

**THE ELECTROCHROMIC
ENHANCEMENT OF LATENT
FINGERPRINTS ON METAL SURFACES**

Thesis submitted for the degree of

Doctor of Philosophy

at the University of Leicester

by

Ann L. Beresford MChem

Department of Chemistry

University of Leicester

2013

The Electrochromic Enhancement of Latent Fingerprints on Metal Surfaces

by

Ann L. Beresford MChem

Fingerprints are unique to individuals and have been used as a method of identification in criminal investigations since the late nineteenth century. The majority of fingerprints are *latent*, i.e. non-visible, and require enhancement for their visualisation. Although many methods have been developed for this purpose, the recovery rate in the form of a *useable* print, is still disappointingly low for metallic surfaces, especially from discharged cartridges. This work aimed to explore the application of a new technique to utilise the insulating properties of fingerprint deposits, on a range of metallic surfaces. Fingerprint residue can 'mask' the surface preventing the electrochemical deposition of a reagent on the bare surface. Here, this takes the form of two different electrochromic polymers, polyaniline and poly-3,4-ethylenedioxythiophene, to produce a negative image of the print. Fingerprint samples were subjected to diverse environments for a range of time intervals. The enhancements were graded on a five point scale devised by Bandey, where prints graded 0-2 are considered unusable and prints graded 3-4 are usable for identification purposes. Using this scale the technique was assessed in a comparative study with existing methods (powder dusting, wet powder and superglue fuming). The outcomes identified superglue fuming as least effective and poly-3,4-ethylenedioxythiophene to be the material of choice when an sample's history was unknown. Exploitation of the polymer's electrochromic properties (oxidation/reduction via applied electric potential), to optimise contrast between print and substrate, resulted in the upgrading (from unusable to useable) of 16 % of samples. Project objectives were achieved; the technique was applied to challenging surfaces via the progression from model substrates to alloys to evidentially viable items. Latent fingerprints were enhanced on stainless steel, nickel plated brass, copper, lead and most importantly previously fired brass cartridges.

Acknowledgements

I would first like to thank Prof. Rob Hillman for giving me the opportunity to take my chemistry career to a level I never imagined I would achieve. I am extremely grateful for the acknowledgement and involvement I have been given for the innovation of this project. I would also like to thank Dr. John Bond OBE for his time, honesty and encouragement. For funding contributions I would like to acknowledge the University of Leicester, Northamptonshire Police and the Innovation Fellowship. For going beyond the call of duty, Greg Gregory, thank you for taking the time to share your knowledge and enthusiasm with me. Graham Clark, thank you for showing me the Raman and SEM ropes. And thank you to the anonymous fingerprint donors.

Specific to Chapter 6 I owe thanks to Rachel Brown for her contributions, Mark Rowe and his team at Northamptonshire Police Forensic Lab for their time, patience and ultimately the use of their equipment. Also, Trudy Loe for allowing Rachel and I to set up camp in her office whilst we waited for samples to be fumed or dried.

This experience has been a rollercoaster of sorts, but what has kept me going has been the friends I made along the way and my close family back in Shropshire:

Becky Williams, Alex Goddard, Rachel Brown, Michal Fornalczyk, Charlotte Beebee, Gemma Geary, Abdul Yavuz, Poppy Jones and Virginia Ferreira. Whether it was keeping me entertained during tea breaks playing Sporcle and eating cake, or lifting my spirits out of hours watching hospital dramas, or sharing my passion for fancy dress, cocktails and dancing, it all helped!

Mum, Dad, GranTed, Custard and DT. Thank you for always believing in me; for your unconditional love and support.

I would also like to give a special mention to three lovely ladies; Rosie Graves, Kathryn Pugh and Claire Fullarton who have had to live with me through some tough times. Thank you for still wanting to be my friend and for all the fun we have had together over the past seven plus years!

Finally, to my Mister. For your incredible patience and for being my light at the end of the tunnel.

Contents

1. Introduction.....	1
1.1. Fingerprints.....	1
1.1.1. History of Fingerprints and their use in Solving Crime.....	1
1.1.2. Modern Fingerprint Searching.....	6
1.1.3. Fingerprint Deposits.....	7
1.1.4. Sweat Types.....	9
1.1.5. Print Types.....	11
1.2. Developing Latent Fingerprints.....	16
1.2.1. History of Fingerprint Development.....	16
1.2.2. Established Methods for Developing Fingerprints.....	17
1.2.3. Recent Advances in Latent Fingerprint Development.....	24
1.2.4. Development of Fingerprints from Metal Substrates.....	26
1.2.5. Fingerprints Acting as a Chemical Resist.....	28
1.3. Polymers.....	30
1.3.1. Electrochromism.....	33
1.3.2. Polyaniline.....	35
1.3.3. Poly-3,4-ethylenedioxythiophene.....	36
1.4. Project Objectives.....	37
1.5. References.....	40
2. Principles of Methodology.....	51
2.1. Overview.....	51
2.2. Potentiostats.....	51
2.2.1. Chronoamperometry.....	54
2.2.2. Cyclic Voltammetry.....	56
2.3. Visualisation.....	60
2.3.1. Digital Photography.....	60
2.3.2. Optical Microscopy.....	61
2.3.3. Scanning Electron Microscopy.....	62

2.4. Characterisation.....	64
2.4.1. Raman Spectroscopy.....	64
2.5. Profilometry.....	65
2.6. References.....	67
3. Experimental.....	70
3.1. Fingerprints.....	70
3.2. Fingerprint Deposits.....	70
3.3. Substrates.....	71
3.4. Metal Plating.....	75
3.5. Electrolyte.....	77
3.6. Monomer.....	78
3.7. Polymer Deposits.....	79
3.8. Pre-treatment.....	80
3.9. Other Enhancement Techniques.....	81
3.10. Visualisation.....	83
3.10.1. Digital Imaging.....	83
3.10.2. Optical Microscopy.....	84
3.10.3. Scanning Electron Microscopy.....	84
3.11. Characterisation.....	84
3.11.1. Raman Spectroscopy.....	85
3.11.2. Energy-Dispersive X-ray Spectroscopy.....	85
3.12. Profilometry.....	86
3.13. References.....	87
4. Novel Fingerprint Development using Polyaniline on Stainless Steel.....	89
4.1. Overview.....	89
4.2. Film Electrochemistry.....	89
4.3. Film Thickness.....	92
4.4. Fingerprint Images.....	97
4.4.1. Digital Images – <i>Ex-situ</i>	98

4.4.2. Digital Images – <i>In-situ</i>	99
4.4.3. Optical Microscopy	101
4.5. Grading	103
4.6. Stainless Steel Knives	118
4.7. Conclusion	120
4.8. References	124
5. Application of Polymer Enhancement to Fingerprints on Diverse Metal Surfaces	127
5.1. Overview	127
5.2. Fingerprint Development from Brass	129
5.3. Fingerprint Development from Copper	150
5.4. Fingerprint Development from Nickel Plated Brass	156
5.5. Fingerprint Development from Lead	163
5.6. Conclusions	173
5.7. References	175
6. Comparative Study of Electrochromic Enhancement of Latent Fingerprints with Existing Development Techniques	179
6.1. Overview	179
6.2. Experimental Procedures	180
6.3. Enhancement Technique Performance According to Pre-Treatment	183
6.3.1. Ambient Conditions	184
6.3.2. Immersion in Water	189
6.3.3. Acetone Wash	192
6.3.4. Exposure to High Temperature	196
6.3.5. Soap Wash	198
6.3.6. Summary	202
6.4. Optimum Enhancement of Samples According to a Incompletely Known History	206
6.5. Conclusions	213

6.6. References.....	216
7. Conclusions.....	219
8. Appendices.....	223

List of Abbreviations

A	Anion
AFR	Automatic Fingerprint Recognition
BCE	Before Common Era
CE	Counter Electrode
CRT	Cathode-Ray Tube
CV	Cyclic Voltammetry
DFO	1,8-Diazofluoren-9-one
DNA	Deoxyribonucleic Acid
EDOT	Ethylenedioxythiophene
EDX	Energy-Dispersive X-ray
ESEM	Environmental Scanning Electron Microscope
FTIR	Fourier Transform Infrared
GSR	Gunshot Residue
HOMO	Highest Occupied Molecular Orbital
JPEG	Joint Photographic Experts Group
LED	Light Emitting Diode
LUMO	Lowest Unoccupied Molecular Orbital
M	Metal
MA	Metal Salt
MALDI	Matrix-Assisted Laser Desorption Ionisation
NAFIS	National Automated Fingerprint Intelligence System
PAni	Polyaniline
PEDOT	Poly-3,4-ethylenedioxythiophene
PTSA	<i>p</i> -Toluenesulphonic Acid

RE	Reference Electrode
RTD	Residence-Time Distributions
SCE	Saturated Calomel Electrode
SDS	Sodium Dodecylsulphate
SEM	Scanning Electron Microscope
SKP	Scanning Kelvin Probe
SIMS	Secondary Ion Mass Spectrometry
UK	United Kingdom
UV	Ultraviolet
WE	Working Electrode

Chapter One

1. Introduction

1.1. Fingerprints

Fingerprints have long been recognised as a form of identification, so much so that the word 'fingerprint' has been adopted by many sciences to describe characteristic information: DNA 'fingerprint' and the 'fingerprint' region of an infrared spectrum are two obvious examples. The importance of fingerprints is due to their uniqueness to individuals; the intricate patterns found on the fingertips are persistent through life and can be used to identify individuals after death.¹

DNA is hereditary, therefore portions of which will be identical to those of blood relations. Fingerprints are not. Fingerprints are unique: there is a 64 billion to one chance of finding two identical prints.² This is why fingerprinting is so important and can be exploited for criminal investigations.

1.1.1. History of Fingerprints and their use in Solving Crime

The Chinese were the first culture known to use friction ridge detail as a form of personal identification from approximately 221 BCE to 220.³ However it was not until centuries later that the first recorded study of fingerprints in 1684 by Nehemiah Grew (1641-1721) was carried out. Originally an English plant morphologist, Grew (Figure 1.1) is thought of as the first real fingerprint pioneer who not only wrote about the subject but published many accurate drawings of the different intricate patterns depicted by the ridges and furrows of fingerprints.⁴

In 1788 it was recognised by a German anatomist, J. C. A. Mayer, that friction ridge detail was unique. He wrote

*'Although the arrangement of skin ridges is never duplicated in two persons, nevertheless the similarities are closer among some individuals. In others the differences are marked, yet in spite of their peculiarities of arrangement all have a certain likeness.'*⁵



Figure 1.1. Image of Dr Nehemiah Grew featured in his publication (1701) ‘Cosmologia sacra, or a discourse of the universe as it is the creature and kingdom of God’.³

The first recorded academic study of fingerprints, however, was published nearly a century and a half later in 1823 by Joannes Evanelista Purkinje (1787-1869). Best

known for his discovery of Purkinje cells, he also discovered sweat glands and covered in his thesis the functions of ridges, furrows and pores present on the tips of the fingers. Also covered were the classification of different patterns (see Section 1.1.5) into nine categories; one arch, one tent, two types of loop and five types of whorl, Figure 1.2.³

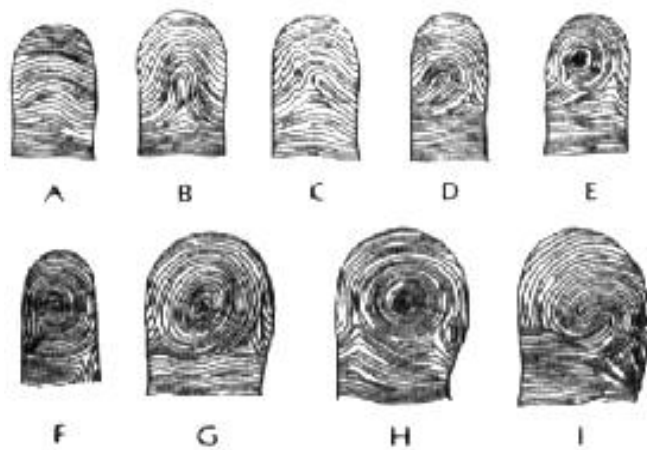


Figure 1.2. Purkinje's nine fingerprint patterns described as; a) transverse curves; b) central longitudinal stria; c) oblique stria; d) oblique sinus; e) almond; f) spiral; g) elliptical whorl; h) circular whorl; i) double whorl.³

Just under forty years later a study into how fingerprints change over time was carried out by Sir William Herschel (1833-1917). Herschel took his own palm prints in 1860 and again in 1888, see Figure 1.3; the print pattern and ridge detail remained unchanged, with the exception of a few extra crease lines.³

Around the same time as Herschel, Dr Henry Faulds (1843-1930) was fingerprinting his patients then removing the printed skin. He allowed the skin to re-grow then

fingerprinted them again, making the observation of identical patterns to the original prints. Faulds is thought of as the first fingerprint pioneer to recognise the significance of crime scene application, writing

*'An English jury...would only, in any case, have to compare two figures similarly enlarged, one being of the accused person's fingers, taken while in custody, and the other...a smudgy mark from some blotting-pad, window-pane, drinking-glass, bottle, or the like.'*⁶

He went on to solve at least two crimes in Japan using fingerprint evidence.³

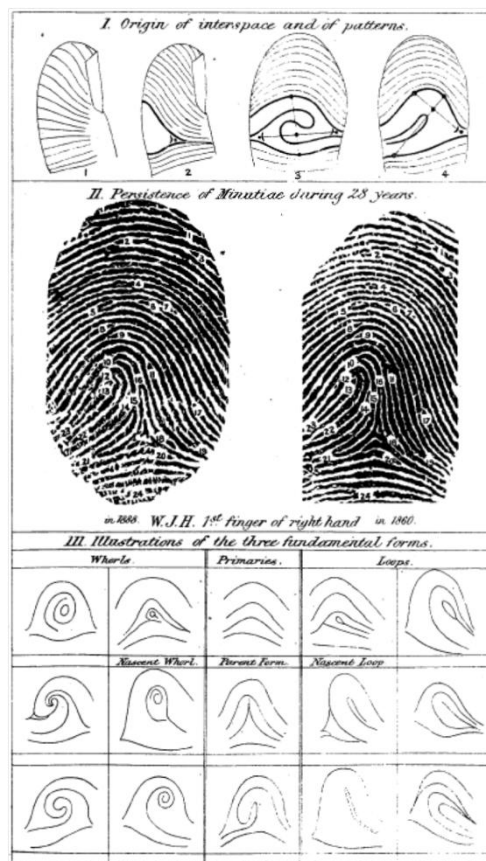


Figure 1.3. Taken from Galton's 'Identification of Finger-tips', published in 1891. Section II shows the persistence of minutiae, *secondary detail* (see Section 1.1.5), after 28 years.⁷

In the late 19th century Sir Francis Galton (1822-1911) conducted an extensive study into fingerprints, which stemmed from his initial interest in thumb impressions. The discovery of the uniqueness of fingerprints led to the decline in common anthropometric methods and the immediate implementation of fingerprints as a more efficient method of identification.⁸

At the turn of the 20th century, Sir Edward Henry (1850-1931), influenced by Sir Galton's *Finger Prints*, made his own important advance in fingerprint identification, known as the 'Henry System'. His method involved the mathematical indexing of fingerprints using a ten print classification system⁹ whereby each whorl (see Section 1.1.5) is given a numerical value based on the finger on which it is found. Assuming all ten prints from an individual are obtained they are paired together as follows; right thumb and right index; right middle and right ring; right little finger and left thumb; left index and left middle; left ring and left little finger. The first of the pair is the numerator and the second the denominator. When a whorl occurs in the first pair it counts 16, in the second it counts 8, in the third 4, in the fourth 2 and in the fifth 1; a value of 0 is given where a loop (or arch– see Section 1.1.5) is found. The sum of the numerators and the sum of the denominators provide a new fraction to which 1 is added to both sides and the fraction inverted. The outcome is a primary classification number that would be used to file and later locate the fingerprints of individuals, from a possible 1024 classes.¹⁰

1.1.2. Modern Fingerprinting Searching

The use of fingerprints as a form of personal identification was legally implemented and used as a standard procedure in forensic science in the early 20th century. Fingerprint agencies were set up and fingerprint databases were established. Every man or woman, who has been arrested and charged, reported or summonsed for a crime has their fingerprints taken. Depending on the country in which this takes place, the prints are added to the appropriate regional/national database, if not already present, where they will remain indefinitely for comparison and identification of individuals. Prior to 1970, the task of fingerprint comparison and identification was long and arduous as the information was kept on a series of card indices that would be filed, searched and recovered by hand. The Automatic Fingerprint Recognition (AFR) technology put an end to the demanding process and was used to develop the computer based system NAFIS (National Automated Fingerprint Intelligence System). As an example, in the UK, by 2001 every police force in England and Wales had the technology available to them. A special algorithm is used to select a number of characteristics that can determine the closest matches between a suspect's fingerprint, held in the database, and a print recovered from a scene.¹ The system has enormous benefits; allowing for quick and simple checking between various fingerprint bureaux across the country.

Tenprints is an example of a bureau used by Northumbria Police. The name Tenprints comes from the recording of an individual's ten distinct fingerprints by the use of an ink pad and paper. Hundreds of fingerprint forms are sent to Northumbria's bureau each day, which holds roughly 700,000 of them. Each set of fingerprints is then fed into the IDENT1 database.¹¹ IDENT1 replaced NAFIS in April 2005 and is now the central national database for searching and comparing the fingerprint details of offenders

within the UK.¹² As of June 2012 the IDENT1 database held: 8.9 million known individuals' ten-prints and 12 million palm print pairs as well as a further 1.9 million unidentified marks and impressions.¹³

Fingerprints recovered from scenes of crime are scanned into respective bureaux and where applicable colour inversion of the image is carried out so that ridges appear black on a white background, Figure 1.4. The fingerprint expert marks up individual characteristics from the scene print and the computer establishes likely matches from within the database. The overall decision on identification, if any, lies with the fingerprint expert. The type of fingerprint pattern, the finger type (left or right hand, thumb, etc.) and the ridge characteristics, (discussed in more detail in Section 1.1.5.) are what the fingerprint expert will be looking for when making the comparison. Until recently there was a minimum requirement of 16 matching characteristics for a positive identification to be made in the UK. However this has now been eradicated, with no minimum quantitative criterion: it is solely the fingerprint expert's decision over the identification.²

1.1.3. Fingerprint Deposits

Humans have on the soles of their feet and palms of their hands ridges which form unique patterns, also known as friction ridge skin. They form roughly twenty-eight weeks after conception when one is still in the foetal stage. Despite their name, there is still debate over whether the friction ridges are primarily to aid grip, to hold items or to secure footing when one has bare feet. It would appear that to be born without fingerprints does hinder activities that require delicate handling such as turning the

pages of a book.¹⁴ However, a research group in Manchester reported that having fingerprints reduces the contact area and thus the friction between the fingers and the opposing surface.¹⁵ Whatever their intended use, they are considered a powerful tool that remain unchanged throughout life, providing no deep cuts or scarring occur, and can be used to identify individuals at *post mortem*.¹

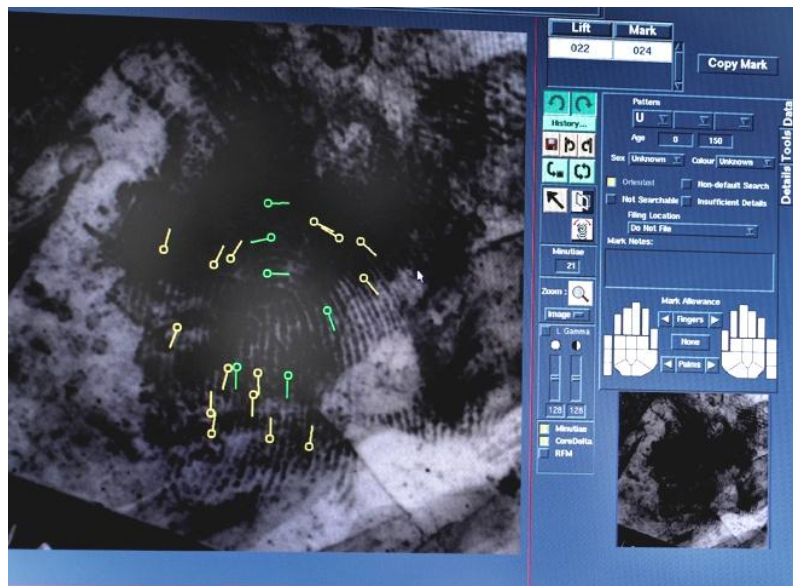


Figure 1.4. An example screenshot of TenPrints, an Automated Fingerprint Identification System and bureau used by Northumbria Police.¹¹

When friction ridge skin comes into contact with a surface, a print is left behind, following Locard's principle that every contact leaves a trace. Fingerprints are created by the perspiration secreted from the sweat pores that are found along the friction skin ridges present on hands and feet (Figure 1.5).¹⁶ The ridge patterns found on the tips of the fingers are often used as a way of identifying a person, usually taken from a crime scene with the intention of discerning who committed the crime. The composition of a

print can be varied, not only can it contain the contents secreted from the relevant sweat glands but material from other glands, cosmetics, perfume and food residues.¹⁷⁻¹⁸



Figure 1.5. A photograph captured by a Nikon Fabre Photo EX microscope (x66 magnification) of friction skin ridges with micro-droplets of sweat being secreted from their sweat pores.¹⁹

1.1.4. Sweat Types

There are three main types of sweat gland: eccrine, apocrine and sebaceous.¹ Eccrine glands are located throughout the body but are in highest density on the soles of the feet and palms of the hands. Water, as much as 98%, can be found in eccrine sweat along with both organic and inorganic constituents. Sebaceous glands are most commonly observed in areas containing hair follicles. Sebaceous sweat is greasier than eccrine sweat as it is made up of only organic components, mostly triglycerides and fatty acids. Apocrine glands are found in the genital, breast, axillary and inguinal regions. Little work has covered the inclusion of apocrine secretions where fingerprint detection is

concerned.²⁰ Due to the location of these glands it is rare to find apocrine sweat as one of the dominant constituents of a print, but its presence may have significance in a crime of a sexual nature.²¹ The main constituents secreted from the three types of glands are outlined in Table 1.1, nevertheless fingerprint composition remains complex.

Source	Inorganic constituents	Organic constituents
Eccrine glands	Chlorides Metal ions Ammonia Sulphate Phosphate	Amino acids Urea Lactic acids Sugars Creatinine Choline Uric acid
Apocrine glands	Iron	Proteins Carbohydrates Cholesterol
Sebaceous glands	-	Fatty acids Glycerides Hydrocarbons Alcohols

Table 1.1. The main constituents of secretions of the sweat glands (excluding water).⁴

The age of both the donor and the print can affect the quality of enhancement of a fingerprint. Due to chemical differences in fingerprint deposits, enhanced prints from children are generally of poorer quality to adults.²²⁻²³ The composition of fingerprint residue can also change over time; the aging process can follow many different pathways and at considerably different rates. Significant physical and chemical changes, such as evaporation, degradation, drying, migration and oxidation can occur.²⁴ These will depend on a number of factors including the initial composition of the fingerprint, the surface the residue resides on and the environmental conditions it is subjected to.

1.1.5. Print Types

When an object or surface is handled, the transfer of material in the form of a print occurs. In some circumstances fingerprints are made *visible* by the transfer of a substance such as paint, blood or foodstuffs from the hands to a surface (Figure 1.6a). In other circumstances impressions are created by the ridges and furrows of a print in a ‘soft’ substrate, a *plastic* print (Figure 1.6b). Yet the majority of fingerprints deposited are *latent* (not visible to the naked eye – Figure 1.6c); their composition is dependent on the eccrine sweat (~98 % water) secreted from pores located on the fingertips.³ However it is common for this sweat to become contaminated simply by touching one’s face which excretes sebaceous sweat from some of its pores.²⁵ Sebaceous sweat is responsible for giving fingerprint deposits oily, tacky characteristics due to the triglycerides and fatty acids it contains. Unlike *visible* or *plastic* fingerprints, which can in most cases be photographed with no further treatment, *latent* prints require enhancement in order to visualise them.

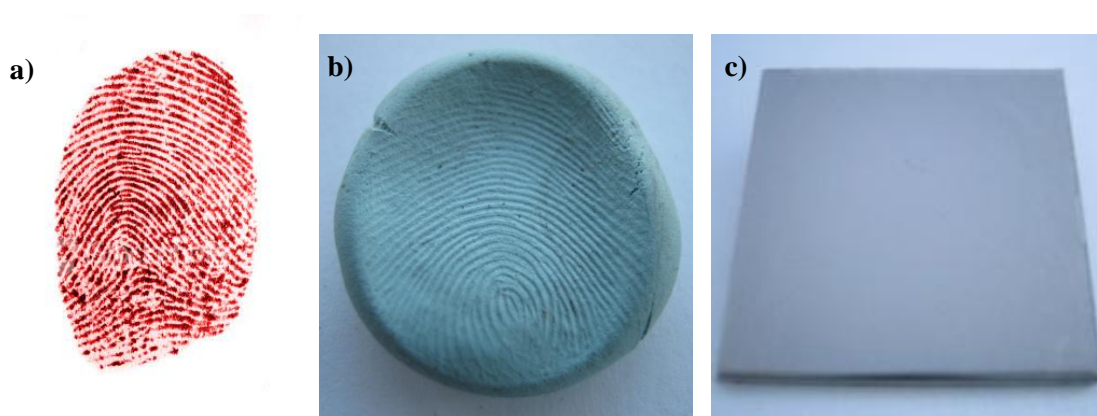


Figure 1.6. Examples of print types a) visible; b) plastic; and c) latent.

Ridges make up patterns, of which there are three main groups, whorls, loops and arches (Figure 7). Large percentages of individuals will share one of these *primary detail* patterns. However it is the distinguishing features, *secondary detail*, such as deltas, lakes, bifurcations and ridge endings which make fingerprints unique. Deltas, which resemble the Greek letter delta and occur in the friction ridges at the point of divergence between two type lines have the added importance that they can help to distinguish between some *primary detail* patterns.



Figure 1.7. The main fingerprint patterns a) whorl; b) loop; c) arch; and an example of a delta d) circled.

Loops are the most common fingerprint pattern; they require at least one ridge to run from one side of the fingertip curve round the ‘core’, the centre and then exit the tip on the same side as the one it entered. Loops have one delta and are classified into either ulnar or radial, named after the bones in the forearm. An ulnar loop joins the pattern on the same side as the little finger; the radial loop joins on the same side as the thumb (Figure 1.8).²

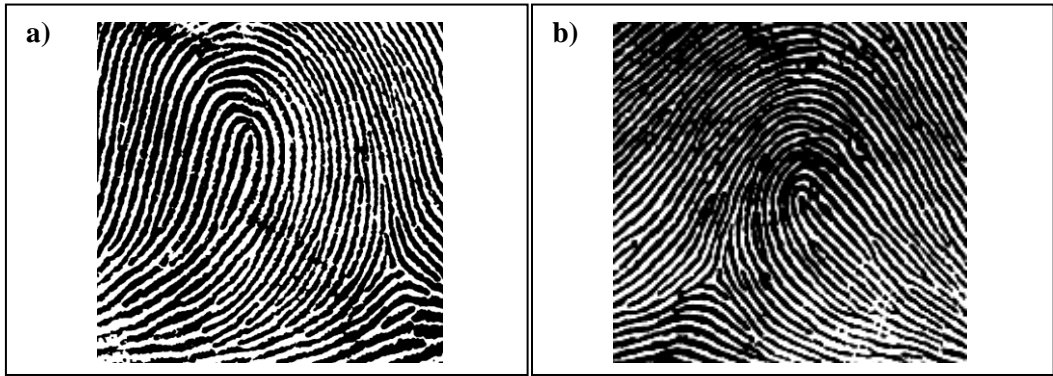


Figure 1.8. Examples of fingerprint patterns a) an ulnar loop from a left hand; b) a radial loop from a left hand. These would be reversed if taken from a right hand.

Arches can be classified into two groups: the plain arch or the tented arch (Figure 1.9).² The plain arch has ridges that flow from one side of the fingertip to the other with a smooth rise in the middle. The tented arch has a significant up-thrust ridge at the core of the print that the other ridges flow over, creating a tent like pattern. Arches by definition do not possess deltas; if one is present then it is a loop and if there are two it is in fact a whorl.

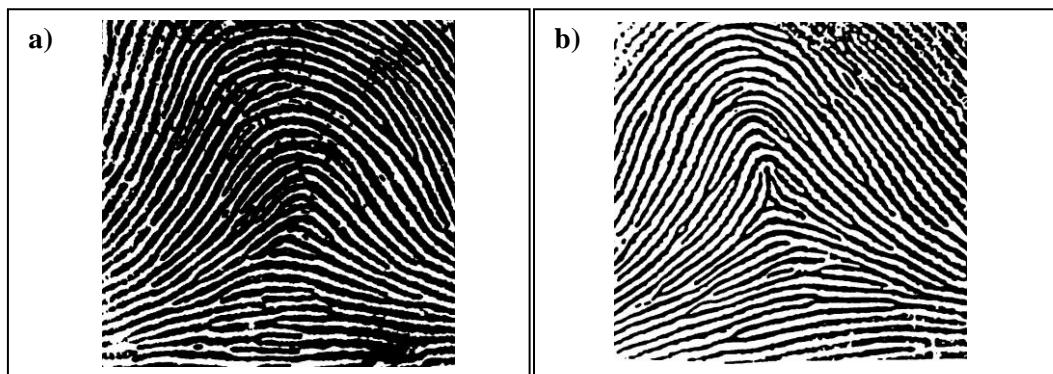


Figure 1.9. Examples of fingerprint patterns a) plain arch; b) tented arch.

Whorls can be defined in several ways: plain, central pocket, double loop and accidental (Figure 1.10).² To be classified as a whorl the print must have one delta either side of the core. A plain whorl consists of one or more ridges that are on the verge of making or make a complete circuit. If one ridge encircling the core is encountered whilst passing from one delta to another it is classified as a plain whorl. However a central pocket whorl consists of at least one re-curving ridge and when passing from one delta to another one of these re-curving ridges is not met. The double loop pattern involves two loops, one entering from either side of the finger in between two deltas. The existence of two deltas excludes the double loop from the loop classification. Finally the accidental whorl; this classification contains patterns that cannot be fitted into any of the previously mentioned categories, including those that consist of a combination of two or more pattern types.

Within one pattern type any combination of *secondary detail* can be found, below is a list of the different types of classification, see Figure 1.11.

- I. **Ridge ending** – when a ridge stops abruptly
- II. **Bifurcation** – a single ridge that divides into two
- III. **Dot** – an individual ridge that is similar in width and length
- IV. **Ridge crossing** – the intersection of two ridges
- V. **Lake** – a ridge that splits into two then reconnects shortly afterwards to form a single ridge again
- VI. **Bridge** – a short ridge that connects two parallel ridges
- VII. **Island** – where a ridge starts and ends without contact with the main part of the pattern, an independent ridge

VIII. **Spur** – similar to a bifurcation, a short ridge branching off a much longer ridge

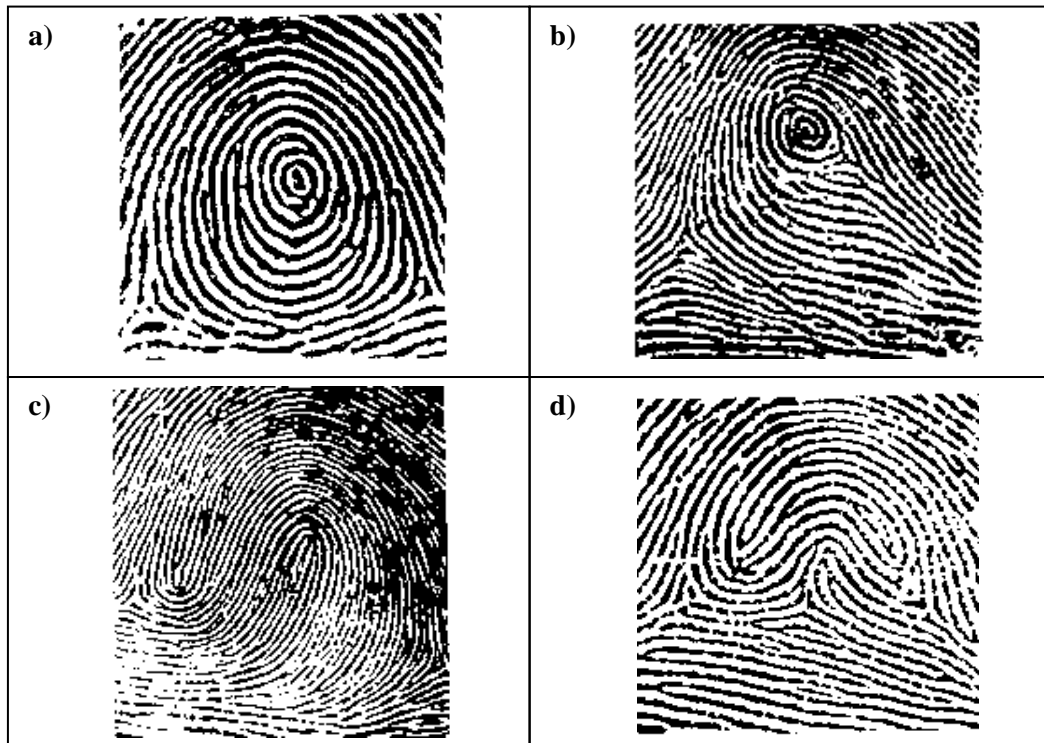


Figure 1.10. Examples of fingerprint patterns a) plain whorl; b) central pocket whorl; c) double loop; d) accidental.

The width of individual ridges and the position of the sweat pores present on them are *tertiary detail*.² This level of detail is rarely used when matching a print, but should not be completely ruled out.

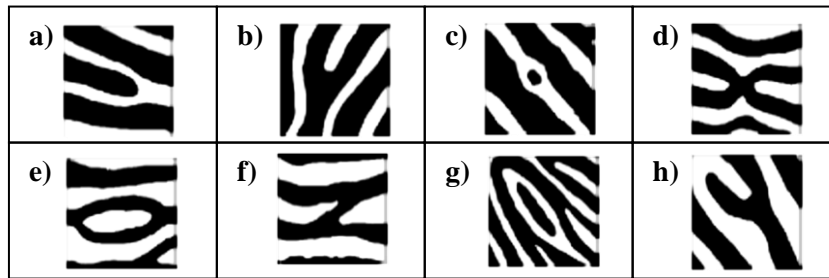


Figure 1.11. Examples of *secondary detail* a) ridge ending; b) bifurcation; c) dot; d) ridge crossing; e) lake; f) bridge; g) island; h) spur.

1.2. Developing Fingerprints

1.2.1. History of Fingerprint Development

Since it was first recognized that fingerprints could be used as a form of identification several methods have been explored to ‘capture’ these prints. Capturing the fingerprint allows revisiting of the image for assessment and comparison to possible matches. Methods have evolved from storing the item or surface to which the print has been located, to a vast digital library of developed fingerprint images (see previous Sections 1.1.1-1.1.2). The type of fingerprint prior to development will depend on the method of retrieval and therefore capturing of the image. It is possible that both a physical and digital copy of the fingerprint could be taken. This next section describes the way in which a latent fingerprint is made visible via different means of development. These include dusting,²⁶⁻³³ superglue fuming,³⁴⁻⁴⁰ photographing⁴¹⁻⁴⁴ and the use of chemical dyes.⁴⁵⁻⁵⁰

1.2.2. Established Methods for Developing Fingerprints

Some bulkier items or surfaces that may possess fingerprint evidence will remain as part of their crime scene, in their original environment. However, some smaller items or more crucial evidence may be removed from the scene to a laboratory for techniques that cannot be completed at the scene. This will usually be carried out if it is thought that a better contrast between the fingerprint and the substrate can be achieved.

A systematic approach should be taken to achieve the highest quality from a fingerprint deposit.² The choice of technique must be thoroughly considered as the approach will differ depending on the type of fingerprint and the substrate it is found on, see Figure 1.12. The type of substrate has great importance as this can determine which technique to employ; some techniques will simply not work on certain surfaces. The surface could be porous (paper document), semi-porous (wooden handle of a weapon) or non-porous (glass window), and may be rough or smooth, shiny or dull, multi-coloured or colourless.

The recovery of fingerprints is a very important process. It is of great consequence to choose the right method of retrieval, as in most cases there will only be one attempt at getting the perfect image and no further enhancement can occur once the print is developed. Once the print has been recovered, an image is required. The image of the fingerprint will be uploaded to a database to search for a match. It is possible that only a small region of the fingerprint is recovered, this is a *partial print*. When this occurs it can be harder to determine *primary detail* which puts more emphasis on *secondary detail* and possibly *tertiary detail*.

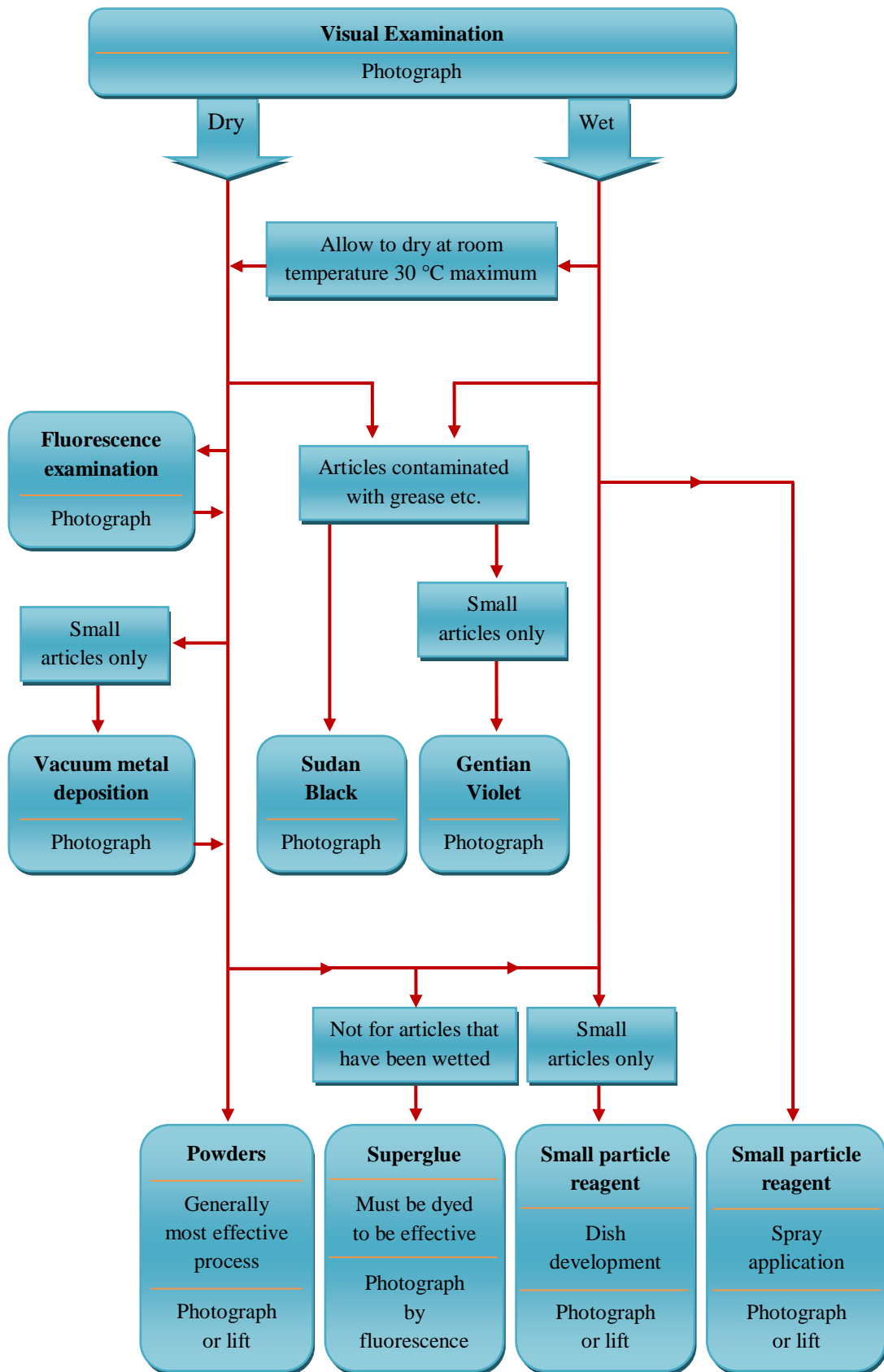


Figure 1.12. The systematic approach taken when developing a fingerprint from a non-porous surface. Adapted from Jackson and Jackson (2004).²

One of the oldest procedures for the development of latent prints is powder dusting. This is a physical method that relies upon the adherence of the powder to the fingerprint residue. The use of a brush to dust over the substrate can have destructive effects on ridge detail but gives instant development. It remains one of the most common and reliable methods. Generally there are four types of powders:

I. **Regular** – contain a resinous polymer for adhesion and colorant for contrast. Commonly used adhesives include rosin, starch and silica gel.²⁶ The colorant used may be an inorganic salt or an organic derivative. An example of a black fingerprint powder is manganese dioxide powder (manganese dioxide 45 %, black ferric oxide 25 %, lampblack 25 %, rosin 5 %).⁴ Other combinations include titanium dioxide and kaolin, ferric oxide and rosin, and lampblack and fuller's earth.⁵¹ However in recent years the use of fingerprint powders containing inorganic salts has deteriorated due to their toxicity and potential health hazards.

II. **Luminescent** – contain natural and/or synthetic compounds that fluoresce or phosphoresce under ultraviolet (UV) light, laser light and other light sources.^{27,52-55} These powders are most useful for the visualisation of latent prints deposited on multicoloured surfaces.

III. **Metallic** – the most common metallic powder used at a crime scene is aluminium powder.² However, there are magnetic powders, referred to as magna-powders, that are applied by the use of a magnetic applicator.²⁷ The powders originally incorporate coarse spherical iron particles with conventional powders. The magnetic iron acted as a carrier for the non-magnetic particles producing a 'brush' when the powder was picked up by the magnetic applicator.⁵⁶⁻⁵⁷ The fine particles would adhere to print detail when the applicator was passed over the suspecting surface. Flake metal powders replaced the standard magna-powders; the presence of the coarse iron was no

longer needed as all of the flake powder could be picked up by the applicator and used for development of prints.⁵⁷⁻⁵⁹ Metallic powders have proved successful when recovering latent prints from leather or plastic substrates and superior for print detection on rough surfaces.⁶⁰⁻⁶¹

IV. **Thermoplastic** – these powders include photocopier toners or dry inks that develop latent fingerprints by fusing to the substrate upon exposure to heat.⁴

Another physical method is that of the small particle reagent that relies upon the adherence of fine particles to the fatty constituents of the latent residue.⁶²⁻⁶⁸ Molybdenum disulfide was originally used. Now fine titanium dioxide⁶²⁻⁶⁴, iron oxide⁶⁵⁻⁶⁶ or zinc carbonate⁶⁷⁻⁶⁸ particles are suspended in a solution containing a surfactant. The solution is sprayed or swabbed onto the substrate and the developed fingerprint appears as a dark or light grey colour. This technique has been successful on a variety of substrates including metal, concrete and wood. However, due to the colour of the developed fingerprint, contrast with the substrate can suffer.

When powders are applied, lifting tape can be used to remove the developed fingerprints from the crime scene for subsequent examination.⁵⁷ A wide range of different types of tape are available for the purpose of lifting powdered fingerprints from a range of surfaces, including human skin.⁶⁹ Regardless of the type of tape being used, the principle of the process is the same. A short length of tape is pressed down onto the developed print, taking care to ensure no air bubbles are present. The tape is then slowly removed from the surface and transferred to a backing sheet.⁷⁰ Lifting tape, or more specifically adhesive tape, has been used in conjunction with many

spectroscopic techniques to analyse contaminants within the acquired fingerprint deposit, such as drug metabolites^{29,70-71} and explosives⁷².

There are two techniques which employ the fuming of a substance. The first and less widely used involves iodine. Iodine crystals are warmed, producing a purple vapour which is absorbed by the fingerprint residue to give a pale brown developed print.⁷³⁻⁸⁰ Although iodine fuming is a simple technique, it has several disadvantages: its vapours are toxic and corrosive, developed prints fade rapidly upon standing in air and aged prints are difficult to develop.⁴ Attempts at prolonging the developed colour by chemical fixing have been carried out using starch, steam or water,⁷⁵⁻⁷⁶ benzoflavone reagents⁷⁷⁻⁷⁸ and most recently a brucine-based reagent⁷⁹. Several decades ago it was found that iodine fuming could also be used to retrieve prints from live human skin.⁸⁰

The second and much more common fuming technique is the use of cyanoacrylate (superglue).³⁴⁻⁴⁰ Latent prints are exposed to ethyl-cyanoacrylate vapour in an enclosed chamber. When the cyanoacrylate monomer comes into contact with the fingerprint residue a white polymer grows along the ridges of the print.³⁵ The polymerisation is anionic: OH⁻, the anionic initiator, reacts with the monomer to create a reactive species that can react with subsequent monomers to make a polyethylene product, Figure 1.13. Wargacki *et al* concluded that water was not the initiator responsible for polymer chain growth. It was found to be the primary components of eccrine sweat (lactate and alanine) that initiated polymerisation via their carboxylate functionality.³⁶ The quality of an obtainable print can decrease as it ages. However, the use acetic acid as an enhancement agent has allowed for greater observed enhancement of these prints. The

carboxylic acid functionality, present in acetic acid, initiates and polymerises the cyanoacrylate vapour.³⁷

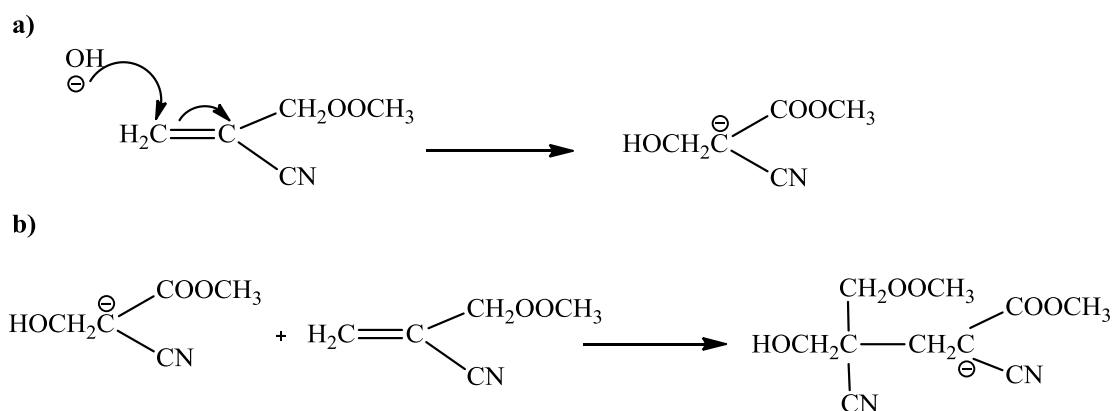


Figure 1.13. Mechanism for superglue polymerisation in a base catalysed reaction, a) monomers are activated; and b) chain propagation follows.³⁵

Prints developed via superglue fuming can sometimes be difficult to visualise or there may be a lack of contrast, therefore further enhancement of this process is required.⁸¹⁻⁸⁶ Dusting powders⁸¹ have been applied as a post-treatment, but luminescent or fluorescent dyes⁸²⁻⁸⁵ have been most useful especially on multicoloured backgrounds and most recently vapour-phase staining.⁸⁶ The overdevelopment of a print can occur, where the polymer forms on the ridges as well as between the ridges, reducing contrast. This could be classed as a disadvantage as it requires someone to observe the technique to decide when the appropriate development has taken place.

For fingerprints on porous surfaces, such as paper and cardboard, the most widely used reagents are ninhydrin and 1,8-diazofluoren-9-one (DFO) and physical developer.⁸⁷

The techniques involve the respective reagent solution being sprayed or swabbed onto the substrate or the substrate being submerged in the solution. Where print detail is present a colour change will occur. The change in colour is a result of a reaction with amino acids present in the fingerprint deposit (Figure 1.14).⁷³ Optimal results have been achieved at higher temperature and humidity,⁷³ and in more recent years analogues of ninhydrin have also been used.^{46,48,88-90} One specific example, 1,2-indandione that is becoming a recognised replacement for ninhydrin and DFO, does not result in an intense colour development. Instead it fluoresces when excited under certain wavelengths of light (473 – 550 nm), allowing visualisation.^{48,91}

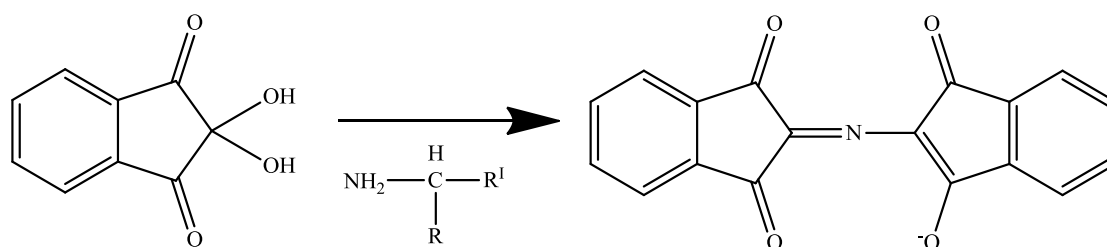


Figure 1.14. Chemical reaction between ninhydrin and a primary or secondary amine to give Ruhemann's purple.

Many more different types of chemical dye are available that are suited to more specific scenarios. Crystal violet, also known as Gentian Violet, is purple in colour and stains the fatty acid components of sweat. It proves particularly useful in the development of fingerprints from adhesive surfaces such as Sellotape® but has also been effective on latex gloves.² Gentian Violet is also a product when Leuco Crystal Violet (colourless) is oxidised by the presence of blood and hydrogen peroxide (Figure 1.15).⁹²⁻⁹³ Sudan Black has been shown to work well in developing prints from adhesive surfaces but is especially effective when surfaces have been covered in oil or

grease.⁹⁴⁻⁹⁵ A blue-black colouration occurs when the dye interacts with the fatty constituents of the fingerprint residue. As well as the surfaces listed above, Sudan Black has been used to develop lip prints from human skin.⁹⁶

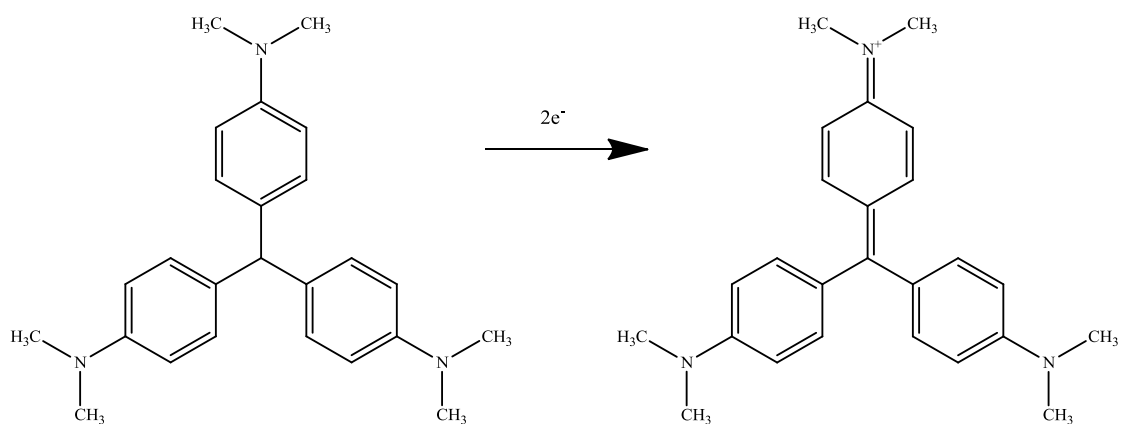


Figure 1.15. Colourless Leuco Crystal Violet seen to oxidise in the presence of blood to give purple Gentian Violet.⁹²

1.2.3. Recent Advances in Latent Fingerprint Development

A common occurrence with the methods described above is that the contrast between print and substrate can suffer when the substrate is dark or multicoloured. In recent years there have been some interesting advances to overcome this issue. Fourier Transform Infrared (FTIR) spectroscopy has been implemented to image prints using differences in the functional groups and molecular components of fingerprint deposits and substrates, rather than visual contrast.⁹⁷⁻¹⁰⁰ This is a non-invasive method that also overcomes the difficulty of fingerprints found on backgrounds made up of writing or images, such as drinks cans and bank notes.

Additional chemical imaging techniques include matrix-assisted laser desorption ionisation (MALDI) and secondary ion mass spectrometry (SIMS).¹⁰¹⁻¹⁰³ These techniques have been used to visualise latent fingerprints through the presence and identification of fingerprint contaminants such as drug metabolites and condom lubricants. In very recent work, the effect of the low pressure environment experienced during both MALDI and SIMS were investigated.¹⁰⁴ The results indicated a 26 % mass loss of the fingerprint residue (fatty acids and water) under 2×10^{-5} Torr for 1 hour. The loss of these constituents has implications for enhancement techniques that rely on their presence. It was therefore concluded that in some circumstances vacuum based techniques such as MALDI and SIMS should not be used due to the effect they may have on subsequent development.

The use of functionalised nanoparticles to both detect and visualise fingerprints has been demonstrated.¹⁰⁵⁻¹⁰⁹ Substrates are immersed in a solvent containing photoluminescent nanocrystals that target the carboxylic acid functionalities of fingerprint constituents. Figure 1.16 represents the general mechanism, the carboxylic acid representing the fingerprint and the amine the nanocomposite. The use of nanoparticles to visualise prints by the presence of drug metabolites has also been shown.¹¹⁰⁻¹¹² Leggett *et al* demonstrated the ability to visualise fingerprints of smokers due to the presence of cotinine, a metabolite of tobacco, in their fingerprint sweat deposits.¹¹² The gold nanoparticles were functionalised with an anti-cotinine antibody which would bind to the cotinine and, tagged with either Alexa Fluor 546 or Alexa Fluor 488, would be visualised under fluorescent light. Alexa Fluors are a series of

fluorescent dyes that have been found to be more fluorescent and more photostable than their commonly used spectral analogues such as Lucifer Yellow and Rhodamine 6G.¹¹³

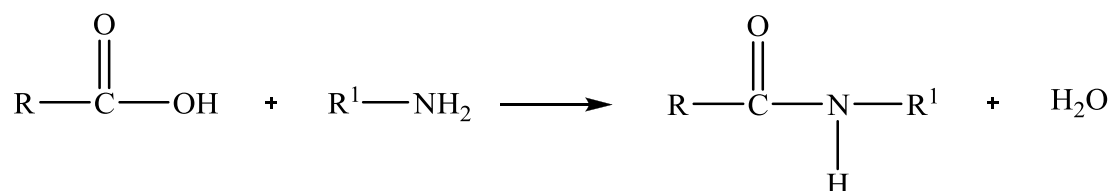


Figure 1.16. General scheme of amide formation from acid and amine.

The majority of fingerprint techniques discussed above are destructive. As previously mentioned, the recovery of the fingerprint is very important so a non-invasive technique is desirable, such as FTIR. It is rare to find a technique that does not involve pre-treatment to the print residue before visualisation can occur. However using spectroscopic imaging on untreated samples has produced positive results.⁹⁷ The implication of such techniques is that they tend not to be speculative, thus require prior knowledge of the location of the print.

1.2.4. Development of Fingerprints from Metal Substrates

Studies involving the development of fingerprints from metal surfaces have increased in recent years, particularly those on ammunition cartridges.¹¹⁴⁻¹²⁰ The visualization of latent fingerprints on spent ammunition cartridges can offer significant forensic evidence, particularly if the cartridge is recovered at the scene of a crime where a firearm has been discharged. These circumstances can provide a link between an individual and a cartridge before it was fired via fingerprint deposits and, potentially,

provide a link to the perpetrator of the crime. However, the visualization of latent fingerprints on spent ammunition cartridges, where fingerprints have been previously deposited, is problematic. Inhibition of subsequent fingerprint visualization has been shown to be caused by the increased temperature due to the firing process, especially blowback,¹²⁰ and abrasive friction caused by loading and ejection of the cartridge.¹²¹ Another issue that makes the visualisation of fingerprints from gun cartridges harder is that of the curved surface.

The Scanning Kelvin Probe (SKP) is a technique that uses the Volta potential difference (ΔV) between the vibrating probe tip and sample to map out an image of the sample surface.¹²² Sweat deposited by the fingertips causes a change in the *work function* at the metal/sweat interface. Work function (ϕ) is a quantity that determines the extent to which photoelectric emission will occur according to Einstein's photoelectric equation¹²³

$$E_k = h\nu - \phi \quad (1.1)$$

where h is Planck's constant and E_k is the kinetic energy of an electron ejected from a metal, when exposed to a certain frequency of radiation (ν).¹²⁴ The magnitude of this potential difference is affected by the water soluble inorganic salts (such as NaCl) present in the fingerprint deposits and the resultant extent of fingerprint corrosion to the metal surface. The non-conducting material, typically air, between the tip and sample constitutes the dielectric.

The electrochemical redox reactions that can occur between latent fingerprints and the metal have been explored extensively by Bond.¹²⁵⁻¹²⁷ It was shown how fingerprint deposits on brass produced sufficient corrosion of the metal to enable the fingerprint to be visualized even after attempts had been made to remove the residue of the fingerprint deposit. Bond used a novel technique that sees the application of an electrical potential to a brass surface and the introduction of a conducting carbon powder that preferentially adhered to the corroded areas of the metal allowing for visualisation of the fingerprint.¹¹⁵

Fingerprints on a variety of surfaces including paper, pottery and cotton, have been visualised by the polymerisation of $(SN)_x$ in the presence of S_2N_2 vapour.^{114,128} Although the mechanism has not yet been confirmed, Kelly *et al* speculate that it is the nitride that interacts with one or more of the components present in fingerprint deposits. When exposed to S_2N_2 , polymerisation occurs as a blue/black polymer along possible ridge detail. Work includes the interaction with corrosion products of fingerprints on metallic surfaces.¹¹⁴

1.2.5. Fingerprints Acting as a Chemical Resist

The techniques described above rely upon the relative reagent to either react with or illuminate components of the fingerprint deposit. The methods discussed in this section are complementary; the fingerprint residue acts as a chemical resist to the ‘reagents’ interaction with the background substrate.^{121,129-133}

A method to develop fingerprints from both unfired and fired brass cartridge cases involves the deposition of palladium onto the metal surface via a displacement process involving the simultaneous oxidation of zinc and to a less extent copper (Equations 1.2-1.3).^{121,129} It was however concluded that further work would have to be done in order to eventually visualise fingerprints on fired cartridges for practical forensic use.



Migron *et al.* also looked at the visualisation of fingerprints via selenation and silver deposition onto three types of cartridge cases.¹²¹ Both methods involved the immersion of the printed sample into a respective solution of $\text{H}_2\text{SeO}_3/\text{HNO}_3$ (Gunblue)



and ammoniacal silver



The results showed the respective precipitation of CuSe and silver was prevented by the presence of fingerprint residue. However, only partial prints were obtained from a few experiments from only one of the types of cartridge case treated, M16.

A new process was proposed in 2001 for the visualization of fingerprints on metal surfaces using the electropolymerisation of pyrrole, the idea being that the fingerprint deposit acts as an insulator to the metal inhibiting deposition of the polymer.¹³⁰ Bersellini *et al.* showed an enhanced fingerprint previously deposited onto a gold sovereign, the polymer forming around the sweat deposit giving a negative image of the print.

Since Bersellini *et al.*'s work similar electrochemical studies has been done to enhance latent fingerprints from stainless steel.¹³¹⁻¹³⁴ Amongst this work is the control of spatially selective electrochemiluminescence to achieve both positive and negative images of the fingerprint residue.¹³⁴

1.3. Polymers

A *polymer* is a large substance that is made up of much smaller repeating units. The formation of polymers involves the joining of *monomers* through chemical reaction. This is commonly referred to as *polymerisation* in which an addition reaction or elimination of a small molecule during the reaction can occur, known as *addition polymerisation* or *condensation polymerisation* respectively. There are a large number of naturally occurring polymers such as rubber, starch in plants and glycogen in animals. Also considered to be polymers are proteins, nucleic acids and silicates generated in rock-formation.¹²³ Polymers can generally be divided into one or more of the following four groups:

I. **Synthetic polymers** – Polymeric organic materials (plastics), manufactured by utilising one of the unique properties of carbon, its ability to form long chains of atoms.

II. **Homopolymers** – These are formed from a single type of monomer, for example ethene (CH_2CH_2) that forms polyethylene, typically via addition reactions involving unsaturated molecules, Figure 1.17.

III. **Heteropolymers** – Also known as *copolymers*, are formed from two (or more) different monomers. Condensation polymerisation is the usual process of formation with the elimination of a simple molecule such as ammonia or water.

IV. **Stereospecific polymers** – If constituent subunits are repeated along a polymer chain in a regular way, a stereospecific polymer may result. It may be that there is always a particular group along one side of the main chain, which would make the polymer *isotactic*, Figure 1.18a. Alternatively, the polymer is *syndiotactic*, the group alternates from side to side of the chain, Figure 1.18b.

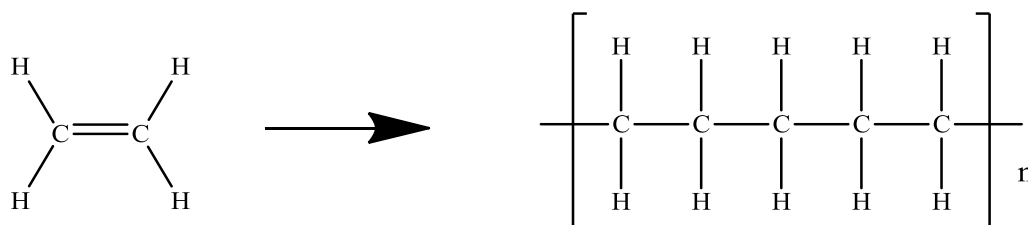


Figure 1.17. Addition polymerisation of ethene to form polyethylene, a homopolymer.

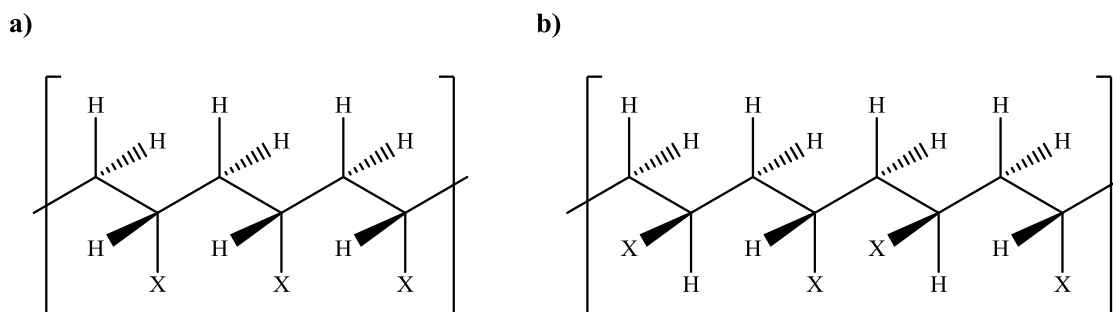


Figure 1.18. Types of stereospecific polymer, a) isotactic; b) syndiotactic.

A continuous network of adjacent unsaturated carbon atoms are found within conjugated polymers, *i.e.* carbon atoms in the sp^2 hybridised state. Each of these sp^2 C-atoms has three σ -bonds, and a p_z atomic orbital involved in π -overlap with the p_z -orbitals of the adjacent sp^2 hybridised C-atom. This chain of atoms with π -overlap of the p_z -orbitals causes the formation of a delocalised π -electron system along the polymer chain, Figure 1.19.¹³⁵ As a result of this conjugation a high density of states in both the highest occupied molecular orbital (HOMO) and lowest unoccupied molecular orbital (LUMO) energy levels is formed. One major feature of the delocalised π -electron system is the ease at which oxidation and reduction can occur. In addition to the covalent frame of the polymer backbone, Van der Waals forces are found between the strands of individual polymer chains.

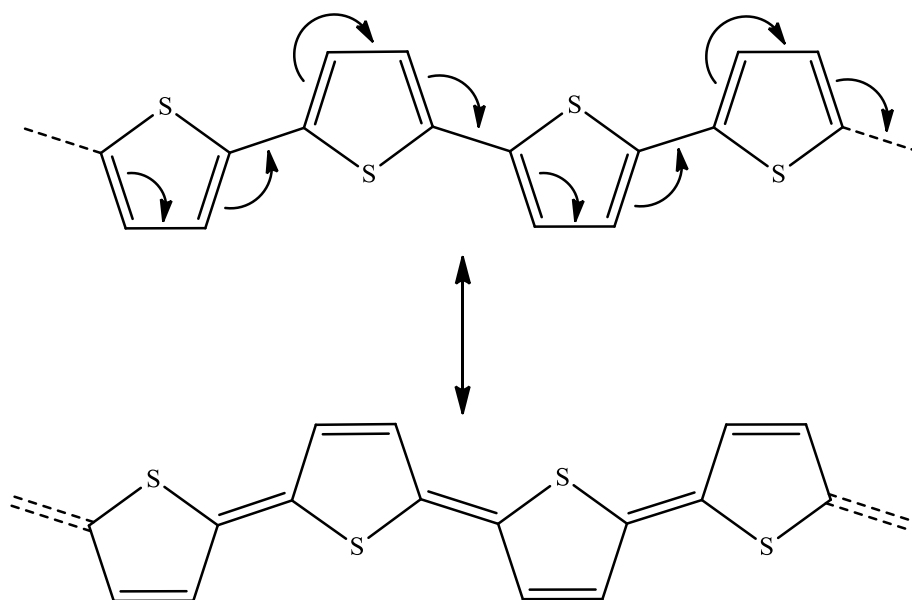


Figure 1.19. The structure of polythiophene demonstrating the change of geometry from benzenoid to quinoid via the delocalised π -electron system.

1.3.1. Electrochromism

There are many ways of achieving electrochromism; electrochemistry is just one example. *Electrochromism* is the phenomenon observed when a material changes colour through the application of a voltage, e.g.; the electrochemical switching between redox states. The colour change results from the generation of different visible region electronic absorption bands. Materials that exhibit these characteristics are known as *electrochromic* materials and there are many types including, but not limited to; transition metal oxides,¹³⁶⁻¹³⁹ Prussian blue,¹³⁹⁻¹⁴¹ viologens^{139,142-143} and conducting polymers.^{139,144-147} The electrochromic properties of conjugated polymers are of primary relevance to this thesis.

Conducting polymers undergo a doping process (oxidation) resulting in the formation of a *polaron*, a major charge carrier. During oxidation, ‘p-doping’, a counter anion is incorporated. Upon anion exit, or the incorporation of an electrolyte cation, the ‘p-doped’ conducting polymer is reduced and its electronic conjugation removed, giving the ‘undoped’ (neutral) form. A negatively charged polymer state is achieved by ‘doping’ the neutral form, through the insertion of a cation (‘n-doping’), balancing the injected charge. The addition of electrons, in excess, to any conjugated polymer chain leads to new electronic states within the otherwise forbidden electron energy gap, as portrayed in Figure 1.20.

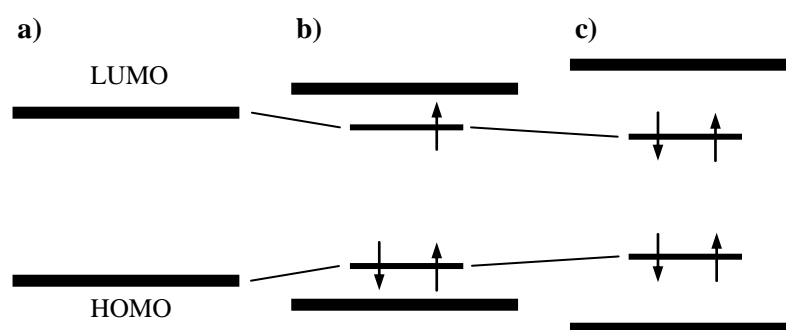


Figure 1.20. An energy level scheme of the self-localised states in conjugated polymers: a) band level of neutral polymer; b) polaron state formed upon the addition of an extra electron; and c) bipolaron state formed upon the addition of a second electron.¹⁴⁸

The energy gap between the HOMO (valence band) and the LUMO (conduction band) determines the optical properties of these materials.¹³⁹ Redox switching gives rise to optical absorption bands in addition to the transportation of electronic charge and

counter ions within the polymer matrix. The magnitude of the band gap of the undoped polymer determines the contrast of colour between the undoped and doped states.¹⁴⁹

1.3.2. Polyaniline

Polyaniline (PAni) is a heterochain polymer, it contains more than one atom type in its backbone and is classed as a carbon-nitrogen polymer; a polyamine. The formation of PAni is a condensation process; two hydrogens are lost from each monomer to form the polymer chain (Figure 1.21).¹⁴⁴ The electro-oxidation of aniline produces a polymer film that is electroactive where the oxidation reaction is chemically reversible.

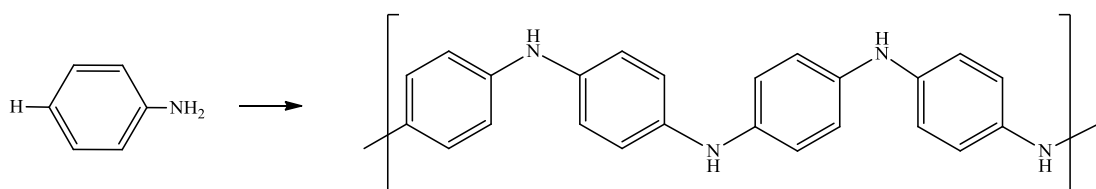


Figure 1.21. Condensation polymerisation of aniline to form leucoemeraldine.

PAni has a special electronic structure which possesses different redox states due to different electrical and chemical behaviour.¹⁵⁰ PAni is an electrochromic conducting polymer that can be found in one of the following oxidation states; leucoemeraldine (yellow/clear), emeraldine (green/blue), or pernigraniline (blue/violet) (Figure 1.22). However it is only the emeraldine salt that is electrically conductive, due to the partially filled conduction band, seen previously in Figure 1.20. Electrical charge is transported through the polymer by the presence of a conjugated π -electron system consisting of alternating single and double bonds along the polymer chain backbone.

When the polymer is doped with an electron donor or acceptor; an electron imbalance occurs resulting in the new electron population to move along the backbone when electric potential is applied.

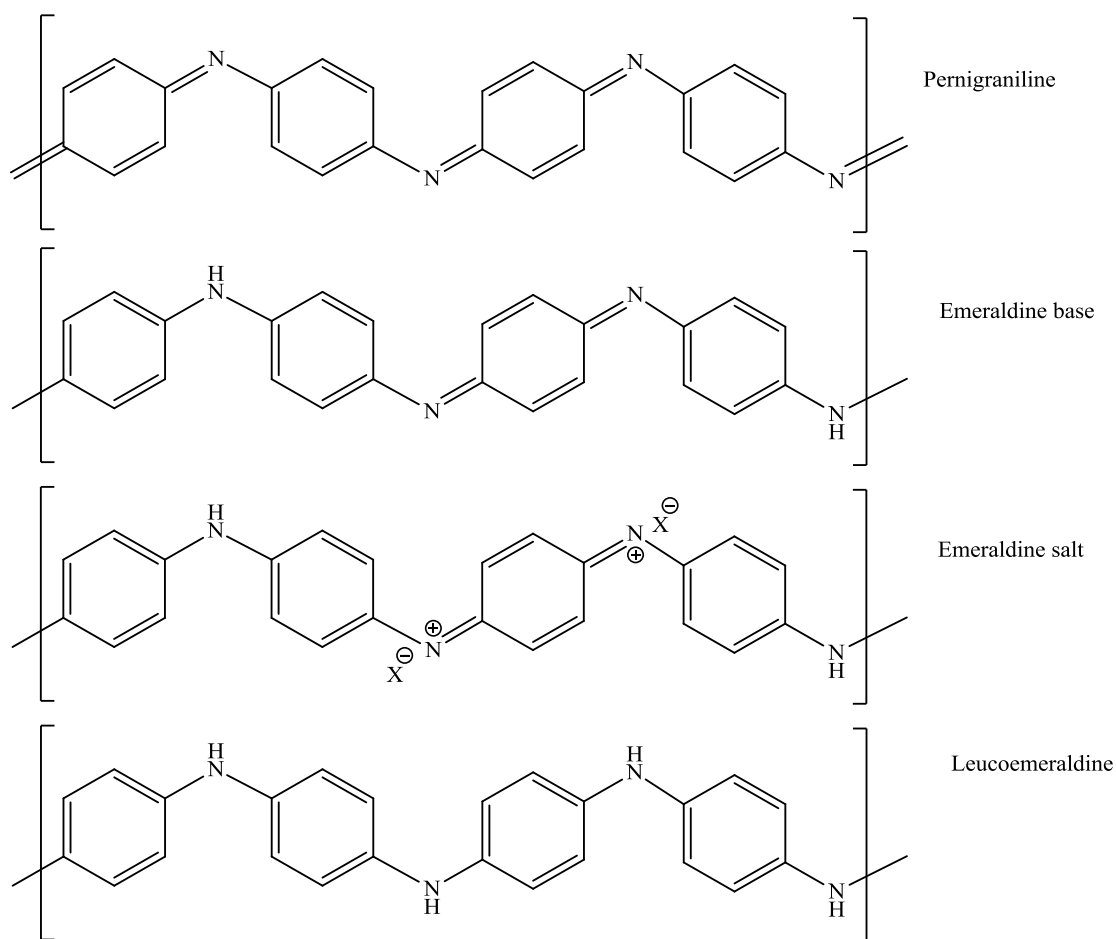


Figure 1.22. Polyaniline in its three oxidation states.

1.3.3. Poly-3,4-ethylenedioxythiophene

Poly-3,4-ethylenedioxythiophene (PEDOT) is a conjugated heteropolymer containing both carbon and sulphur. Similarly to PANi, polymerisation occurs via a condensation

mechanism whereby each monomer unit loses two hydrogens from the C-2 and C-5 positions on the thiophene ring as shown in Figure 1.23.

PEDOT, like PANi, is an electrically conducting electrochromic polymer. PEDOT possesses three oxidation states: when neutral (undoped) it is dark blue in colour and when oxidised (doped) a positive charge is, on average, shared over three monomer units giving a light blue colour. The final oxidation state is reduced (n-doped) which cannot be reached within the solvent window of an aqueous electrolyte.¹⁴⁴

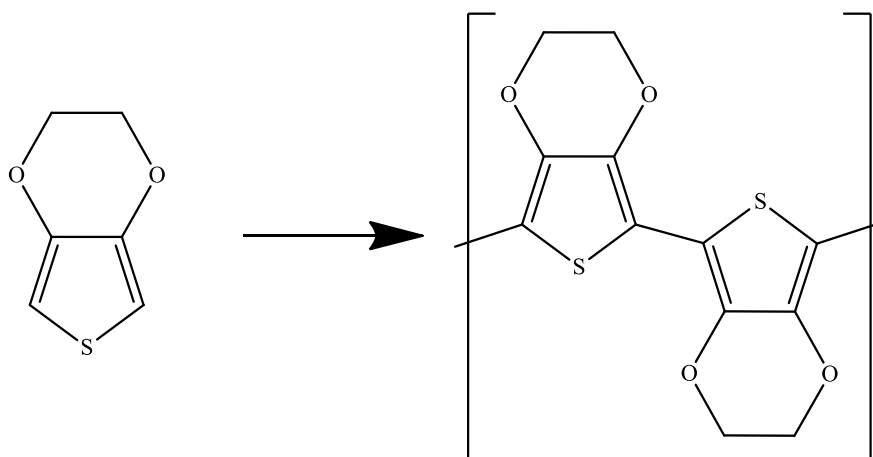


Figure 1.22. The condensation polymerisation of (ethylenedioxythiophene) EDOT to PEDOT.

1.4. Project Objectives

The visualization of latent fingerprints on metallic surfaces, such as spent ammunition cartridges, knives or tools, can offer significant forensic evidence. The value in recovering such items from the scene of a crime is considerable, particularly where it is

strongly believed that item was handled by the offender. Under these circumstances a link can be made between an individual and what could be an integral piece of evidence through the deposition of a fingerprint, potentially providing a link to the perpetrator of the crime. However, the visualization of latent fingerprints on metallic items specifically spent ammunition cartridges, where fingerprints have been previously deposited, is problematic.

The purpose of this work is to recover latent fingerprints from a selection of metallic surfaces, which have prospective forensic value, by the electropolymerisation of a polymer. The work aims to utilise fingerprint residues to 'protect' the metal surface from polymer deposits resulting in a negative image of the print. It is intended, where applicable, to exploit the electrochromic properties of the deposited polymer for the contrast between print and substrate to be optimised.

The goal is to assess the technical performance of polymer enhancement in diverse environments, in a comparison with existing enhancement techniques to identify individual strengths and weaknesses. The comparison is intended to address viable environments and conditions to which a print may be subject to prior to recovery and thus enhancement. As well as environment, the study should cover a range of fingerprint donors and ages of fingerprint deposits to consider the effects these might have on their subsequent enhancement.

The facility to visualise fingerprints from a range of metal surfaces is desirable. Therefore the aim of enhancing different types of prospective items using the polymer method is proposed. The ultimate objective is to apply the technology to more challenging surfaces via the progression from model surfaces to elemental metals to alloys to evidentially viable items.

1.5. References

1. P. C. White, *Crime Scene to Court the Essentials of Forensic Science*, 2004, **2**, The Royal Society of Chemistry, Cambridge, UK.
2. A. R. W. Jackson, J. M. Jackson, *Forensic Science*, 2004, Pearson Prentice House, Harlow, UK.
3. J. G. Barnes. *The Fingerprint Sourcebook*, 2011, ch. 1, U.S. Department of Justice, Office of Justice Programs, 810 Seventh Street N.W. Washington, DC 20531.
4. H. C. Lee, R. E. Gaensslen, *Advances in Fingerprint Technology*, 2001, **2**, CRC Press, London, UK.
5. Scottish Police Services Authority, http://www.spsa-forensics.police.uk/services/history_science/history_1788 (Accessed on 17th December 2012).
6. H. Faulds, *Dactylography or the study of Finger-prints*, ch. 5, **pg 61-75**, XXth Century Science Series.
7. F. Galton, *Nineteenth Century*, 1891, **30**, 303.
8. S. M. Stigler, *Genetics*, 1995, **140**, 857.
9. Henry Classification System, *International Biometric Group*, 2003, New York.
10. E. R. Henry, *Classification and Uses of Finger Prints*, 1900, George Routledge and Sons Ltd, London, UK.
11. Northumbria Police, Crime Scene Investigation, http://www.northumbria.police.uk/about_us/csinorthumbria/fngerprintbureau/tet-enprin/ (Accessed on 24th January 2013).

12. National Policing Improvement Agency,
<http://www.npia.police.uk/en/10504.htm> (Accessed on 14th January 2013).
13. Homeland Security, <http://www.homelandsecurity-technology.com/projects/ident1-automated-fingerprint-system-northrop-grumman-uk/> (Accessed 30th April 2013).
14. National Geographic News
http://news.nationalgeographic.com/news/2006/09/060922-fingerprints_2.html
(Accessed on 14th January 2013).
15. P. H. Warman, A. R. Ennos, *J. Exp. Biol.*, 2009, **212**, 2016.
16. R. D. Sr. Olsen, *Fingerprint and Identification Magazine*, 1972, **53**, 10.
17. A. Girod, R. Ramotowski, C. Weyermann, *Forensic Sci. Int.*, 2012, **223**, 10.
18. C. Ricci, S. G. Kararian, *Surf. Interface Anal.*, 2010, **42**, 386.
19. Nikon Rumours, <http://nikonrumors.com/2009/10/05/nikon-fabre-photo-exportable-stereoscopic-microscope-review.aspx/> (Accessed on 21st November 2012).
20. A. M. Knowles, *J. Phys. E. Sci. Instrum.*, 1978, **11**, 713.
21. H. C. Lee, R. E. Gaensslen, *Advances in Fingerprint Technology*, 2001, **2**, CRC Press, London, UK. Pg 63-104.
22. M. V. Buchanan, K. Asano, A. Bohanon, *P. Soc. Photo-Opt. Ins.*, 1996, **2941**, 89.
23. A. M. Bohanan, *J. Forensic Ident.*, 1998, **48**, 570.
24. C. Weyermann, O. Ribaux, *Sci. Justice*, 2012, **52**, 68.
25. R. S. Croxton, M. G. Baron, D. Butler, T. Kent, V. G. Sears, *Forensic Sci. Int.*, 2010, **199**, 93.
26. G. S. Sodhi, J. Kaur, *Forensic Sci. Int.*, 2001, **120**, 172.

27. M. J. Choi, T. Smoother, A. A. Martin, A. M. McDonagh, P. J. Maynard, C. Lennard, C. Roux, *Forensic Sci. Int.*, 2007, **173**, 154.
28. M. J. Choi, A. M. McDonagh, P. J. Maynard, R. Wuhrer, C. Lennard, C. J. Roux, *Forensic Ident.*, 2006, **56**, 756.
29. M. J. West, M. J. Went, *Spectrochim Acta. A-M.*, 2009, **71**, 1984.
30. R. K. Garg, H. Kumari, R. Kaur, *Egypt J. Forensic Sci.*, 2011, **1**, 53.
31. B. J. Jones, A. J. Reynolds, M. Richardson, V. G. Sears, *Sci. And Just.*, 2010, **50**, 150.
32. D. C. Wade, *J. Forensic Ident.*, 2002, **52**, 551.
33. J. Brozowski, *Probl. Forensic Sci.*, 2005, **64**, 333.
34. B. K. Cheshier, J. M. Stone, W. F. Rowe, *Forensic Sci. Int.*, 1992, **57**, 163.
35. P. Czekanski, M. Fasola, J. Allison, *J. Forensic Sci.*, 2006, **51**, 1323.
36. S. P. Wargacki, L. A. Lewis, M. D. Dadmun, *J. Forensic Sci.*, 2007, **52**, 1057.
37. S. P. Wargacki, L. A. Lewis, M. D. Dadmun, *J. Forensic Sci.*, 2008, **53**, 1138.
38. M. Paine, H. L. Bandey, S. M. Bleay, H. Wilson, *Forensic Sci. Int.*, 2011, **212**, 130.
39. D. Algaier, D. Baskaran, M. Dadmun, *React. Funct. Polym.*, 2011, **71**, 809.
40. B. J. Jones, R. Downham, V. G. Sears, *J. Forensic Sci.*, 2012, **57**, 196.
41. H. Scott, *J. Forensic Sci. Soc.*, 1963, **4**, 60.
42. K. E. Creer, *Forensic Sci. Int.*, 1983, **23**, 149.
43. R. H. Hooker, K. E. Creer, J. S. Brennan, *Forensic Sci. Int.*, 1991, **51**, 297.
44. E. M. Robinson, G. B. Richards, *Crime Scene Photography*, 2nd edn., 2010, 367-397.
45. D. Sapse, N. D. K. Petraco, *J. Mol. Model.*, 2007, **13**, 943.
46. C. Conn, G. Ramsay, C. Roux, C. Lennard, *Forensic Sci. Int.*, 2001, **116**, 117.

47. J. Almog, A. Klein, I. Davidi, Y. Cohen, M. Azoury, M. Levin-Elad, *J. Forensic Sci.*, 2008, **53**, 364.
48. S. Berdejo, M. Rowe, J. W. Bond, *J. Forensic Sci.*, 2012, **57**, 509.
49. N. Porpiglia, S. Bleay, L. Fitzgerald, L. Barron, *Sci. And Just.*, 2012, **52**, 42.
50. Q. Chen, W. T. Kerk, A. M. Soutar, X. T. Zeng, *Appl. Clay Sci.*, 2009, **44**, 156.
51. G. C. Goode, J. R. Morris, *Latent fingerprints: A review of their origin, composition and methods for detection*, 1983, Atomic Weapons Research Establishment, Aldermaston.
52. G. S. Sodhi, J. Kaur, *Defence Sci. J.*, 2000, **50**, 213.
53. M. J. Choi, K. E. McBean, P. H. R. Ng, A. M. McDonagh, P. J. Maynard, C. Lennard, C. Roux, *J. Mater. Sci.*, 2008, **43**, 732.
54. L. Liu, S. K. Gill, Y. Gao, L. J. Hope-Weeks, K. H. Cheng, *Forensic Sci. Int.*, 2008, **176**, 163.
55. M. Algarra, J. Jiménez-Jiménez, R. Moreno-Tost, B. B. Campos, J. C. G. Esteves da Silva, *Opt. Mater.*, 2011, **33**, 893.
56. H.L. MacDonell, *Ident. News*, 1961, **11**, 7.
57. B. Wilshire, *Endeavour*, 1996, **208**, 12.
58. J. D. James, C. A. Pounds, N. Phil, B. Wilshire, *J. Forensic Sci.*, 1991, **36**, 1368.
59. J. D. James, C. A. Pounds, B. Wilshire, *Powder Metall.*, 1991, **34**, 39.
60. J. D. James, C. A. Pounds, B. Wilshire, *J. Forensic Sci.*, 1993, **38**, 391.
61. L. K. Seah, U. S. Dinish, W. F. Phang, Z. X. Chao, V. M. Murukeshan, *Forensic Sci. Int.*, 2005, **152**, 249.
62. G. Polimeni, B. F. Foti, L. Saravo, G. De Fulvio, *Forensic Sci. Int.*, 2004, **1465**, S45.

63. P. Cucè, G. Polimeni, A. P. Lazzaro, G. De Fulvio, *Forensic Sci. Int.*, 2004, **1465**, S7.
64. A. J. Reynolds, B. J. Jones, V. Sears, V. Bowman, *J. Phys. Conf. Ser.*, 2008, **126**, 012069.
65. F. Haque, A. D. Westland, J. Milligan, F. M. Kerr, *Forensic Sci. Int.*, 1989, **41**, 73.
66. B. J. Jones, R. Downham, V. G. Sears, *Surf. Interface Anal.*, 2010, **42**, 438.
67. O. P. Jasuja, G. D. Singh, G. S. Sodhi, *Sci. And Just.*, 2008, **48**, 141.
68. G. S. Sodhi, J. Kaur, *Egypt. J. Forensic Sci.*, 2012, **2**, 45.
69. M. Trapecar, *Sci. And Just.*, 2009, **49**, 292.
70. M. J. West, M. J. Went, *Forensic Sci. Int.*, 2008, **174**, 1.
71. F. Rowell, K. Hudson, J. Seviou, *Analyst*, 2009, **134**, 701.
72. F. Rowell, J. Seviour, A. Y. Lim, C. G. Elumbaring-Salazar, J. Loke, J. Ma, *Forensic Sci. Int.*, 2012, **221**, 84.
73. C. Champod, C. Lennard, P. Margot, M. Stoilovic, *Fingerprints and Other Ridge Skin Impressions*, 2004, CRC Press, Boca Raton, FL.
74. O. P. Jasuja, G. Singh, *Forensic Sci. Int.*, 2009, **192**, e11.
75. J. Almog, Y. Sasson, A. Anati, *J. Forensic Sci.*, 1979, **24**, 431.
76. R. B. Michael, *Chesapeake Examiner*, 2008, **46**, 5.
77. F. Haque, A. Westland, F. M. Kerr, *Forensic Sci. Int.*, 1983, **21**, 79.
78. K. Flynn, P. Maynard, E. Du Pasquier, C. Lennard, M. Stoilovic, C. Roux, *J. Forensic Sci.*, 2004, **49**, 1.
79. O. P. Jasuja, A. Kaur, P. Kumar, *Forensic Sci. Int.*, 2012, **223**, e47.
80. M. A. Feldman, C. E. Meloan, J. L. Lambert, *J. Forensic Sci.*, 1982, **27**, 806.
81. L. Liu, Z. Zhang, L. Zhang, Y. Zhai, *Forensic Sci. Int.*, 2009, **183**, 45.

82. S. Morimoto, A. Kaminogo, T. Hirano, *Forensic Sci. Int.*, 1998, **97**, 101.
83. A. Zamir, E. Springer, B. Glattstein, *J. Forensic Sci.*, 2000, **45**, 687.
84. E. R. Menzel, M. Takatsu, R. H. Murdock, K. Bouldin, K. H. Cheng, *J. Forensic Sci.*, 2000, **45**, 770.
85. C. A. Steele, M. S. Ball, *J. Forensic Sci.*, 2003, **48**, 1314.
86. M. Takatsu, O. Shimoda, H. Teranishi, *J. Forensic Sci.*, 2012, **57**, 515.
87. V. Bowman editor, *Manual of fingerprint development techniques*, 2nd edn. Sandridge, UK: Police Scientific Development Branch, Home Office 2004.
88. C. J. Lennard, P. A. Margot, M. Stoilovic, R. N. Warrenner, *J. Forensic Sci. Soc.*, 1988, **28**, 3.
89. J. Almog, V. G. Sears, E. Springer, D. F. Hewlett, S. Walker, S. Wiesner, R. Lidor, E. Bahar, *J. Forensic Sci.*, 2000, **45**, 538.
90. D. B. Hansen, M. M. Joullié, *Chem. Soc. Rev.*, 2005, **34**, 408.
91. D. E. Bicknell, R. S. Ramotowski, *J. Forensic Sci.*, 2008, **53**, 1108.
92. L. C. A. M. Bossers, C. Roux, M. Bell, A. M. McDonagh, *Forensic Sci. Int.*, 2011, **210**, 1.
93. N. Praska, G. Langenburg, *Forensic Sci. Int.*, 2013, **224**, 51.
94. S. J. Cadd, S. M. Bleay, V. G. Sears, *Sci. And Just.*, Available online December 2012.
95. A. Castello, M. Alvarez, F. Verdu, *Color Technol.*, 2002, **118**, 316.
96. E. Navarro, A. Castello, J. A. Lopez-Alfaro, F. Verdu, *J. Forensic Legal Med.*, 2007, **14**, 340.
97. N. J. Crane, E. G. Bartick, R. Schwartz Perlman, S. Hoffman, *J. Forensic Sci.*, 2007, **52**, 48.

98. M. Tahtouh, P. Despland, R. Shimmon, J. R. Kalman, B. J. Reedy, *J. Forensic Sci.*, 2007, **52**, 1089.
99. A. Hemmila, J. McGill, D. Ritter, *J. Forensic Sci.*, 2008, **53**, 369.
100. C. G. Worley, S. S. Wiltshire, T. C. Miller, G. J. Havrilla, V. Majidi. *J. Forensic Sci.*, 2006, **51**, 57.
101. M. I. Szyrkowska, K. Czernski, J. Rogowski, T. Paryjczak, A. Parczewski, *Forensic Sci. Int.*, 2009, **184**, e24.
102. M. J. Bailey, N. J. Bright, R. C. Croxton, S. Francese, L. S. Ferguson, S. Hinder, S. Jickells, B. J. Jones, B. N. Jones, S. G. Kazarian, J. J. Ojeda, R. P. Webb, R. Wolstenholme, S. Bleay, *Anal. Chem.*, 2012, **84**, 8514.
103. R. Bradshaw, R. Wolstenholme, L. S. Ferguson, C. Sammon, K. Mader, E. Claude, R. D. Blackledge, M. R. Clench, S. Francese, *Analyst*, 2013, **138**, 2546.
104. N. J. Bright, T. R. Wilson, D. J. Driscoll, S. M. Reddy, R. P. Webb, S. Bleay, N. I. Ward, K. J. Kirkby, M. J. Bailey, *Forensic Sci. Int.*, 2013, <http://dx.doi.org/10.1016/j.forsciint.2013.03.047>.
105. E. R. Menzel, S. M. Savoy, S. J. Ulvick, K. H. Cheng, R. H. Murdock, M. R. Sudduth, *J. Forensic Sci.*, 2000, **45**, 545.
106. K. K. Bouldin, E. R. Menzel, M. Takatsu, R. H. Murdock, *J. Forensic Sci.*, 2000, **45**, 1239.
107. E. R. Menzel, J. R. Schwierking, L. W. Menzel, *J. Forensic Ident.*, 2005, **55**, 189.
108. M. Bruchez Jr., M. Moronne, P. Gin, S. Weiss, A. P. Alivisatos, *Science*, 1998, **281**, 2013.
109. E. R. Menzel, M. Taskatsu, M. R. Murdock, K. Bouldin, K. H. Cheng, *J. Forensic Sci.*, 2000, **45**, 770.

110. P. Hazarika, S. M. Jickells, K. Wolff, D. A. Russell, *Angew. Chem. Int. Ed.*, 2008, **47**, 10167.
111. P. Hazarika, S. M. Jickells, Russell DA. *Analyst*, 134, 2009, 93-96.
112. R. Leggett, E. E. Lee-Smith, S. M. Jickells, D. A. Russell, *Angew. Chem. Int. Ed.*, 2007, **46**, 4100.
113. N. Panchuk-Voloshina, R. P. Haugland, J. Bishop-Stewart, M. K. Bhalgat, P. J. Millard, F. Mao, W. Leung, R. P. Haugland, *J. Histochem. Cytochem.*, 1999, **47**, 1179.
114. S. M. Bleay, P. F. Kelly, R. S. P. King, *J. Mater. Chem.*, 2010, **20**, 10100.
115. J. W. Bond, *J. Forensic Sci.*, 2008, **53**, 812.
116. G. Williams, N. McMurray, Latent, *Forensic Sci. Int.*, 2007, **167**, 102.
117. G. Williams, H. N. McMurray, D. A. Worsley, *J. Forensic Sci.*, 2001, **46**, 1085.
118. G. Williams, *Fingerprint Whorld*, 2010, **36**, 51.
119. A. A. Cantu, D. A. Leben, R. Ramotowski, J. Kopera, J. R. Simms, *J. Forensic Sci.*, 1998, **43**, 294.
120. B. W. Given, *J. Forensic Sci.*, 1976, **21**, 587.
121. Y. Migron, G. Hocherman, E. Springer, J. Almog, D. Mandler, *J. Forensic Sci.*, 1998, **43**, 543.
122. M. Nonnenmacher, M. P. Oboyle, H. K. Wickramasinghe, *Appl. Phys. Lett.*, 1991, **58**, 2921.
123. J. Daintith editor, *Oxford dictionary of chemistry*, 4th edn., 2000, Oxford University Press, Oxford, UK.
124. P. Atkins, J. de Paula, *Elements of Physical Chemistry*, 4th edn., 2005, Oxford University Press Inc., New York, USA.

125. J. W. Bond, *J. Forensic Sci.*, 2011, **56**, 999.
126. J. W. Bond, *Physica B*, 2011, **406**, 1582.
127. J. W. Bond, *J. Phys. D. Appl. Phys.*, 2009, **42**, 235301.
128. P. F. Kelly, R. S. P. King, R. J. Mortimer, *Chem. Commun.*, 2008, 6111.
129. Y. Migron, D. Mandler, *J. Forensic Sci.*, 1997, **42**, 986.
130. C. Bersellini, L. Garofano, M. Giannetto, F. Lusardi, G. Mori, *J. Forensic Sci.*, 2001, **46**, 871.
131. A. L. Beresford, A.R. Hillman, *Anal. Chem.*, 2010, **82**, 483.
132. A. L. Beresford, R. M. Brown, A. R. Hillman, J. W. Bond, *J. Forensic Sci.*, 2012, **57**, 93.
133. R. M. Brown, A. R. Hillman, *Phys. Chem. Chem. Phys.*, 2012, **14**, 8653.
134. L. Xu, Y. Li, S. Wu, X. Liu, B. Su, *Ange. Chem. Int. Ed.*, 2012, **51**, 8068.
135. W. R. Salaneck, R. H. Friend, J. L. Brédas, *Phys. Rep.*, 1999, **319**, 231.
136. S. K. Deb, *Sol. Energ. Mat. Sol. C.*, 1992, **25**, 327.
137. H. Gomathi, M. Jayalakshmi, J. Joseph, R. Vittal, *B. Electrochem.*, 2003, **19**, 9.
138. K. A. Gesheva, T. M. Ivanova, G. Bodurov, *Prog. Org. Coat.*, 2012, **74**, 635.
139. R. J. Mortimer, *Chem. Soc. Rev.*, 1997, **26**, 147.
140. S. Demiri, M. Najdoski, J. Velevska, *Mater. Res. Bull.*, 2011, **46**, 2484.
141. M. Ishizaki, K. Kanaizuka, M. Abe, Y. Hoshi, M. Sakamoto, T. Kawamoto, H. Tanaka, M. Kurihara, *Green Chem.*, 2012, **5**, 1537.
142. R. J. Mortimer, T. S. Varley, *Chem. Mater.*, 2011, **23**, 4077.
143. G. Bar, N. Larina, L. Grinis, V. Lokshin, R. Gvishi, I. Kiryushev, A. Zaban, V. Khodorkovsky, *Sol. Energ. Mater. Sol. C.*, 2012, **99**, 123.

144. T. A. Skotheim, *Handbook of Conducting Polymers*, Marcel Dekker, Inc., New York, 1986, **1**.
145. J. Padilla, T. F. Otero, *Bioinspir.Biomim.*, 2008, **3**, 035006.
146. F. Carpi, D. De Rossi, *Opt. Laser. Technol.*, 2006, **38**, 292.
147. S. Xiong, F. Yang, G. Ding, K. Y. Mya, J. Ma, X. Lu, *Electrochim. Acta.*, 2012, **67**, 194.
148. W. R. Salaneck, R. H. Friend, J. L. Brédas, *Phys. Rep.*, 1999, **319**, 231.
149. R. J. Mortimer, A. L. Dyer, J. R. Reynolds, *Displays*, 2006, **27**, 2.
150. G. Ballum, G. Harsányi, 2003, 26th International Spring Seminar on Electronics Technology, Slovak Republic.

Chapter Two

2. Principles of Methodology

2.1. Overview

In this chapter the basic principles behind the methods used during this study are discussed. The following chapter, Chapter 3, describes the experiments carried out using the following techniques.

2.2. Potentiostats

A *potentiostat* is a device that maintains the potential of a *working electrode* at a constant level relative to a *reference electrode*.¹ The cell voltage is the sum of several potential differences which can be affected to different degrees when a current flows through the cell. In order for practically all the change in potential to be observed at the *working electrode* a highly reversible *counter electrode* or one which is much larger than the *working electrode* must be used.²

Changes in potential at the *working electrode* are controlled versus a *reference electrode*, such as a saturated calomel electrode (SCE) or silver/silver chloride electrode ($\text{Ag}|\text{AgCl}$)³, in a three electrode measurement, Figure 2.1. The third electrode is the *counter electrode* whose purpose is to complete the circuit with the electrolyte in order to apply a potential to the *working electrode*. The *reference electrode* carries practically no current which means the current will flow through the circuit between the *working* and the *counter electrodes*, while the potential is controlled in a second circuit with the *reference* and *working electrode*. The potential at the *counter electrode* can change substantially however this still has no influence over that of the *working*

electrode with respect to the *reference electrode*. This would work the same way if the current was being controlled and potential was being measured between the *working* and *counter electrodes*. Figure 2.2 shows an equivalent circuit where Z_1 is the cell resistance between the *counter electrode* and the *reference electrode*; Z_2 is the cell resistance between the *reference electrode* and the *working electrode*.

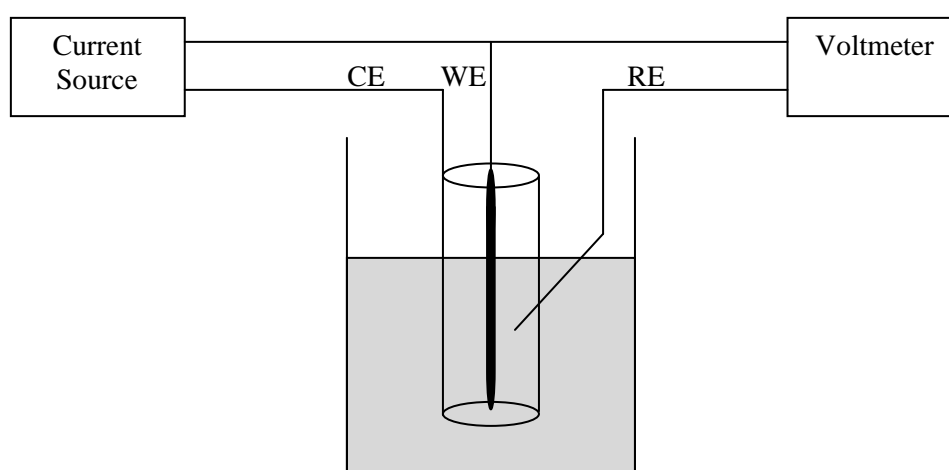


Figure 2.1. Schematic representation of a one compartment three-electrode cell, the *working electrode* (WE) is connected to a *reference electrode* (RE) through a high-input-resistance voltmeter and is connected to the *counter electrode* (CE) through a low-input-resistance current source.²

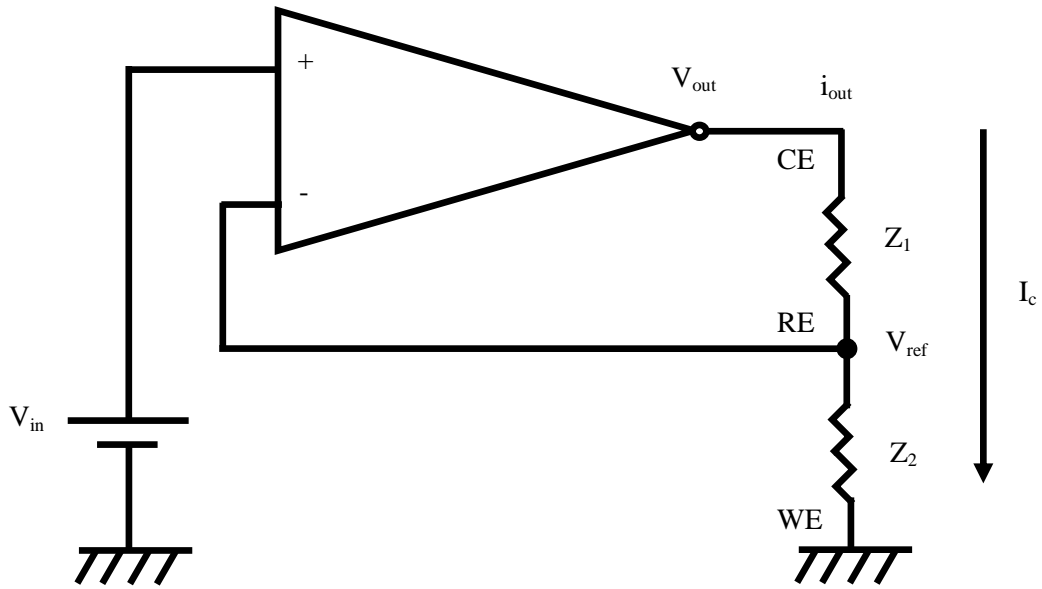


Figure 2.2. Equivalent circuit of the one compartment three electrode cell circuit.⁴

The potentiostat works to keep V_{in} and V_{out} equal and that the cell current I_c is supplied by an operational amplifier to maintain this requirement,¹ see Equation 2.1.

$$V_{out} = V_{in} = V_{ref} + I_c Z_2 = V_{ref} + E_c \quad (2.1)$$

where E_c is the cathode potential, equal to the potential difference between the *reference electrode* and the *working electrode*. V_{in} and V_{ref} are constants therefore $I_c Z_2$ must also be constant. If Z_1 or Z_2 changes during a measurement the amplifier output voltage changes to maintain

$$E_c = I_c Z_2 \quad (2.2)$$

is at a constant level. If Z_2 increases due to an increase in cell resistance the output voltage of the potentiostat decreases leading to a decrease in I_c . Likewise if Z_2 decreases, the output voltage increases correspondingly to maintain a constant E_c .¹

A drop in the potential, known as the residual potential drop, can be observed between the *working* and *counter electrodes* which is caused by the distance between the two electrodes. In an attempt to compensate for the drop in residual potential, the best geometry would be to have spherical electrodes (the *working electrode* located in the centre of a spherical *counter electrode*); to reduce the resistance in solution and the potential drop would be decreased. When this is not an option (most cases) a cylindrical geometry is adopted where the *counter electrode* surrounds the *working electrode*, similar to Figure 2.1. The worst results are achieved when the geometry is planar.

2.2.1. Chronoamperometry

Chronoamperometry is a potentiostatic method in which the potential between the *working* and the *reference electrodes* is compared to a value determined externally, the difference is amplified and a current is passed between the *working* and *counter electrodes*, of such magnitude and sign as to reduce the difference to a very small value typically 1 mV or less.⁵ The maintenance of potential of the *working electrode*, at which the analytical reaction occurs, is at a constant level such that quantitative oxidation/reduction of the analyte occurs without involvement of the less active species in the sample or solution.⁶ The current is initially high but decreases rapidly and approaches zero as the analyte is removed from solution in the vicinity of the electrode, Figure 2.3.

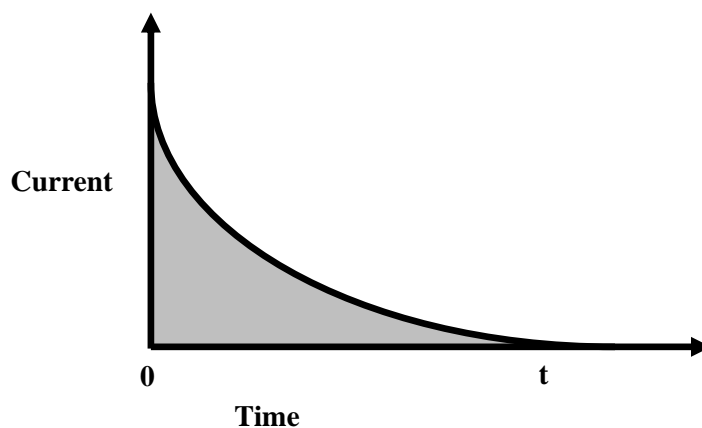


Figure 2.3. For a current that varies with time, the quantity of charge Q in a time t is equal to the shaded area under the curve, obtained by integration of the current-time curve, Equation 2.3.⁶

$$Q = \int_0^t i dt \quad (2.3)$$

Generally potentiostats are automated and equipped with a computer or an electronic current integrator that gives the charge, in coulombs, necessary to complete the reaction as shown in Figure 2.3.

When an experiment is conducted potentiostatically both the active dissolution region and passive region are observed. The potential of an electrode with respect to a *reference electrode* represents its oxidising or reducing power. It is possible to determine the course of an electro-organic synthesis to produce one desired product or another by careful choice of potential.⁵

2.2.2. Cyclic Voltammetry

Cyclic voltammetry (CV) is an electroanalytical technique used to study the electroactivity of species in electrochemistry,⁷⁻⁸ inorganic chemistry,⁹⁻¹⁰ organic chemistry¹¹⁻¹² and biochemistry.¹³⁻¹⁴ CV uses a three electrode cell (Figure 2.1) with a supporting electrolyte to suppress migration of charged reactants or products. A triangular waveform is imposed as the potential on the *working electrode*, Figure 2.4, with simultaneous measurement of the current.¹⁵ After crossing the potential region in which an electrode reaction takes place, the direction of the potential is reversed. Often during the reverse scan it is possible to detect the electrode reactions of the intermediates and products formed by the forward scan.⁷ Depending on the nature of the experiment one full cycle, a partial cycle, or several cycles can be used to gain the necessary result.¹⁶

By measuring the current at the *working electrode* during a potential scan a voltammogram can be obtained, displaying current versus potential, see Figures 2.5 and 2.6. Potential varies linearly with time so in theory the horizontal axis could also be thought of as the time axis. As the scan rate is controlled the time scale for the process can be calculated and then used to interpret the data further.

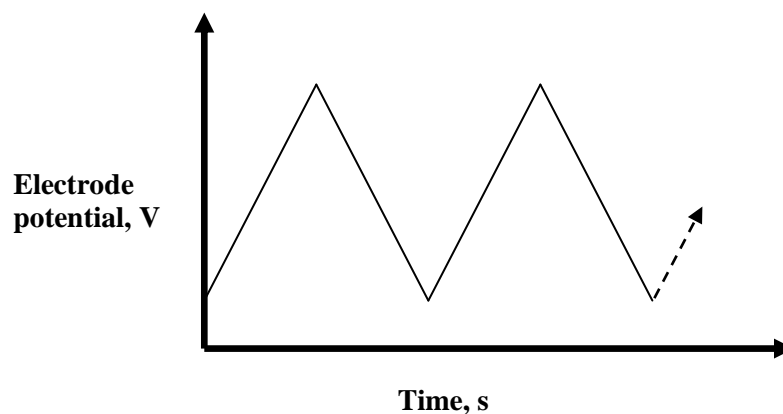


Figure 2.4. Potential-time behaviour at the *working electrode* typical of cyclic voltammetry.¹⁵

The voltammetric response for two solution species can be found in Figure 2.5. For a solution species with reversible electrochemistry (Figure 2.5a)

$$\Delta E_p = E_{p,c} - E_{p,a} \quad (2.4)$$

$$i_{p,a}/i_{p,c} = 1 \quad (2.5)$$

where the peak potential E_p is independent of the scan rate v , $E_{p,c}$ is the peak cathodic potential and $E_{p,a}$ is the peak anodic potential. The peak current i_p is proportional to $v^{1/2}$, where $i_{p,a}$ is the peak anodic current and $i_{p,c}$ is the peak cathodic current.

For a solution species with irreversible electrochemistry, Figure 2.5b, peak height is governed by diffusion and wave shape is controlled by kinetics.¹⁶ Electron transfer is much slower; therefore a greater driving force is required for a given current i . *Hysteresis*, the separating of peaks, is observed with increasing scan rate.

For a surface immobilised species, Figure 2.6, no transport is involved. The system is reversible where

$$\Delta E_p = 0 \quad (2.6)$$

with Equation 2.5 also being applicable. However the peak current i_p is proportional to scan rate v , and

$$\int i = Q = \Gamma/nFA \quad (2.7)$$

where Q (C) is charge, n is the number of electrons lost per molecule of the depositing species, A (cm²) is the deposition area, F is Faraday's constant and Γ (mol cm⁻²) is the number of moles in the deposit, referred to as *coverage*.

The potentials at which reversal of voltage takes place are called *switching potentials*. Switching potentials are specifically chosen for the intended experiment to observe a controlled oxidation and reduction of one or more species.¹⁷ The initial scan can either be in the negative or positive direction. A scan in the direction of more negative potentials is referred to as the *forward scan* and one in the direction of more positive potentials is deemed the *reverse scan*.

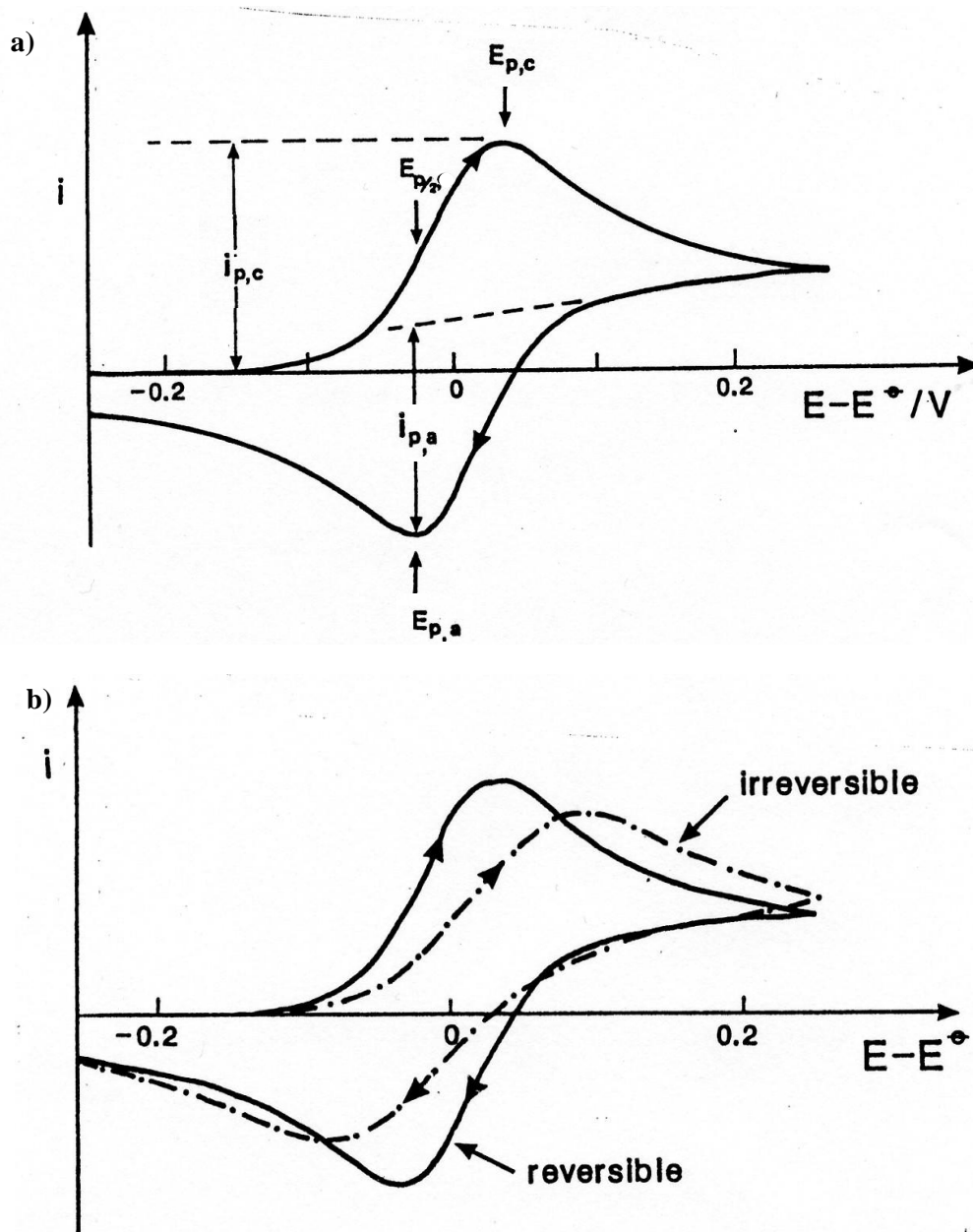


Figure 2.5. Voltammogram examples of; a) a solution species with reversible electrochemistry; b) solution species with irreversible electrochemistry compared to one with reversible electrochemistry.¹⁶

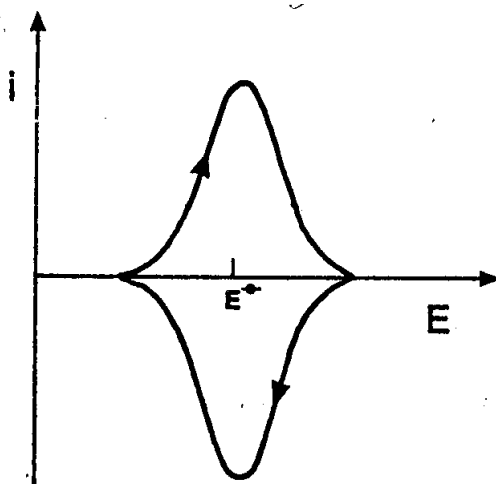


Figure 2.6. An example of a voltammogram for a surface immobilised species.

A rise in the current observed indicates the oxidation of a species. A current response of zero, within a potential range, is due to the absence of any oxidizable or reducible species. When the current is found to drop this can be attributed to the reduction of a species.

2.3. Visualisation

2.3.1. Digital Photography

Digital images can be captured by several different means, such as cameras, videos and scanners. Digital photography is acquired through the use of a digital camera. When the camera is on and the shutter button is pressed, the aperture opens allowing light to pass through the lens and strike the light-sensitive sensor.¹⁸ There are a range of electronic sensors found in digital cameras; however they all serve the same purpose, to record the photographic image as a series of pixels. The more pixels a sensor has, the more information that can be captured, resulting in well defined detail and high clarity

images.¹⁸ The image is then stored in a format that can be later opened and viewed in appropriate computer software. The most common format is the JPEG.

When capturing the image there are several options; including resolution, zoom and focus to be considered. When the subject is small and delicate a close-up image may be required. However, using the zoom function can lead to loss in resolution.¹⁸ Therefore digital cameras often have the option of photographing in ‘macro’ or ‘super-macro’ mode, which allows the camera to be closer to the subject for a high resolution image to be captured. The slightest shake of the camera can be amplified by the extreme closeness to the subject, therefore attaching the camera to a tripod can help to stabilise the shot giving a sharper image.¹⁸ ‘Autofocus’ allows the most important element of the image to be locked into focus. Once the image is captured the focus will not shift allowing for additional images to be taken if necessary.

2.3.2. Optical Microscopy

Optical microscopy is used to view samples on a larger scale than possible with the naked eye. An optical trinocular (three eyepieces) microscope uses reflected visible light to illuminate the sample.¹⁹ Two of the eyepieces are used to view the sample directly. However, a digital camera or video camera can be attached to the third eyepiece to allow for the enlarged images to be recorded and viewed on a computer system.²⁰⁻²¹

2.3.3. Scanning Electron Microscopy

The resolution of optical microscopy is limited by diffraction effects to about the wavelength of light. Considerably higher resolution surface information can be obtained, but not limited to, using *Scanning Electron Microscopy* (SEM). An image is obtained by sweeping the solid surface in a *raster pattern* with a finely focused beam of electrons or suitable probe. A *raster pattern* is a scanning pattern in which the electron beam is first swept across the surface in a straight line (x direction), then returned to its starting position, and shifted downward (y direction) by a standard increment.²¹ The process is repeated until the desired area of the surface has been scanned. During this process several types of signals are produced, including backscattered, secondary, and Auger electrons; X-ray fluorescence, and various energies of other photons. A suitable detector is used to receive the signals, above the surface (z direction), during the scanning process. The information is stored on a connected computer system and converted using a transducer into an image. The most common signals used for surface studies, as the basis of SEM, are backscattered and secondary electrons.

Figure 2.7 shows a schematic of an SEM, depicting an electron gun source, electron focusing system and electron detector. The electron focusing system is made up of a magnetic condenser lens and magnetic objective lens. Their purpose is to reduce the final spot size on the sample to be imaged, typically between 5 – 200 nm. The condenser lens is responsible for the throughput of the electron beam reaching the objective lens. The objective lens is responsible for the size of the electron beam focused on the sample surface. Located within the objective lens are two pairs of electromagnetic coils. One pair deflects the beam across the sample in the x direction,

and the other pair deflects the beam in the y direction. Varying the electrical signal to the pairs of coils allows the sample to be scanned as a function of time. The signals that drive the electron beam in the x and y directions also drive the horizontal and vertical scans of a cathode-ray tube (CRT). An image is produced through the output of a detector to control the intensity of the spot on the CRT. Through a one-to-one correlation between the signal produced at a particular location on the sample and a corresponding point on the CRT, a map of the sample is constructed.

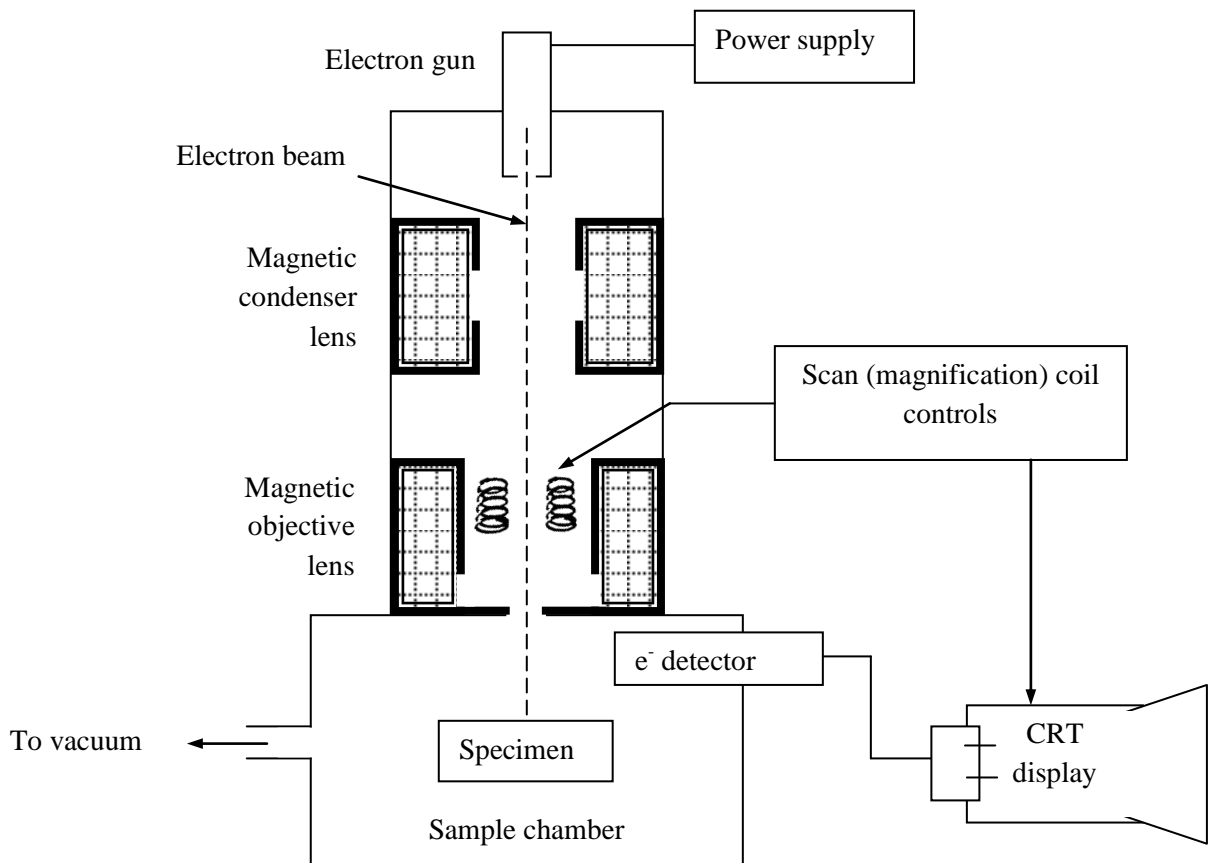


Figure 2.7. Schematic of an SEM.²¹

The sample chamber is fitted with a large-capacity vacuum pump to accelerate the switch from ambient pressure to 10^{-4} Torr or less. The sample stage can be moved in the x , y , and z directions as well as rotated about each axis, allowing the sample to be viewed from almost any perspective.

Samples that are both conductors of electricity and heat are the easiest to study. This is due to the unhindered flow of electrons, thus a build up of charge and the likelihood of thermal degradation are minimised.

2.4. Characterisation

2.4.1. Raman Spectroscopy

A powerful laser source, of visible or near infrared monochromatic radiation, is used to radiate a sample to acquire Raman spectra. The scattered radiation is measured at an angle, often at 90° . A Raman spectrum depicts the wavenumber shift ($\Delta\tilde{\nu}$) which is defined as the difference in wavenumbers (cm^{-1}) between the observed radiation and that of the source.²²

There are three components that Raman spectroscopy consists of; a laser source, a sample illumination system and a suitable spectrometer. An example of a Raman spectrometer can be found in Figure 2.8.

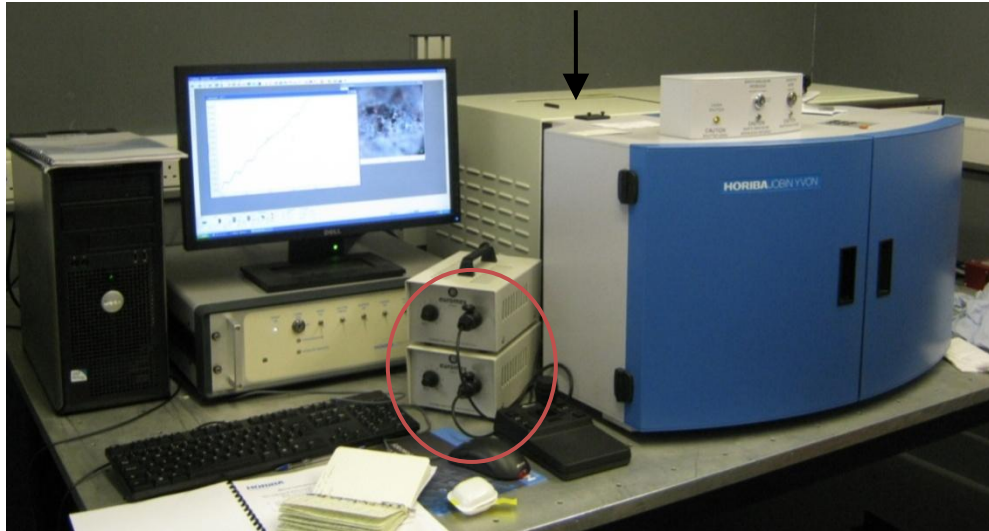


Figure 2.8. Photograph of a Horiba Jobin Yvon, LabRAM HR Raman spectrometer connected to a computer system. An optical microscope is situated within the sample chamber (behind blue doors), with a fiber-optic light source, controlled externally (circled in red), to aid with spectral analysis and visualisation of the test substrate. The laser source is situated in the container behind the sample chamber (see arrow).

When an electric field of the radiation interacts with an electron cloud of a bond within the sample, a dipole moment is induced. The deformability of the bond in an electric field is a constant measure known as *polarizability*.²² For a bond to be Raman active its polarizability must vary as a function of the distance between nuclei.

2.5. Profilometry

Profilometry is a relatively simple technique that maps the topography of a sample's surface through the use of a stylus. The sensitive probe is moved across the surface in one direction for a set distance and is most commonly used to measure surface texture and step heights of coatings.²³ Figure 2.9 shows an example of a profilometer.



Figure 2.9. Photograph of a Silver Surtronic 3+ profilometer, stylus is circled in black.

2.6. References

1. D. A. Skoog, F. J. Holler, T. A. Nieman, *Principles of Instrumental Analysis*, 5th edn., 1998, **pg 628-631**, Thomson Learning, USA.
2. E. Gileadi *Physical Electrochemistry*, 2011, **pg 17-27**, Wiley-VCH, Weinheim, Germany.
3. P. T. Kissinger, W. R. Heineman, *J. Chem. Educ.*, 1983, **60**, 702.
4. R. G. Kelly, J. R. Scully, D. W. Shoesmith, R. G. Buchheit, *Electrochemical Techniques in Corrosion Science and Engineering*, 2003, Marcel Dekker Inc, New York.
5. E. Gileadi *Physical Electrochemistry*, 2011, **pg 37**, Wiley-VCH, Weinheim, Germany.
6. D. A. Skoog, D. M. West, F. J. Holler, S. R. Crouch, *Fundamentals of Analytical Chemistry*, 8th edn., 2004, **pg 643-660**, Brooks/Cole, Thomson Learning Inc., USA.
7. D. H. Evans, K. M. O'Connell, R. A. Petersen, M. J. Kelly, *J. Chem. Educ.*, 1983, **60**, 290.
8. G. Mohseni, M. Negahdary, H. Faramarzi, S. Mehrtashfar, A. Habibi-Tamijani, S. H. Nazemi, Z. Morshedtalab, M. Mazdapour, S. Parsania, *Int. J. Electrochem. Sci.*, 2012, **7**, 12098.
9. P. Siega, V. Vrdoljak, C. Tavagnacco, R. Dreos, *Inorg. Chim. Acta*, 2012, **387**, 93.
10. R. E. Moss, J. J. Jackowski, M. de Souza Castilho, M. A. Anderson, *Electroanal.*, 2011, **23**, 1718.
11. T. Yamagata, J. Kuwabara, T. Kanbara, *Eur. J. Org. Chem.*, 2012, **27**, 5282.

12. S. Kato, S. Shimizu, H. Taguchi, A. Kobayashi, S. Tobita, Y. Nakamura, *J. Org. Chem.*, 2012, **77**, 3222.
13. L. D. Pinto, P. A. L. Puppim, V. M. Behring, D. H. Flinker, A. L. R. Mercê, A. S. Mangrich, N. A. Rey, J. Felcman, *Inorg. Chim. Acta*, 2010, **363**, 2624.
14. K. Ataka, B. Richter, J. Heberle, *J. Phys. Chem. B*, 2006, **110**, 9339.
15. C. H. Hamann, A. Hamnett, W. Vielstich, *Electrochemistry*, 2nd edn., 2007, **pg 261**, Wiley-VCH, Weinheim, Germany.
16. A. R. Hillman, 2007, Electroanalytical Chemistry Lecture 1, University of Leicester.
17. D. A. Skoog, D. M. West, F. J. Holler, S. R. Crouch, *Fundamentals of Analytical Chemistry*, 8th edn., 2004, **pg 694-699**, Brooks/Cole, Thomson Learning Inc., USA.
18. P. K. Burian, *Mastering Digital Photography and Imaging*, 2004, Sybex, Alameda, USA.
19. Meiji Techno, *MT7000 Series Metallurgical Microscopes for Reflected Light Observation*, 08. 03. 323.10,000 V1, Japan.
20. Meiji Techno, *Metallurgical Microscope Instruction Manual*, 03. 09. 2,000 V1, New York Microscope Company Inc., Japan.
21. R. Oldfield, *Light Microscopy An Illustrated Guide*, 1994, Wolfe Publishing, England.
22. D. A. Skoog, F. J. Holler, T. A. Nieman, *Principles of Instrumental Analysis*, 5th edn., 1998, **pg 549-553**, Thomson Learning, USA.
23. D. A. Skoog, F. J. Holler, T. A. Nieman, *Principles of Instrumental Analysis*, 5th edn., 1998, **pg 429-444**, Thomson Learning, USA.
24. Taylor Hobson Precision, *Surtronic 3+ Operating Instructions*, HB – 103, UK.

Chapter Three

3. Experimental

3.1. Fingerprints

Fingerprint samples were taken from a minimum of four different donors for each experiment studied. The donors varied in age (21 – 42 years old), gender and ethnicity. No previous grooming of the donors' fingerprints took place and where possible separate donors were used for individual pieces of study. Fingerprints were taken as closely as possible within the time frame, 12:00pm – 3:00pm.

3.2. Fingerprint Deposits

Three kinds of fingerprint deposit were used; where necessary the specific type is stated in the results. One kind of fingerprint deposit was 'unknown' or natural; the donors were asked to deposit prints without record of the time since the donor last washed their hands, handled food or other substances or surfaces. The remaining two fingerprint types were more controlled: eccrine and sebaceous. Prior to fingerprint deposition, the subject's hands were thoroughly washed with soap, rinsed with water and dried with paper towel. To produce a sebaceous print the fingertips were rubbed around the nose and forehead region. An even spread of perspiration was achieved by rubbing the fingertips together and over the palm of the hand. To produce an eccrine print, a powder free nitrile glove was worn for 15 minutes.¹ Fingerprints were deposited on the substrates by application of minimal pressure. Their subsequent development was carried out over a wide time period following their deposition, between 2 hr – 39 days.

3.3. Substrates

Several forms of substrate were used in this study. Initial work was carried out on *model substrates*, substrates that were representative of a specific clean flat metal for analysis. Work was extended on some metals to corresponding metallic items of viable forensic value, such as knives and cartridges (see Chapter 5 Section 5.1).

Model stainless steel plates (grade 316, area 6.25 cm², thickness 0.1 cm), Figure 3.1a, were washed in warm water containing a few drops of commercially available detergent to remove the protective grease. All stainless steel plates were polished if not otherwise stated. One side, intended for fingerprint deposition and subsequent enhancement, of the stainless steel was polished with Brasso™ (Brasso, Reckitt Benckiser plc, Slough, UK) for approximately 5 min, until a mirror-like finish was achieved. The samples were then washed again in warm water containing a few drops of commercially available detergent and left to dry in air.

Knives possessing blades and handles made from stainless steel (grade 304, Figure 3.1b) were washed in warm water containing a few drops of commercially available detergent. The knives were then dried with paper towel prior to fingerprint deposition.

Model brass plates (area 6.25 cm², thickness 0.1 cm) Figure 3.2a, were prepared by polishing to a mirror like finish using Brasso™. Following polishing, samples were washed in warm water containing a few drops of commercially available detergent; the metal was rubbed with a non-abrasive cloth to effectively remove any grease or polish

remaining on the surface. Samples were then rinsed with acetone and patted dry with paper towel.



Figure 3.1. Photographs of a stainless steel a) plate; b) knife.

Brass cartridges (Federal American Eagle® calibre .223 Remington) were removed from their original packaging and loaded into a firearm by an ungloved hand. Once fired, the spent cartridges (Figure 3.2b) were gathered and stored in a polythene bag until their development.

Model copper plates (area 6.25 cm^2 , thickness 0.1 cm) Figure 3.2c, were prepared by polishing to a mirror like finish using Brasso™. Following polishing, samples were washed in warm water containing a few drops of commercially available detergent; the metal was rubbed with a non-abrasive cloth to effectively remove any grease or polish remaining on the surface. Samples were then rinsed with acetone and patted dry with paper towel.

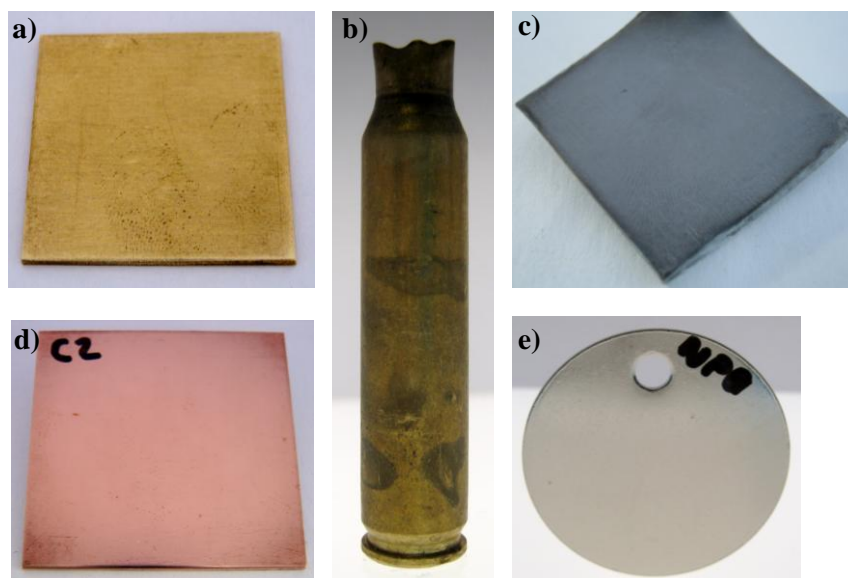


Figure 3.2. Example photographs of a) brass; b) previously fired brass cartridge; c) lead; d) copper; e) nickel plated brass (dog tag).

Lead plates (area 3.25 cm^2 or 6.25 cm^2 , thickness 0.15 cm) Figure 3.2d, were prepared by polishing with an abrasive polishing block until an even visible change to the surface occurred removing the outer most passivated layer. Following polishing, samples were washed in warm water containing a few drops of commercially available detergent. Samples were then rinsed with acetone and patted dry with paper towel.

Pet identification tags (referred to in later chapters as dog tags) were used as model substrates for nickel plated brass (area 4.90 cm^2 , thickness 0.1 cm), Figure 3.2e. The samples were washed in warm water containing a few drops of commercially available detergent, then rinsed with acetone and patted dry with paper towel prior to fingerprint deposition.

Both fired and safely disarmed nickel plated brass cartridges (Federal Premium® calibre .308 Winchester) were studied. The cartridges that were fired through a rifle were removed from their original packaging (Figure 3.3a) and loaded directly into a firearm by an ungloved hand (Figure 3.3b). Once fired, the spent cartridges were placed in their original packaging until their development. In order to study cartridges that had not been fired through a rifle, a series of procedures to disarm them were carried out to ensure safety. The ammunition is secured in a holder that grips the base of the cartridge, Figure 3.4a. The bullet is then inserted and secured into a hammer device with the bullet end facing down, Figure 3.4b. Once securely in place the hammer is then struck against a solid surface Figure 3.4c; allowing for the removal of the bullet and propellant (Figure 3.4d), a nitrocellulose based powder coated in graphite to allow for a smooth exit from the barrel of the firearm. The cartridge is then removed from the device and placed in a vice; the base of the cartridge is struck with a hammer which should be followed by a loud bang, signalling the removal of the primer.

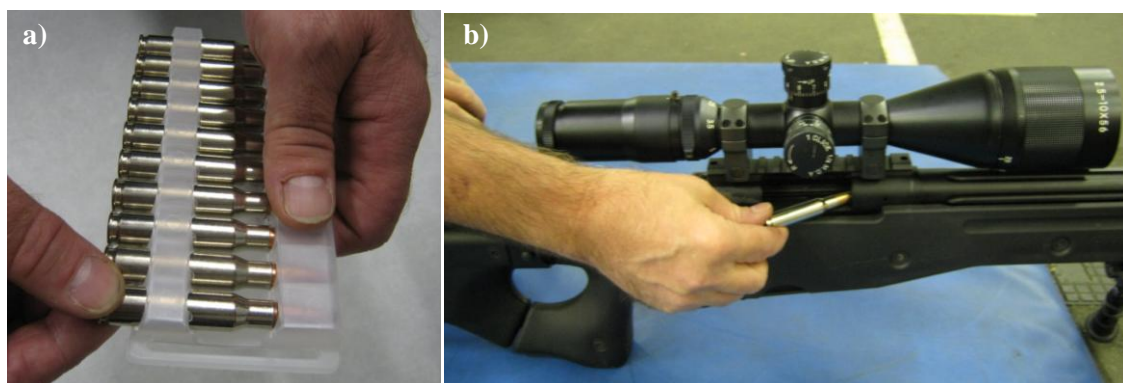


Figure 3.3. Photographs of a cartridge a) being removed from its original packaging; b) being loaded into a firearm.

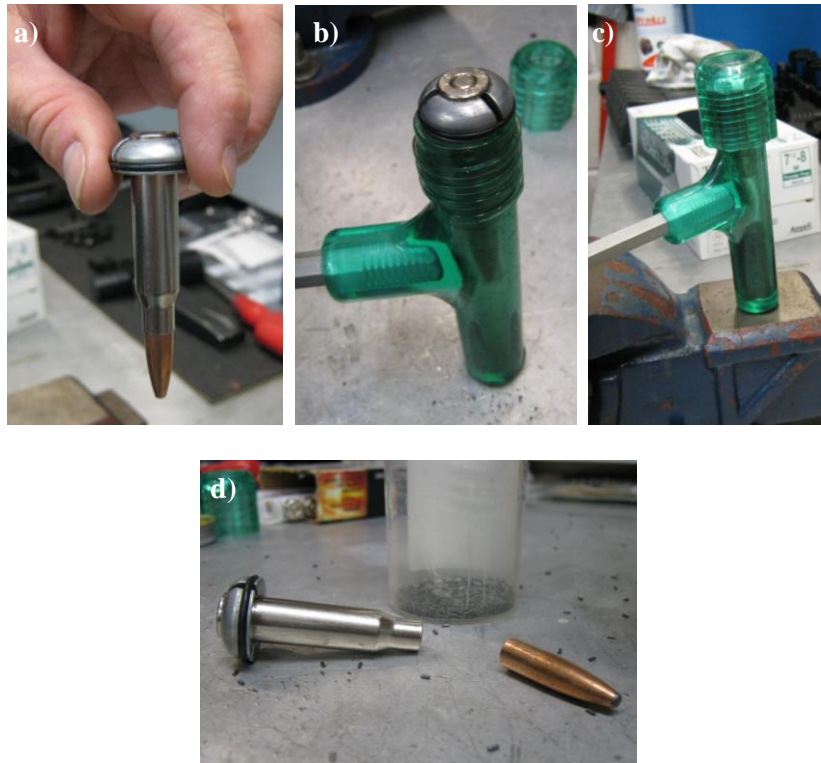


Figure 3.4. Photographs of the processes involved to disarm the ammunition a) securing the cartridge in the holder; b) bullet facing downwards into hammer device; c) striking the hammer device; d) disarmed cartridge, propellant (in container) and bullet.

3.4. Metal Plating

A nickel Watts plating solution was prepared by heating 250 ml of deionised water to approximately 60 °C. Whilst stirring, 150 g nickel sulphate, 45 g nickel chloride and 22.5 g boric acid were added slowly to the water. Once all solids had dissolved the solution was made up to 500 ml with additional deionised water. The pH of the solution was tested over several days, adjusting with concentrated sulphuric acid/sodium hydroxide until an optimum value (3 - 4.5) was reached.²

Brass substrates were prepared as describe above, however no fingerprints were deposited. Insulating tape was used to section off part of the metal, an area of 7.5 cm² for brass plates and 10.2 cm² for brass cartridges were exposed for plating. A Thurlby-Thandar Instruments Ltd. (32 V – 2 A) power pack was used for metal plating. Figure 3.5 illustrates the experimental set up used for the brass plates, a cylindrical mesh of iridium oxide coated titanium was used when plating the cartridges. A range of brass plated samples were produced by varying the current applied, to achieve a range of current densities, Table 3.1. Current density J (mA cm⁻¹) was calculated using Equation 3.1

$$J = \frac{I}{A} \quad (3.1)$$

where I (mA) is the current applied and A (cm²) is the area to be plated.

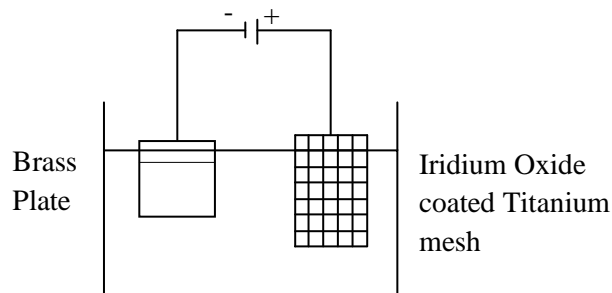


Figure 3.5. Schematic of the experimental set for nickel plating, showing the masked section of the brass plate.

Samples were held at these fixed current densities for 5 minutes before being removed and rinsed with water. On visual appearance alone the samples that produced the most uniform nickel coating were found at 17.5 mA cm⁻² and 15.0 mA cm⁻². Further samples

were prepared using these two current densities for varying lengths of time (1 - 4 mins). Profilometry was used to calculate the depth of the nickel coating. Average thicknesses, calculated over four or more measurements, are used where relevant in later chapters.

A current density of 15.0 mA cm^{-2} was used for plating the brass cartridges; thus a current of 153 mA was applied, for 3 mins, with an observed voltage of 2.11 V.

Current density/ mA cm^{-2}	Current/ mA	Voltage observed/ V
20.0	150	2.50
17.5	131	2.41
15.0	113	2.34
12.5	94	2.29
10.0	75	2.26
7.5	56	2.20

Table 3.1. Shows the required current for a range of current densities, for a surface area of 7.5 cm^2 .

3.5. Electrolyte

The driving force for migration is the electric field in solution. To eliminate this effect a higher concentration of supporting electrolyte, compared to that of the electroactive species, is added. The supporting electrolyte is chosen on the basis that it will not take part in the charge-transfer process but will reduce the electric field by increasing conductivity in solution.³ The inert ions in solution carry most of the electricity so that the contribution of the electrical field to the rate of mass transport is negligible and

therefore assumed to have been eliminated unless otherwise stated. However, this is not always the case and should be noted specifically for films formed on the electrode that mass transport through the film may depend on migration.³

Different electrolyte solutions of varying concentration were used to optimise development and complement chemistries of the working electrode metal substrate.

Sulphuric acid (Fisher Chemical, reagent grade >95 %), H₂SO₄, was used as a background electrolyte in the deposition of both PANi and PEDOT (with the presence of sodium dodecylsulphate [Acros Organics, for biochemistry 99 %], SDS, [0.01 M]) onto stainless steel (0.5, 1.0 M), and PANi onto lead (0.1, 1.0, 5.0 M). Sodium oxalate (Hogg Laboratory Suppliers, laboratory reagent), Na₂C₂O₄, was used for PANi deposition onto brass (0.05, 0.1, 1.0 M), copper (0.2 M) and nickel plated brass (0.2 M). Nickel plated brass substrates were also developed using PANi in *p*-toluenesulphonic acid (Lancaster Synthesis, >98 %), PTSA, (0.2 M) and PEDOT in lithium perchlorate (Sigma Aldrich, ACS reagent ≥95 %), LiClO₄, (0.1 M) with the presence of SDS, (0.01 M).

3.6. Monomer

Aniline (Sigma Aldrich, reagent plus 99 %), (0.01 - 1.0 M) and EDOT (Sigma Aldrich, 97 %), (0.01 M) were chosen because of their polymers electrochromic properties. The choice of PANi and PEDOT as electrochromic polymers was based on the facility to operate in aqueous media, their exceptional chemical stability and general robustness in

thin film form.⁴⁻⁵ In the case of PANi, the added opportunity to access three optically distinct oxidation states aided the selection.

3.7. Polymer Deposits

All polymer films were deposited using a μ AUTOLAB type II potentiostat in a conventional three electrode cell, with a Ag|AgCl|saturated KCl reference electrode and either a Pt flag or an iridium oxide coated titanium mesh as a counter electrode. Secondary reference electrodes consist of a metal (M), an insoluble salt of same metal (MA) and solution with same anion (A).⁶ An Ag|AgCl is an example of a secondary electrode, which are preferred over primary electrodes as their potential is more stable and more reproducible.

For stainless steel substrates potentiostatic deposition (0.9 V) was used to deposit both PANi and PEDOT, with respective deposition times in the range 200 - 2400 s and 140 - 3600 s, in a background electrolyte of H₂SO₄ (SDS also present when depositing PEDOT). Subsequent fingerprint visualization was carried out potentiodynamically ($-0.2 < E/V < +0.9$; scan rate, $v = 20 \text{ mV s}^{-1}$) in monomer-free aqueous 1M H₂SO₄.

The development of brass substrates was carried out via potentiostatic deposition (0.5, 0.6, 0.7 V) of PANi, with deposition times in the range 8 – 140 s. Potentiodynamic deposition (within the range $-0.4 < E/V < +1.8$; scan rate, $v = 2, 5, 10, 20 \text{ mV s}^{-1}$) was also used in the development of brass substrates in a background electrolyte of sodium oxalate.

Potentiostatic deposition (0.6, 0.7 V), with deposition times in the range 80 – 300 s, and potentiodynamic deposition (within the range $-0.2 < E/V < +1.2$; scan rate, $v = 5, 10, 20 \text{ mV s}^{-1}$) of PANi, was used for the development of copper substrates in a background electrolyte of sodium oxalate.

Nickel plated brass substrates were developed using the potentiodynamic deposition of PANi, in the range $+0.2 < E/V < +1.6$; scan rate, $v = 20, 25, 50, 100 \text{ mV s}^{-1}$, in a background electrolyte of *p*-toluenesulphonic acid. Both the potentiostatic deposition (0.9 V, deposition time in the range 55 – 160 s) and potentiodynamic deposition (within the range $-1.0 < E/V < +1.7$; scan rate, $v = 10, 20, 50 \text{ mV s}^{-1}$) of PEDOT was also carried out on nickel plated brass substrates, in a background electrolyte of lithium perchlorate and SDS. The development of nickel plated brass cartridges via potentiostatic (0.6 V) and potentiodynamic deposition (within the range $-0.2 < E/V < +1.2$; scan rate, $v = 10, 20, 50 \text{ mV s}^{-1}$) of PANi was carried out in a background electrolyte of sodium oxalate.

Potentiodynamic deposition of PANi, within the range $-0.2 < E/V < +1.85$; scan rate, $v = 5, 10, 20, 50, 100 \text{ mV s}^{-1}$, was carried out on lead substrates in a background electrolyte of H_2SO_4 .

3.8. Pre-treatment

If not otherwise stated samples were left on the bench in the laboratory after the fingerprint deposit was made but before development was carried out. Different

environments, the conditions of which can be found below, were used to simulate probable scenarios for which a piece of evidence could be subject to prior to analysis.

Chapter 5 includes the removal of fingerprints from both brass and copper substrates prior to their development. The substrates were left for either one month, one week or alternatively were checked twice a day until the area beneath the sweat deposit started to darken, before they were washed in warm water with a few drops of commercially available detergent. A non-abrasive cloth was used to remove any remaining traces of fingerprint deposit in accordance with Paterson *et al.*⁷

Chapter 6 involves the aging (1 – 28 days) and exposure of fingerprints to five different environments, prior to their enhancement, Table 3.2. The prints were left overnight under ambient conditions before being subjected to their respective environments. In the case of the one day old prints, pre-treatment commenced approximately four hours after fingerprint deposition.

3.9. Other Enhancement Techniques

Chapter 6 compares the polymer deposition technique with three existing fingerprint development methods which are described below.

Environment	Sample Conditions
Ambient	Kept in open box until enhancement
High Temperature	Placed on metal tray stored in oven at 150 °C until enhancement
Under Water	Kept submerged under water until enhancement
Soap Wash	Rubbed in warm (40°C) soapy water for 30s, rinsed in soap free water. Left to dry naturally, stored as ambient until development
Acetone Wash	Agitated in acetone for 30s, rinsed in water. Left to dry naturally, remained at ambient conditions until development

Table 3.2. The specific conditions used for the five environments studied.

Samples developed by dusting with black granular powder (WA Products), according to Fingerprint Powders Guidelines,⁸ were gently dusted back and forth with a mop head squirrel brush.

A mixture of iron oxide and detergent (Codeco and distilled water), referred later to as wet powder, was made to a consistency viscous enough to coat a surface but sufficiently optically transmitting that one could see the underlying surface through the resultant film. Wet powdered samples were developed by painting on the mixture in perpendicular directions to ensure particles attached to the deposited fingerprint ridges. Samples were then rinsed under slow running water to remove excess wet powder mixture and placed in a drying cabinet (60 °C) for 1 hour.

Development of samples by superglue fuming was carried out in a fuming cabinet (MVC 5000, Foster and Freeman, Evesham, UK), prepared by the addition of distilled water and sufficient cyanoacrylate to cover the incorporated hot plate. Samples were placed in the cabinet set to Auto Glue. 78.9% humidity was reached after approximately 8 minutes; this was followed by 15 minutes of fuming at 119.4 °C. The samples were then removed from the cabinet and dipped in a solution of Basic Yellow 40 dye (2 g l⁻¹ in aqueous 60% ethanol) then rinsed under slow running water. Samples were left in a drying cabinet (60 °C) for 1 hour.

3.10. Visualisation

It was stressed in Chapter 1 the importance of capturing an image of the developed print therefore visualisation plays a major part in this project. Three different visualisation techniques were implemented to acquire *primary*, *secondary*, and *tertiary* detail.

3.10.1. Digital Imaging

Samples were photographed immediately prior to and following polymer enhancement. Photographs were taken using either a Pentax Optio M40 or Canon PowerShot A480 digital camera. In both cases the Super Macro mode and automatic focus was used which allowed for images to be captured when the samples were approximately 15 cm from the camera. The photographs that appear in this thesis are the original raw images, unless otherwise stated in their respective figure legends that brightness has been altered for the purposes of printing.

Specific to Chapter 6, samples kept in an oven or under water, were removed from their environments and left to reach ambient conditions (cool/dry, respectively) naturally in air before being photographed. Samples developed by dusting and wet powder were photographed using a Canon PowerShot A480 digital camera. Images of samples developed by superglue fuming were captured with DCS-3 Image-ProPlus 5.0.1.11 image software acquired by a Fuji FinePix S2 Pro digital camera with a 55mm Nikkor micro lens and visualised through a 476 nm filter by a 4x4 crime-lite LED ($\lambda = 430\text{-}470\text{ nm}$).

3.10.2. Optical Microscopy

A Meiji Techno MT7100 trinocular microscope was used to obtain *secondary* and *tertiary detail* of the polymer enhancements. The microscope was linked to a computer and operated using uEye Demo, Copyright 2003-2008 IDS Imaging Development System GmbH.

3.10.3. Scanning Electron Microscopy

A Philips XL30 Environmental Scanning Electron Microscope (ESEM) was used to obtain *secondary* and *tertiary detail* of the polymer enhancements, as well as measurements of the thickness of nickel coatings on brass substrates.

3.11. Characterisation

Following electrochemical treatment of the metal substrates, analysis was carried out in order to characterise any alterations to the surface's chemistry. Assessment of

repeatability and thickness measurements were required to ensure comparable nickel coatings, to those found on nickel plated brass cartridges, were achieved in the laboratory.

3.11.1. Raman Spectroscopy

A Horiba Jobin Yovn, LabRAM HR Raman spectrometer was used to obtain characteristic information from substrates. The spectrometer was connected to a computer and an Olympus U-5RE-2 optical microscope (x 50 magnification) with a euromex Holland fiber-optic light source (EK-1), to aid with spectral analysis and visualisation of the test substrate. A silicon wafer was used for calibration of the 532.11 nm laser with 1200 grating, through a slit of 100 μm . The optical density filter (25 % - 50%), confocal pinhole (100 - 300 μm) and acquisition (RTD 1 s, exposure time 10 - 30 s, accumulation 2) were varied to optimise spectral measurements in the range 100 - 2000 cm^{-1} .

3.11.2. Energy-Dispersive X-ray Spectroscopy

Elemental analysis of the nickel plated brass substrates was acquired using a Philips XL30 ESEM in conjunction with an Oxford Inca Energy-Dispersive X-ray (EDX) system.

3.12. Profilometry

Profilometry measurements were taken using a Silver Surtronic 3+, the interface settings applied were 8 mm x 10 μm . TalyProfile software was used to collect measurements.

3.13. References

1. V. G. Sears, S. M. Bleay, H. L. Bandey, *Sci. Justice.*, 2012, **52**, 145.
2. W. Canning, *The Canning Handbook of Electro-Plating*, 1978, **pg 368-459**, Canning & Co. Ltd., Birmingham, UK.
3. E. Gileadi, *Physical Electrochemistry*, 2011, **pg 29-54**, Wiley-VCH, Weinheim, Germany.
4. T. A. Skotheim, R. L. Elsenbaumer, J. R. Reynolds, *Handbook of Conducting Polymers*, 1998, Marcel Dekker, New York.
5. A. A. Argun, P. H. Aubert, B. C. Thompson, I. Schwendeman, C. L. Gaupp, J. Hwang, N. J. Pinto, D. B. Tanner, A. G. MacDiarmid, J. R. Reynolds, *Chem. Mater.*, 2004, **16**, 4401.
6. D. J. G. Ives, G. J. Janz, *Reference Electrodes*, 1961, **pg 179-230**, Academic Press Inc., London, UK.
7. E. Paterson, J. W. Bond, A. R. Hillman, *J. Forensic Sci.*, 2010, **55**, 221.
8. H. L. Bandey, *Fingerprint Powders Guidelines*, Sandridge: Police Scientific Development Branch, Home Office, 2007; Publication No.:09/07.

Chapter Four

4. Novel Fingerprint Development using Polyaniline on Stainless Steel¹

4.1. Overview

In this chapter a novel method for the visualisation of latent fingerprints is discussed. The strategy is demonstrated on stainless steel, chosen in view of its widespread use in common objects (handles, tools, knives) of forensic relevance, onto which is electrochemically deposited an electrochromic PANi film. PANi was selected on the basis of the facility to operate in aqueous media, but more significantly its exceptional stability to redox cycling, and the possibility of electrochemically accessing multiple optically distinct oxidation states.^{2,3}

4.2. Film Electrochemistry

This technique employs the idea that a fingerprint deposit acts like a resist, preventing the deposition of the polymer onto the metal surface directly below, see Figure 4.1. The polymerisation of four aniline monomers, to form the electrically conductive structure of PANi (emeraldine salt - Figure 1.23), was carried out. At a constant potential ($E = 0.9$ V), the polymer films were deposited onto the stainless steel substrates (Chapter 3, Section 3.7). In background electrolyte, the polymer film's optical properties could be accessed either via cycling of potential in the range $-0.2 < E/V < +0.9$, or maintaining a constant potential within the same range (versus a Ag|AgCl|saturated KCl reference electrode). The participation of both proton (cation) and anion transfers to maintain electroneutrality upon changing polymer charge state ensures rapid switching in aqueous media.⁴ These attributes have prompted application in electrochromic

devices^{3,5} in which the goal is the opposite of that here, namely laterally *uniform* colouration of the surface, be it an element of a display device⁶ or an architectural glazing unit.⁷

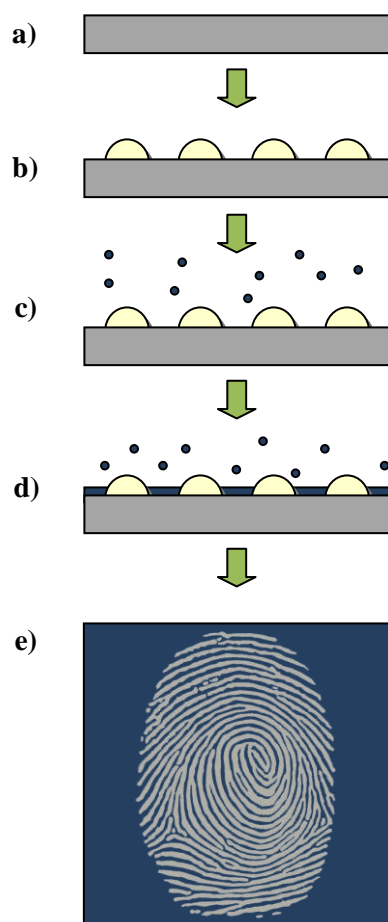


Figure 4.1. Strategy schematic of technique. Side view of a) metal surface, b) fingerprint deposit, c) polymerisation of polymer, d) deposition of polymer, and aerial view of e) enhanced fingerprint.

An example of a cyclic voltammogram (CV) can be seen in Figure 4.2. This CV was the tenth cycle of a previously deposited (potentiostatically, $E = 0.9$ V) PANi film used to enhance a fingerprint on stainless steel. The shape of the CV is similar to those

previously reported for PANi on stainless steel and other metals,⁸⁻¹⁰ where the redox peaks are found at slightly different potentials depending on the substrate and electrolyte.

In Figure 4.2 the large peak at approximately $E = 0.4$ V can be attributed to the oxidation of the PANi film from leucoemeraldine to emeraldine. The formation of pernigraniline, which appears at more positive potentials to the previous transition, was observed here at $E = 0.9$ V. It was found that when the polymer film was taken higher than $E = 0.9$ V the film began to detach from the stainless steel and as a result ridge detail was lost. The middle peak ($E = \sim 0.64$ V) is related to the degradation products trapped within the PANi film.¹¹

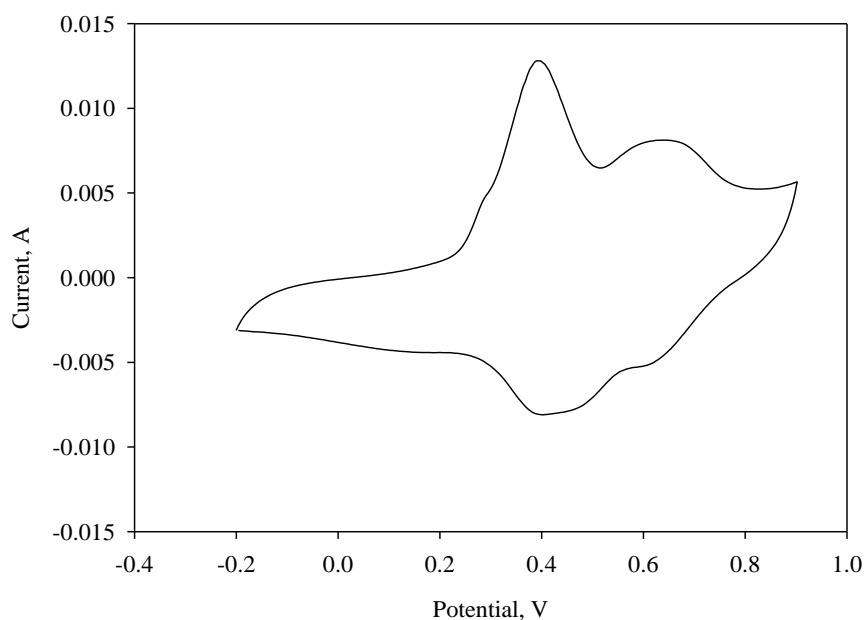


Figure 4.2. Typical CV of PANi film previously potentiostatically deposited ($E = 0.9$ V) onto fingerprinted stainless steel in monomer free (1 M H_2SO_4) electrolyte. Scan rate, $\nu = 20$ mV s^{-1} ($-0.2 < E/\text{V} < 0.9$).

4.3. Film Thickness

The intention here is not to determine an optimum film thickness for an automated fingerprint enhancement, but for pure interest. It is possible to estimate the thickness of the polymer deposit coulometrically using Faraday's Law. As previously mentioned in Chapter 2 Section 2.2.2, the potential axis of the voltammogram (Figure 4.2) can also be considered as a time axis. As the scan rate is known the charge Q (C) can be calculated

$$Q = \int_0^t i dt \quad (4.1)$$

Once Q is known Equation 4.2 can be used to determine number of moles of aniline in the polymer deposit, coverage Γ (mol cm⁻²)

$$\Gamma = \frac{Q}{nFA} \quad (4.2)$$

where n (0.5) is the number of electrons lost per molecule of aniline to form the emeraldine salt, A is the area (cm²) of the polymer deposit on the substrate and F is Faraday's constant (9.648 x 10⁴ C mol⁻¹). From the density ρ (g cm⁻³) and molar mass M_r (g mol⁻¹), along with the coverage, the thickness is calculated using Equations 4.3 and 4.4;

$$c = \frac{\rho}{M_r} \quad (4.3)$$

$$h = \frac{\Gamma}{c} \quad (4.4)$$

where c (mol cm⁻³) is the concentration and h (cm) is the height (thickness). The calculated value is an estimate that refers to a compact dry polymer film. During the CV measurements, the presence of different species within the film will cause it to swell; increasing the thickness.¹²⁻¹³ A non-uniform coverage across the available

deposition area, caused by the presence of the fingerprint residue, will also affect the calculation of the true thickness of the polymer film.

Using the data found in Figure 4.2, an example of the calculations carried out to determine a sample's thickness is shown below. The CV data acquired by the potentiostat, and collected by the connected computer, are transferred to Origin 6.0. Here, the cathodic current as a function of time can be determined digitally. The sum total gives the sample's charge Q as 2.52×10^{-1} C (Equation 4.1). For this specific sample, an image of which can be found in Section 4.4.1 Figure 4.5, the area A , of stainless steel exposed to solution during deposition was calculated to be 4.52 cm^2 . This was determined by using

$$A = \pi r^2 \quad (4.5)$$

where r , the radius of the circle was measured as 1.2 cm. However, due to the presence of the fingerprint not all of the available area was covered in polymer. On individual assessment it was estimated that just over 60 % of the sample was covered in polymer, amounting to a polymer deposit area, A , of 2.83 cm^2 . Substituting both the charge and the area covered by polymer into Equation 4.2

$$\Gamma = \frac{2.52 \times 10^{-1}}{0.5 \cdot F \cdot 2.83} = 1.85 \times 10^{-6} \text{ mol cm}^{-2} \quad (4.6)$$

gives the number of moles of aniline in the sample film. The density (1.02 g cm^{-3}) and molar mass (93.13 g mol^{-1}) of aniline, which will be the same for all samples studied, are used in Equation 4.3

$$c = \frac{1.02}{93.13} = 0.0129 \text{ mol cm}^{-3} \quad (4.7)$$

which gives the concentration of aniline monomer units in the sample film. Substituting the concentration and number of moles of aniline in the sample film into Equation 4.4

$$h = \frac{1.85 \times 10^{-6}}{0.0129} = 1.43 \mu m \quad (4.8)$$

gives an estimated thickness of 1.43 μm . As a result of these calculations it can be estimated that the polymer film thickness for the samples studied were in the range 61.3 nm – 1.93 μm , according to the individual deposition times used.

Recent work has shown that under ambient conditions the mass of fingerprint residue, over a period of approximately 5 weeks, can reduce by 26 %.¹⁴ Quantifying the fingerprint residue deposited, in terms of thickness, has also been studied.¹⁵ Thomas and Reynoldson found that the topography of the residue became irregular and viscosity increased with the age of the print deposit. The height of a fingerprint deposit can vary widely (from 10 nm to 2 μm) according to load,¹⁵ so the present experiments span a range from low trench filling (between the ridges) to substantial trench over-filling.

Prints were developed from 2 hours up to 39 days following their deposition. Figure 4.3 shows just four examples of the sweat deposited, after being given the same instructions, by different donors. The examples were viewed under an optical microscope within a couple of hours following their initial deposition. They show the difference in the quantity and quality that can be produced from different donors. Some donors appear to produce a generous distribution of sweat (Figure 4.3a), showing clear ridge detail and positions of sweat pores. Other donors do not produce as much residue, but a clear distinction between ridges and substrate can still be made, Figure 4.3b. Alternatively, an unbalanced distribution of sweat can occur, Figure 4.3c, where a subtle deposit appears in localised regions of the print. The reduced level of residue may be insufficient for enhancement to take place, allowing polymer deposition in the

localised regions with no ridge definition. In contrast, a much heavier deposit, which fills the furrows of the print, can also occur (Figure 4.3d). In this scenario the excess of residue may prevent polymer deposition in the localised regions, again losing ridge definition.

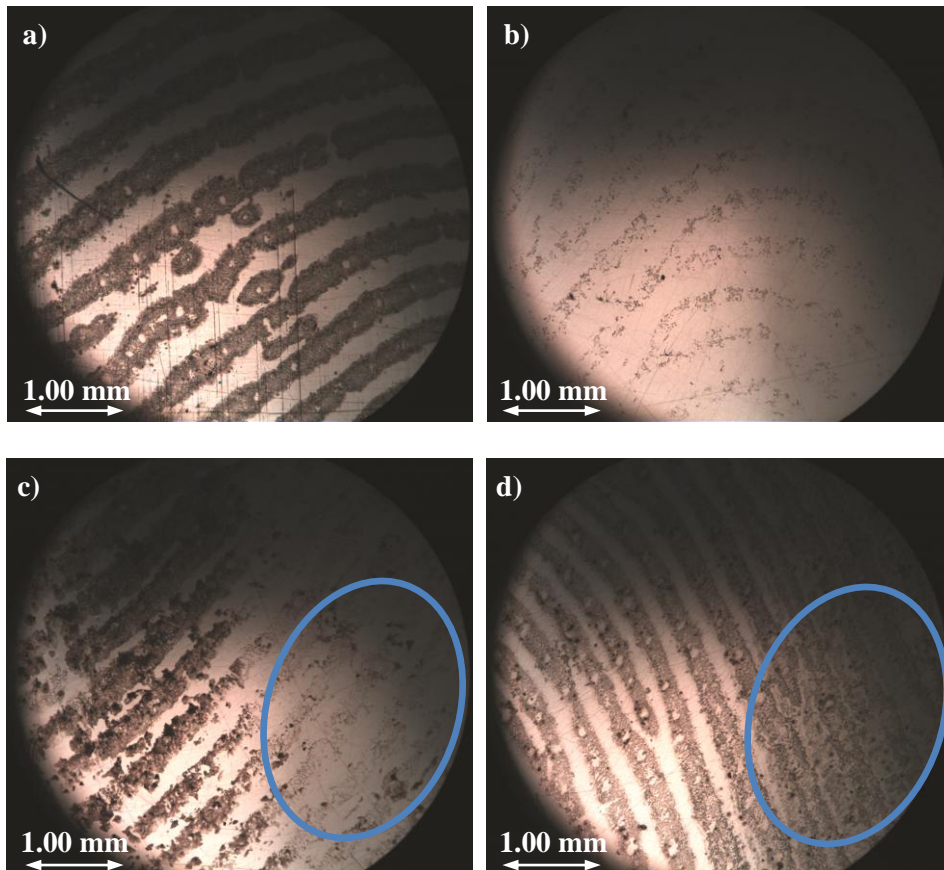


Figure 4.3. Optical microscopy images demonstrating the variance in quality and quantity of sweat deposits from four different donors (within 2 hrs following deposition); a) clear detail and heavy deposit; b) clear detail and light deposit; c) light deposit in localised area (circled); d) heavy deposit in localised area (circled). The consequence of differences is discussed in the text.

It could be assumed that a thin layer of fingerprint deposit would require an equally thin deposit of polymer, in order for the print to be visualised Figure 4.4a. For a thicker

fingerprint residue, a longer deposition time and therefore a thicker polymer deposit could occur, Figure 4.4b, before a print showed signs of overdeveloping. On the basis that the residue degrades over time, the thickness of print residue and therefore thickness of possible polymer deposited would be expected to decrease too. However, the results indicate there to be no correlation between polymer thickness and age of the print residue. The thickest polymer deposit recorded (1.93 μm) was for one of the oldest fingerprint deposits (39 days old). This suggests, according to Thomas and Reynoldson that the initial fingerprint residue height was substantially high and remained so for the ageing period. The thinnest polymer deposit recorded (61.3 nm) was for one of the freshest fingerprint deposits (2 days old), which could suggest that a fairly light residue was initially deposited. This can be explained by the fact a range of donors were used, and therefore the difference in the initial 'load' of residue was varied.

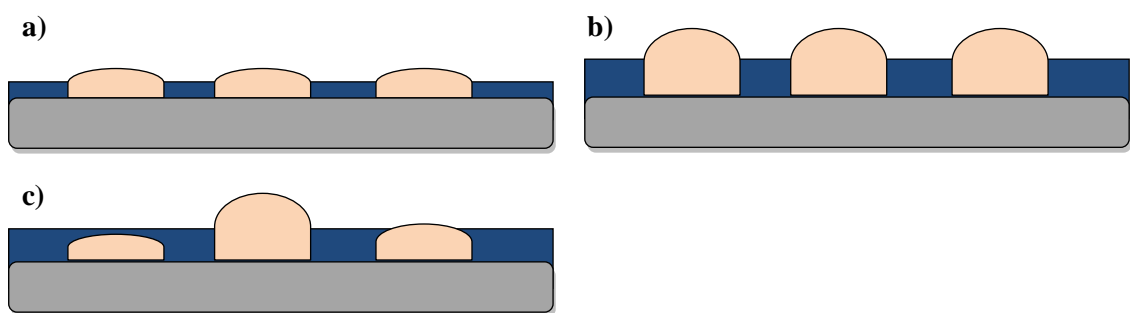


Figure 4.4. Diagrams displaying the variability of sweat residue and subsequent polymer deposits, a) thin residue and polymer deposit; b) thick residue and polymer deposit; c) variable residue thickness with compromised polymer deposit.

As will be seen further on in this chapter (Sections 4.4 and 4.5), not all prints are enhanced perfectly and for the majority of cases ridge detail is incomplete. One cause

of incomplete ridge detail is the variation in the distribution of sweat across one fingerprint, resulting in enhancement as can be seen in Figure 4.4c. The height of the polymer is consistent yet the height of the residue can vary, in some cases overdevelopment of ridge detail will occur due to the lack of residue in a localised area. In these cases, when ridge detail has been obscured, the ability to access PANi's different optical densities becomes extremely advantageous, see Section 4.5. Accessing a lesser optical density state, will allow for better resolution of ridges that have started to be covered, and visualisation of ridges that have been completely covered by the polymer film.

4.4. Fingerprint Images

Capturing the image of an enhanced fingerprint has great importance; it is this image that will be used to search for a potential match. Samples were photographed according to the procedure outlined in Figure 4.5. It must be noted that as the project progressed, the quality of digital images captured greatly improved as more experience was acquired. A number of 'set ups' were implemented ranging from a white paper background to the use of a light box and tripod. As well as digital images, optical microscopy was used to obtain images of enhanced prints on stainless steel.

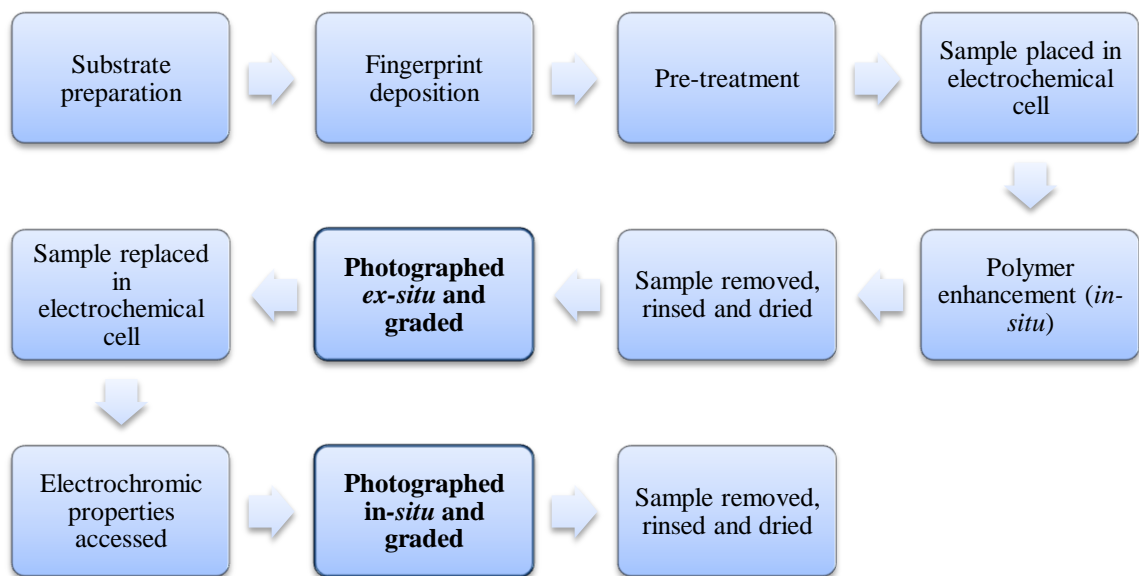


Figure 4.5. A flowchart describing the procedure from sample preparation and enhancement to image capture and grading.

4.4.1. Digital Images – *Ex-situ*

Ex-situ digital images were taken of individual samples prior to and following their enhancement, an example of which can be seen in Figure 4.6. The purpose was to compare any initial visibility of residue to the enhanced ridge detail. The detail visible before enhancement varied: some donors produced considerably more residue than others when asked to deposit their prints. The purpose of multiple donors was to test the technique’s ability to enhance a range of print deposits, with the intention they all be latent. However as it can be seen in Figure 4.6a not all samples were latent. Some, like this one, were visible but lacked ridge definition. The quantification of residue deposited was beyond the scope of this study and therefore not controlled.

Before enhancement there was little ridge detail visible apart from the beginnings of some ridges circled on the left hand side, Figure 4.6a. The successful enhancement of the sample can be seen in Figure 4.6b, albeit not all of the print, but considerably more than the original undefined detail. Interestingly, following enhancement the circled area is not as well defined as some of the main body of the print. Figure 4.6c-d highlights the enhancement that has taken place; from the appearance of an unclear image where ridge detail is barely visible to some fairly well defined *secondary detail*.

4.4.2. Digital Images – *In-situ*

In-situ digital images were taken, when necessary, in monomer free 1 M H₂SO₄ following a sample's enhancement. With small variations of the potential applied the colour of the polymer changes. The colour change signifies a change in oxidation state. The three distinct colours found are: clear/yellow ($E = \sim -0.2$ V), green ($E = \sim 0.4$ V) and blue ($E = \sim 0.9$ V), see Figure 4.7. This process is repeatable and reversible. There are localised areas where the polymer has deposited more heavily than others (circled in Figure 4.7a-c). As optical density is decreased these areas appear much paler in colour and for some parts become transparent.

Upon removal from solution the samples were allowed to dry. The natural oxidation of the polymer was observed, settling at a consistent green colour. It was also observed that the polymer remains the same colour and therefore presumably the same oxidation state, providing it is stored in a sealed container out of direct sunlight, for up to three

years. Samples of a similar age were re-examined *in-situ* where the range of PANi's colours was still accessible, an indication to the robustness of the polymer film.

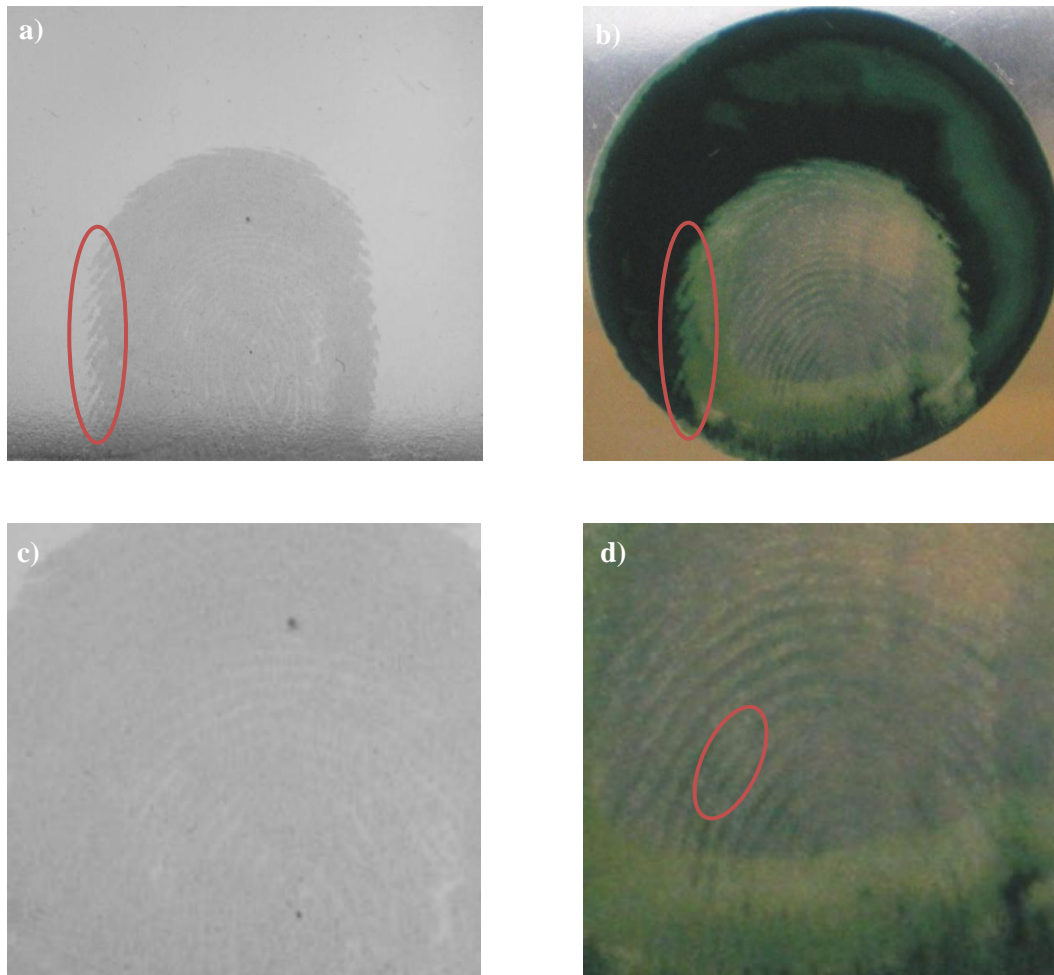


Figure 4.6. *Ex-situ* photographic images of the same sample a) before enhancement; b) following enhancement and their corresponding enlarged regions c) before enhancement; d) following enhancement (ridge ending circled). Images have been brightened for the purposes of printing.

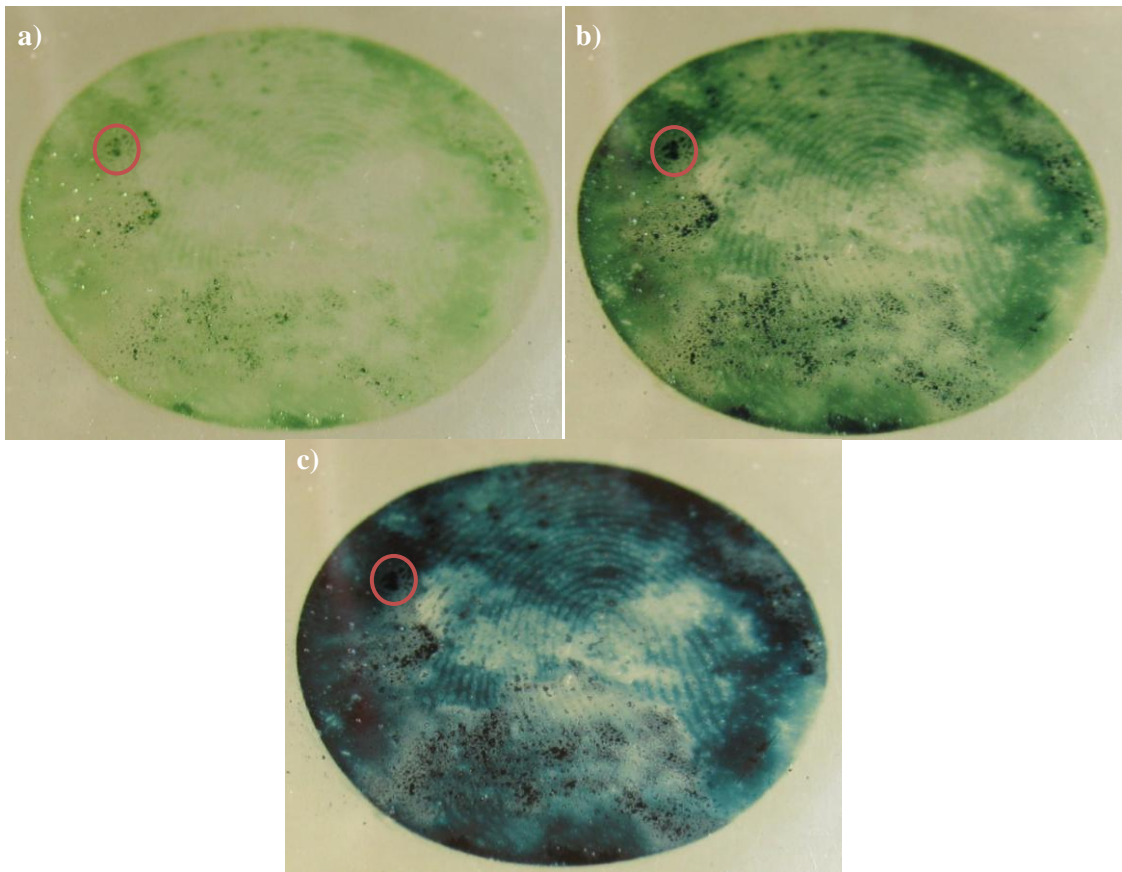


Figure 4.7. *In-situ* photographic images of a sebaceous 35 day old fingerprint on stainless steel, previously enhanced via potentiostatic deposition of PANi ($E = 0.9$ V, 400 s), viewed under potential control (E) at; a) -0.2 V; b) 0.4 V; c) 0.9 V.

4.4.3. Optical Microscopy

With the use of an optical microscope it is possible to see that the polymer has filled the spaces between the ridges of the fingerprint deposit. What appears as bare stainless steel in Figure 4.8, are the ridges of a fingerprint deposit that have prevented against the deposition of the green PANi film. It is also possible to see that the polymer has started to grow across the ridge detail, along scratches on the stainless steel substrate. Preferential deposition along the scratches has occurred rather than an even coating across the ridges, following the filling of the furrows.

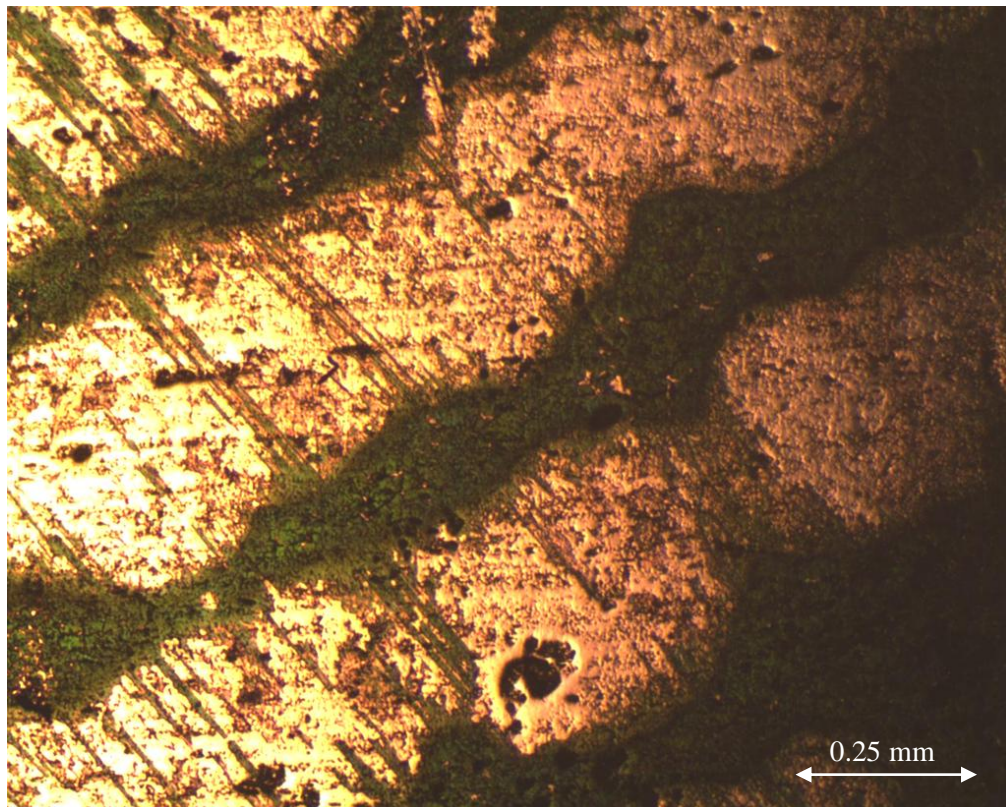


Figure 4.8. Optical microscopy image of a sebaceous print on stainless steel enhanced via potentiostatic deposition of PANi.

Secondary detail, such as the ridge endings and island circled in Figure 4.8a, are easily identified using optical microscopy. Figure 4.9 shows an example of a print in a series of images with increasing magnification. This demonstrates how the polymer first fills between the ridges before it can spill over into the furrows of the print detail. In the centre of Figure 4.9d the polymer free stainless steel can be seen.

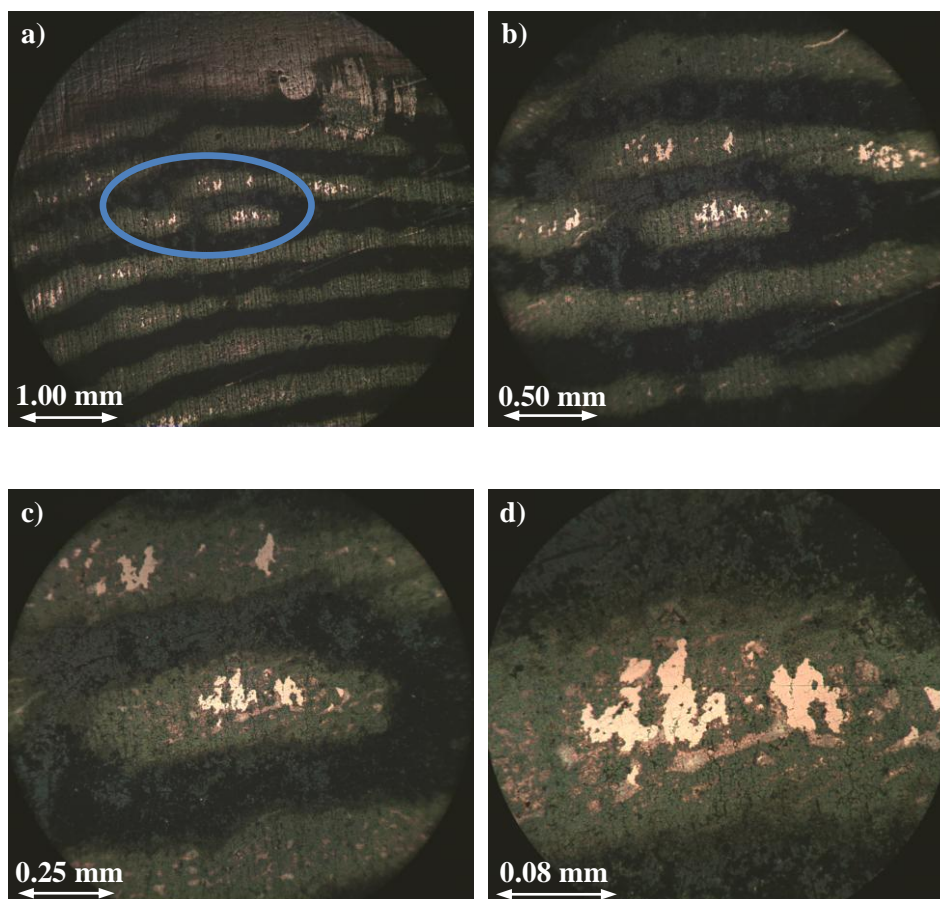


Figure 4.9. A 38 day old fingerprint on stainless steel enhanced via potentiostatic deposition of PANi ($E = 0.9$ V, 400 s) viewed *ex-situ* at the following magnifications; a) 5x; b) 10x; c) 20x; d) 50x.

4.5. Grading

It was not possible to enhance all of the samples to a level of high quality that would allow for an identification to be made. The samples were varied - generated by different sweat inducement times, individual donors, ambient conditions and deposition pressure, and aged for different periods (2 hrs – 39 days) representing a plausible spectrum of print quality. As a way of assessing the quality of enhanced prints, via new and existing techniques, the Home Office implemented a grading scheme, Table 4.1. A grade 0 is given to samples that it has not been possible to develop a print from.

Samples that are given a grade 1 are those that show it is apparent a fingerprint deposit is present but it is not possible to distinguish ridge characteristics. A grade 2 is given to samples that possess some discernible ridge detail amounting to one third of the fingerprint. Grade 3 developed prints possess continuous detail over two thirds of the sample. When a print is fully developed a grade 4 is given. According to the Bandey scale a grade 3 or above is required for a positive identification to be made, with the aim of a conviction in court.

Grade	Fingermark characteristics
0	No development
1	No continuous ridges; all discontinuous or dotty
2	One third of mark comprises continuous ridges; remainder shows no development or is dotty
3	Two thirds of mark comprises continuous ridges; remainder shows no development or is dotty
4	Full development: whole mark comprises continuous ridge detail

Table 4.1. Grading scheme for accessing the quality of fingerprint ridge detail.¹⁶

Once the enhanced samples had been photographed, they were graded. Out of a set of 50 samples, 20 qualified as grades viewed as *useable*. Figure 4.10 shows examples of the range in quality of enhancement, Figure 4.11 shows their corresponding CV response following enhancement via potentiostatic deposition of PANi.

It may appear obvious that there once was a fingerprint on each of the samples found in Figure 4.10, however the detail that has been made available following enhancement is very different. A grade of 1 was given to the examples in Figure 4.10a and 4.10b; there is sufficient detail to signify the presence of a fingerprint yet insufficient ridge detail to begin a search for a match. The example found in Figure 4.10c shows significantly more ridge detail over a larger area, however due to lack of clarity in localised areas in the centre of the print it can only be given a grade of 3. The final example in Figure 4.10d was given a grade 4; the ridges have been enhanced consistently across the whole region which will allow for accurate identification of a match.

When the sample in Figure 4.10a is observed, a large proportion of the deposition area is polymer free, most likely due to a smudged fingerprint deposit preventing the film from adhering to the substrate. This may explain the CV (Figure 4.11a), which is not typical of PANi unlike the other examples found in Figure 4.11. There is no apparent cathodic peak that can be attributed to the oxidation of the PANi film from leucoemeraldine to emeraldine, like those found in Figures 4.11b-c ($E = 0.40 - 0.41$ V). On visual appearance alone however it would appear that a PANi film was deposited. Figure 4.11a does have some slight peaks at $E = 0.58$ V and 0.75 V, which could be attributed to degradation products.

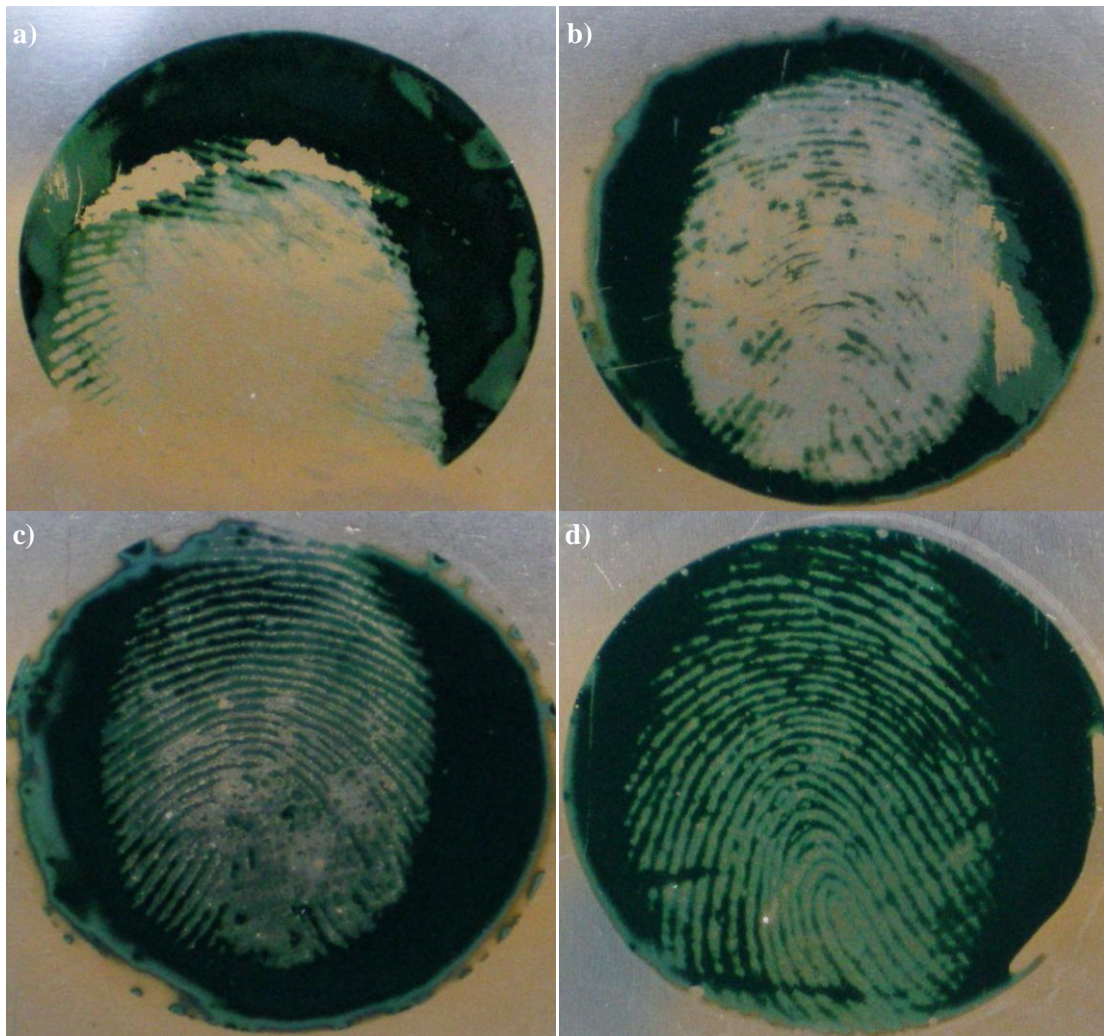


Figure 4.10. Photographic images of fingerprints on stainless steel enhanced via the potentiostatic deposition of PANi ($E = 0.9$ V, varying deposition times), a) 39 days old, 800 s, $1.93 \mu\text{m}$, grade 1; b) 34 days old, 400 s, $1.2 \mu\text{m}$, grade 1; c) 34 days old, 400 s, $0.6 \mu\text{m}$, grade 3; d) 35 days old, 400 s, $0.5 \mu\text{m}$, grade 4.

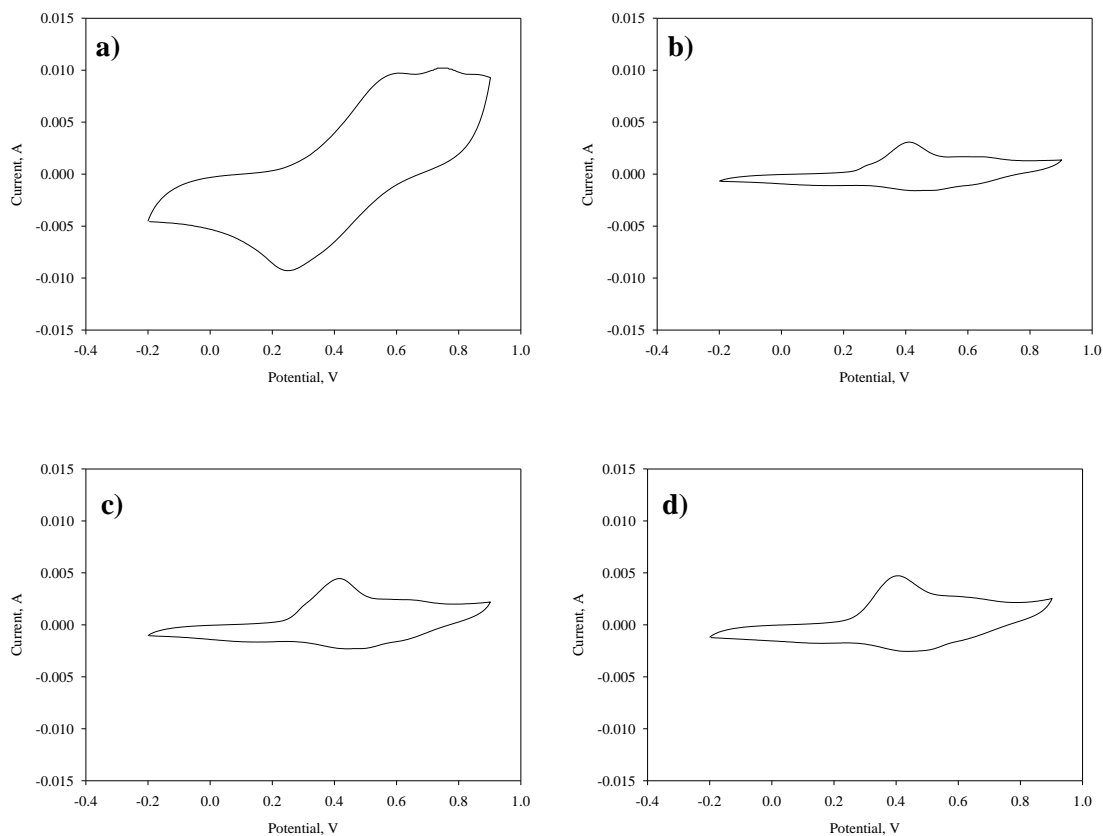


Figure 4.11. The corresponding tenth scan ($-0.2 < E/V < +0.9$, 20 mV s^{-1}) in $1 \text{ M H}_2\text{SO}_4$, of previously deposited PANi onto stainless steel, of the samples found in; a) Figure 4.9a; b) Figure 4.9b; c) Figure 4.9c; d) Figure 4.9d.

To allow for a direct comparison of the magnitude of current drawn during the CV measurements, the graphs in Figure 4.11 share the same scaled axis. As a consequence the redox peaks are less pronounced for Figures 4.11b-c. They do however share a very similar shape to one another with cathodic peaks at approximately $E = 0.40 \text{ V}$, 0.64 V and 0.90 V . The peaks indicate the transition from leucoemeraldine to emeraldine, the presence of degradation products and the formation of pernigraniline, respectively.

The ages of the fingerprints, at the point of enhancement, of 50 samples (10 prints from 5 donors) were compared against the grade they were given individually, see Figure 4.12. From this assessment it can be concluded that there is no apparent correlation between the age of the fingerprint deposit and the possible quality of the developed print. It was shown that a grade 3 or above was possible with fresh prints (2 hrs old) and aged prints (up to 38 days old). Of the samples aged over 13 days old none were given a grade 0. Therefore some degree of distinguishing detail was developed identifying the presence of a fingerprint despite the print residue being on the substrate for over 2 weeks. Multiple samples of the same age, which resulted in the same grade, are illustrated by a red dot. For samples whose age and grade were unique a blue dot has been used.

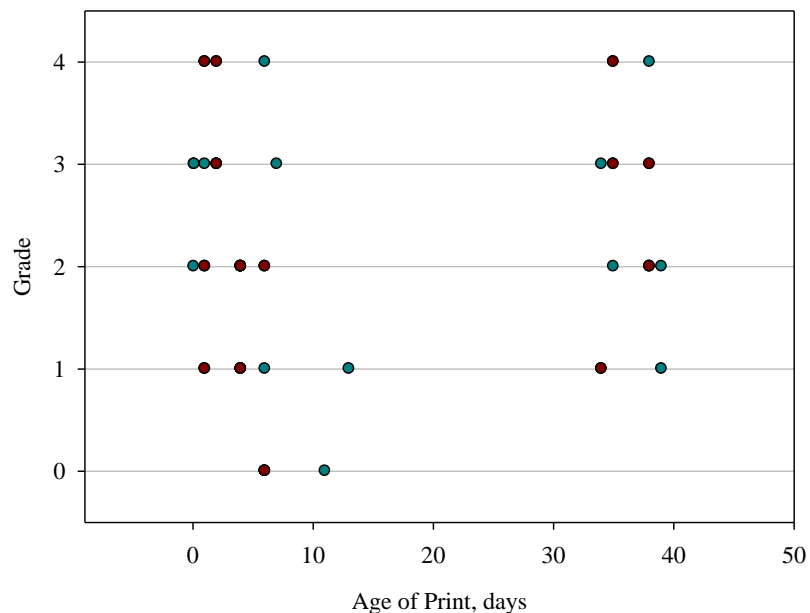


Figure 4.12. A graph showing the data from 50 samples; the age of the fingerprints compared to the grades they were given. Blue dots indicate one sample, whereas red dots indicate more than one sample that fits the same data point.

Deposition time, the time taken to enhance the print or the time taken to draw the conclusion no enhancement of detail was possible, was compared against the corresponding grade (Figure 4.13). Figure 4.13 shows it was possible to achieve a grade 3 after 20 minutes, but also that a grade 4 could be accomplished in just under 5 minutes. For samples that required the same length of time to be enhanced to the same grade, a red dot has been used. Blue dots signify an individual sample of unique deposition time and grade. For this set of samples the average deposition time was 645.2 s and the mode was 400 s. Therefore the majority of samples were developed between 6 - 10 minutes. It would appear, based on this data, that deposition times above 20 minutes will not lead to a useful fingerprint enhancement. The longer the polymerization time, the thicker the film will be and the more likely that overdevelopment will occur. However there was no correlation between the grade and the deposition time; suggesting that the grade of the enhanced prints is dependent on the initial quality of the fingerprint deposit.

With the knowledge that polyaniline possesses more than one oxidation state, each of which exist as a different colour, it was observed how these colours contrasted against the stainless steel substrate. The concept was to observe the potential at which each sample gave the best contrast between polymer deposit and substrate. Since the substrate is fairly pale in colour and the darkest polymer state was accessed at $E = 0.9$ V, samples were assessed *in-situ* commencing at this applied potential and then at 0.1 V decrements down to the palest polymer state at $E = -0.2$ V. After each potential was applied a photograph was taken. A series of images, found in Figure 4.14, demonstrate this process.

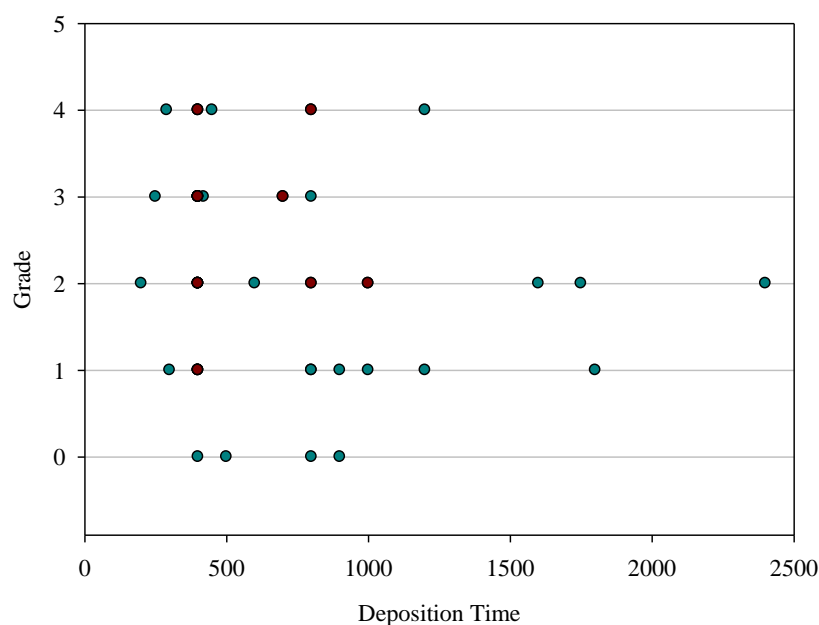


Figure 4.13. A graph showing the data of 50 samples; the time taken to enhance the fingerprints compared to the grades they were given. Blue dots indicate one sample, whereas red dots indicate more than one sample that fits the same data point.

This specific sample has been overdeveloped; the polymer film has been allowed to fill in between and over the ridges into the furrows. However, what these images demonstrate are not only the range of colours available with the PANi deposit, but also by varying the potential, ridge detail can be optimised. In Figures 4.14a-h ridge detail can be seen, but as the applied potential drops below $E = 0.1$ V (Figures 4.14i-l) it becomes increasingly difficult to determine the difference between print and substrate. It is also difficult to determine the *primary detail* of the print as only the very top of the core is visible. Despite this, *secondary detail* such as ridge endings and bifurcations are visible and the print would be a grade 3 on the Bandey scale.

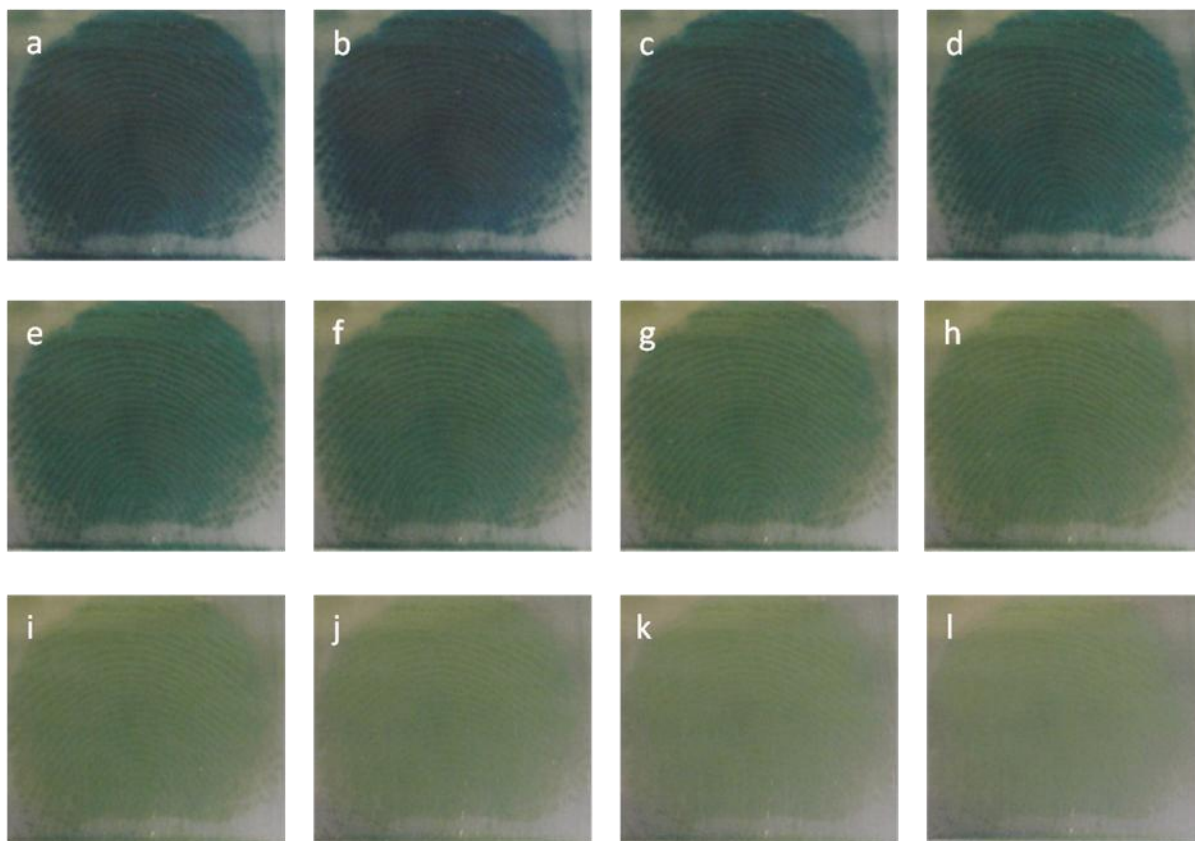


Figure 4.14. A series of *in-situ* photographic images of a previously enhanced, via potentiostatic deposition of PANi, 1 day old fingerprint following a constant potential (10 s) of; a) 0.9 V; b) 0.8 V; c) 0.7 V; d) 0.6 V; e) 0.5 V; f) 0.4 V; g) 0.3 V; h) 0.2 V; i) 0.1 V; j) 0 V; k) -0.1 V; l) -0.2 V. Images have been brightened for the purposes of printing.

The corresponding CV response of the sample in Figure 4.14 can be seen in Figure 4.15. Presented on a different scaled axis to the CVs in Figure 4.11, the peaks can be seen more clearly. However, the CV is not typical of PANi; similarly to the CV in Figure 4.11a there is the absence of the cathodic peak that can be attributed to the oxidation of the film from leucoemeraldine to emeraldine. There are two distinct cathodic peaks at $E = 0.54$ V and 0.61 V, which could be attributed to degradation products. Figures 4.14d-e show the visual response at these approximate potentials, similar in colour with the latter more green than blue indicating a change in the state of

the film. At $E = 0.9$ V a peak is emerging which could indicate the formation of the pernigraniline form of PANi. Figure 4.14a shows a dark blue film which is characteristic of the pernigraniline state. From the images seen in Figure 4.14 there is quite clearly an electrochromic material present on the surface of the stainless steel despite the CV obtained.

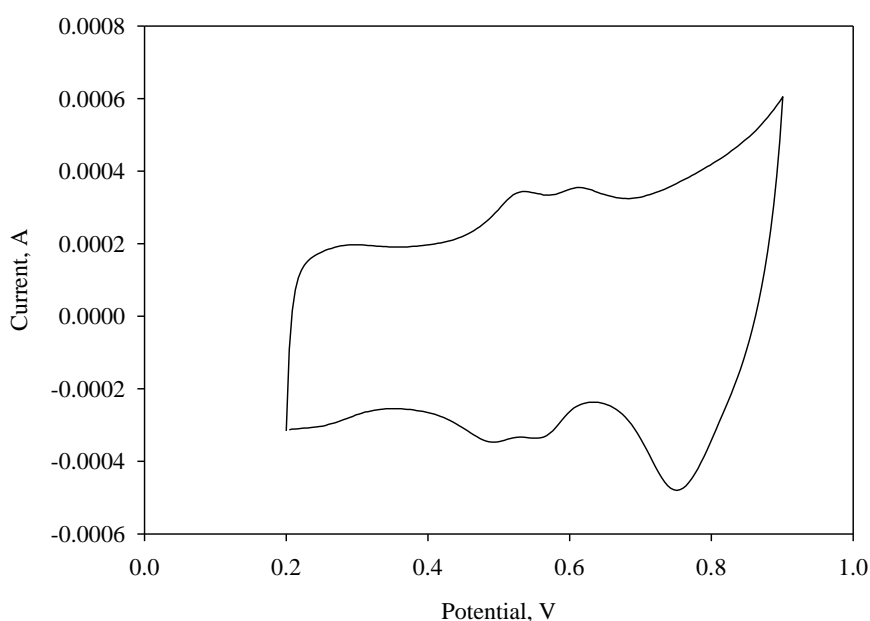


Figure 4.15. The tenth scan of potential ($-0.2 < E/V < +0.9$, 20 mV s^{-1}) in $1 \text{ M H}_2\text{SO}_4$, of the sample found in Figure 4.13, previously deposited PANi (0.9 V , 450 s) to enhance a 1 day old fingerprint on stainless steel.

The overdevelopment of a sample, in localised areas, was not uncommon. Using optical microscopy this occurrence was observed, see Figure 4.16a. In the circled area an excess of polymer has obscured accurate definition of the ridges below. This is most likely the result of a sample that has an unbalanced distribution of residue upon print

deposition, similar to that shown previously in Figure 4.3c. Excess polymer has been deposited due to the lack of ridge detail available to prevent polymerization. An implication that could occur with an overdeveloped sample is the mis-identification of ridge characteristics. For example polymer that spans across more than one ridge could be mistaken for a *bridge* or *ridge crossing* (Chapter 1, Section 1.1.3). In contrast, a sample that has an excess of sweat residue, similar to that in Figure 4.3d, is likely to result in an enhancement like that found in Figure 4.16b. When compared to the rest of the image, the circled area lacks contrast between the fingerprint deposit (substrate) and polymer deposit. This is an example of underdevelopment, which could be a result of a smudged region of a print.

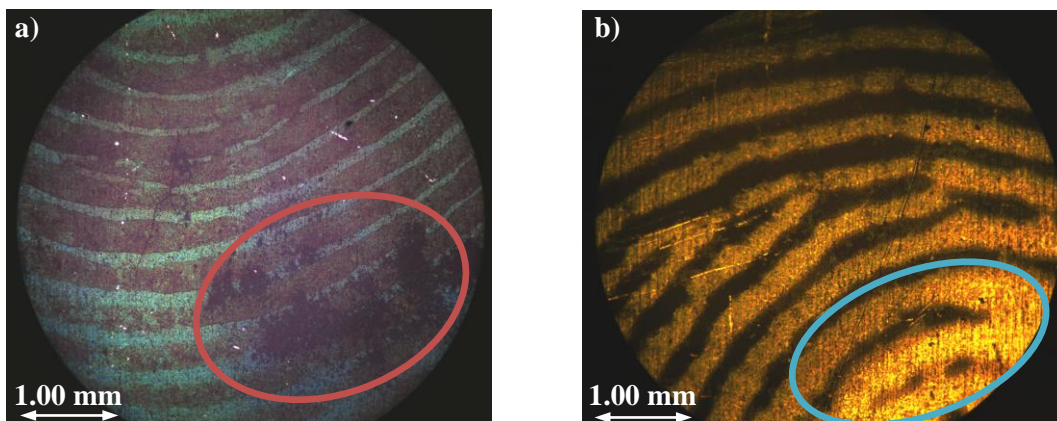


Figure 4.16. Optical microscopy images of fingerprints enhanced via potentiostatic deposition of PANi ($E = 0.9$ V, 800 s) showing a) over-filled furrows, b) under-filled furrows.

Demonstrated in Figure 4.17 is the ability to alter the colour contrast, and ultimately the visibility of ridge detail. This has the practically important attribute of exploiting maximum optical density (accessed at higher potential) for under-filled furrows and

lesser optical density (accessed at lower potential) for fully- or over-filled furrows. Figure 4.17 shows how ridge detail can be made apparent by varying the potential applied to a sample and therefore the contrast; in this case, as potential is increased more detail is visible.

The corresponding CV of the sample in Figure 4.17 can be found in Figure 4.18. The shape is typical of PANi. The cathodic peak at $E = 0.4$ V indicates the transition of states from leucoemeraldine to emeraldine, confirmed by the visual response seen in Figure 4.17c as a green film. The cathodic response at $E = 0.9$ V attributes to further oxidation of the film to the pernigraniline state, the visual result seen below in Figure 4.17f as a dark blue film. At $E = -0.2$ V (Figure 4.17a) the polymer film is at its most reduced form, shown as very pale green to almost transparent in some areas. For some samples accessing this level of optical density would allow for additional enhancement of ridge detail. However, here the best enhancement is found at the highest optical density, $E = 0.9$ V. The main pattern of the print is identifiable as a plain whorl. *Secondary detail*, such as a spur circled in Figure 4.17e and creases in the skin can easily be seen. This level of enhancement would justify a grade 4 on the Bandey scale.

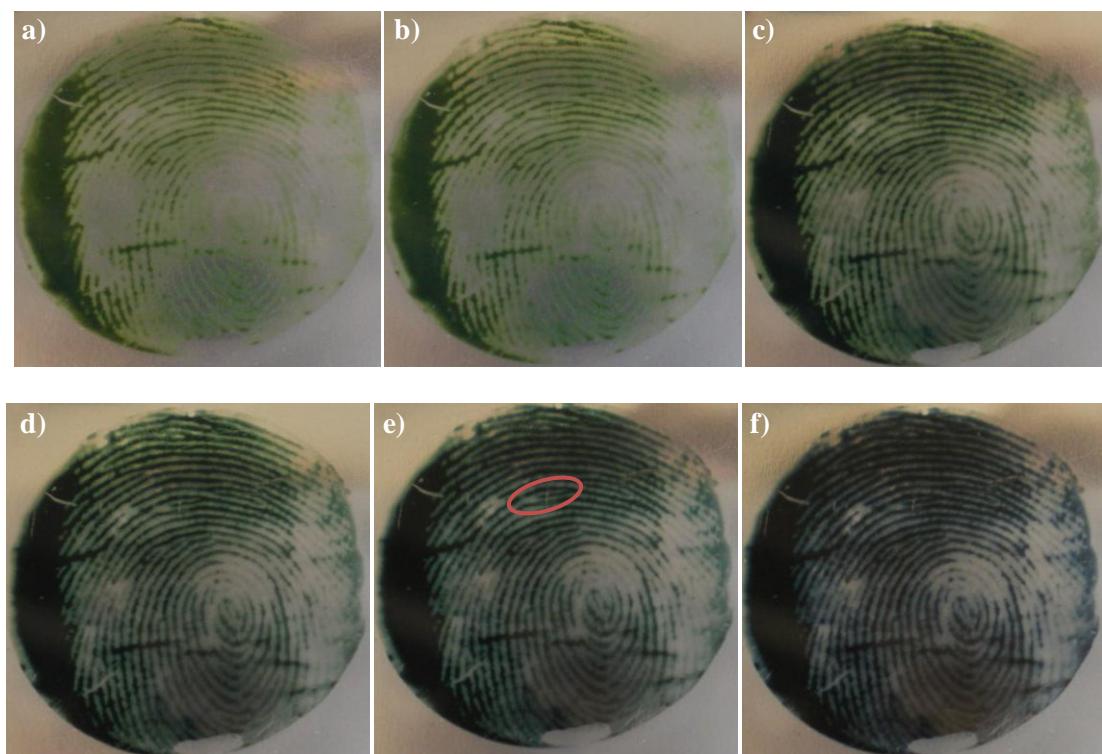


Figure 4.17. 38 days old sebaceous fingerprint on stainless steel enhanced via potentiostatic deposition of PANi ($E = 0.9$ V, 400 s), *in-situ* (1 M H_2SO_4) images taken whilst sample is maintained under potential control; a) -0.2 V; b) 0.1 V; c) 0.4 V; d) 0.6 V; e) 0.7 V (spur circled in red); f) 0.9 V.

It would be expected that as stainless steel is pale in colour the best contrast would be found when the polymer is at its maximum optical density, darkest colour. It was found, however, that a range of applied potentials gave the best contrast and not just at maximum optical density, see Figure 4.19. There is a general trend that as the potential applied is decreased fewer samples were found to display their best contrast. This shows that each sample is unique in its development, just as fingerprint detail is unique to individuals.

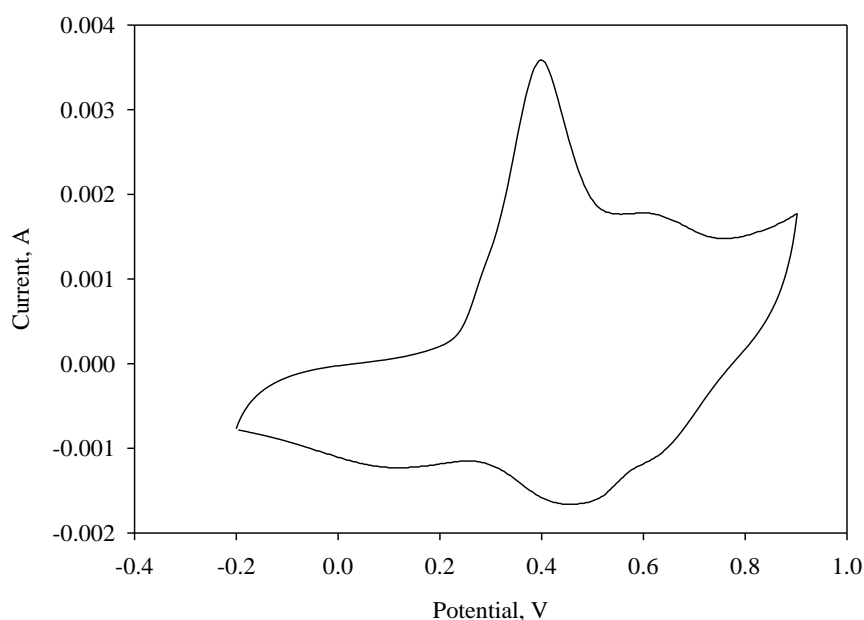


Figure 4.18. The tenth scan of potential ($-0.2 < E/V < +0.9$, 20 mV s^{-1}) in $1 \text{ M H}_2\text{SO}_4$, of the sample found in Figure 4.16, previously deposited PANi ($E = 0.9 \text{ V}$, 400 s) to enhance a 38 day old fingerprint on stainless steel.

As previously discussed, once a sample is *ex-situ* it resides to its natural oxidation state which is green in colour. Seen in the figures above, this colour can also be accessed by applying a constant potential in the range $E = 0.3 \text{ V} - 0.5 \text{ V}$. Referring to Figure 4.19, the combined number of samples giving the best contrast in the potential range $E = 0.3 \text{ V} - 0.5 \text{ V}$ are lower than the combined number of samples for the remaining potentials. With this in mind, it was considered whether the original grades assigned to the developed samples could be improved. The same 50 samples were re-graded by assessing the *in-situ* contrast between print and substrate at an applied potential of $E = 0.9 \text{ V}$, and then at 0.1 V decrements down to $E = -0.2 \text{ V}$. The outcomes are summarized in Figure 4.20.

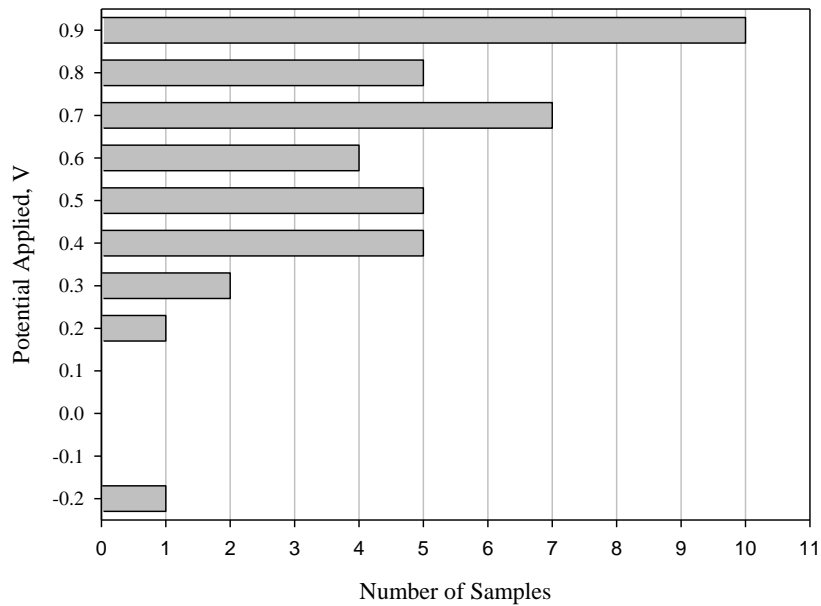


Figure 4.19. A chart showing the distribution of constant potentials (E/V) that produced the best contrast for data set one. Ten of the samples were excluded due to no improved contrast from their natural state.

Insufficient fingerprint residue was present on the four samples previously graded 0 and therefore further enhancement was ineffectual. Out of those eleven formerly given a grade of 1, five were enhanced to a grade 2. Of those fifteen graded 2 a total of eight were taken up to a grade 3. From the twelve samples previously graded 3, two were improved. As for the grade 4 samples improvement was unnecessary.

The average grade of the samples when viewed *ex-situ* was $2.2 (\pm 1.2)$, this increased to $2.5 (\pm 1.2)$ when the samples were re-graded *in-situ*. The critical feature however is a shift of the mode from grade 2 (not useful) to grade 3 (useful). A numerical assessment shows that 20 of the initial prints were grade 3 or 4, but enhancement raised this to 28,

i.e. an increase in the number of useable fingerprints by 16 % to a total of 56 % of the whole data set.

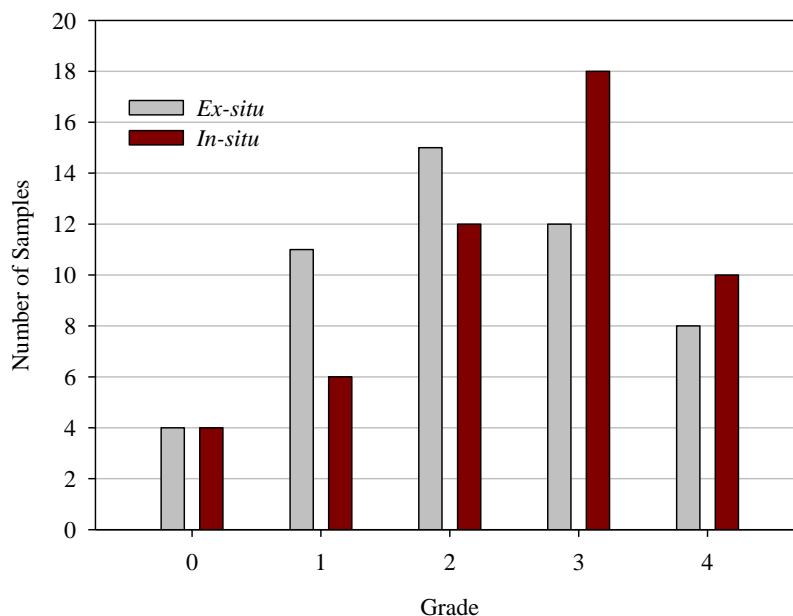


Figure 4.20. Chart showing distribution of sample quality according to the scheme of Bandey. Grey bars represent graded enhancements viewed *ex-situ*. Red bars represent the same samples graded following enhancement whilst viewed *in-situ* under potential control.

4.6. Stainless Steel Knives

Knife crime can appear within many different types of crime: homicide, attempted murder, rape, sexual assault and robbery.¹⁷ In England and Wales, during the year ending June 2012, 29,513 offences involving a knife or sharp instrument were recorded by the police.¹⁷ Despite this number being the lowest it has been in the past four years, it still contributes 51 % of attempted murders and 39 % of homicides. This is why it is incredibly important to ensure development techniques are in place to provide the

greatest possible enhancement they can. Stainless steel is a common material for knife blades, door handles and components of tools such as screwdriver blades, crow bars and jaws of bolt cutters. Therefore the work discussed above has great potential to be applicable to such items.

The work discussed previously involved deposition onto flat plates of stainless steel. With evidentially viable objects such as knives the principles should still apply, with one main difference being the geometry of the substrate. It is widely known that when setting up a one compartment three electrode cell the counter and working electrode should be facing one another. The counter electrode should have at best a similar surface area, but ideally a larger surface area, than the working electrode.¹⁸ Therefore an alternative counter electrode to that used for flat substrates was required, seen previously in Figure 2.1. Fingerprints were deposited onto the stainless steel handles of 25 pieces of cutlery by 4 different donors. An example of an enhancement from a knife can be seen in Figure 4.21a.

A clear and fairly well defined print (grade 3) can be seen in Figure 4.21b, the *primary detail* of the print is a loop and *secondary detail* such as a spur (circled) can be identified. The polymer has also deposited uniformly over the rounded geometry. The ability of the polymer to deposit over a large non-planar area in one step has its advantages, it is not always known where a fingerprint will be present on an item therefore the technique has valuable application to real evidence.



Figure 4.21. Photographic images of a fingerprint (2 days old) on a stainless steel knife, enhanced via potentiostatic deposition of PANi ($E = 0.9$ V, 500 s); a) full image; b) zoomed image of handle with spur circled in red.

4.7. Conclusion

The enhancement of latent fingerprints on stainless steel has been demonstrated, via the selective deposition of PANi. The fingerprint residue acted as a mask to the metal substrate preventing polymerisation in these localised areas. Via different means of visualisation this theory was confirmed. It was possible to identify *primary*, *secondary* and *tertiary detail* through the use of both digital imaging and optical microscopy. The ability to access all three levels of detail would allow a fingerprint expert to correctly identify a positive fingerprint match.¹⁸

In addition to the enhancement of *latent* fingerprints, the technique demonstrated it is applicable to *visible* prints that are lacking in clarity of ridge definition. It was shown that for these samples further ridge definition and *secondary detail* was achievable.

There were, however, samples where variation in the residue height resulted in a varied level of enhancement across a print. In regions where residue heights were low definition was lost, yet the remaining print area where residue height was higher ridge detail was visible. Therefore some samples were overdeveloped: the polymer film filled the furrows of the print before extending deposition across the ridges.

After grading a set of 50 samples it was found that a grade 3 or above for fresh and aged prints, short and long deposition times were achievable. Parameters such as the age of the fingerprint deposit and the time lapsed for the development of the print were compared against the given grades. No correlation between the two parameters and the grade was found. Also individual donors produced fingerprint deposits that when developed were not all given the same grade. It would appear that the quality of the fingerprint deposit at the time of deposition is the factor that determines the impending grade given to any one sample. This would be the case with any technique, as prints can be smudged or there be a lack of sweat to create a useful print. Each sample, like donors fingerprint detail, was found to be unique. This can be attributed to the many variables; type of fingerprint deposit, polymerization time and thickness of polymer, which can all contribute to the overall quality of the enhancement.

By accessing PANi's electrochromic properties upon transfer of the polymer-coated substrate to a monomer-free electrolyte, the optimal visual contrast between fingerprint and polymer was obtained. Therefore varying the potential applied to under- and overdeveloped samples made it possible to visualise ridge detail that was both undefined and present below an excess of polymer, respectively. This procedure

resulted in 16% of the samples, previously unusable, to be given a grade that would be usable in court for a conviction. In previous fingerprint development techniques the ability to ultimately choose the colour/contrast has not been demonstrated.

Once samples were removed from the electrolyte solution they were rinsed; the majority of samples (97.75 %) were left unaffected by this process maintaining their original grades. However ridge detail was lost from two samples, where the polymer film had detached from the metal surface resulting in the samples being down-graded. The polymer films also showed that, under appropriate storage conditions, they have a shelf life of at least three years; the three distinct colours still accessible *in-situ* after this time. This robust feature could be quite significant in a criminal case where evidence is re-evaluated.

As well as the successful enhancement of fingerprints from *model* substrates, print residue from evidentially viable items was demonstrated. The application of the technique to an item whose geometry is not planar is advantageous. Very few pieces of evidence are likely to be flat sections of metal.

Although a high percentage of the samples (90%) developed were made up of sebaceous deposits, it was these samples that gave higher quality developed prints rather than the eccrine deposits. Most established techniques for the development of latent prints rely on the presence of fatty constituents from sebaceous residues. This method is no different, sebaceous deposits most likely gave higher quality prints due to the constituents being less soluble in the aqueous electrolyte. Pure eccrine deposits are

less common as sweat produced from the fingertips is easily contaminated with sebaceous sweat, once hands have been washed, either by touching ones face or hair.

It proved difficult to measure accurately the area that the polymer had deposited onto due to the development taking place between the ridges, leaving some of the substrate polymer free. Generally the polymer deposit covered half of the whole possible area for development therefore it can be assumed that the actual thickness of the polymer deposit is twice that of the calculated values, which has been taken into account for all values stated here. However some samples were overdeveloped so polymer deposit spanned the entire deposition area, therefore each sample must be considered individually.

4.8. References

1. A. L. Beresford, A. R. Hillman, *Anal. Chem.*, 2010, **82**, 483.
2. T. A. Skotheim, *Handbook of Conducting Polymers*, 1st edn., 1986, Marcel Dekker, Inc., New York.
3. A. A. Argun, P. H. Aubert, B. C. Thompson, I. Schwendeman, C. L. Gaupp, J. Hwang, N. J. Pinto, D. B. Tanner, A. G. MacDiarmid, J. R. Reynolds, *Chem. Mater.*, 2004, **16**, 4401.
4. A. R. Hillman, A. M. Mohamoud, *Electrochim. Acta.*, 2006, **51**, 6018.
5. C. Yang, L. Huang, Y. Chih, W. Lin, F. Liu, T. Wang, *Polymer*, 2007, **48**, 3237.
6. G. H. Shim, M. G. Han, J. C. Sharp-Norton, S. E. Creager, S. H. Foulger, *J. Mater. Chem.*, 2008, **18**, 594.
7. B. P. Jelle, A. Gustavsen, T. N. Nilsen, T. Jacobsen, *Sol. Energ. Mat. Sol. C.*, 2007, **91**, 342.
8. J. L. Camalet, J. C. Lacroix, T. D. Nguyen, S. Aeiyaich, M. C. Pham, J. Petitjean, P. C. Lacaze, *J. Electroanal. Chem.*, 2000, **485**, 13.
9. M. Mazur, P. Predeep, *Polymer*, 2005, **46**, 1724.
10. K. R. Prasad, N. Munichandraiah, *Synthetic Met.*, 2001, **123**, 459.
11. S. Pruneanu, E. Veress I. Marian, L. Oniciu, *J. Mater. Sci.*, 1999, **34**, 2733
12. E. Piccinini, M. Giacinti Baschetti, G. C. Sarti, *J. Membrane Sci.*, 2004, **234**, 95.
13. H. Schenderlein, A. Voss, R. W. Stark, M. Biesalski, *Langmuir*, 2013, **29**, 4525.
14. N. J. Bright, T. R. Wilson, D. J. Driscoll, S. M. Reddy, R. P. Webb, S. Bleay, N. I. Ward, K. J. Kirkby, M. J. Bailey, *Forensic Sci. Int.*, 2013, <http://dx.doi.org/10.1016/j.forsciint.2013.03.047>.
15. G. L. Thomas, T. E. Reynoldson, *J. Phys. D: Appl. Phys.*, 1975, **8**, 724.

16. H. L. Bandey, Fingerprint development and imaging newsletter: the powders process, study 1. Sandridge: Police Scientific Development Branch, Home Office, 2004; Report No.:54/04.
17. G. Berman, Knife Crime Statistics, *House of Commons Library*, SN/SG/4304, 2012.
18. A. R. W. Jackson, J. M. Jackson, *Forensic Science*, 2004, Pearson Prentice House, Harlow, UK.

Chapter Five

5. Application of Polymer Enhancement to Fingerprints on Diverse Metal Surfaces

5.1. Overview

The previous chapter demonstrated how a new technique has been developed to enhance latent fingerprints on stainless steel surfaces. Stainless steel is a common material for evidentially viable items, but there are clearly many different metal types that also hold the potential to be of forensic value. Whereas the following chapter, Chapter 6, describes the effect of parameters such as exposure time and fingerprint donor, this chapter focuses on expanding the application of the technique to a range of different metal surfaces. The surfaces discussed below have been chosen for their potential forensic value.

Metal theft, the act of stealing metal on a large scale, is amongst the many crimes for which metal can be one of the pieces of evidence retrieved for fingerprint analysis. Amongst those metals targeted in metal theft are brass, copper, and lead,¹⁻³ this is the reason for their inclusion in this study. As well as evidentially valuable ‘model’ surfaces, evidentially viable items, such as spent cartridges, of different elemental composition have been investigated for two reasons. The first is to broaden the scope of metal surfaces beyond those previously mentioned. The second is to assess the polymer deposition technique’s ability to enhance fingerprints on a surface that possesses a unique geometry.

A *cartridge* encompasses all the components required for a round of ammunition, Figure 5.1 illustrates these. The bullet, propellant and primer are the key components. The bullet is the part that is discharged from the gun when it is fired; it is firmly set in to the end of the cartridge. Behind the bullet, in the cartridge, is the tightly packed propellant which fuels the exit of the bullet.⁴ At the base of the cartridge is the primer, which is a high-explosive that can be detonated by a quick shock, such as a fast moving firing pin. Once the firing pin hits the primer it will explode, igniting the propellant.⁴ The gases produced are strong enough to push the bullet from the cartridge and down the barrel of the gun, leaving the cartridge behind.⁵ The cartridge bears the brunt of the explosion;⁶ abrasive friction is caused leaving marks on the cartridge from its subsequent ejection from the gun chamber.⁷

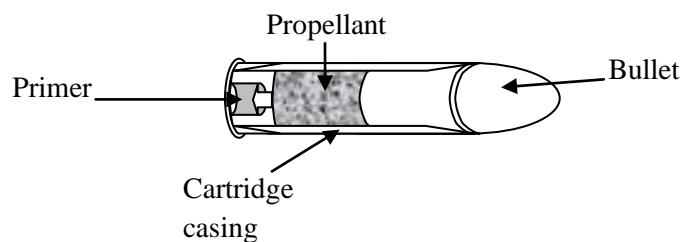


Figure 5.1. An example of a cartridge and the components that make ammunition.⁸

The metals considered in this chapter have different properties for which the process of polymer deposition, and therefore their fingerprint enhancement, will differ somewhat from that of stainless steel. As previously discussed in Chapter 3, lead, copper and brass can form passive layers on their surfaces when exposed to certain conditions.

5.2. Fingerprint Development from Brass

Brass is a commonly used material in the manufacturing of bullets and their cartridges. Some criminals, prefer their ammunition to be aesthetically pleasing and will polish their brass bullets.⁹ This would allow for better deposition of polymer, if the surface is clean and highly polished. However it is more likely that the ammunition recovered for fingerprint analysis is that of previously fired cartridges, which may have even been recycled.⁹ Inhibition of subsequent fingerprint visualization has been shown to be caused by the increased temperature due to the firing process, especially blowback,⁶ and abrasive friction caused by loading and ejection of the cartridge.⁷ The heat produced within the chamber of the gun can cause the fingerprint to no longer be visible to the naked eye. However, this does not necessarily mean that the detail is gone. During this process the residue may change the chemistry of the cartridge surface in localised areas, thus requiring treatment in order for subsequent visualisation.

The electrochemical redox reactions that can occur between latent fingerprints and the metal have been explored extensively by Bond.¹⁰⁻¹² It was shown how fingerprint deposits on brass produced sufficient corrosion of the metal to enable the fingerprint to be visualized even after attempts had been made to remove the residue of the fingerprint deposit.

Polymers, such as polyaniline and its derivatives, possess protective properties and for this reason have been previously electrochemically synthesised onto a range of different metals, including brass, to prevent corrosion.¹³⁻¹⁵ However there are

complications when electrochemically depositing onto brass in the form of dezincification, see Equation 5.1



When measured against a Ag|AgCl|saturated KCl reference electrode the anodic dissolution of brass occurs at approximately -0.18 V in 0.2 M sodium oxalate ($\text{Na}_2\text{C}_2\text{O}_4$); at approximately +0.26 V passivation should be complete.¹³ A complex mechanism results from the formation of insoluble copper and zinc oxalate compounds. An increase in the current at approximately +0.30 V, which is attributed to the oxidation of CuO to Cu_2O on the brass substrate, has previously been measured.¹³ As a consequence four passivation layers arise. Despite these complications successful deposition of PANi, from a $\text{Na}_2\text{C}_2\text{O}_4$ solution, onto brass has been achieved.¹³ Therefore $\text{Na}_2\text{C}_2\text{O}_4$ was used as the background electrolyte in the deposition of PANi.

The effect of $\text{Na}_2\text{C}_2\text{O}_4$ on polished brass was assessed alongside electrolyte with the monomer aniline present. The results can be seen in Figure 5.2. There was a distinct difference having the aniline present under these conditions, both chemically and visually. The current drawn, scanning in the potential range $-0.4 < E/\text{V} < +1.8$, was considerably lower with aniline present, Figure 5.2a. The current passed, under the same conditions, stayed consistently higher for the monomer free solution, particularly between $+1.0 < E/\text{V} < +1.8$, Figure 5.2b. Both the anodic and cathodic peaks obtained for each solution appeared at different potentials, indicating that different reactions were occurring. By the end of potential cycling with aniline present, the solution had turned from colourless to pale yellow. The solution containing only $\text{Na}_2\text{C}_2\text{O}_4$ became increasingly clouded by the precipitation of a blue substance, $\text{Cu}(\text{OH})_2$. The presence

of aniline resulted in a pale brown fairly uniform coverage to the substrate. The absence of aniline gave an irregular blue/green treatment to the substrate.

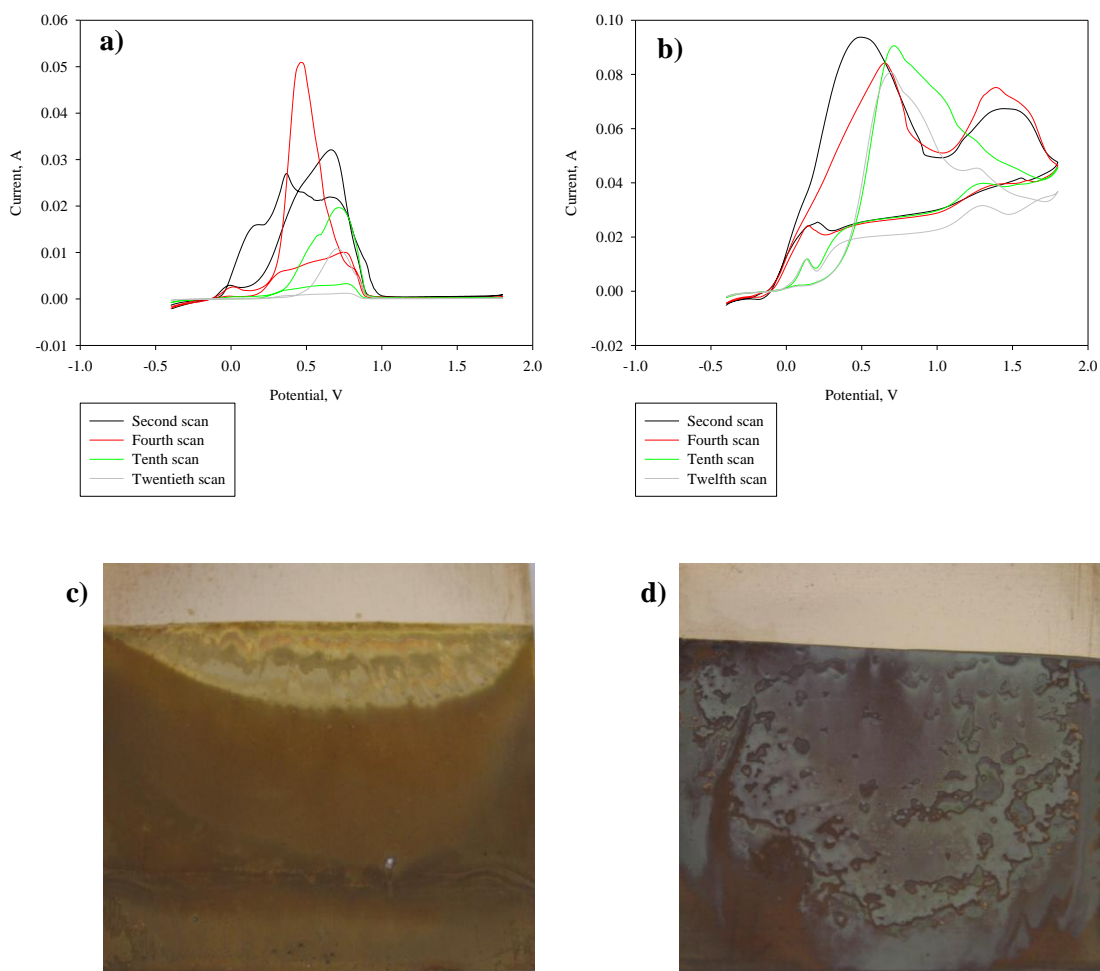


Figure 5.2. The second, fourth, tenth and twentieth scan of potential, in the range $-0.4 < E/V < +1.8$, of polished flat brass in a) 0.12 M aniline, 0.2 M $\text{Na}_2\text{C}_2\text{O}_4$ at 20 mV s^{-1} ; b) 0.2 M $\text{Na}_2\text{C}_2\text{O}_4$ at 20 mV s^{-1} ; *ex-situ* photographic images of the resulting samples c) and d) respectively.

A combination of donors, time periods and cleaning regimes were used in the analysis of polymer treatment on model brass substrates. Both positive and negative images of

fingerprints, from three proposed scenarios, occurred in the development of the brass substrates. A negative enhancement can be determined by a visible change to the background substrate. Therefore, if a reagent appeared white following enhancement on a black background, the latent print would appear black on a now white background, Figure 5.3a. A positive enhancement can be determined by a visible change to the regions covered by the latent print. Therefore, if a reagent appeared white following enhancement on a black background, the latent print would appear white on the still black background, Figure 5.3b.



Figure 5.3. Examples of enhancements on black substrates a) negative; b) positive.

The first scenario, in accordance with the results discussed in Chapter 4 and previous work,¹⁶⁻¹⁸ found the sweat deposited acted as an insulator to the brass surface when aged for up to two days, Figure 5.4. Negative enhancements of the fingerprints left on the surface showed clear ridge detail and even *tertiary detail* such as the position of sweat pores, circled in Figure 5.4a.

Samples that were aged for longer than two days, up to a week, had started the corrosion process and mixed results were achieved. Ridge detail was not as well defined and polymer deposition was patchy. As the prints age, fewer components, that were present at the time of deposition, will be found on the metal surface. The composition of fingerprint residue can change over time; the aging process can follow many different pathways and at considerably different rates. Significant physical and chemical changes, such as evaporation, degradation, drying, migration and oxidation can occur.¹⁹ If the entire fingerprint deposit was to degrade from the metal surface there would no longer be an electrical insulator to prevent polymer deposition, therefore a relatively uniform polymer deposit should be achieved. The results however contradicted this and patchy polymer deposits were observed. Through the knowledge that brass naturally forms an oxide layer on its surface, and that leaving fingerprint deposits on brass under the same conditions for several days can produce corrosion products, it is proposed that the natural oxide layer formed prevented polymer deposition.



Figure 5.4. An *ex-situ* photograph of a negative enhancement via PANi deposition ($-0.4 < E/V < +1.8$, 20 mVs^{-1}) of a two day old fingerprint on previously polished brass, a) full print; b) enlarged region with *secondary detail* (ridge ending, circled in red) and *tertiary detail* (pore position, circled in blue) visible.

The second proposed scenario involved samples that were washed prior to enhancement, removing any remaining fingerprint deposit, in accordance with Paterson *et al.*²⁰ Despite a thorough cleaning regime, negative enhancements of the prints were obtained. Therefore the insulating qualities could no longer be the responsibility of the previously placed sweat deposit. Very clear ridge detail was attained and as before the position of the sweat pores were visible, Figure 5.5. As all traces of the sweat deposit had been removed, another surface alteration must have occurred to still achieve a visible image of a print. Most likely, the sweat deposit, prior to its removal, triggered the corrosion of the brass thus changing the chemistry of the surface. The initiation of the process is caused by the presence of chloride ions in the sweat deposit, which have been shown to react with both zinc and copper to form complex metal chlorides.²¹ In terms of copper, the process is initiated by the formation of CuCl at the

brass/fingerprint interface followed by further reaction with chloride ions to form the complex



which can then form copper (I) oxide via hydrolysis



In an acidic environment, brass dissolution is more thermodynamically favourable because at equilibrium the reaction lies in favour of the oxidised species of Equation 5.4



where the overall standard potential is $E^\circ = -0.76$ V, for Equations 5.4-5.5. Therefore the production of hydrogen ions causes the corrosion process to accelerate.²² Zinc complexes can also be formed through interaction with chloride ions or with the copper (II) chloride complex



Similarly, this zinc complex can undergo hydrolysis, forming zinc oxide with the production of hydrogen ions



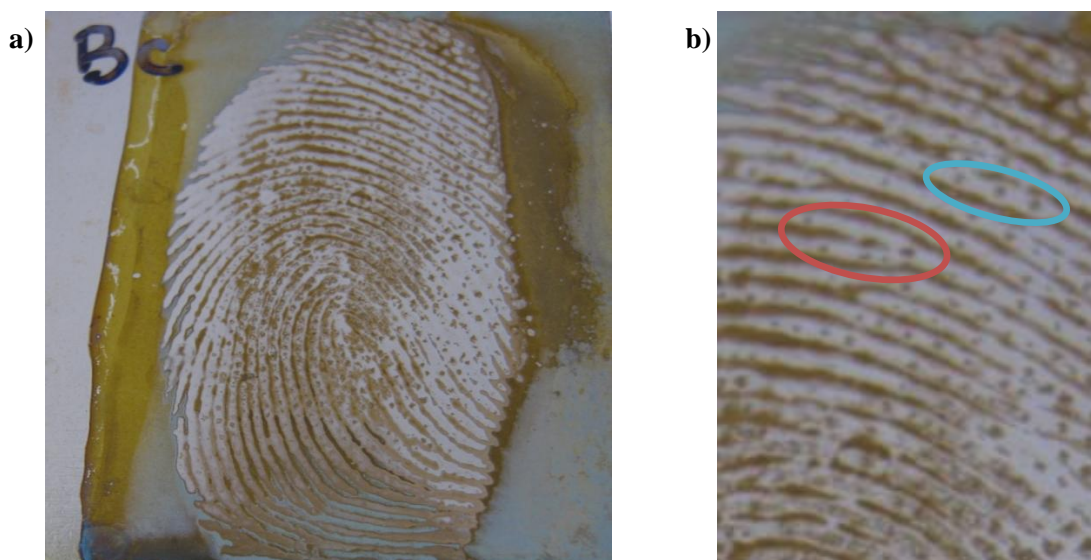


Figure 5.5. An *ex-situ* photograph of a negative enhancement via PANi deposition ($-0.4 < E/V < +1.8$, 20 mVs^{-1}) following removal of a month old fingerprint on previously polished brass, a) full print; b) enlarged region with *secondary detail* (bifurcation, circled in red) and *tertiary detail* (pore position, circled in blue) visible.

The production of chloride ions, seen in Equations 5.3 and 5.8, allows the corrosion process to continue until the water content in the sweat has evaporated, thereby inhibiting the mobility of ions in the remaining deposit. The regions of brass once covered by the fingerprint remain polymer free, with the deposition occurring around the ridge detail. This can be explained with the aid of Figure 5.6a that shows an equivalent circuit for the one compartment three electrode set up, in which the current flow has a choice of pathways, shown in detail in Figure 5.6b. As stated previously, this oxide layer above the brass could be copper (I) oxide, zinc oxide or, more likely, a mixture of the two.²³ The majority current flow is determined by the path of least electrical resistance. Therefore the regions of brass once covered by the fingerprint

must offer a higher resistance to the surrounding area, so preferential deposition of the polymer occurs between the ridge details.

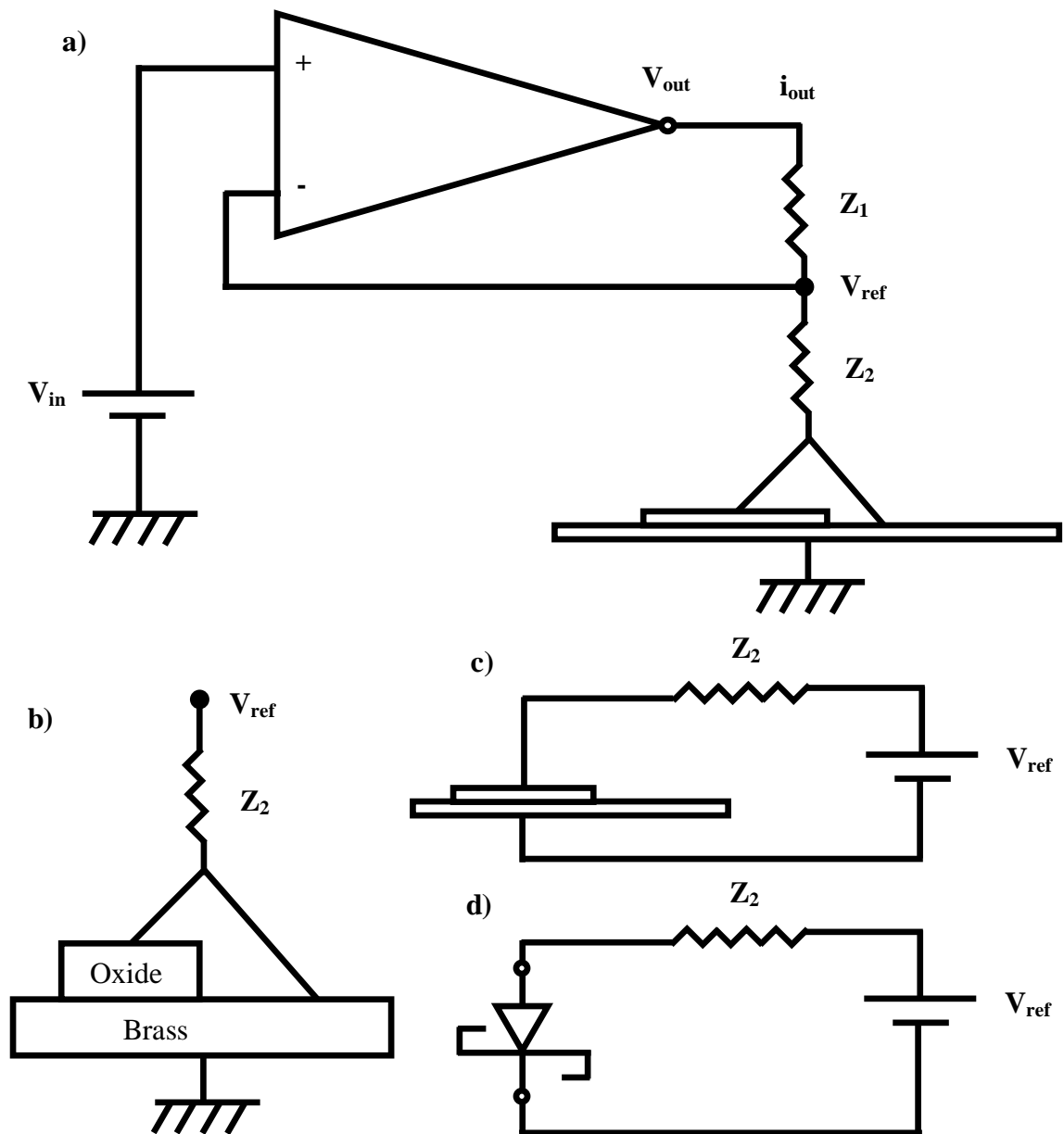


Figure 5.6. Schematic diagrams of a) the circuit; b) what is happening at the working electrode; c) the equivalent circuit found at the working electrode; d) the equivalent circuit showing the forward biased Schottky diode.

The third and final scenario was found amongst the samples that had undergone a post print cleaning regime, prior to enhancement. Fingerprint detail was achieved; however, some results were unexpected. Positive enhancements of the print were acquired, Figure 5.7.

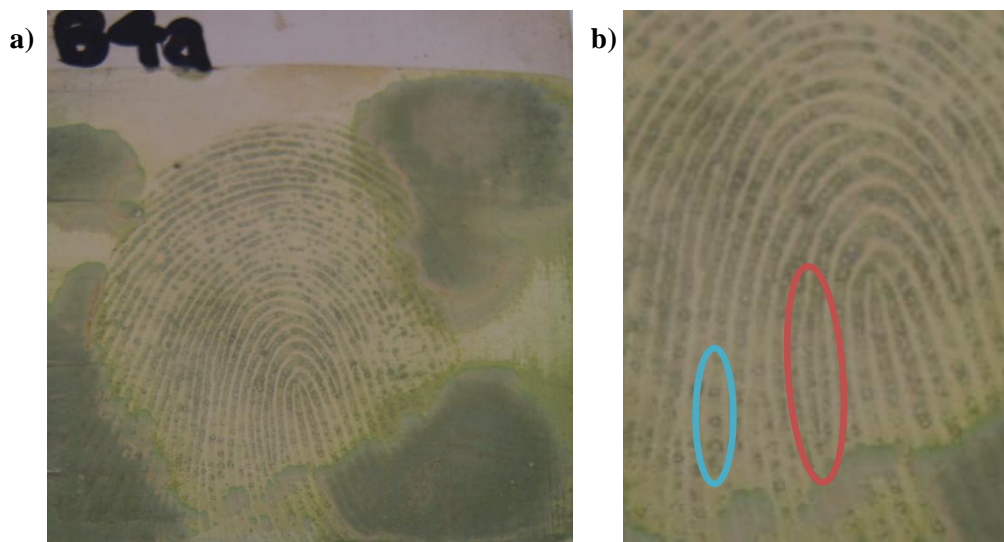


Figure 5.7. An *ex-situ* photograph of a positive enhancement via PANi deposition ($-0.4 < E/V < +1.8$, 20 mVs^{-1}) following removal of a four day old fingerprint on previously polished brass, a) full print; b) enlarged region with *secondary detail* (large lake, circled in red) and *tertiary detail* (pore position, circled in blue) visible.

The polymer was found to deposit along the ridges rather than between them, as would be expected. The detail obtained from the positive enhancements was as good as the negatively enhanced prints showing *tertiary detail* that is illustrated by the use of SEM in Figure 5.8. The SEM image shows positive enhancement of both pore and ridge detail. The small slightly rounded breaks in the deposition are the positions of the sweat pores along the ridges. Between the ridges small amounts of deposition that has started to occur can be seen.

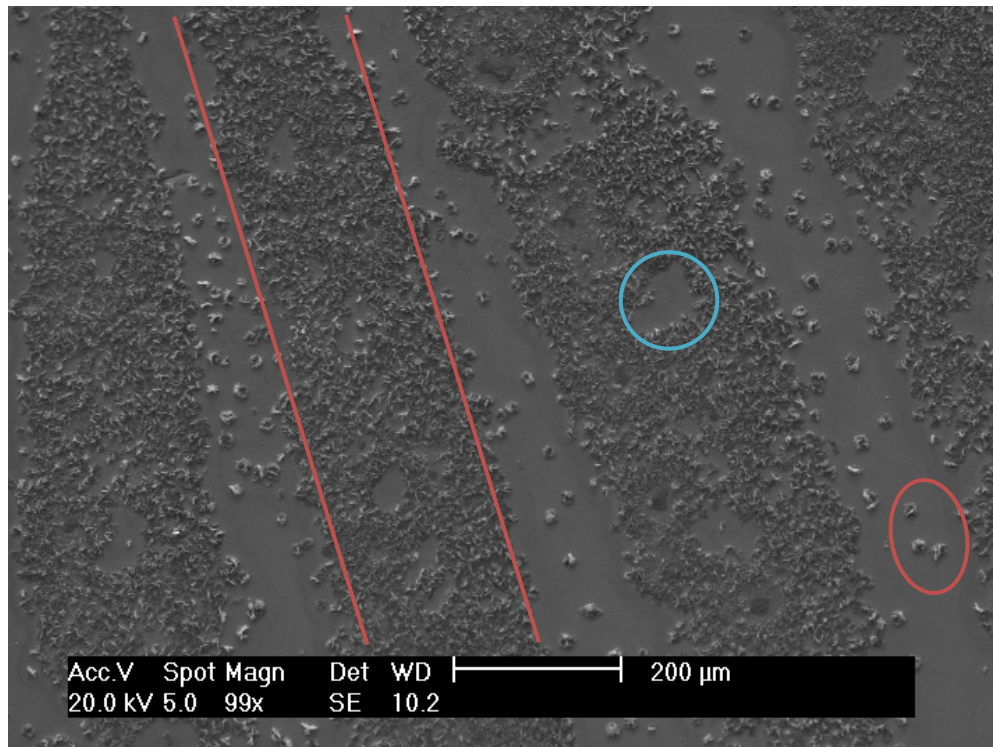


Figure 5.8. SEM image of positive enhancement (polymer on ridges, between red lines) small amount of over development (polymer between ridges, circled in red) tertiary detail visible (pore circled in blue).

The fingerprint donor is the only variable within each age of fingerprint deposit; it is hypothesised that the consistency of the donors sweat be a factor in the corrosion of the brass surface.²⁴ The same eight donors were used for the different time periods of prints deposited; amongst them one donor's prints always produced a positively enhanced image. The remaining positively enhanced prints made up just under one third of the total number of samples. The path of least resistance has therefore changed in Figure 5.6b from the brass to the oxide route. As stated above, the oxide, discussed previously, can either be copper (I) oxide (p-type semiconductor) or zinc oxide (n-type semiconductor), or a mixture of the two. A semiconductor is a substance with electrical conductivity intermediate between that of a conductor and an insulator.²⁵ The orbitals

of their electrons overlap and their individual energy levels are separated out into energy bands. The net movement of electrons in the conduction band, and empty states called 'holes' in the valence band constitute conduction within the semiconductor. Electrons and holes are charge carriers. Where the majority carriers are electrons the semiconductor is n-type; a p-type semiconductor therefore has holes as the majority carrier.²⁵

If V_{ref} (Figure 5.6b) is greater than zero then, at the working electrode, the equivalent circuit given in Figure 5.6c will be the more appropriate model. Previous work has shown how electrochemical oxidation can give rise to the formation of a Schottky barrier diode between the corrosion product copper (I) oxide or zinc oxide and its brass substrate.¹¹ In the configuration shown in Figure 5.6c, for this diode to be forward biased, the oxide must be p-type and therefore has to be copper (I) oxide, rather than zinc oxide,¹¹ Figure 5.6d. To aid in the understanding of this, firstly an energy diagram (Figure 5.8) for a *n-type* semiconductor in close contact with a metal, such that a Schottky barrier forms, is described.²⁶ In Figure 5.9, Φ_m is the work function of the metal and Φ_n is the work function of the semiconductor. E_C , E_f and E_v represent the semiconductor conduction, Fermi level and valence bands respectively. Also, χ = electron affinity, E_g = energy gap, ψ_{bi} = built in potential and Φ_{bp} = potential barrier.

Figure 5.9a shows the energy levels of the metal and semiconductor when in separate systems. As they are brought into the same system and the gap δ is reduced ($\delta = 0$, Figure 5.9b), the built in potential increases. This is the potential seen by the electrons in the conduction band when trying to move from the semiconductor to the metal.

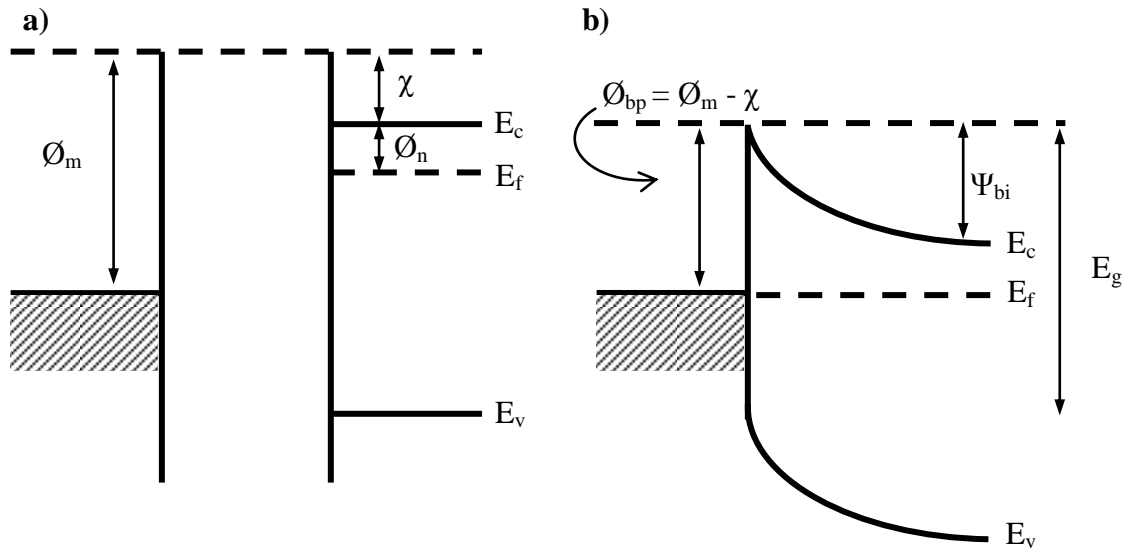


Figure 5.9. Energy diagram for a metal and an ‘n-type’ semiconductor; a) in separate systems; b) connected into one system resulting in the formation of a Schottky barrier. The dotted line at the top of each diagram represents the vacuum level.²⁶

For a p-type semiconductor, in close proximity with a metal, the direction of bending of the energy bands is reversed. The built in potential for a p-type semiconductor is the potential seen by holes in the valence band when trying to move from the semiconductor to the metal and has been measured by Bond¹² as approximately 0.4 V for a brass/copper (I) oxide junction formed from fingerprint corrosion of the brass. Similarly, the potential barrier (Φ_{bp}) has previously been measured at 0.50 ± 0.04 V¹² and this potential must be overcome before a forward biased current can flow.

The potential applied in these experiments exceeds both the built in potential and potential barrier therefore, with a forward bias, the copper (I) oxide readily acts as a conductor allowing polymer deposition to occur along the ridge detail thus a positive print is obtained. It can be seen in Figure 5.8 that polymer has not only deposited along the ridges but has also started to deposit on the surrounding area. It would appear that

instead of the corrosion acting as an electrical insulator it is now offering comparable or lower electrical resistance to the surrounding area. Alternatively, as the potential is being cycled it is possible that when the potential is below ϕ_{bp} , between -0.2 V and 0.4 V, the copper (I) oxide is now electrically insulating and allowing polymer deposition to occur on the surrounding area, which can be seen previously in Figure 5.7. If the oxide layer had been predominantly zinc oxide, then, in this experimental configuration, the Schottky barrier would have been reversed biased, resulting in a negligible local current flow.

Brass cartridges, where handling prior to firing was by ungloved hands, were analysed for fingerprint detail. The majority of the cartridges displayed no visible fingerprint detail prior to their attempted development via polymer deposition. Of the twenty-five cartridges assessed, four resulted in some degree of development of detail. Similarly to the model brass substrates, both positive and negative enhancements of fingerprints occurred in the development of the brass cartridges.

To achieve a representative example of the first of the above proposed scenarios, bullet cartridges were made safe, therefore were not fired to ensure that the sweat deposit was on the surface of the cartridge acting as an insulator rather than corrosion. As previously discussed, the development of fingerprints from previously fired cartridges is problematic. The sweat deposit can suffer a degree of degradation due to aspects of the firing process. Therefore by enhancing a deposited print on a cartridge that has been made safe will show the level of detail possible from a 'clean' brass cartridge. No prior grooming of the fingerprints deposited for the study took place; therefore there was no guarantee of enhancement to all fingerprints deposited. Figure 5.10 shows a negative

enhancement (as would be expected); this is determined by the coverage of green polymer to the main body of the cartridge. The ridge detail has prevented polymer deposition and is viewed as the same colour as the original brass background. In some areas of the enhancement pore position can be seen, Figure 5.10c, polymer has been able to deposit in these regions.

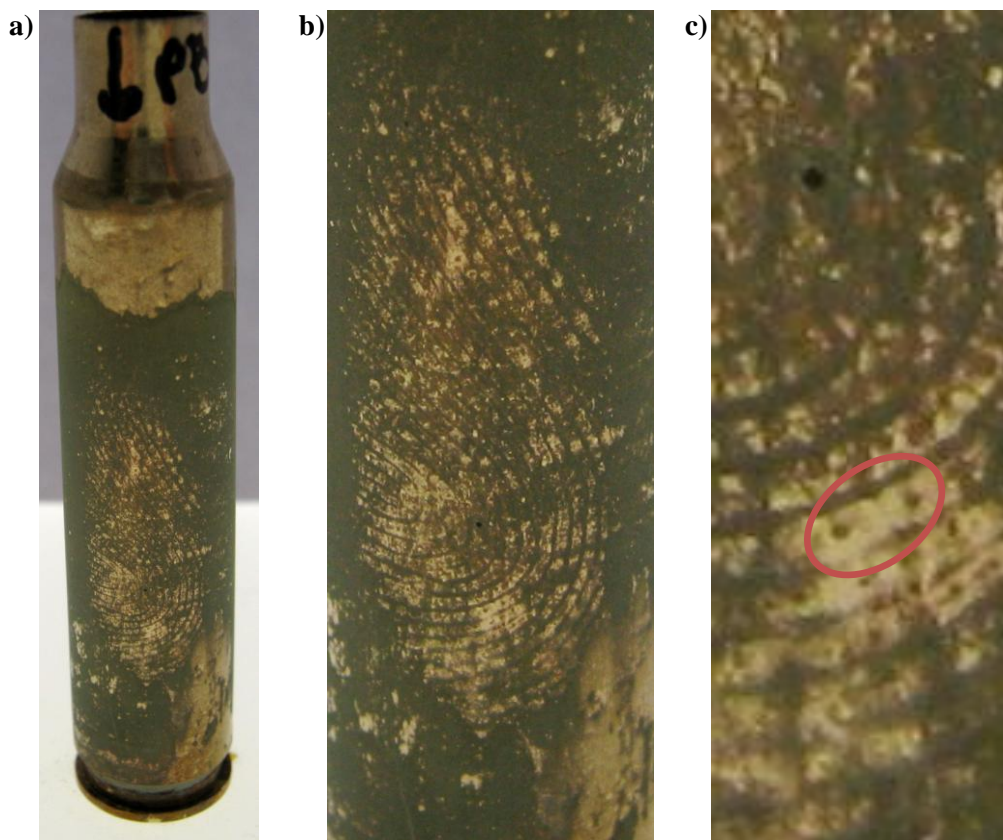


Figure 5.10. An *ex-situ* photograph of a negative enhancement, via one full scan of potentiodynamic deposition in the range $-0.2 < E/V < +0.6$ in 0.1 M aniline, 0.1 M $\text{Na}_2\text{C}_2\text{O}_4$, of a two day old print on a cartridge that has been made safe a) the full cartridge; b) enlarged region showing ridge detail; c) enlarged region showing visible pore position.

The remaining brass cartridges used in this study were fired through a rifle, following their loading by an ungloved hand. No further treatment/cleaning of these cartridges

took place prior to their development. A large percentage of the cartridges did not provide enhancement of print detail following development as would be expected. The cartridges that resulted in a successful enhancement can be seen in Figures 5.11 and 5.12. A negative enhancement of two overlapping prints was visualised, Figure 5.11. The polymer has covered the main body of the cartridge and ridge detail can be visualised as the original colour of the brass substrate. The image gives the appearance that the cartridge had been handled as if picked up by the thumb and forefinger. The first of the two prints, Figure 5.11a, is much clearer to see than the second, Figure 5.11c. Where it is apparent ridge detail has been developed, it is difficult to ascertain *secondary detail* such as bifurcations and spurs. This is due to some overlap of polymer onto the regions where the fingerprint was deposited. The result of a negative enhancement, following the firing of the cartridge, suggests the insulating component would no longer be that of the fingerprint sweat but, as discussed previously, the corrosion product caused by the sweat deposit. Therefore the sample would be categorized into the second proposed scenario given above.

Corresponding with the third proposed scenario on model brass substrates, positive enhancements were also obtained on the brass cartridges, Figure 5.12. This is best shown in Figure 5.12a_{ii} where deposition has occurred along the ridge detail as well as the surrounding area but detail is still distinguishable, such as a crossover and bifurcation. A definite *partial print* can be seen in Figure 5.12b, the enhancement of which is positive. Due to the lack of extensive ridge detail enhanced it is difficult to distinguish *secondary detail*; however from the portion of core detail visible, a loop or possibly a central pocket whorl, but not an arch, is suggested as its *primary detail*.



Figure 5.11. A series of *ex-situ* photographs of a negative enhancement, via potentiostatic deposition of PANi at 0.6 V in 0.3 M aniline, 0.1 M $\text{Na}_2\text{C}_2\text{O}_4$ for 85 s. Two fingerprints on a previously fired brass cartridge a) first print; b) the overlap of the two prints; c) second print; with their respective enlarged print regions.

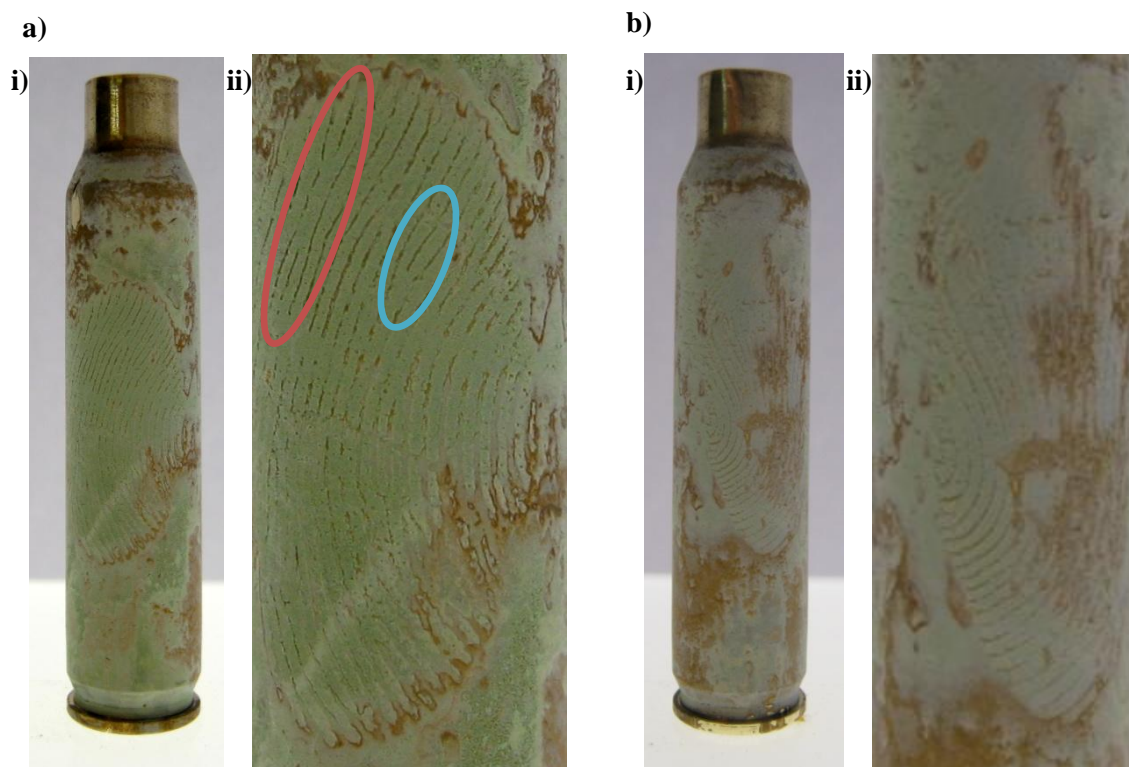


Figure 5.12. *Ex-situ* photographs of positively enhanced, previously fired brass cartridges developed by potentiostatic deposition of PANi at 0.6 V in a) 0.1 M aniline, 0.1 M Na₂C₂O₄ for 90 s, i) full print; ii) enlarged region showing a crossover (circled in red) and bifurcation (circled in blue); b) 0.1 M aniline, 0.05 M Na₂C₂O₄ for 120 s, i) *partial print*; ii) enlarged region showing core detail.

It is possible to analyse cartridges in one step by submersing the entire length during the polymer enhancement. Therefore it is not necessary to know the exact location of the print prior to development, making this a speculative technique for cartridges. It is not guaranteed that a print will always be found in the same location on a particular item, which has been demonstrated by the prints enhanced on the brass cartridges. The series of images in Figure 5.11 show the tips of two fingerprints slightly overlapping, giving the impression that the cartridge was handled as if one was writing with a pen. The overlapping prints are quite close to the top of the cartridge, whereas the other

prints enhanced are positioned more centrally. The prints found in Figures 5.10 and 5.12a are perpendicular to the cartridge while that in Figure 5.12b is parallel to the cartridge and also upside down. This suggests that different donors handled their ammunition differently when loading them into the weapon.

Raman spectra of a previously fired brass cartridge were recorded before and following electrochemical treatment, Figure 5.13. The peaks at 1348, 1470 and 1597 cm^{-1} , which can be found in both spectra, can be attributed to the presence of contaminants on the brass cartridge.²⁷⁻²⁹ Described in Chapter 3 Section 3.3 are the components required for a round of ammunition, all of which are encompassed in the *cartridge*. Two of these components, the primer and the propellant, constitute the majority of the trace evidence, gunshot residue (GSR) that is produced when a firearm is fired.²⁸ GSR is a combination of the burnt and unburnt particles as a result of the combustion process within the cartridge.²⁹ Once the ammunition has been discharged from the firearm, trace GSR can be found on the shooter, the firearm, the target and the ejected components; bullet and cartridge, as well as the area in close proximity to the shooting.³⁰ In recent years there has been work done to investigate the issues that arise due to GSR contamination.³¹⁻³³ The work suggests that the particles are easily transferred from person to person, object to object, person to object and *vice versa*. The cartridges used in this study will have spent some time on the floor of the firing range, before their collective storage in a polythene bag prior to enhancement. Therefore, the probability of GSR contamination of the cartridges is extremely high.

Nitrocellulose and nitroglycerine are commonly used as propellant; the NO_2 groups readily decompose during the ignition process.²⁷ 2,4-dinitrotoluene is commonly used as a stabilizer in propellant.²⁸⁻²⁹ The peaks found at 1348 cm^{-1} and 1597 cm^{-1} can be attributed to the symmetric and asymmetric stretching of the NO_2 groups present in nitrate esters and dinitrotoluene, respectively.²⁷⁻²⁹ As well as the compounds previously mentioned, the presence of metals, originating from the cartridge primer, such as lead, antimony and barium are found in GSR.^{27-28,31,33} Therefore the peak found at 1470 cm^{-1} could be attributed to the asymmetric stretching of the CO_3 groups present in BaCO_3 .²⁷

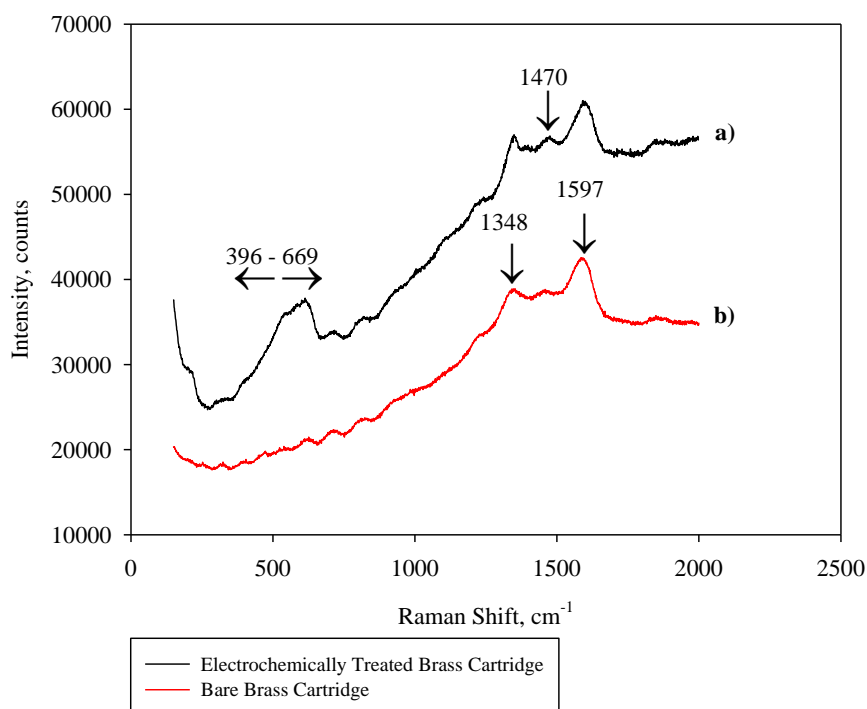


Figure 5.13. Representative Raman spectra of previously fired brass cartridges a) following electrochemical treatment with 0.3 M aniline, 0.1 M $\text{Na}_2\text{C}_2\text{O}_4$; b) no treatment undertaken.

A change to the surface chemistry of the brass cartridge, following electrochemical treatment in the presence of the aniline monomer, can be observed in the Raman spectrum (spot size 300 μm), Figure 5.13a. This is apparent due to the appearance of a broad band between 396 and 669 cm^{-1} . As stated previously the three peaks at 1348, 1470 and 1597 cm^{-1} are still present following treatment. However, their positions are observed in a region that peaks are commonly located for PANi (Table 5.1). When PANi is fully reduced the most dominant bands, which are key for *p*-disubstituted benzene rings, have previously been found at 1191 cm^{-1} and 1623 cm^{-1} .³⁴ The appearance of further bands, see Table 5.1, accompanied by a decrease in the intensity of the 1191 cm^{-1} band, characterise the formation of semiquinone radical cations.³⁴ Once PANi is fully oxidised a further three bands can be found which have been attributed to the formation of the quinone imine biradical.³⁴ This makes it difficult to decipher whether polymer is present following the electrochemical treatment. However there is very little change to the positioning of the three peaks which suggests one of two things. First, the quantity of PANi present is too insignificant to alter the intensity and position of the peaks. Second, there is no PANi present, but due to the appearance of a broad band between 396 and 669 cm^{-1} a definite chemical alteration to the brass surface has occurred.

PAni	Peak Position
Fully reduced	1191 cm^{-1} and 1623 cm^{-1}
-0.15 V	1623, 1222, 1342, 1525 and 1584 cm^{-1}
Fully oxidised	1261, 1478 and 1518 cm^{-1}

Table 5.1. Observed peak positions for a Raman spectrum of PANi.³⁴

The use of $\text{Na}_2\text{C}_2\text{O}_4$ on copper and brass surfaces has been previously investigated.³⁵⁻³⁶ The most prominent peaks are those found at approximately 1500 cm^{-1} and 560 cm^{-1} , which can be attributed to the presence of copper oxalate; the symmetric stretching vibration of the COO group and the C-C bond of the oxalate ion.³⁵ From the spectrum obtained it could be argued that these peaks are present. The large band suggests more than one constituent responsible such as CuO and Cu_2O , whose major peaks can be found in the range 250 cm^{-1} to 786 cm^{-1} .

In summary, the visualisation of latent fingerprints from brass substrates has been achieved via an electrochemical treatment with the presence of a monomer unit. The polymer technique also revealed fingerprints on previously fired cartridges. In addition both positive and negative enhancements of fingerprints have been identified. More examples of negative and positive development can be found later in this chapter.

5.3. Fingerprint Development from Copper

Copper is targeted for metal theft so it would be useful to enhance fingerprints from this substrate. Copper slowly oxidises in atmospheric oxygen to develop an oxide layer that does not extend to the bulk metal.³⁷ The formation of this oxide layer will affect the way in which fingerprints will be enhanced on its surface. Copper will also slowly oxidise when exposed to certain electrochemical conditions. The oxidation of copper and the deposition of the polymer will then be in competition with one another.

As copper is one of the two constituents of brass, similar results were found for these two substrates of which more discussion will be found further on in this chapter. It is known that both copper and brass surfaces can be corroded by fingerprint deposits; work has been published on this topic,³⁸⁻⁴³ and therefore addressed in this chapter.

Polished substrates were investigated; fingerprint deposits were allowed to corrode the metal surface prior to enhancement. Potentiostatic and potentiodynamic deposition of PANi were used to enhance corroded fingerprints on copper substrates. The data discussed here are representative of a larger study. The samples discussed have been replicated ten or more times.

The previous deposition of polymers onto copper have been for similar reasons to that of brass, to protect the surface from corrosion.⁴⁴ The monomer and electrolyte combination were chosen due to their proven use for depositing PANi onto copper.⁴⁵ The majority of samples reached their optimum enhancement before a full cycle of potential was complete, therefore incomplete cyclic voltammograms were obtained, Figure 5.14a. Those that were complete showed typical peaks of PANi indicating the changes in oxidation state of the polymer film. Figure 5.14b shows a representative cyclic voltammogram of the deposition of PANi onto copper, the peaks at approximately 0.7 V and 0.9 V represent the oxidation of the monomer and polymer, respectively. Very few samples required a complete scan of potential, within the intended range, for enhancement to take place. This led to the decision of potentiostatic deposition. Figure 5.14d shows the electrochemical data for the development of a sample via potentiostatic deposition.

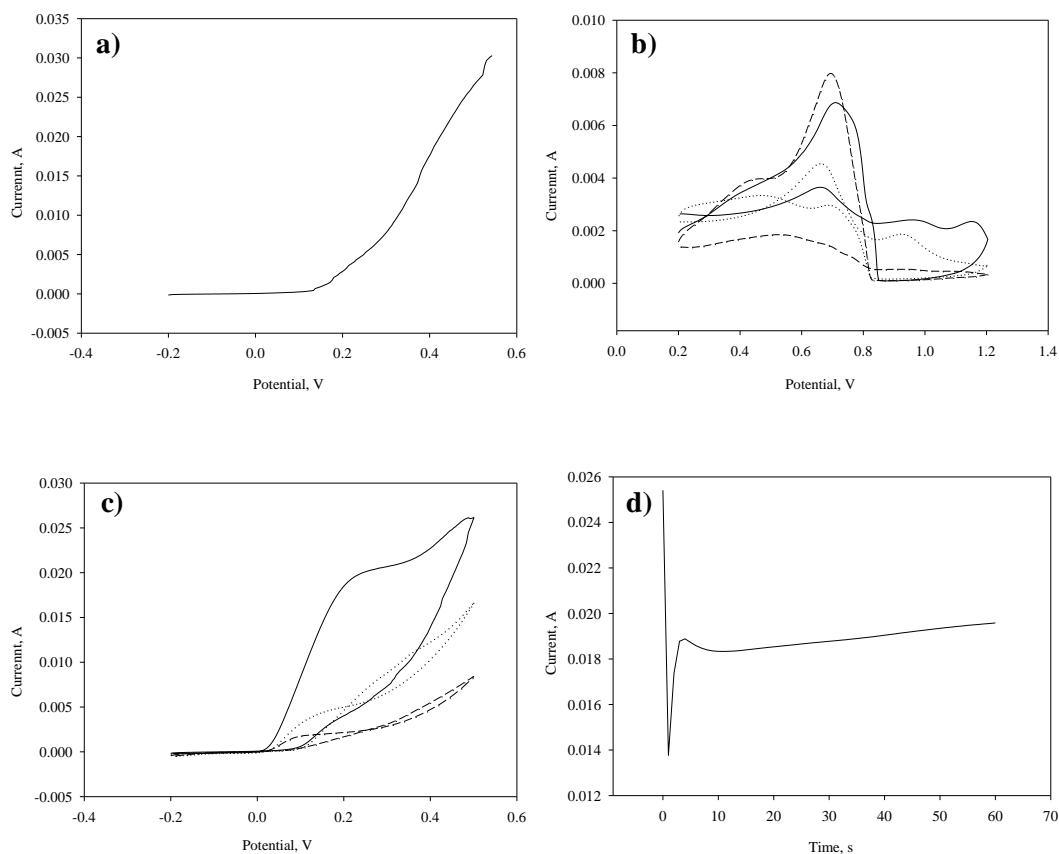


Figure 5.14. The enhancement of fingerprinted copper substrates via the deposition of PANi a) the partial scan of potentiodynamic deposition, in the range $-0.2 < E/V < +0.6$, using 0.3 M aniline, 0.2 M $\text{Na}_2\text{C}_2\text{O}_4$ at 5 mV s^{-1} ; b) the third, fifth and tenth scan of potentiodynamic deposition, in the range $+0.2 < E/V < +1.2$, using 0.15 M aniline, 0.2 M $\text{Na}_2\text{C}_2\text{O}_4$ at 10 mV s^{-1} ; c) the first, second and third scan of potentiodynamic deposition, in the range $-0.2 < E/V < +0.5$, using 0.3 M aniline, 0.2 M $\text{Na}_2\text{C}_2\text{O}_4$ at 10 mV s^{-1} ; d) potentiostatic deposition at $+0.6 \text{ V}$ for 60 s using 0.15 M aniline, 0.2 M $\text{Na}_2\text{C}_2\text{O}_4$.

The visual appearances of the polymer films were assessed in terms of their uniformity and colour contrast to the copper substrate. Figure 5.15 shows a month old print before and after its development via potentiodynamic deposition. Due to the time period the fingerprint had been present on the copper substrate, a heavily corroded and thus

visible image of the print was already available, Figure 5.15a. A print so well defined would not require enhancement, and as can be seen in Figure 5.15b ridge detail has been lost following development, its purpose however is to demonstrate the colour contrast and uniformity possible from PANi when deposited onto copper. The green deposit is highly visible against the copper substrate giving good contrast.

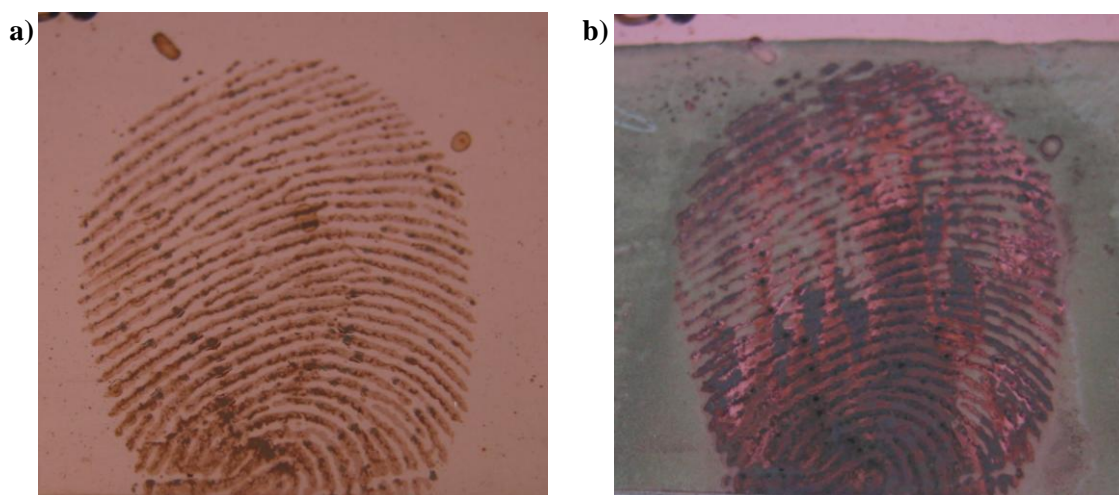


Figure 5.15. *Ex-situ* photographs of a month old print on previously polished copper a) before enhancement; b) following two full scans of potentiodynamic deposition, in the range $-0.2 < E/V < +1.2$, using 0.15 M aniline, 0.2 M $\text{Na}_2\text{C}_2\text{O}_4$ at 10 mV s^{-1} .

Similarly to the brass substrates, contradicting enhancements were achieved on previously polished copper. A range of ages, gender and ethnic background were considered for the fingerprint donors, which could explain the opposing results. The samples found in Figure 5.16 are following their enhancement, but the way in which this has been achieved is very different. The differing composition of the donors' sweat has created two very different environments, one in which the deposition of PANi is prevented and another in which it is promoted. How can it be decided whether the

development is a negative or positive copy of the fingerprint? One approach would be to assess the surrounding area. If the main body of the substrate has been chemically/visibly changed following development, the enhancement is most likely to be negative, leaving the fingerprint deposit free from polymer. Negative enhancements (Figure 5.16a), where polymer deposited around the ridge detail, was the most common result. If the chemical/visible change has occurred to limited regions of the substrate, such as the areas previously exhibiting fingerprint sweat, the enhancement is most likely to be positive. Positive enhancements (Figure 5.16b) were also found, the polymer deposition occurred on the corrosion products of the fingerprint detail. It has already been addressed, earlier in this chapter, that the corrosion of brass is triggered by the presence of chloride ions in the sweat deposit. The formation of CuCl initiates the corrosion process of brass, so it can therefore be expected to occur on a copper substrate at the copper/fingerprint interface, followed by further reactions outlined previously in Equations 5.2 and 5.3.

The examples shown in Figure 5.16 have been enhanced to very similar levels of detail, despite being developed by different electrochemical processes and displaying opposite enhancement images. It must be stated that not all samples developed via potentiodynamic deposition resulted in negative enhancements; 25 % of the samples were positively enhanced. Not all samples developed via potentiostatic deposition resulted in positive enhancements; 62.5 % of the samples were negatively enhanced. Both potentiostatic and potentiodynamic developments gave encouraging results, successfully enhancing the fingerprints from the copper substrate. There did not appear

to be a distinct difference between the two processes; ridge detail was enhanced, on 75 % of samples, by both potentiostatic and potentiodynamic development.

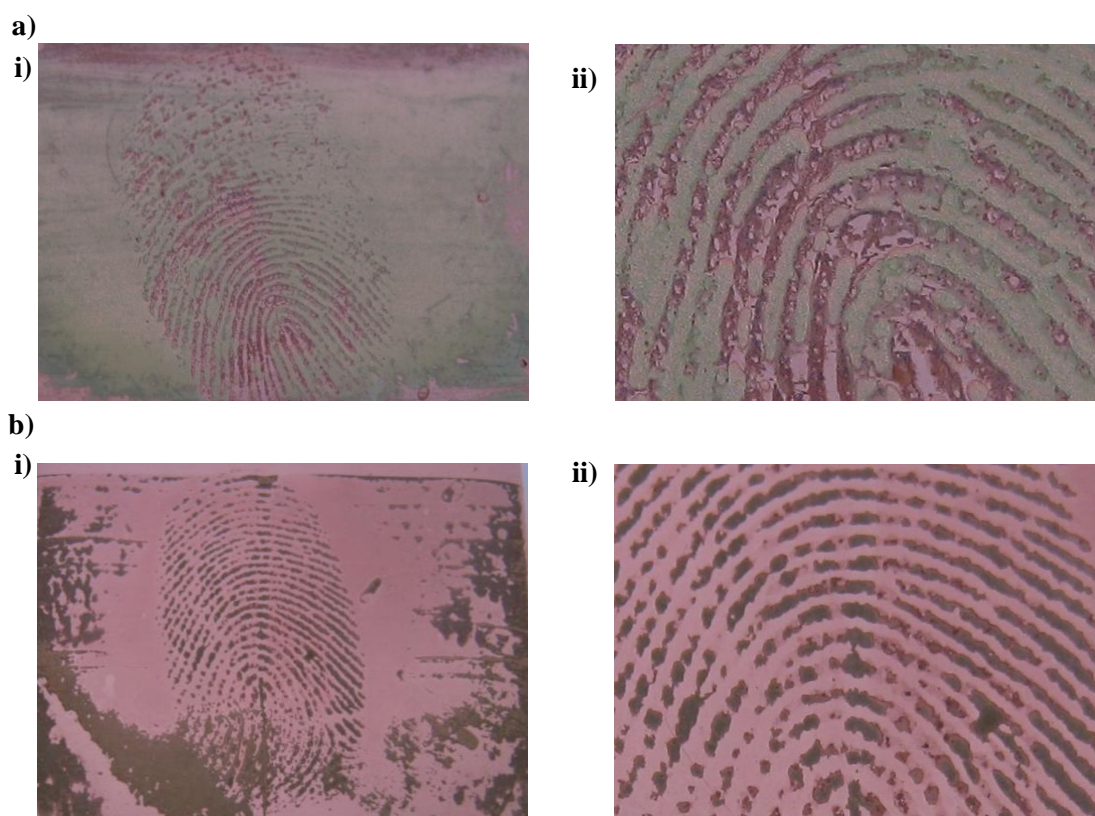


Figure 5.16. *Ex-situ* photographs of corroded prints on previously polished copper, following enhancement via a) potentiodynamic deposition in the range $-0.2 < E/V < +0.6$, using 0.3 M aniline, 0.2 M $\text{Na}_2\text{C}_2\text{O}_4$ at 10 mV s^{-1} , i) negative enhancement of full print, ii) enlarged region showing *secondary detail*; b) potentiostatic deposition at +0.6 V for 60 s using 0.15 M aniline, 0.2 M $\text{Na}_2\text{C}_2\text{O}_4$, i) positive enhancement of full print, ii) enlarged region showing *secondary detail*.

The differing selective deposition onto previously polished and fingerprinted copper substrates were assessed using optical microscopy and SEM. Figure 5.17a and 5.17b show the quality of detail attainable by either a positive or negative image of the

fingerprint. Figure 5.17a shows a very high quality negative image of a delta. Figure 5.17b shows a positive image of ridge detail. Also circled is visible corrosion of the copper from the previously deposited fingerprint. The SEM revealed that even more detail was feasible; Figure 5.17c shows a sweat pore surrounded by polymer deposit. The concave nature of the sweat pores present on the ridges results in tiny holes in the contact area between fingerprint and substrate. In this particular case the sweat pore position has been untouched by the polymer deposit which has formed along the ridge containing the pore.

Raman spectroscopy was carried out on a week old print, developed via potentiodynamic deposition in the range $-0.2 < E/V < +0.8$ at 10 mV s^{-1} . The Raman spectrum can be seen in Figure 5.18. The peaks are more characteristic of oxides of copper than of PANi; the peak at 620 cm^{-1} can be assigned to the presence of either or both Cu_2O and CuO . The intensity and peak positions related to that of PANi can be greatly affected by the laser that is implemented. Peaks can either be exaggerated or minimised, the latter of which may be the case here, especially as the films in question are thin enough for the background substrate, copper, to suppress the emission of PANi.

5.4. Fingerprint Development from Nickel Plated Brass

Nickel plated brass bullet cartridges are fairly common, but can be more expensive than brass cartridges. Fingerprints on fired nickel plated cartridges might be expected to behave similarly to those on fired brass cartridges in that enhancement is required to visualise any remaining ridge detail following the destructive processes during firing.

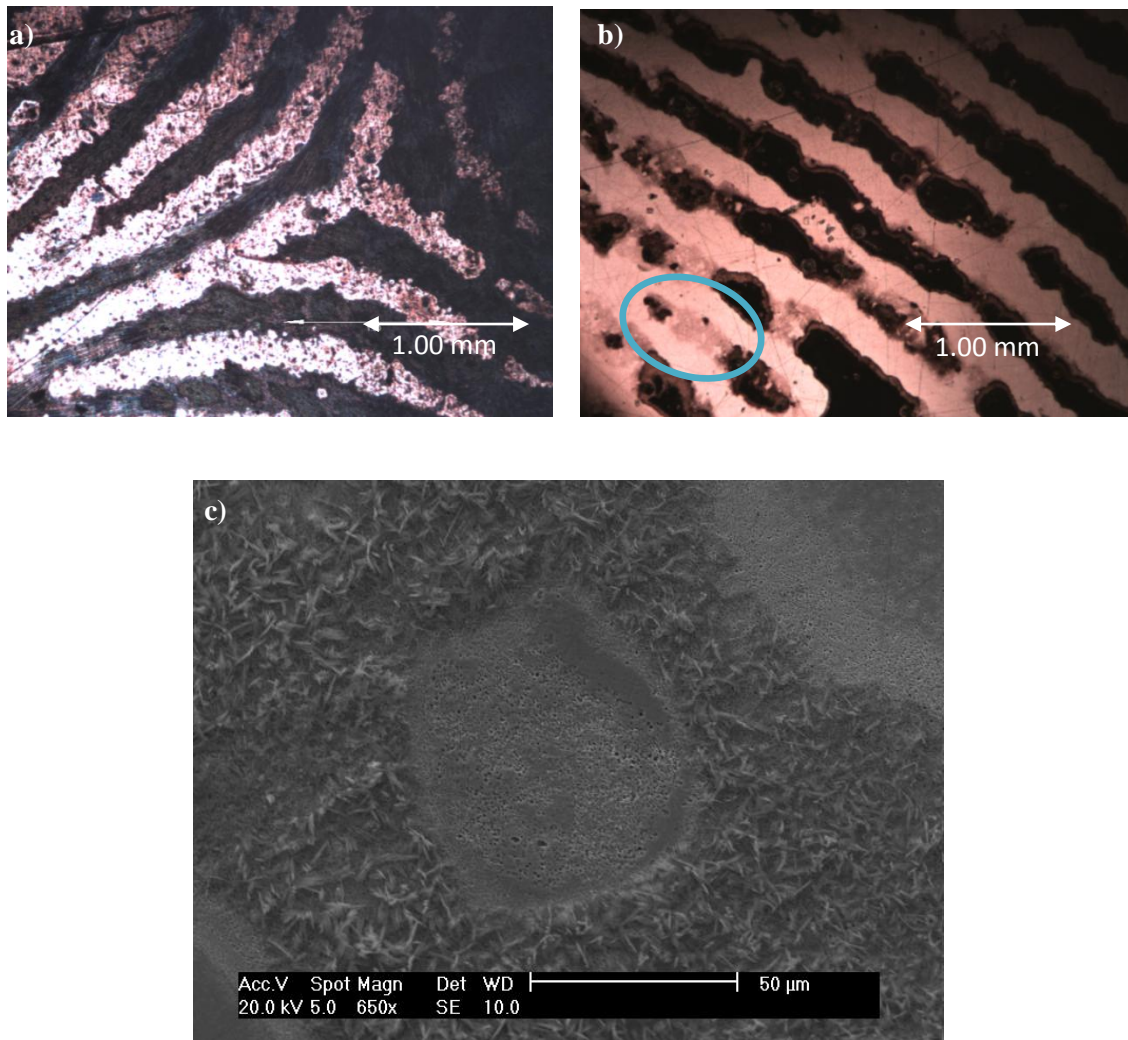


Figure 5.17. Optical images of a) a negatively enhanced delta viewed under optical microscopy; b) positively developed ridge detail viewed under optical microscopy (corrosion circled); c) a sweat pore positively enhanced viewed under SEM.

As before, model surfaces, in the form of dog tags, were used prior to the cartridges themselves. Successful PANi deposition and fingerprint enhancement on nickel plated brass dog tags were achieved, Figure 5.19. The monomer and electrolyte combinations were chosen due to their proven use for depositing PANi onto nickel substrates as a form of protection against corrosion.⁴⁶⁻⁴⁷ The data discussed here are representative of a

larger scope of study consisting of 26 model substrates and 46 cartridges; specific samples discussed where appropriate.

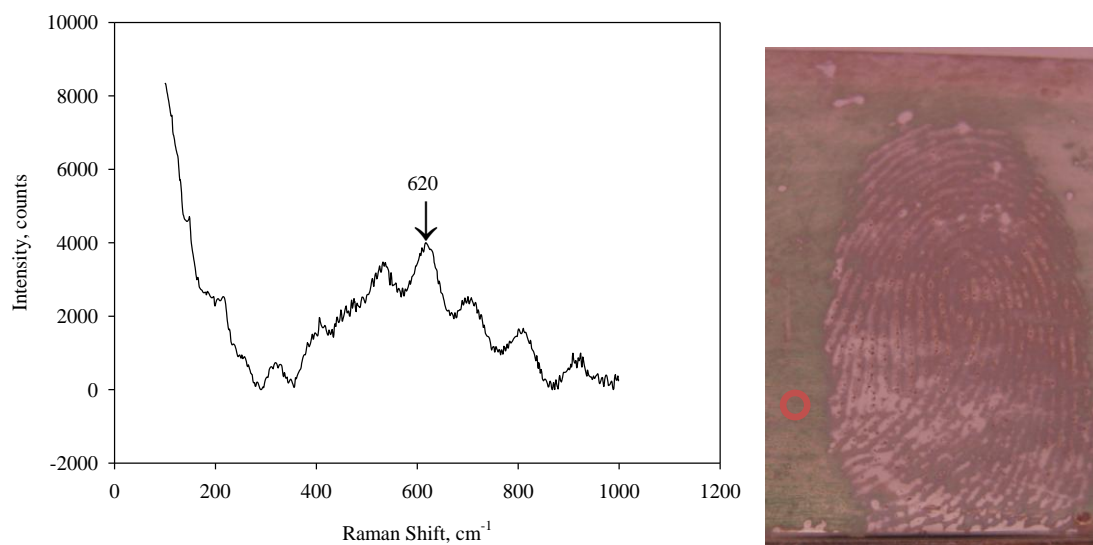


Figure 5.18. Raman spectra of an electrochemically treated brass surface developed via potentiodynamic deposition in the range $-0.2 < E/V < +0.8$ at 10 mV s^{-1} and an *ex-situ* photograph of the negatively enhanced corresponding sample with approximate location of measurement.

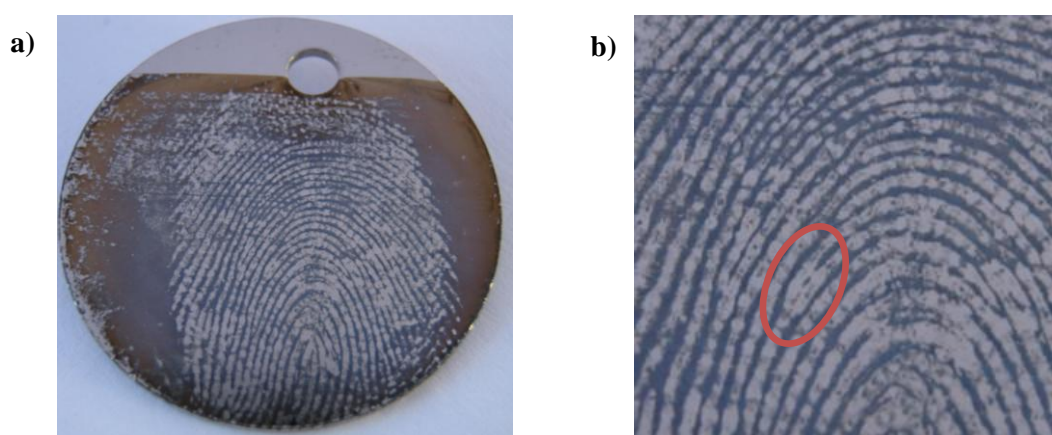


Figure 5.19. An *ex-situ* photograph of a negative enhancement on nickel plated brass, developed via potentiodynamic deposition in the range $+0.2 < E/V < +1.2$ at 50 mV s^{-1} , in 0.2 M PTSA, 0.1 M aniline, a) full print; b) enlarged region showing *secondary detail* such as a bifurcation circled in red.

The same conditions were applied to previously fired nickel plated brass cartridges; however, the results were inconsistent. Polymer either did not deposit or required extensive cycling in order for the film to be visible. The films were non-uniform and no fingerprint detail was enhanced. The geometry of the cartridges had previously been addressed therefore the thickness of the nickel plating was questioned. It was determined using SEM that the dog tags had a nickel coating almost six times greater than the nickel coating on the previously fired cartridges. Examples of these thickness measurements can be seen in Figure 5.20.

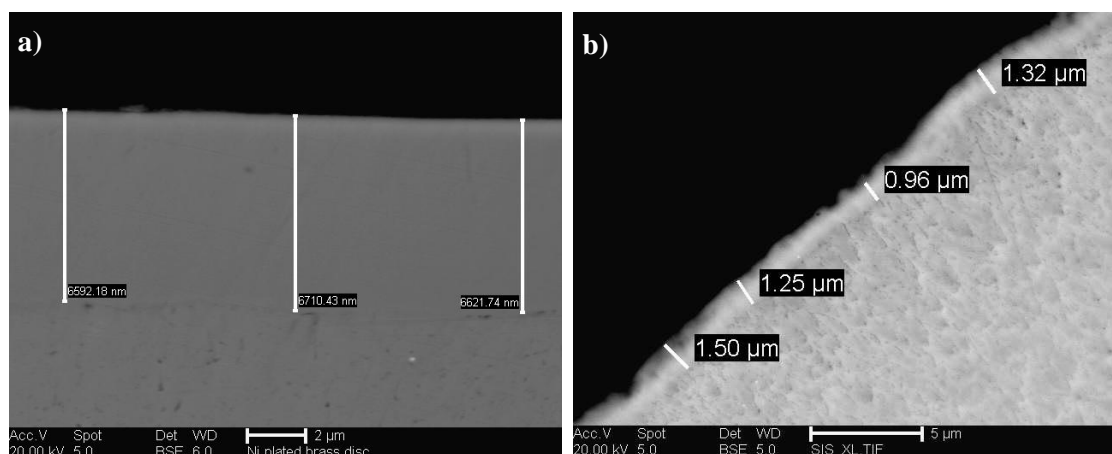


Figure 5.20. Optical images taken with an SEM of the cross sections of a) nickel plated brass dog tag; b) nickel plated brass cartridge.

A series of brass samples were plated with varying thicknesses of nickel including similar depth ($< 1.25 \mu\text{m}$) to those found on the nickel plated cartridges, see Chapter 3, Section 3.4. PANi deposition was then carried out on these samples to determine the minimum thickness of nickel coating at which polymer would deposit successfully. Alongside the flat brass samples a brass cartridge was also nickel plated and PANi

deposition performed, Figure 5.21. Interestingly, the PANi deposited uniformly over the range of nickel thicknesses including that of similar thickness to the nickel plated cartridges and the laboratory prepared nickel plated brass cartridge. Therefore it can be assumed that the thickness of nickel coating was not the factor preventing PANi from depositing onto the cartridges. This led to reservations concerning the porosity, possibly as a result of the method of plating, of the nickel coating found on the cartridges.

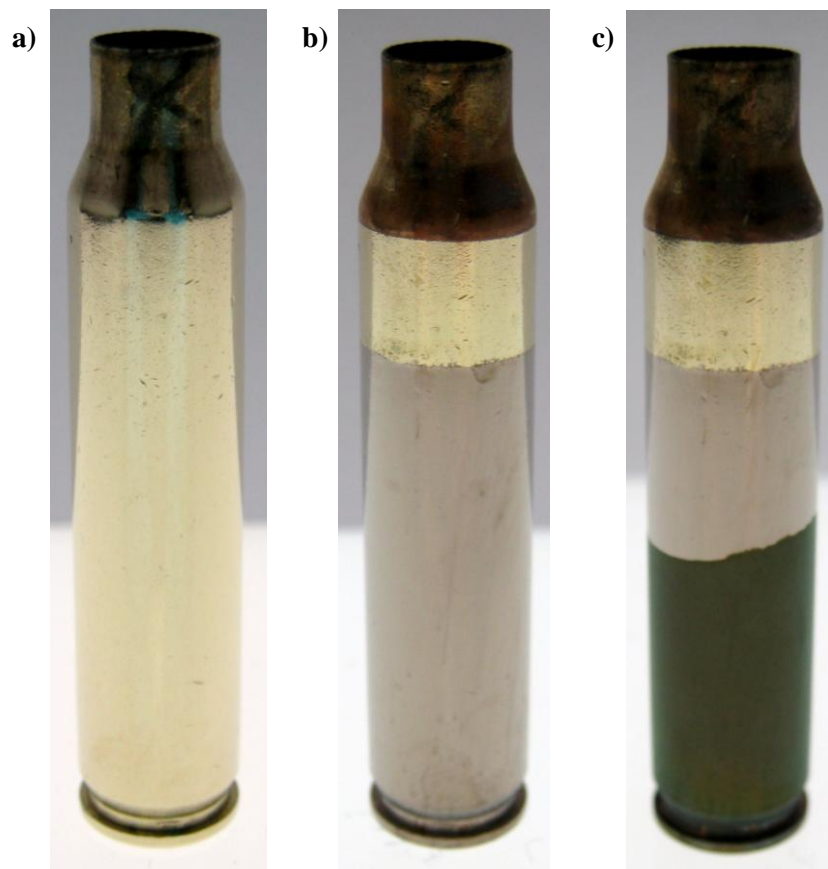


Figure 5.21. A series of *ex-situ* photographs of the same previously fired brass cartridge following a) polishing with Brasso; b) nickel plating; c) PANi deposition.

Using SEM (Figure 5.22a) it was found that there were large craters in the nickel plating, more than adequate for interaction between the electrolyte and the underlying brass to occur. It is proposed that the driving force behind this interaction exceeded that of the polymer deposition onto the nickel substrate. When compared to the nickel coating prepared in the laboratory (Figure 5.22b), which despite being more rough, was more uniform and showed no indication of breaks in the nickel coating.

An alternate electrolyte solution, suited to that of a brass substrate, was tested with the aim of bypassing the nickel plating would be successful. Unfortunately, this did not succeed. An alternate monomer unit EDOT was tested which did deposit and enhance fingerprint detail, Figure 5.23a; however uniformity on the nickel cartridge was questionable resulting in poor resolution of ridge detail, Figure 5.23b. The PEDOT film was patchy and appeared not to deposit in the furrows of the nickel plating. A print is visible but would only achieve a grade 1 on the Bandey scale.

Raman analysis was carried out on both nickel plated substrates following their treatment with the aniline monomer in electrolyte, Figure 5.24. The spectra show similarities, in terms of peaks at 623, 712 and 816 cm^{-1} . A more subtle distinction between the two spectra is the presence of two further peaks at 1351 and 1596 cm^{-1} , which bear similar values to those attributed to PANi (Table 5.1). In the case of the nickel plated flat brass the peaks are very pronounced. However, in comparison, the same peaks found in the spectrum of the nickel plated cartridge are of much lower intensity. The drop in intensity confirms the lack of PANi present on the cartridge following polymer treatment.

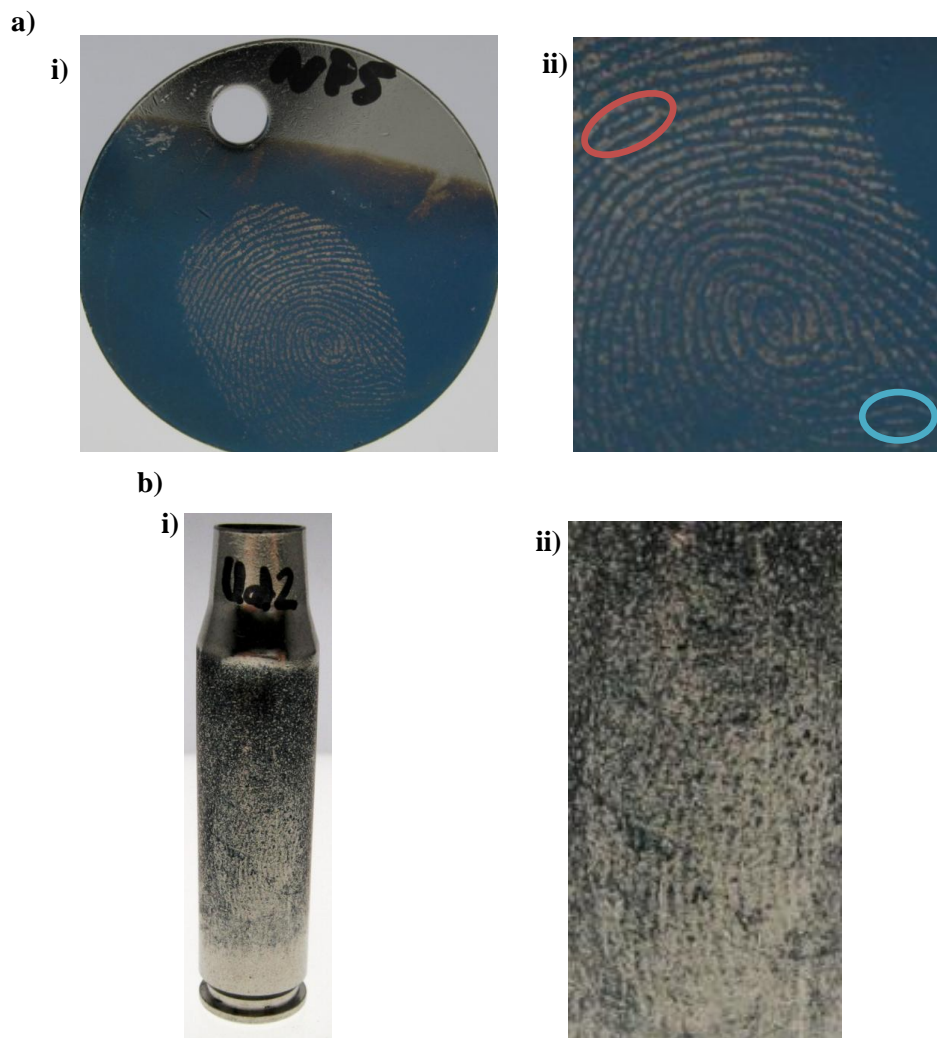


Figure 5.23. *Ex-situ* photographs of PEDOT enhanced fingerprints from nickel plated brass a) a dog tag, i) full print, ii) enlarged region showing *secondary detail* such as a lake (circled in red) and an island (circled in blue); b) a cartridge, i) *partial print*, ii) enlarged region of print barely visible.

5.5. Fingerprint Development from Lead

In the UK, theft of lead is also common, and is mainly associated with building materials, particularly older buildings such as churches and other public buildings that have roofs made predominantly from lead. Since 2007, over £25 million was paid by one insurance company in respect of over 10,000 claims from UK churches related to

the theft of lead from their roofs.³ It would be useful to be able to retrieve fingerprint evidence from these surfaces to aid in the identification and arrest of the perpetrators. The fact that lead, when stolen, is often from an outdoor environment means that the surface will have developed an oxide layer, which will affect the way in which fingerprints will be enhanced from its surface.

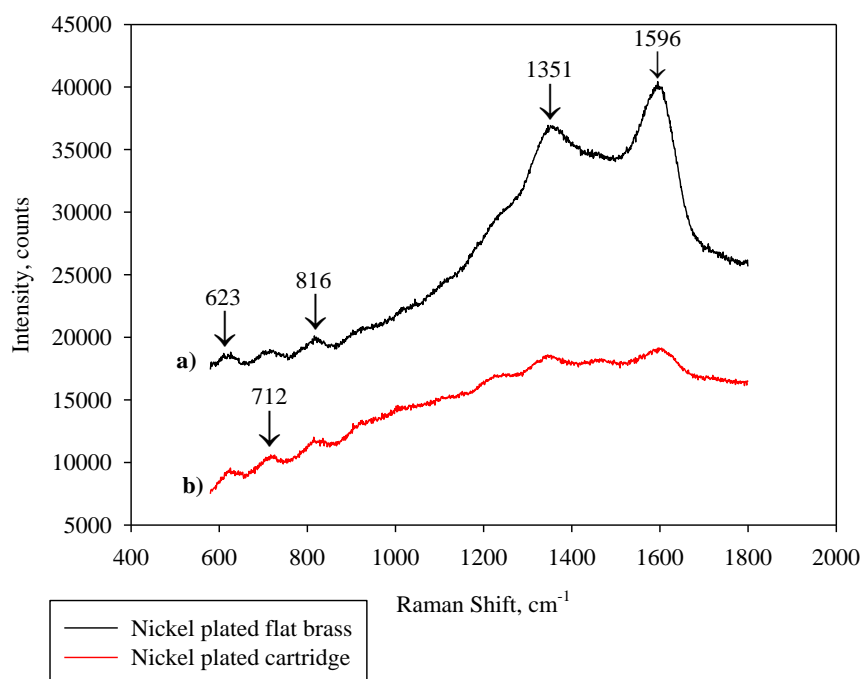


Figure 5.24. Representative Raman spectra of two nickel plated brass substrates following potentiodynamic deposition, in the range $+0.2 < E/V < +1.2$ at 50 mV s^{-1} , in 0.2 M PTSA , 0.1 M aniline , a) dog tag; b) cartridge.

The likelihood of a polished piece of lead being recovered for fingerprint analysis is very slim due to the formation of complex compounds on the surface. However, this type of substrate should not be completely dismissed and serves as a model surface to distinguish the best parameters for polymer deposition. Therefore both polished and non-polished lead substrates will be considered. The data discussed here are

representative of a larger scope of study; each sample type has been successfully replicated 16 or more times.

The monomer and electrolyte combination were chosen due to their proven use for depositing PANi onto lead.⁴⁸ A short survey of parameters was conducted, for which some of the cyclic voltammograms can be seen in Figure 5.25. The cyclic voltammograms obtained for both the deposition and redox chemistry are typical of PANi in that they show two peaks at approximately 0.4 V and 0.9 V indicating the changes in oxidation state of the polymer film. The peak at 0.4 V is a result of the oxidation of neutral PANi, see earlier Figure 1.23 and 1.24, the peak at 0.9 V is a result of further oxidation of the polymer film. In the cases where peaks are found in between, Figure 5.25b and 5.25d, these can be attributed to the degradation of PANi and the presence of ortho-coupled polymers.⁴⁹

The presence of oxygen does not affect the deposition of PANi as this occurs at more positive potentials. It would also be seen as unpractical to require a nitrogen tank when this technique is applied to fingerprint development in the field. Therefore no attempt was made to deoxygenate the solutions; the result of this can be seen by the sloping baselines in Figure 5.25, especially towards the negative potentials where oxygen is reduced causing a negative current.

The visual appearances of the polymer films were assessed in terms of their uniformity and colour contrast to the lead substrate. Figure 5.26 shows a series of bare metal

samples, previously polished (described earlier in Chapter 3 Section 3.3) and prior to fingerprint deposition, then following polymer deposition. It is clear that as the concentration of both monomer and electrolyte are increased the uniformity of the polymer film begins to suffer, localised aggregates form on the surface which could mask and confuse potential fingerprint ridge detail. This undesirable effect is pronounced when scan rate is decreased and the number of cycles is increased, allowing more time for aggregates to grow within a given potential cycle. However, the sample that can be seen in Figure 5.26a iii, despite being grown at the slower scan rate of 50 mV s^{-1} , gives a much brighter film to the equivalent sample grown at a faster scan rate of 100 mV s^{-1} . Therefore it was obvious which monomer/electrolyte concentration and scan rate would produce a suitable deposit for fingerprint enhancement.

Following polymer deposition, samples were cycled in the potential range $-0.2 < E/V < +0.9$, in monomer-free $1 \text{ M H}_2\text{SO}_4$, to assess the electrochromism of the polymer film. Despite the presence of oxidation peaks at 0.3 V and 0.8 V as shown previously in Figure 5.25f, no colour change was visible to the eye. Lead is a dark coloured metal and the films present on the surface lacked sufficient optical density to allow for visualisation. Had the films been thicker, the observation of a colour change may have been apparent. A thicker film was not produced due to the implications it would cause to the visualisation of the fingerprint detail.

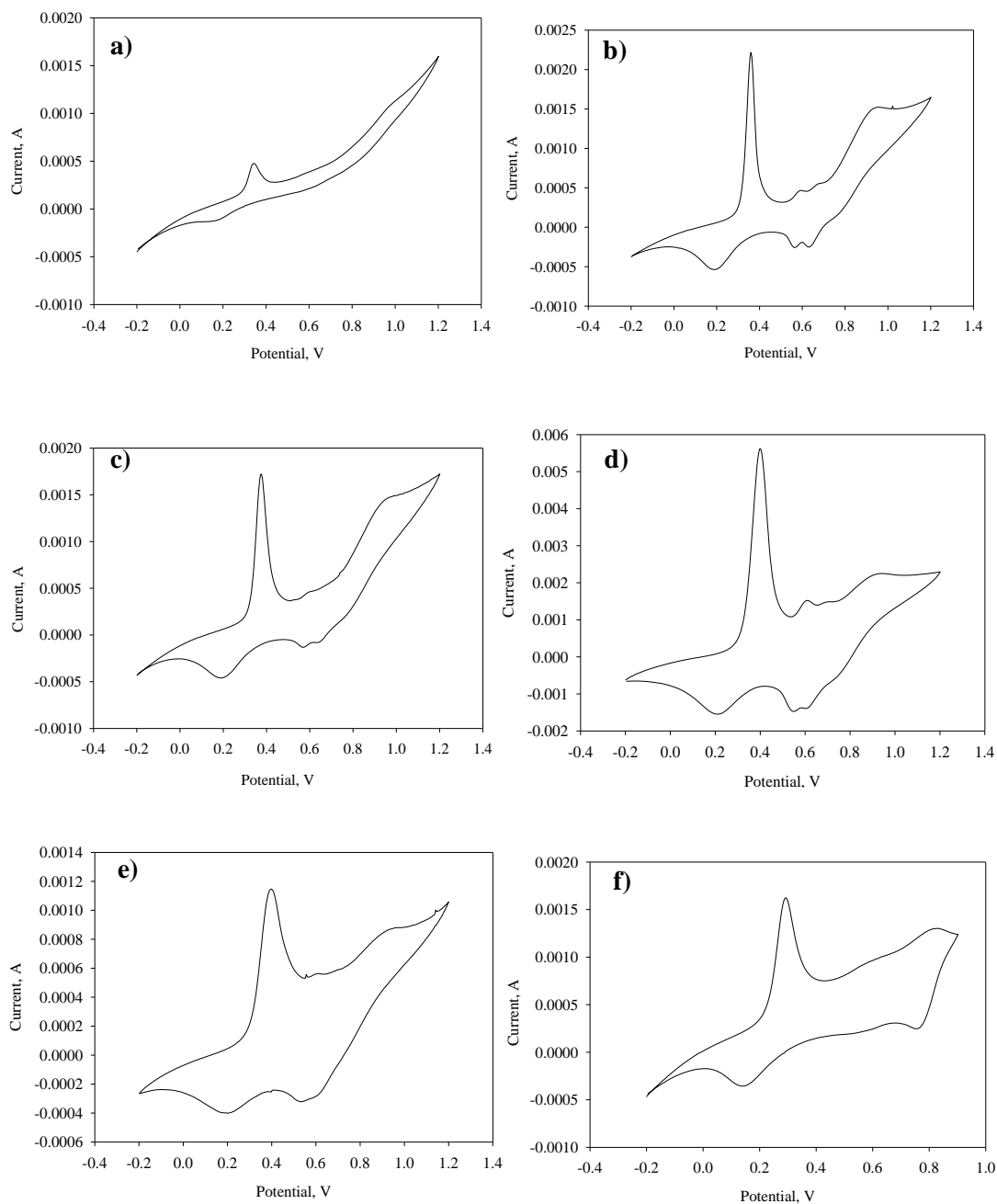


Figure 5.25. The tenth scan of potentiodynamic deposition, in the range $-0.2 < E/V < +1.2$, of PANi onto lead using a) 0.1 M aniline, 5 M H_2SO_4 at 100 mV s^{-1} ; b) 0.5 M aniline, 5 M H_2SO_4 at 50 mV s^{-1} ; c) 0.5 M aniline, 1 M H_2SO_4 at 50 mV s^{-1} . The twentieth scan of potentiodynamic deposition, in the range $-0.2 < E/V < +1.2$, of PANi onto lead using d) 0.1 M aniline, 5 M H_2SO_4 at 100 mV s^{-1} ; e) 0.1 M aniline, 5 M H_2SO_4 at 50 mV s^{-1} . The tenth scan of subsequent potential cycling, in the range $-0.2 < E/V < +0.9$, using f) 1 M H_2SO_4 at 100 mV s^{-1} , deposition conditions 20 scans in 0.1 M aniline, 1 M H_2SO_4 at 100 mV s^{-1} .

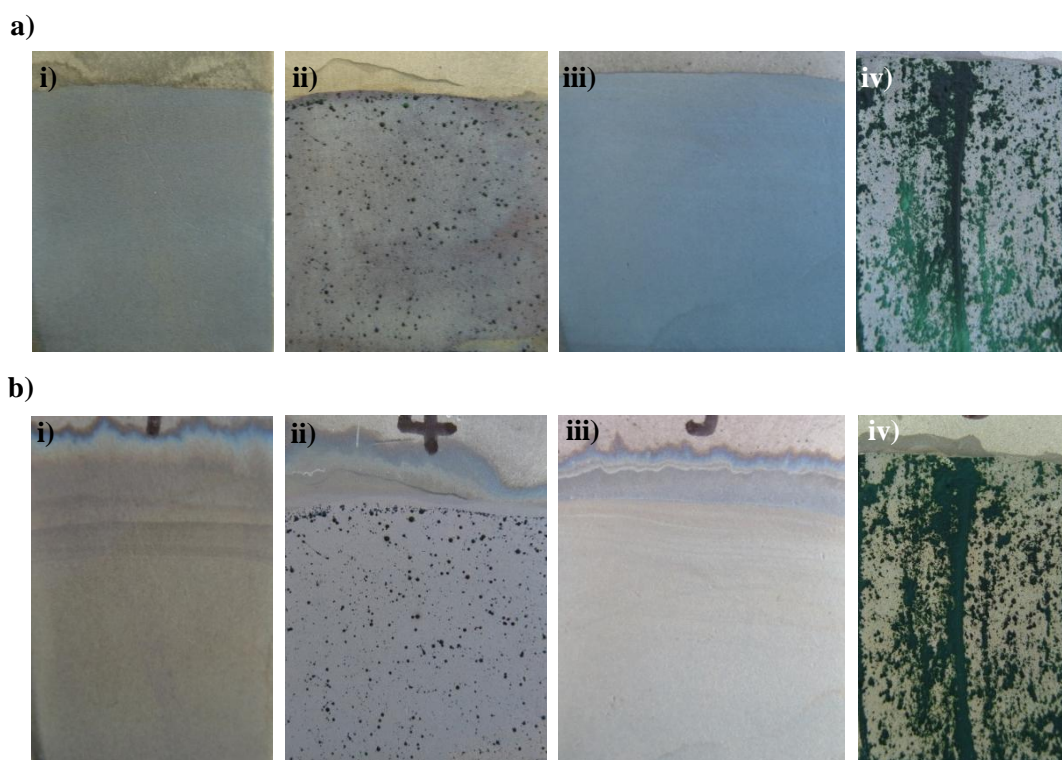


Figure 5.26. A series of *ex-situ* photographs of PANi films on lead a) following potentiodynamic deposition in i) 0.1 M aniline, 1 M H₂SO₄ at 100 mV s⁻¹ for 10 scans; ii) 0.5 M aniline, 5 M H₂SO₄ at 100 mV s⁻¹ for 10 scans; iii) 0.1 M aniline, 1 M H₂SO₄ at 50 mV s⁻¹ for 10 scans; iv) 0.5 M aniline, 5 M H₂SO₄ at 50 mV s⁻¹ for 20 scans, and b) the above samples following subsequent potential cycling in 1 M H₂SO₄ at 100 mV s⁻¹.

As the film is reduced, the optical density decreases as the film becomes lighter in colour. But even as the polymer was oxidised to access its most optically dense state no change was visible. As discussed in Chapter 4, the ability to access the range of colours PANi can deliver is desirable for those samples that bear a non-uniform fingerprint deposit. This allows for optimisation of contrast between the ridge detail and the polymer film. Unfortunately this does not appear to be the case when applied to lead surfaces; the quality of the film was greatly diminished after cycling in monomer free electrolyte, the results of which can be seen in the photographs in Figure 5.26b. It

would appear that following potential cycling in monomer-free electrolyte a thin layer of electrolyte past the line of electrolyte air interface has occurred caused by surface tension.

Optimum deposition of PANi onto lead was via potentiodynamic deposition in the range $-0.2 < E/V < +1.2$ at 100 mV s^{-1} , in a solution of 0.1 M aniline in 1 M H_2SO_4 . However, when applied to polished lead substrates that had day old fingerprints present on their surface, mixed results were achieved. Figure 5.27 shows several samples, one of which that had been cut into two pieces prior to the deposition of a single fingerprint, in theory giving the same fingerprint 'make up' on each half of the substrate. Both sections were treated in exactly the same way to test for repeatability. A uniform coverage of polymer on both samples was achieved; unfortunately a higher proportion of the ridge detail in Figure 5.27a was still visible compared to that in Figure 5.27b, which has been completely covered up by the polymer. Due to the concave nature of the sweat pores along the ridges, polymer deposition can occur as no contact between pore and substrate takes place. Confirmation of the quality of enhancement down to the smallest details, sweat pore position, can be seen in Figures 5.27dii and 5.28a.

The same parameters used for the polished samples were applied to lead substrates that had not been previously polished and therefore possessed complex mixtures on their surfaces. These mixtures will vary depending on the conditions the substrates are exposed to but could consist of PbO_2 , $\text{Pb}(\text{OH})_2$ and PbCl_2 .⁵⁰ The lead that was supplied had a tarnished appearance and some fingerprint detail was visible, presumably

deposited from general handling of the substrate at some unknown time prior to its delivery. The attempts at enhancing these once visible prints were unsuccessful.

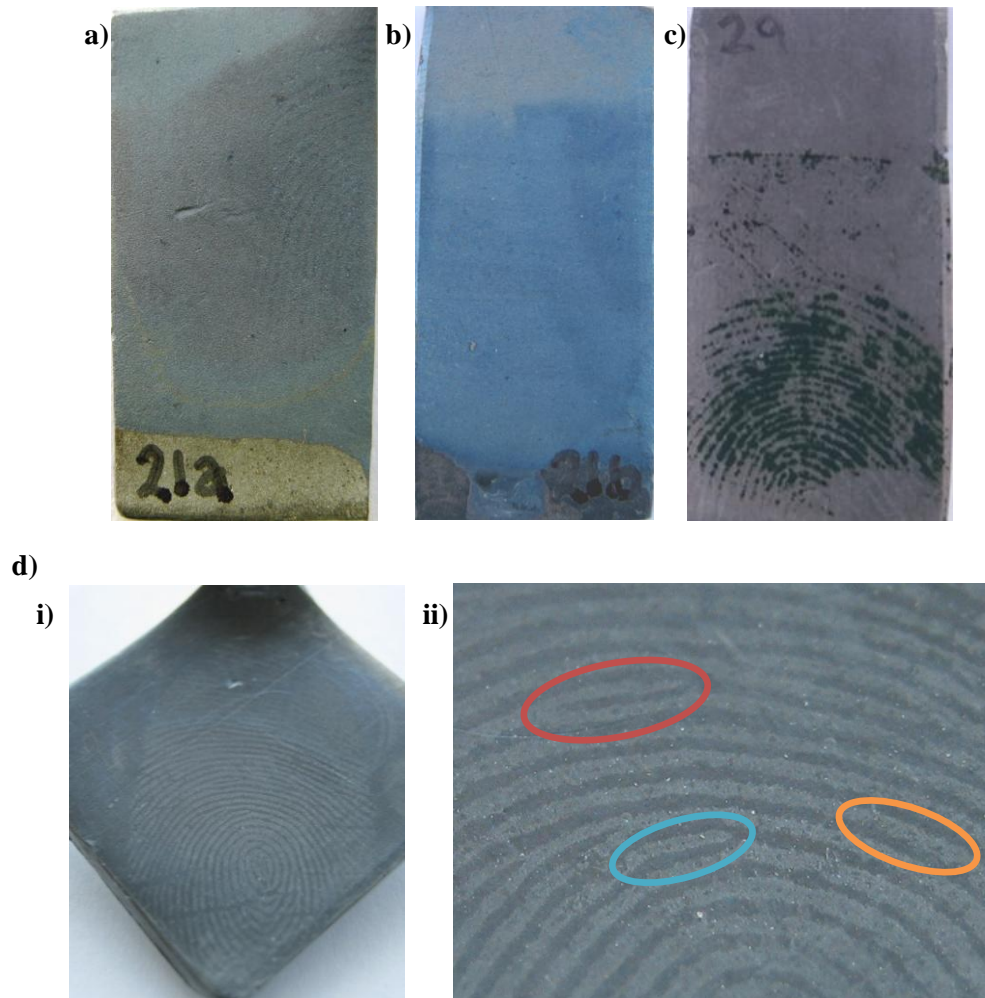


Figure 5.27. A series of graded images of PANi enhanced day old fingerprints on previously polished lead a) grade 2 print; b) grade 1 print; c) non-polished lead, grade 2 print; d) i) grade 4 print, ii) enlarged region with visible *secondary* and *tertiary detail*; a spur (circled in red), ridge ending (circled in blue), and pore position (circled in orange). Images a-c have been brightened for the purposes of printing.

One day old fingerprints on unpolished lead were enhanced using PANi, but the results obtained differed to those from the polished samples. Polymer deposition is more localised to the position of the ridge detail; the bare lead is almost free from polymer deposition. Instead of the fingerprint deposit masking the surface from polymerisation, the areas covered by ridge detail have become the more desirable initiation sites for the polymer to deposit, Figure 5.27c. This suggests that the fingerprint deposit has reacted with the lead substrate in a way that has made the pathway of deposition easier, but not limited to, these localised regions. The colour of the polymer deposited in these localised regions is identical to that of the aggregates formed on the polished substrate when monomer concentration or number of cycles is increased.

The spatially selective deposition on to previously polished and fingerprinted lead substrates was assessed using optical microscopy and SEM. The quality of polymer deposition and, therefore quality of the fingerprint enhancement can be seen in Figure 5.28a. *Secondary detail*, such as ridge endings and bifurcations can be easily observed using both microscopes, as well as *tertiary detail*.

Following cyclic voltammetry in monomer free electrolyte there appeared to be no colour change to the polymer film despite the presence of the oxidation peaks of PANi. Raman spectroscopy was carried out and an example of a Raman spectrum can be seen in Figure 5.29. The wide bands between 1700 cm^{-1} and 1050 cm^{-1} are characteristic of PANi.³⁴ The sharp peak at 980 cm^{-1} and two weaker peaks at 452 cm^{-1} and 439 cm^{-1} can be assigned to the presence of PbSO_4 .⁵¹ The intensity of the PbSO_4 compared to that of the PANi band reiterates that the polymer film is thin.

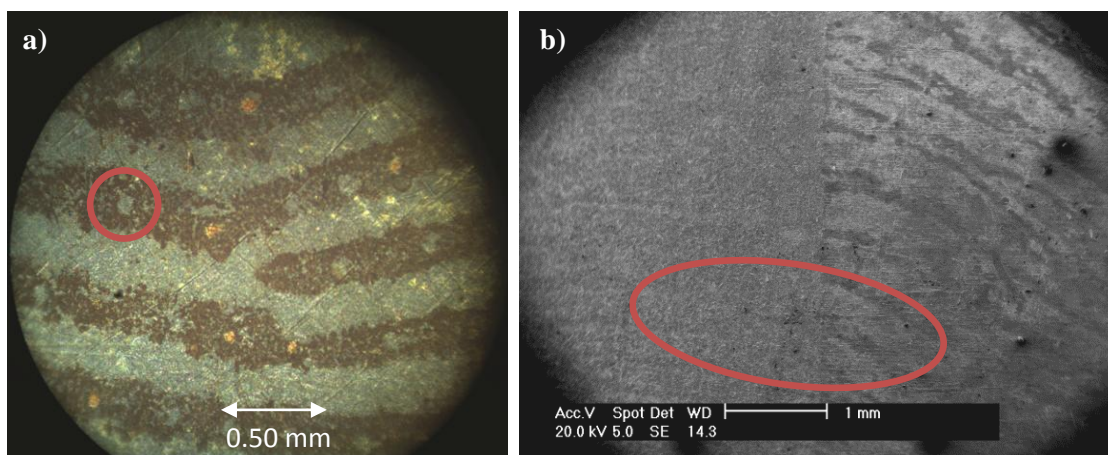


Figure 5.28. Optical images of lead samples following development viewed under a) optical microscopy, pore position visible; b) SEM, bifurcation visible.

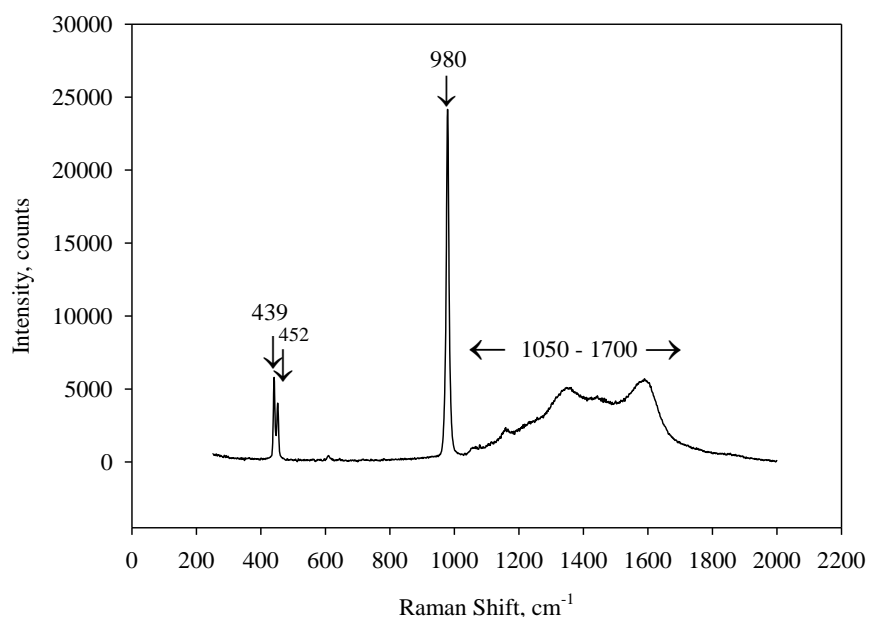


Figure 5.29. Representative Raman spectrum of a PANi film on polished lead.

5.6. Conclusions

The results have proven the electropolymerisation of PANi, and PEDOT, to be a viable technique for enhancing fingerprints on a range of diverse metals, including spent brass cartridges. The results discussed above have also shown the polymer deposition technique to work in a way that would not necessarily be expected. Both positive and negative enhancements have been obtained on brass, copper and lead.

Polymer enhancement of fingerprints on lead has been proven to show positive results on polished substrates. The results from non-polished substrates contradicted the theory that the fingerprint deposit masks the surface from polymerisation. It is unrealistic that evidence made from lead would be highly polished, therefore the application of the polymer treatment should be thoroughly considered as a method for enhancing fingerprints on lead.

Polymer enhancement of fingerprints on nickel plated brass substrates is very dependent on the nickel plating process. Fingerprints have been successfully enhanced from model nickel plated substrates. However, due to the plating process of nickel plated brass cartridges, insufficient resolution of ridge detail is possible on these more evidentially valuable surfaces.

Enhancement on both copper and brass has proven to be the most useful, especially from previously fired brass cartridges, where substantial ridge detail has been developed. Despite the possibility of an enhancement producing either a positive or

negative image, the technique has achieved something that happens rarely, successfully visualising latent ridge detail deposited onto a cartridge prior to its ejection from a firearm.

5.7. References

1. Centre for Problem-Oriented Policing. Theft of scrap metal, guide No. 58 (2010). http://www.popcenter.org/problems/metal_theft (Accessed 4th February 2013).
2. A. Sidebottom, J. Belur, K. Bowers, L. Tompson, S. D. Johnson, *J. Res. Crime Delinq.*, 2011, **48**, 396.
3. Ecclesiastical Insurance Office. Guidance notes theft of metal. <http://www.ecclesiastical.com/Images/Guidance%20notes%20-%20theft%20of%20metal.pdf> (Accessed 4th February 2013).
4. P. C. White, *Crime Scene to Court*, 2nd edn., 2004, The Royal Society of Chemistry, Cambridge, UK.
5. B. Fisher, D. Fisher, J. Kolowski, *Forensics Demystified*, 2007, **pg 133-153**, McGraw-Hill, New York, USA.
6. B. W. Given, *J. Forensic Sci.*, 1976, **21**, 587.
7. Y. Migron, G. Hocherman, E. Springer, . Almog, D. Mandler, *J. Forensic Sci.*, 1998, **43**, 543.
8. A. R. W. Jackson, J. M. Jackson, *Forensic Science*, 2004, **pg 241**, Pearson, Prentice Hall, Gosport, UK.
9. G. Gregory, 2012, Northamptonshire Police Armourer interview, Northamptonshire Police Force Headquarters.
10. J. W. Bond, *J. Forensic Sci.*, 2011, **56**, 999.
11. J. W. Bond, *Physica B.*, 2011, **406**, 1582.
12. J. W. Bond, *J. Phys. D. Appl. Phys.*, 2009, **42**, 235301.
13. A. T. Özyılmaz, N. Çolak, G. Ozyılmaz, M. K. Sangün, *Prog. Org. Coat.*, 2007, **60**, 24.

14. C. B. Breslin, A. M. Fenelon, K. G. Conroy, *Mater. Design*, 2005, **26**, 233.
15. V. Brusic, M. Angelopoulos, T. Graham, *J. Electrochem. Soc.*, 1997, **144**, 436.
16. A. L. Beresford, A. R. Hillman, *Anal. Chem.*, 2010, **82**, 483.
17. R. M. Brown, A. R. Hillman, *Phys. Chem. Chem. Phys.*, 2012, **14**, 8653.
18. A. L. Beresford, R. M. Brown, A. R. Hillman, J. W. Bond, *J. Forensic Sci.*, 2012, **57**, 93.
19. C. Weyermann, O. Ribaux, *Sci. Justice*, 2012, **52**, 68.
20. E. Paterson, J. W. Bond, A. R. Hillman, *J. Forensic Sci.*, 2010, **55**, 221.
21. A. Meekins, J. W. Bond, P Chaloner, *J. Forensic Sci.*, 2012, **57**, 1070.
22. K. R. Trethewey, J. Chamberlain, *Corrosion for Science and Engineering*, 1995, Longman Scientific, Harlow, UK.
23. J. W. Bond, *J. Phys. D. Appl. Phys.*, 2008, **41**, 125502.
24. H. C. Lee, R. E. Gaensslen, *Advances in Fingerprint Technology*, 2nd edn., 2001, CRC Press, London, UK.
25. P. Atkins, J. de Paula, *Elements of Physical Chemistry*, 4th edn., 2005, Oxford University Press Inc., New York, USA.
26. S. M. Sze, K. K. Ng, *Physics of semiconductor devices*, 3rd edn., 2007, John Wiley & Sons Inc, Hoboken, New Jersey.
27. J. Bueno, V. Sikirzhyski, I. K. Lednev, *Anal. Chem.*, 2012, **84**, 4334.
28. M. López-López, J. J. Delgado, C. García-Ruiz, *Anal. Chem.*, 2012, **84**, 3581.
29. M. López-López, J. L. Ferrando, C. García-Ruiz, *Anal. Chim. Acta*, 2012, **717**, 92.
30. F. S. Romolo, P. Margot, *Forensic Sci. Int.*, 2001, **119**, 195.
31. R. E. Berk, S. A. Rochowicz, M. Wong, M. A. Kopina, *J. Forensic Sci.*, 2007, **52**, 838.

32. S. Charles, N. Geusens, *Forensic Sci. Int.*, 2012, **216**, 78.
33. B. Cardinetti, C. Ciampini, S. Abate, C. Marchetti, F. Ferrari, D. Di Tullio, C. D'Onofrio, G. Orlando, L. Gravina, L. Torresi, G. Saporita, *Scanning*, 2006, **28**, 142.
34. L. D. Arsov, W. Plieth, G. Koûmehl, *J. Solid State Electrochem.*, 1998, **2**, 355.
35. H. Jeziowski, B. Moser, *Chem. Phys. Lett.*, 1985, **120**, 41.
36. A. T. Özyılmaz, G. Ozyilmaz, N. Çolak, *Corros. Eng. Sci. Techn.*, 2009, **44**, 12.
37. Z. Ahmad, *Principles of Corrosion Engineering and Corrosion Control*, 2006, ch. 4, Butterworth-Heinemann, Jordan Hill, UK.
38. G. Williams, N. McMurray, *Forensic Sci. Int.*, 2007, **167**, 102.
39. J. W. Bond, C. Heidel, *J. Forensic Sci.*, 2009, **54**, 892.
40. J. W. Bond, *Rev. Sci. Instrum.*, 2009, **80**, 075108.
41. J. W. Bond, *J. Forensic Sci.*, 2009, **54**, 1034.
42. S. M. Bleay, P. F. Kelly, R. S. P. King, *J. Mater. Chem.*, 2010, **20**, 10100.
43. A. J. Goddard, A. R. Hillman, J. W. Bond, *J. Forensic Sci.*, 2010, **55**, 58.
44. S. Patila, S. R. Sainkarb, P. P. Patila, *Appl. Surf. Sci.*, 2004, **225**, 204.
45. A. T. Özyılmaz, T. Tüken, B. Yazıcı, M. Erbil, *Prog. Org. Coat.*, 2005, **52**, 92.
46. A. T. Özyılmaz, *Surf. Coat. Tech.*, 2006, **200**, 3918.
47. A. T. Özyılmaz, G. Kardaş, M. Erbil, B. Yazıcı, *Appl. Surf. Sci.*, 2005, **242**, 97.
48. B. Cheraghi, A. R. Fakhari, S. Borhani, A. A. Entezami, *J. Electroanal. Chem.*, 2009, **626**, 116.
49. S. Pruneanu, E. Veress I. Marian, L. Oniciu, *J. Mater. Sci.*, 1999, **34**, 2733.
50. F. E. Varela, L. M. Gassa, J. R. Vilche, *J. Electroanal. Chem.*, 1993, **353**, 147.
51. R. Varma, C. A. Melendres, N. P. Yao, *J. Electrochem. Soc.*, 1980, **127**, 1416.

Chapter Six

6. A Comparative Study of Electrochromic Enhancement of Latent Fingerprints with Existing Development Techniques¹

6.1. Overview

The previous two chapters have focused on the application of the polymer deposition technique to a range of metal surfaces, including items that were chosen for their potential forensic value. This chapter describes the effect of parameters such as exposure time and fingerprint donor. The purpose is to assess the abilities of the polymer deposition technique in enhancing fingerprints subjected to a range of environments, for varying lengths of time, and comparing the results to those achievable via existing techniques. The study compares the enhancement and visualisation of latent fingerprints on stainless steel substrates using the electrochromic enhancement approach with three classical methods (dusting, wet powder and superglue fuming). Two variants of the electrochromic enhancement method were utilized with PANi and PEDOT as the electrochromic materials.

Overall, the study encompassed 500 samples. From a practical perspective, the objectives were to determine the most appropriate development methods for samples for which the age or environment – or both – were unknown. The effectiveness of the enhancement techniques were addressed by three questions: (i) does the “enhancement” technique actually result in a higher grade print?; (ii) does the enhancement protocol result in a useable print (grade 3 or 4 on the Bandey scale)?; and (iii) for given combinations of circumstances (specified age and/or environment, averaged across five

donors) which enhancement technique results in the largest number of useable (grade 3 or 4) prints? Throughout this chapter the data presented will be referred to in terms of the *fraction improved*, the *fraction useable*, and the *optimum enhancement technique*, respectively. Therefore, in terms of the first question, no negative responses are possible. Similarly, in terms of the second question, a useable print is only achievable with enhancement.

Forensic laboratories take a systematic approach to enhancing a fingerprint.² When developing a new technique it is important to know where it would fit with the existing protocol, where previous environmental conditions can change how an item is processed, as seen previously in Figure 1.12.

6.2. Experimental Procedures

Full details of the experiments carried out for this chapter can be found in Chapter 3, Sections 3.7-3.9. Here is a brief overview of the procedures and reasons for their inclusion in the study.

According to a review carried out by Girod *et al.* a donor's characteristics, including age, ethnic origin, medication and diet, influence the variability of print residue quantity and composition.³ Therefore fingerprint samples were taken from five different donors, three males and two females, varying in age from 21 - 42. Although not quantified, these represented a range of deposit composition and amount, i.e.

quality. The samples were then exposed to different environments for systematically varied intervals of time to give four ages of print; 1 day, 7 days, 14 days and 28 days.

The fingerprint deposits were subject to a range of histories to assess the relative efficacy of the electrochromic enhancement method and more traditional methods. The histories (environments and time scales) that were used are more representative of plausible scenarios that may arise in a criminal investigation than those found in the previous chapters. The surfaces from which the fingerprints were to be recovered were subject to five environments: ambient, extended immersion in water, washing with acetone, extended heating and washing with aqueous soap solution.

When fingerprints are recovered from metal surfaces, the most widely used visualization techniques are dusting, cyanoacrylate fuming (“superglue”) and the use of wet powder.⁴ The most common procedure for the development of latent prints is powder dusting. Whether the powder used is regular, metallic or luminescent (see Chapter 1 Section 1.2.2) the method relies upon physical adherence of the powder to the sticky sebaceous components of the fingerprint residue.⁵⁻⁸ The colour selection of the powder used to achieve maximum contrast is based on the colour of the surface. Here the substrate is pale grey in colour therefore a standard black powder (details found in Chapter 3 Section 3.9.) was used to maximise contrast.

Small particle reagent - sometimes referred to as wet powder - works in much the same way as dusting. This technique has been shown to work well on wet non-porous

surfaces, although the scope of colour variation for the adhering particles is limited for achieving good visual contrast on metal surfaces.⁹⁻¹⁰ It is therefore expected that although contrast may not be as good, for samples exposed to certain environments wet powder should work well at visualising prints.

“Superglue” treatment involves reaction of cyanoacrylate with the fingerprint deposit, leading to polymerisation of the monomer along the ridges of the print.¹¹⁻¹² Superglue fuming often requires an additional step for visualisation. Here Basic Yellow 40 dye was used, which required photographing under illumination with light of an appropriate wavelength, $\lambda = 430-470$ nm. Although widely used, the efficacy of this technique is limited for fingerprints that have either been wetted or that have been aged. Therefore it is expected that superglue will work best for fresher prints and samples that have undergone treatment without the use of water.

Two variants of the electrochromic enhancement method were utilized, PANi and PEDOT, generated by anodic electropolymerization of aniline and EDOT, respectively. While proof of concept of the electrochromic enhancement method has been established for PANi¹³ and PEDOT¹⁴ with fingerprints subject to ambient conditions, the technical performance of this approach under more practical conditions was assessed.

6.3. Enhancement Technique Performance According to Sample Pre-Treatment

To give an impression of the origins of the data, typical outcomes are shown in Figure 6.1 for two nominally identical fingerprints (i.e. taken from the same donor). The first sample was immersed in water for 7 days (Figure 6.1a) then enhanced using PANi (Figure 6.1b). The second sample was heated for 28 days (Figure 6.1c) then enhanced using PEDOT (Figure 6.1d). It is clear that the enhancement processes have, from the starting point of a grade 0 print, revealed significant *secondary detail*. It is not possible to discuss individually all 500 samples. However, throughout this chapter further examples of the enhancements achieved for different donors, time intervals and environmental exposures are given.

In this section the fraction (expressed as a percentage) of samples for which the fingerprint was enhanced to any extent (represented by *fraction improved*) and to a useable level (represented by *fraction useable*) by each technique are considered. In the latter instance, “*useable*” is characterized by a grade of 3 or 4 according to the Bandey scale, discussed previously in Section 4.1 of Chapter 4.¹⁵ The results are shown in Figures 6.2, 6.4, 6.6, 6.8 and 6.10. Each individual figure relates to one exposure environment; within this the effects of varying the age of the fingerprint (moving forwards in the diagram) and the enhancement method are explored. Each column represents the combined outcome from five donors; the figures capture data from 100 prints.

6.3.1. Ambient Conditions

The samples left under ambient conditions were kept in an open box until their enhancement took place. Despite the investigation of time and donor under ambient conditions in previous chapters, these samples were produced by different donors. Therefore a better comparison could be made between the environments investigated.

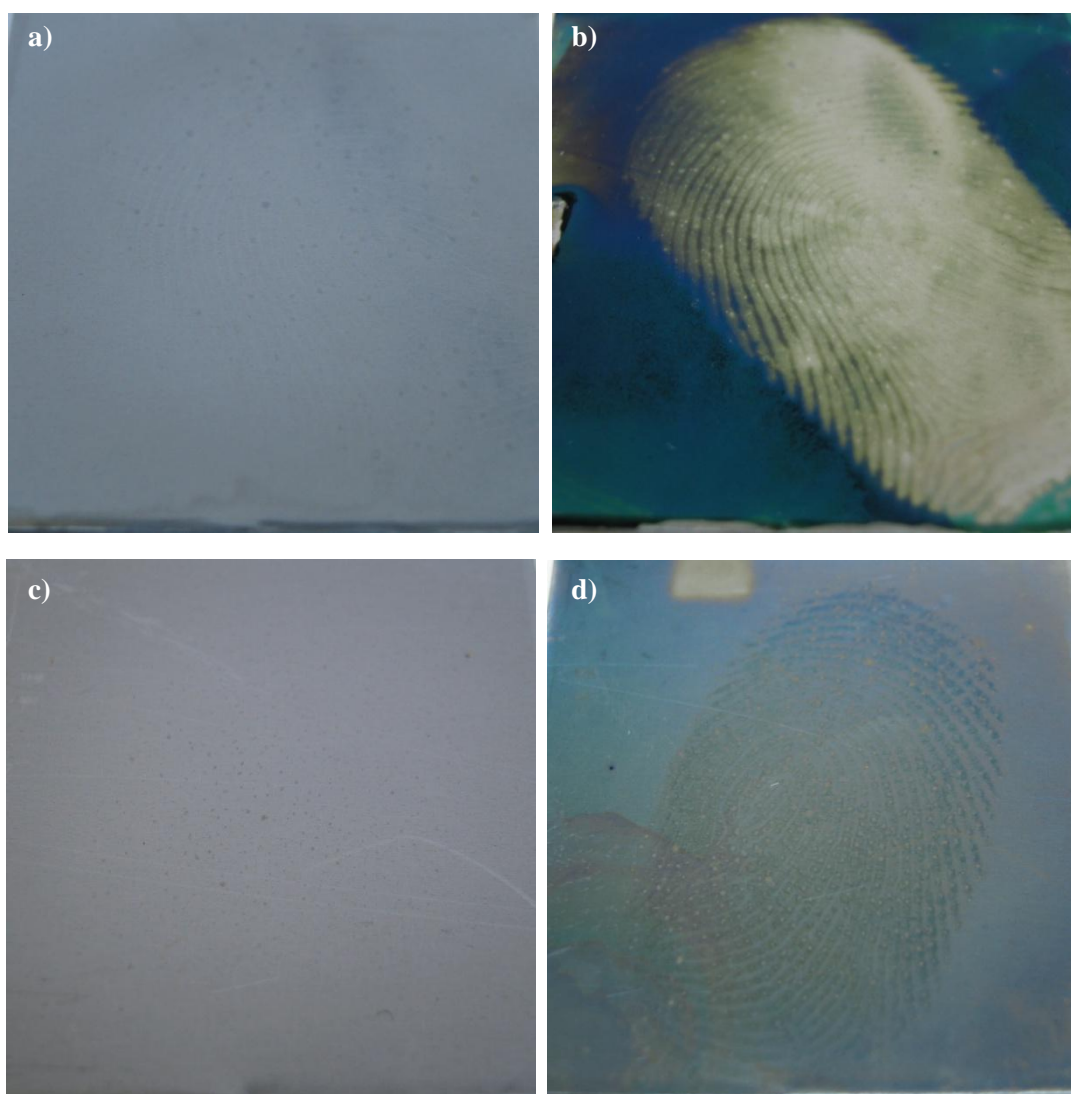


Figure 6.1. Fingerprints deposited by the same donor following; a) immersion for 7 days in water, then; b) subsequent enhancement via PANi deposition; c) exposure to high temperature for 28 days, then; d) subsequent enhancement via PEDOT deposition.

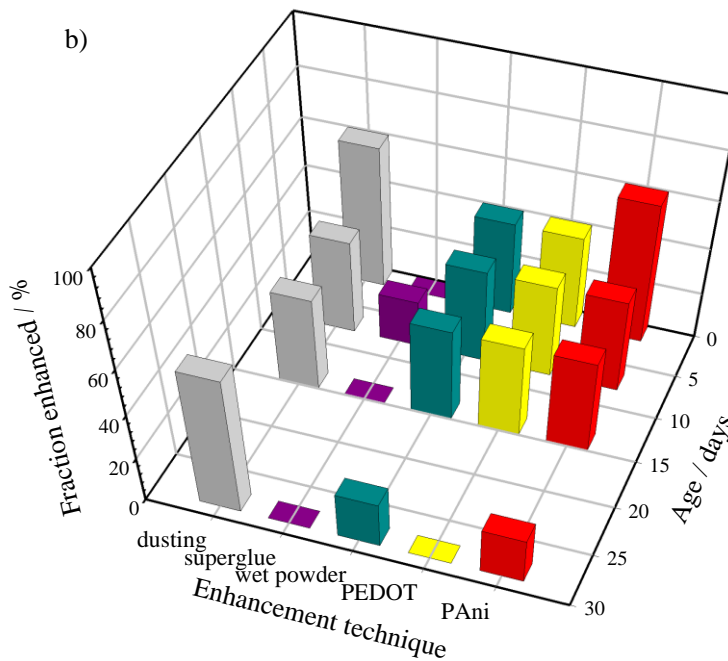
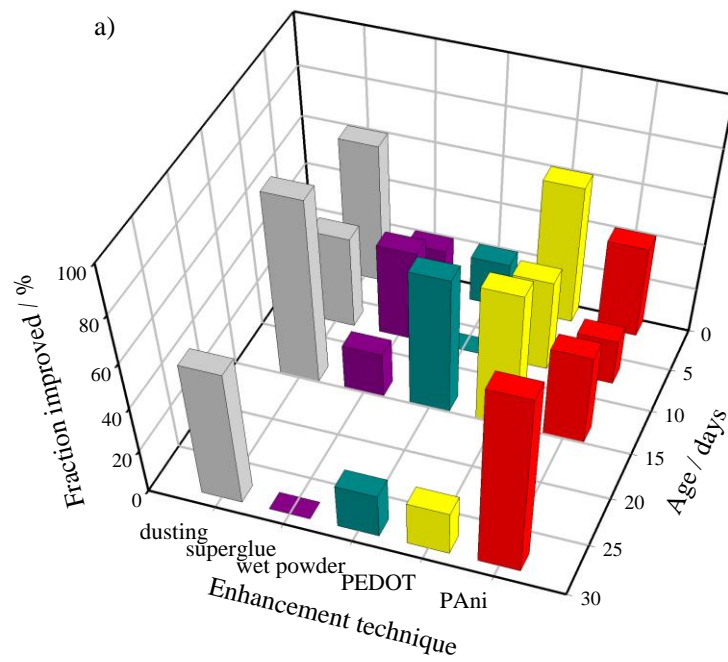


Figure 6.2. Three-dimensional bar charts showing the percentage improvements achieved by each of the development techniques for samples subject to storage under ambient conditions where; a) represents the *fraction improved* by each technique; and b) represents the *fraction useable*.

No attempt was made to remove the residue for the samples kept under ambient conditions; therefore the highest volume of samples improved to some degree should result from this environment. Figure 6.2a indicates that for each time interval at least four of the five techniques were able to improve the visibility of detail on their respective samples. It would appear that for the most part the *fraction improved* by an individual technique was between 40 - 60 %. For 1 and 14 day old samples each technique was able to improve the visibility of ridge detail of at least one sample. Out of all of the samples kept under ambient conditions superglue improved the least number of samples. PEDOT equalled the *fraction improved*, of one or more of the existing techniques, for both the 1 and 7 day time intervals. However PANi was the technique that improved the highest fraction of samples following the 28 day time interval. At 14 days old dusting improved a higher fraction of samples than any other technique.

Of the *fraction improved* not all were of a grade that is viewed as *useable*. It would appear that for the most part the *fraction useable* by an individual technique was 40 %. Figure 6.2b indicates that three of the five techniques were able to enhance at least one sample, to a useable grade, after each time interval. For 1 day old samples all but one technique, superglue, could improve the visibility of ridge detail to a useable grade. In fact superglue fuming only enhanced one sample, 7 days old, to a useable grade. PANi and dusting enhanced the highest *fraction useable* for 1 day old samples, equating to 3 of the 5 donors. One or both of the polymer enhancements equalled the highest *fraction useable* for all but one of the time intervals. At 28 days old dusting enhanced the most

samples, to a useable grade, with wet powder and PA_ni improving just one of their five samples.

The images found in Figure 6.3 show three fingerprints taken after the same time interval, 28 days old. Each fingerprint was deposited by a different donor and enhanced by a different technique, but all were given the same grade 3. All three samples lacked some level of distinguishable ridge detail that meant they could not be given the highest grade 4. Dusting was used to enhance the print in Figure 6.3a, circled is a region where the powder has adhered to both the positions of the ridges and furrows of the print. This is the result of a localised smudge of print residue upon deposition. It could be that as the finger was removed from the substrate, lifting in a wrist to fingertip motion, the tip of the print was slightly dragged across some of the residue deposited. Wet powder was used to enhance the print in Figure 6.3b. Here the core of the print, with *secondary detail* such as the two lakes circled, can be seen perfectly. However, detail is less clear further from the centre of the print. The ridges appear compacted, as if the furrows between them have narrowed. The area of apparent ridge contact is load dependent.¹⁶ According to Thomas and Reynoldson an increase of load from 0.5 to 10 N increases the width of the contact area from 125 to 250 μm . Therefore, if a high pressure was applied by the donor during deposition this could cause the ridges to “flatten out” losing the space and therefore definition between them. PA_ni deposition was used to enhance the print in Figure 6.3c, a lack of ridge definition towards the bottom of the detail could be the result of an uneven pressure applied at the time of residue deposition. *Secondary detail* can be seen in other areas of the print such as the circled lake. When compared to the lakes circled in Figure 6.3b a distinct difference can be

seen; the position of the “reagent’s” adherence is reversed. The wet powder has adhered to the boundary ridges (darker grey) of the lake (paler grey). In contrast PANi has adhered to the lake (green) leaving the boundary ridges (pale grey) free from polymerisation.

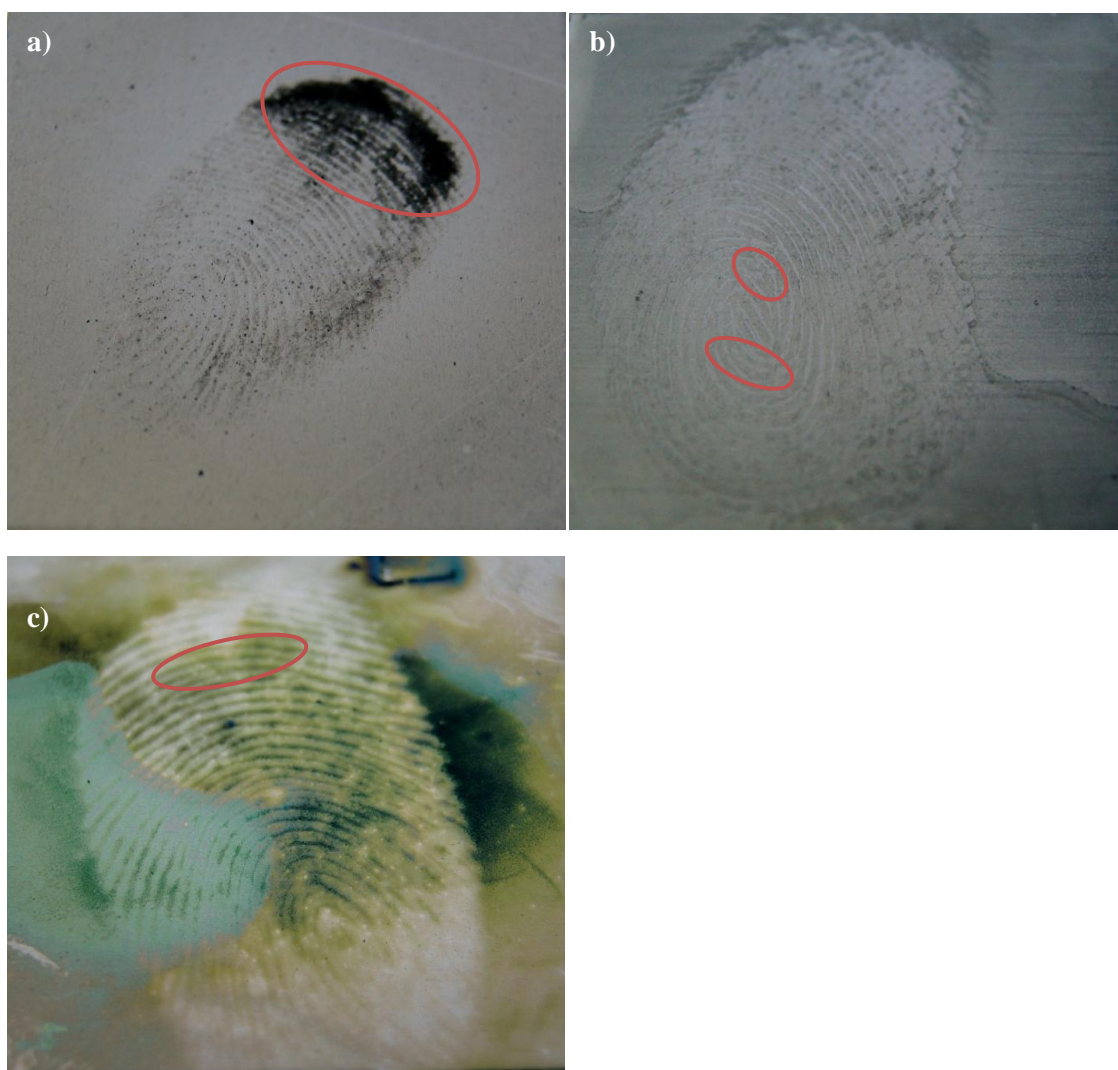


Figure 6.3. Photographic images of grade 3 fingerprints, previously deposited by different donors and stored under ambient conditions for 28 days before their enhancement via; a) dusting; b) wet powder; c) PANi deposition ($E = 0.9$ V, 300 s). Image b has been brightened for the purposes of printing.

6.3.2. Immersion in Water

Samples that were to be kept under water were placed in a container and submerged in water for their time before enhancement. This scenario is representative of a piece of evidence discarded into a waterway. The samples were allowed to dry naturally before their enhancement took place.

For samples that were submerged in water it is very likely that water soluble components of the residue, such as sugars and chlorides, will be removed over time. The results for samples kept under water differed from those under ambient conditions, Figure 6.4. According to Figure 6.4a the vast majority of samples were improved by their respective enhancement technique. Unfortunately wet powder was unable to improve any of the 1 day old samples, but for every other technique and time interval scenario at least one sample was improved. PEDOT and PANi equalled the *fraction improved* made by the existing techniques following the 1 day time interval. For the three remaining time intervals PANi outperformed the other four techniques and after the 7 day time interval 80 % of samples kept under water were improved using PANi. At both 14 and 28 days old PANi improved 60% of the samples, where dusting and wet powder resulted in the next highest *fraction improved*.

Despite the high *fraction improved* not all of the samples resulted in a grade that was *useable*, Figure 6.4b. PEDOT and PANi either excelled or equalled the *fraction useable* made by the existing techniques after three of the time intervals. The highest *fraction useable* by any one technique, at any one time interval, was 40 %. Unfortunately,

neither of the polymer enhancements were able to enhance a sample, to a useable grade, that had been aged for 28 days whilst under water. The dusting techniques each produced one useable print after this time; it would therefore be logical to expect them to work even better after shorter time intervals. This was not observed, so could be a result of dusting techniques producing variable outcomes; due to the end result being very dependent on how the operator works a particular print.

The images found in Figure 6.5 show two fingerprints taken after the same time interval, 7 days old. The fingerprints were deposited by the same donor but enhanced by different techniques. Despite the prints being deposited by the same donor and stored under water for the same amount of time, only one of them was enhanced to a useable grade. Superglue fuming was used to enhance the print in Figure 6.5a. The image of the superglue enhancement shows the ridges as light green on a much darker green background. The light green ridges indicate the location of the dyed polymerisation product, following superglue fuming. It is clear where the print residue was deposited yet not all the ridge detail is visible. There are also a large number of black dots (circled) that prevent the ridges from being continuous. Due to these reasons it is not possible to give a grade that is viewed as useable. PEDOT deposition was used to enhance the print in Figure 6.5b, which was given a useable grade of 3. The ridges enhanced by PEDOT appear, as they did with PANi, as a light grey on a blue background. The core of the print is not visible, however more than adequate surrounding features have been enhanced to justify a useable grade. A bifurcation and a delta have been circled.

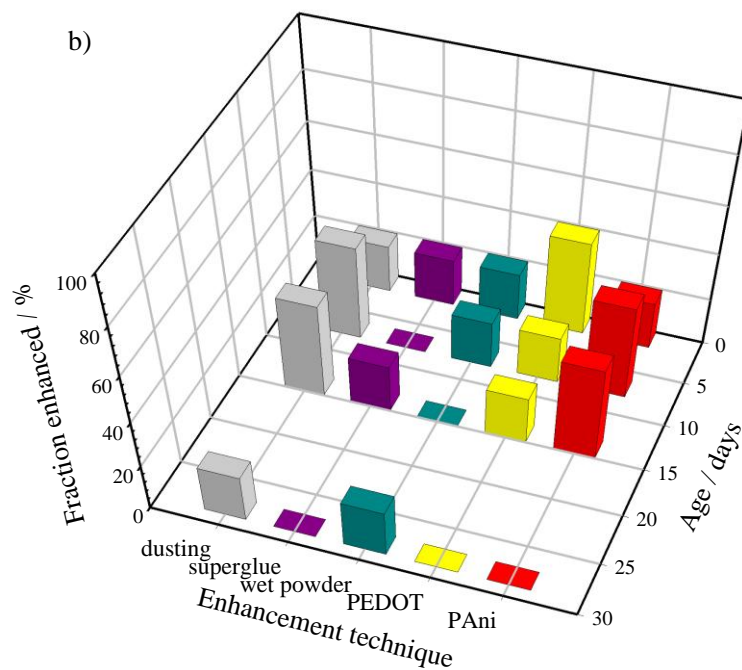
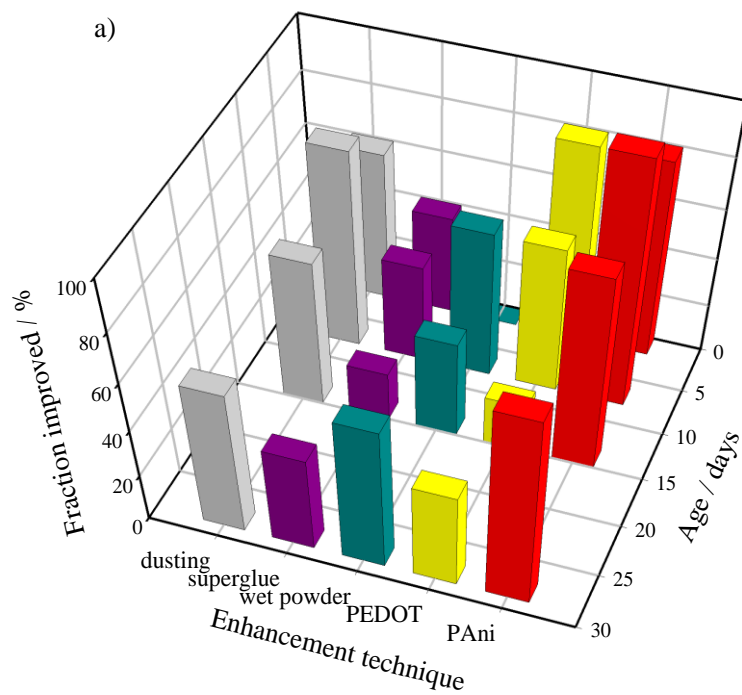


Figure 6.4. Three-dimensional bar charts showing the percentage improvements achieved by each of the development techniques for samples subject to continuous immersion in water; where; a) represents the *fraction improved* by each technique; and b) represents the *fraction useable*.

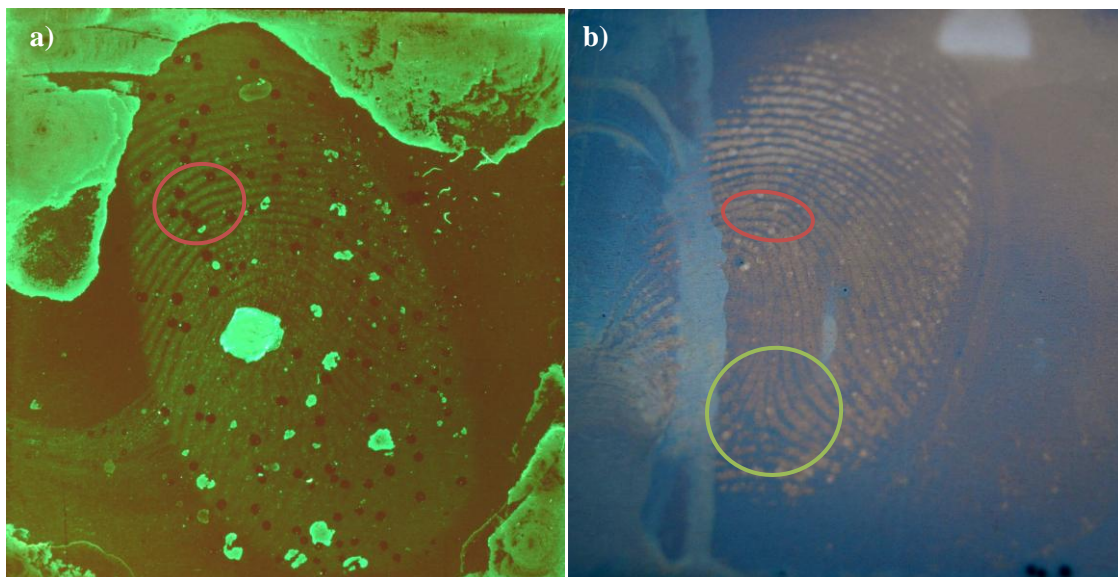


Figure 6.5. Photographic images of fingerprints previously deposited by the same donor and stored under water for 1 day before their enhancement via; a) superglue fuming (grade 2), circled are black dots (see text for more details); b) PEDOT deposition ($E = 0.9$ V, 180 s, grade 3), bifurcation circled in red and a delta circled in green. Image a has been brightened for the purposes of printing.

6.3.3. Acetone Wash

For this scenario samples were agitated in acetone for 30 s before being rinsed in water. The samples were allowed to dry naturally and remained under ambient conditions until their enhancement.

Acetone is a polar aprotic solvent and is commonly used as a degreaser.¹⁷ It has not only been used previously as part of a cleaning regime prior to the deposition of fingerprints,¹⁸⁻¹⁹ but also as a method for the removal of fingerprints prior to visualisation via corrosion.²⁰ All five techniques were able to improve the visibility of

detail for both the 1 and 7 day old samples, Figure 6.6a. PEDOT and wet powder achieved equal *fraction improved* results for the 1 day old samples. Following the 7 day time interval PEDOT improved the highest fraction, 80 %, of the samples. All the techniques, except for superglue, were able to improve 40 % of the samples aged for 14 days. Dusting gave the highest fraction of improvement for the 28 day old samples.

Four of the techniques, including both the polymer enhancements, enhanced at least one of the 1 day old samples to a useable grade, Figure 6.6b. However, for the 7 day old samples only PEDOT was able to result in any degree of *fraction useable*. Additionally, dusting was the only technique to enhance, to a useable grade, a sample after the 14 day time interval. Variable pressure exerted from an individual donor, at the time of residue deposition, can affect the quality and quantity of sweat deposited.¹⁶ It is therefore speculated that when a technique produces better results after a longer time interval, a larger quantity of residue was initially deposited. No improvements were made by any of the techniques following the 28 day time interval. Due to the low *fraction useable* results this suggests that during the samples agitation in acetone the removal of some components did occur, or the acetone wash aided the degradation of the fingerprint residue over time.

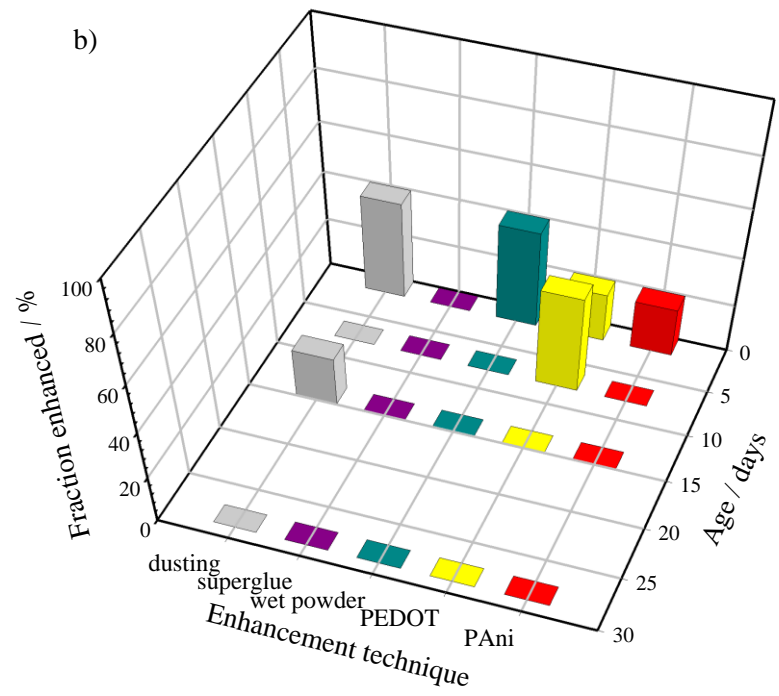
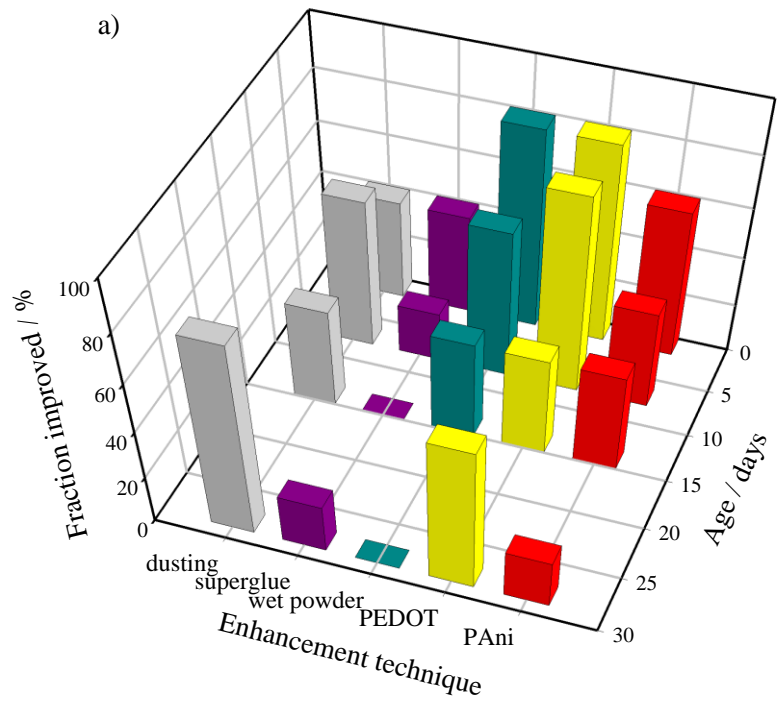


Figure 6.6. Three-dimensional bar charts showing the percentage improvements achieved by each of the development techniques for samples subject to an acetone wash; where a) represents the *fraction improved* by each technique; and b) represents the *fraction useable*.

The images found in Figure 6.7 show two grade 2 fingerprints taken after different time intervals. The fingerprints were deposited by the same donor and were both enhanced via PANi deposition. The appearance of the samples, despite being enhanced in the same way, is very different. The sample found in Figure 6.7a was aged for 7 days following its acetone wash. A considerable amount of the print has been made visible, yet much heavier deposits of polymer, in localised areas, have prevented continuous ridges (circled). Aged for 14 days following its acetone wash, the sample in Figure 6.7b also lacks continuous ridge detail.

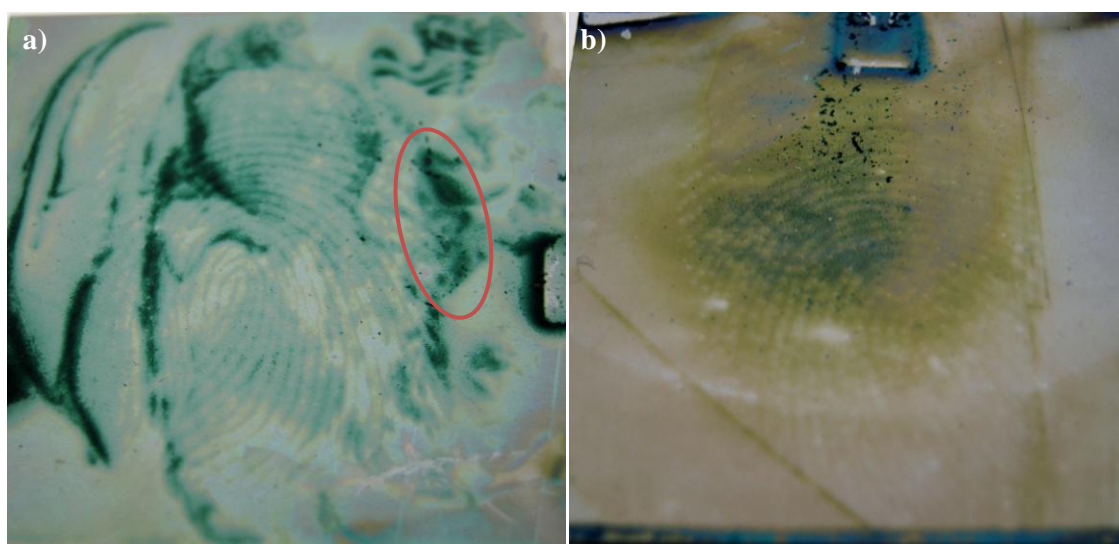


Figure 6.7. Photographic images of grade 2 fingerprints, previously deposited by the same donor, enhanced via PANi deposition ($E = 0.9$ V, 300 s) following an acetone wash and storage under ambient conditions for; a) 7 days; b) 14 days.

6.3.4. Exposure to High Temperature

The high temperature samples were placed on a metal tray and kept in an oven at 150 °C until their enhancement. It was expected that the evaporation of the more volatile components would occur more rapidly than if kept under ambient conditions. Whereas crimes which involve the use of fire would reach much higher temperatures, this scenario represents the possible outcome from such a scene. Before their enhancement they were allowed to cool to room temperature.

At least three of the five techniques were able to improve the visibility of ridge detail after each of the time intervals for samples that were exposed to continuous heating, the results of which can be seen in Figure 6.8a. Both PEDOT and PANi improved 100 % of their 1 day old samples with superglue being the only other technique to make an improvement after that time interval. PEDOT was still able to improve 100 % of its 7 day old samples, where PANi and dusting both improved 40 %. Surprisingly, wet powder, having not improved any samples at 1 and 7 days old, improved the highest fraction for 14 day old samples and 60 % at 28 days old. PEDOT achieved the highest *fraction improved* of samples that had been aged for 28 days; however PANi did not improve any.

The high temperature samples were not exposed to such extremes (>600 °C) as previously reported, where it was found that the water content and volatile organic components of the fingerprint residue can be completely removed.²⁰⁻²¹ However, it was expected that some degree of degradation of the residue would be likely to occur at 150

°C, or at least occur faster than if the sample was exposed to ambient conditions. The results, when compared to those under ambient conditions, support this. Two of the four time intervals (1 day old and 14 days old) did not result in any enhancements, to a useable grade, by any one of the techniques, Figure 6.8b. PEDOT enhanced the highest fraction of samples over all four times intervals and was the only technique to achieve a useable sample that had been aged for 28 days. This suggests that a temperature of 150 °C is more than adequate for the removal of some or the entire fingerprint residue.

The images found in Figure 6.9 show three fingerprints taken after the same time interval, 7 days old. Each fingerprint was deposited by a different donor and enhanced using a different technique. PANi deposition was used to improve the print in Figure 6.9a, which was given a grade of 1. Only small sections of ridge detail have been enhanced (circled). The polymer has deposited around the print region suggesting that after 7 days there are components of sweat residue remaining on the metal substrate preventing polymerisation. During the high temperature exposure the residue could have lost its structural integrity resulting in the ridges merging into one another. However, for prints that had been aged for the same amount of time it was still possible to achieve useable grades. Superglue fuming was used to enhance the print in Figure 6.9b, which was given a grade of 4. The *primary detail* of the print is clearly a loop and *secondary detail* such as the circled bifurcations are visible. PEDOT deposition was used to enhance the print in Figure 6.9c, which was given a grade of 3. The ridges are clear yet less of the print has been enhanced than that of the enhancement by superglue fuming. It was possible to enhance clear ridge detail with some of the samples, but not from all of the donors. Each donor's sweat will have a slightly different consistency,

which when heated will degrade at different rates. Therefore it could be how the donors sweat is affected by the heat that determines the outcome of the enhancement.

6.3.5. Soap Wash

To represent a scenario where a piece of evidence was cleaned in an attempt to remove any fingerprints, samples were washed in warm soapy water. They were then rinsed with soap free water and allowed to dry naturally in air and remained under ambient conditions until their enhancement.

Warm soapy water has been used previously as a method for the removal of fingerprints from metal surfaces.^{20, 22} The soap wash involved the use of a surfactant (commercially available detergent) that can act as a solvent to oils and fats.²³⁻²⁴ Figure 6.10a shows the limited improvements made by each of the techniques. PEDOT was the only technique to improve samples taken after all four of the time intervals; with 100 % improvements for both 1 and 7 day old samples. PANi was able to improve just one sample from the 1, 14 and 28 day time intervals. The conventional techniques each made improvements after one of the time intervals; superglue improved 20 % of 1 day old samples, wet powder improved 20 % of 7 day old samples and dusting improved 40 % of 14 day old samples.

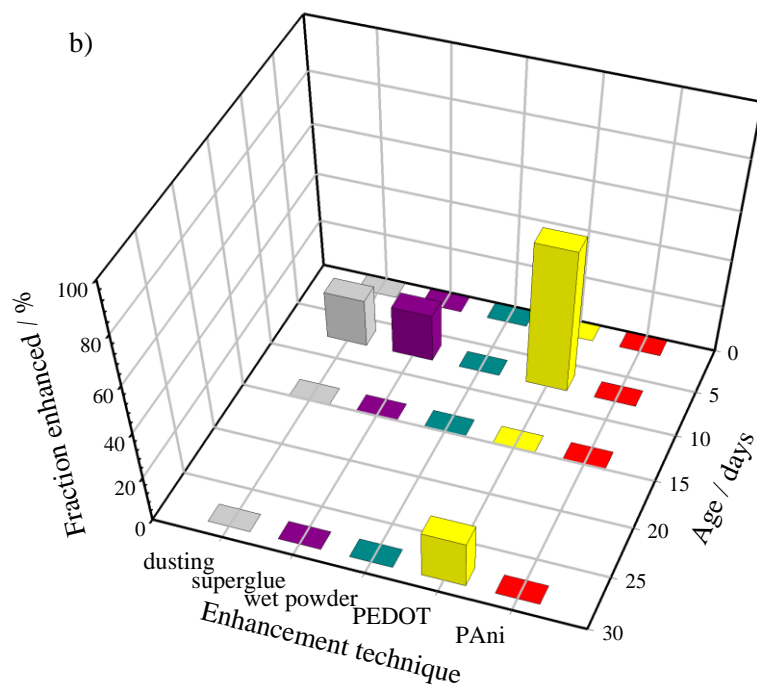
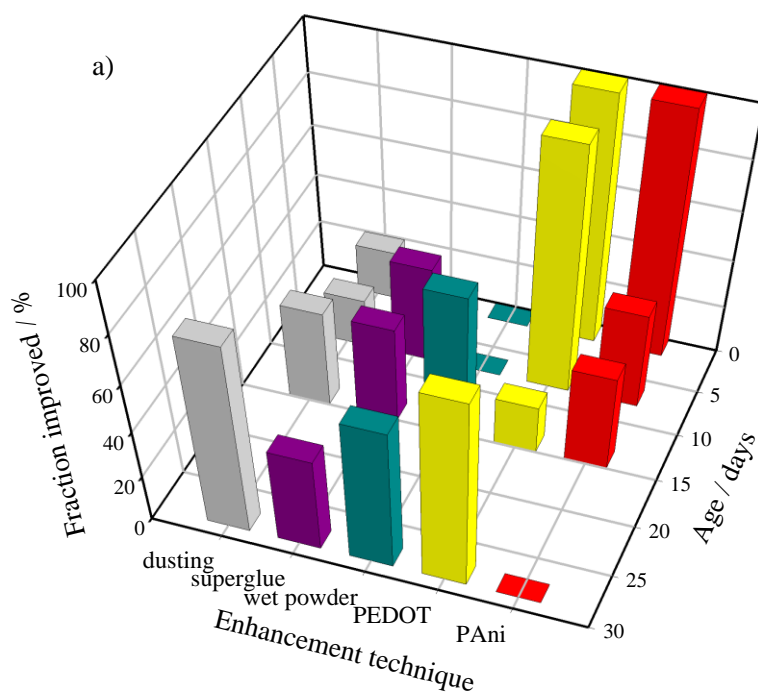


Figure 6.8. Three-dimensional bar charts showing the percentage improvements achieved by each of the development techniques for samples subject to continuous heat treatment at 150 °C; where a) represents the *fraction improved* by each technique; and b) represents the *fraction useable*.

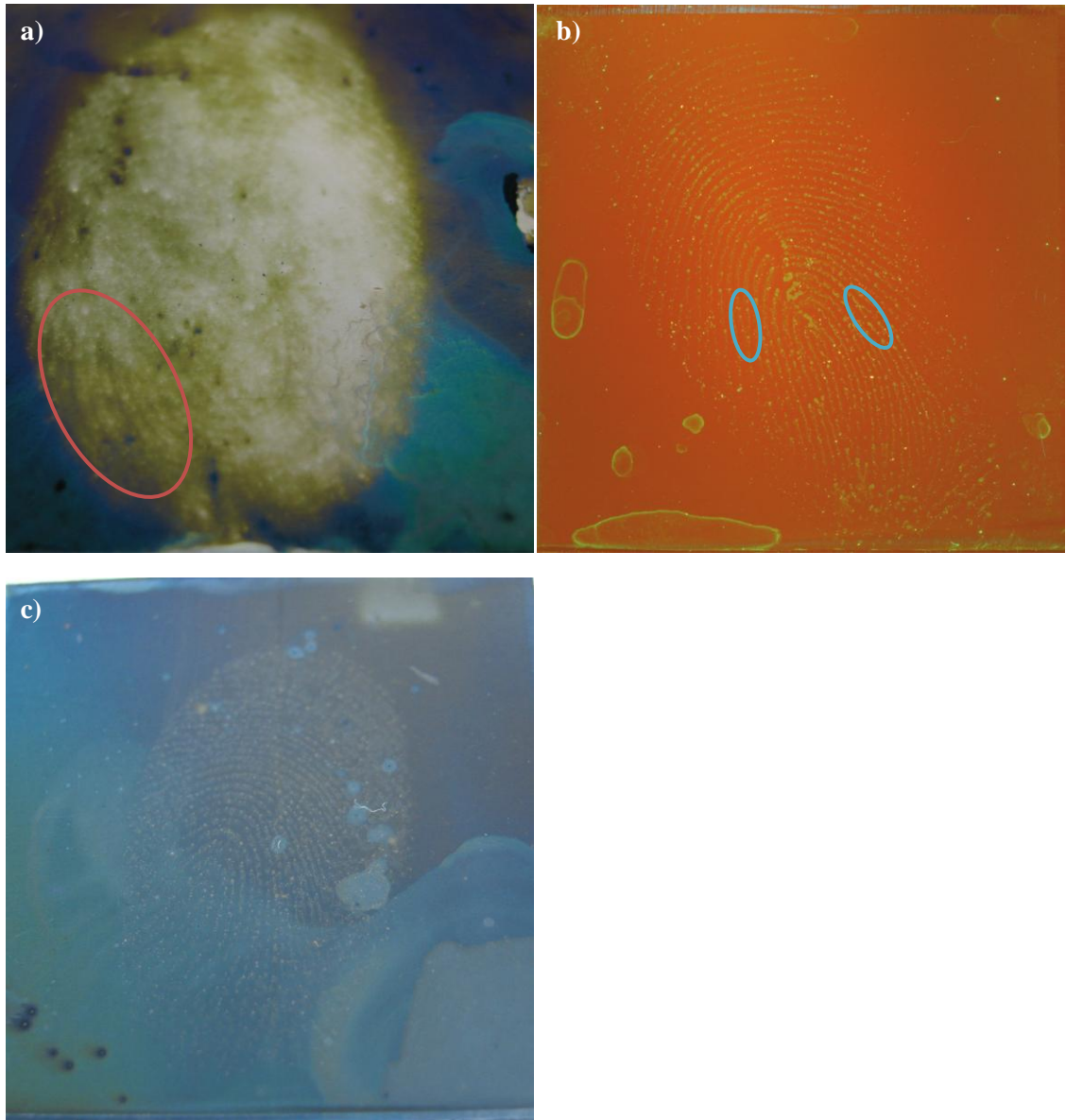


Figure 6.9. Photographic images of fingerprints previously deposited by different donors and stored at high temperature for 7 days before their enhancement via; a) PANi deposition ($E = 0.9$ V, 360 s, grade 1), faint ridges circled in red; b) superglue fuming (grade 4), bifurcations circled in blue; c) PEDOT deposition ($E = 0.9$ V, 150 s, grade 3). Images b-c have been brightened for the purposes of printing.

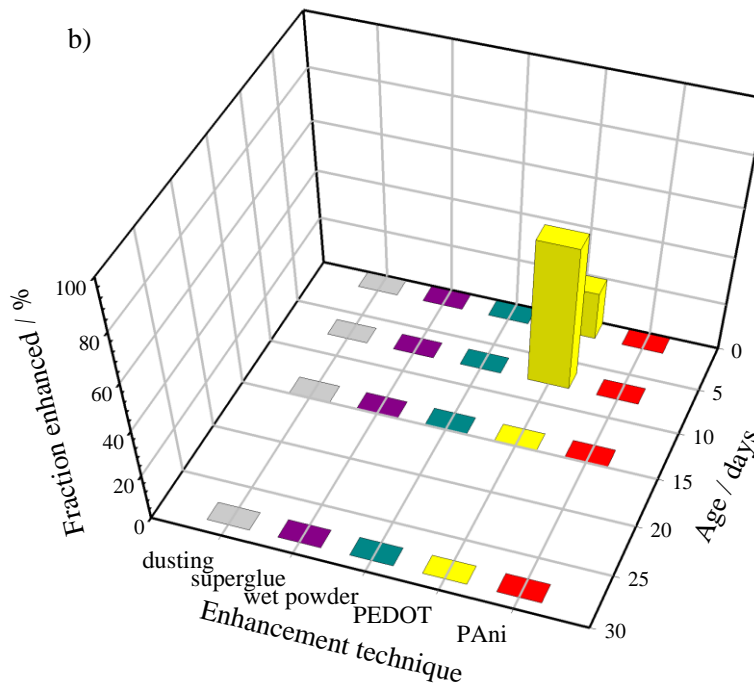
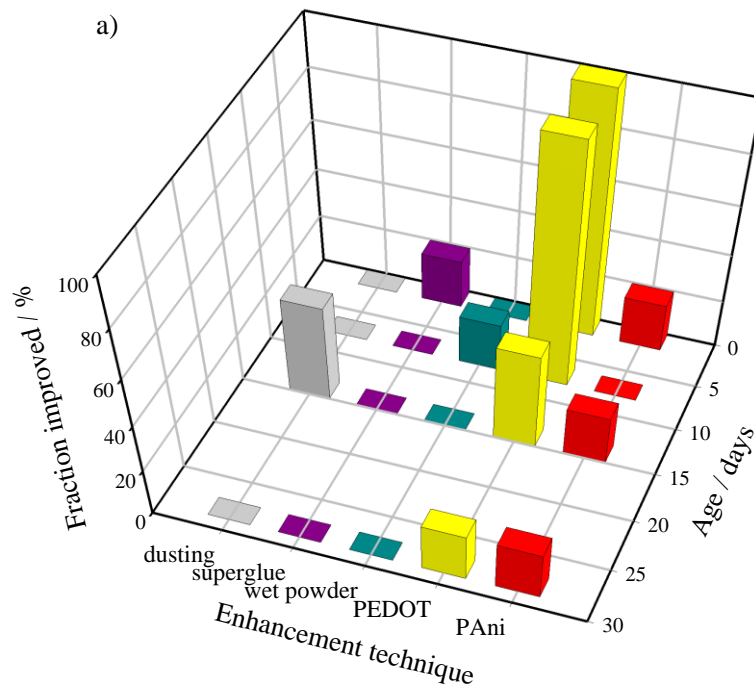


Figure 6.10. Three-dimensional bar charts showing the percentage improvements achieved by each of the development techniques for samples subject to washing with aqueous soap solution; where a) represents the *fraction improved* by each technique; and b) represents the *fraction useable*.

It would appear that the use of a surfactant, to remove fingerprints from metal surfaces, is effective. The least *fraction useable* of the entire study was achieved from samples that had been washed with soap, Figure 6.10b. PEDOT was the only technique to enhance samples to a grade that is deemed useable; one sample that was 1 day old and two that had been aged for 7 days.

The images found in Figure 6.11 show two fingerprints taken after different time intervals. Each fingerprint was deposited by a different donor and enhanced using a different technique. Wet powder was used to improve the 7 day old print in Figure 6.11a. Ridge detail is visible but not well defined; contrast between the wet powder and the substrate is poor. Therefore the sample can only be given a grade of 2. PEDOT deposition was used to enhance the 1 day old print in Figure 6.11b. Less of the print is visible than that of the wet powder sample however the contrast between the substrate and ridges is clearer.

6.3.6. Summary

Inspection of Figures 6.2a, 6.4a, 6.6a, 6.8a and 6.10a shows that, with the exception of soap washed samples, most techniques offered some element of enhancement. This is hardly surprising, but does not reveal whether the enhancement was at a worthwhile level. Interestingly, due to its widespread use on non-porous surfaces, superglue fuming appeared to be the least effective treatment. Simplistically, with obvious variations that are explored below, the most effective procedures were either simple dusting or one of the electrochromic polymer treatments to be assessed.

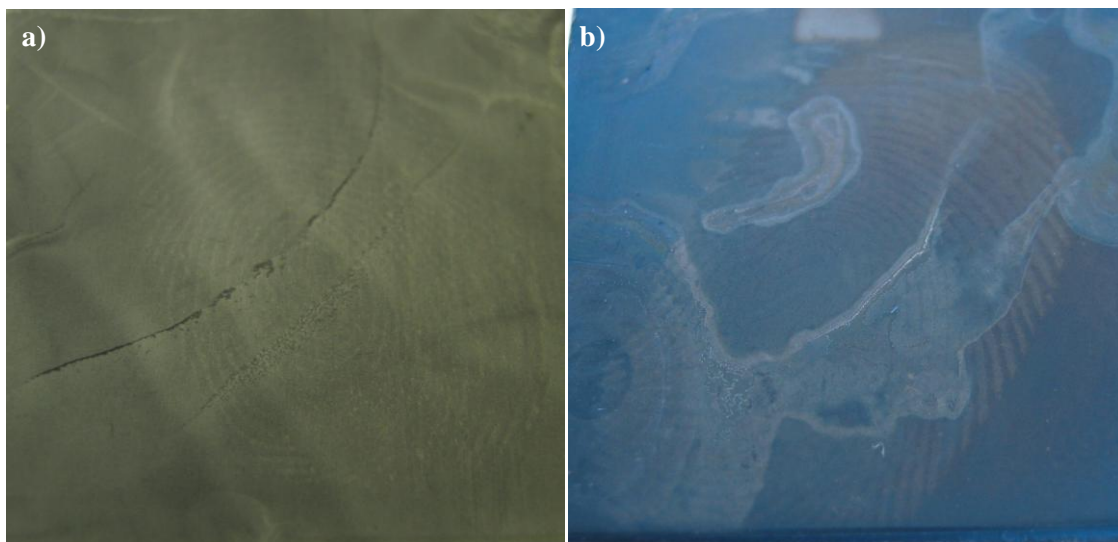


Figure 6.11. Photographic images of fingerprints, previously deposited by different donors, following a soap wash and storage under ambient conditions for; a) 7 days before their enhancement via wet powder (grade 2); b) 1 day before their enhancement via PEDOT deposition ($E = 0.9$ V, 180 s, grade 3). Images have been brightened for the purposes of printing.

Half of the twenty possible time interval and environment combinations resulted in one or more of the polymer treatments improving the highest fraction of samples. In fact only three of the combinations resulted in one or more of the existing techniques improving the most samples. As a consequence the remaining seven combinations were a result of one or more of the polymer treatments improving an equally high fraction of the samples to one or more of the existing techniques.

The more searching question was what level of enhancement was achieved; for this the inspection of Figures 6.2b, 6.4b, 6.6b, 6.8b and 6.10b is required. For ambient conditions (Figure 6.2), the variations in performance of the enhancement methods

were generally not large, for a given age of print. The two exceptions to this were the low enhancement levels from superglue fuming (at all print ages) and the better recovery rate for the oldest prints (28 days) using simple dusting. Overall, with these two exceptions, this relatively unchallenging scenario was tolerant to choice of enhancement procedure.

At the other extreme, this more discriminating survey showed that samples subject to heat treatment (Figure 6.8) or washed with aqueous soap solution (Figure 6.10) were associated with very low recovery levels. PEDOT deposition offered the best prospect of recovery in the former instance and was the only enhancement procedure that appeared to offer any prospect of success in the latter instance.

Between these extremes were the cases of an acetone wash and continuous immersion in water. In the case of the acetone wash (Figure 6.6), dusting was the most effective treatment. Success levels for this treatment were generally very poor for older samples. The reason for this marked decrease in recovery rate with age was not clear, since the acetone wash was early in the storage interval; nevertheless, the outcome was clear. Continuous immersion in water provided more complex outcomes. The effectiveness of wet powder was not high, but it seemed relatively insensitive to the duration of immersion. It would appear that anything removed by water was lost quickly and would in any case be removed by the wet powder treatment. As water is used to rinse samples treated with wet powder (see Chapter 3 Section 3.9), water based components of print residue are unlikely to affect its success. The polymer treatments and dusting

show modest performance over the first 14 days, with only dry powder dusting (and possibly wet powder) effective after 28 days.

An interesting general observation was that recovery rates, for a given sample history/environment and enhancement technique, were relatively insensitive to fingerprint age for the first 14 days, but drop sharply at 28 days. The practical significance of this for scheduling the processing of evidence is obvious.

The polymer treatments gave a greater number of useable prints in more sub-groups than any of the existing techniques: dusting, wet powder and superglue fuming. Equal amounts of useable prints were achieved by one or both of the polymer treatments with one or more of the existing techniques in a quarter of the groups. For each combination of time, environment and development technique no more than three of the five samples were enhanced to a useable grade, this can be seen in Table 6.1. The highest number of useable prints was not surprisingly generated from an ambient environment. The least number of useable prints was achieved from the soap washed samples, all developed using PEDOT. The number of useable prints developed from 1 and 7 day old samples was very similar, following this, as the samples aged, fewer prints were developed to such quality.

1 Day Old						
	Ambient	High Temp.	Water Treated	Acetone Wash	Soap Wash	
Dusting	3	0	1	2	2	0
Superglue	0	0	1	0	0	0
Wet Powder	2	0	1	2	2	0
PEDOT	2	0	2	1	1	1
PAni	3	0	1	1	1	0
7 Day Old						
	Ambient	High Temp.	Water Treated	Acetone Wash	Soap Wash	
Dusting	2	1	2	2	0	0
Superglue	1	1	0	0	0	0
Wet Powder	2	0	1	0	0	0
PEDOT	2	3	1	2	2	3
PAni	2	0	2	0	0	0
14 Day Old						
	Ambient	High Temp.	Water Treated	Acetone Wash	Soap Wash	
Dusting	2	0	2	2	1	0
Superglue	0	0	1	0	0	0
Wet Powder	2	0	0	0	0	0
PEDOT	2	0	1	0	0	0
PAni	2	0	2	0	0	0
28 Day Old						
	Ambient	High Temp.	Water Treated	Acetone Wash	Soap Wash	
Dusting	3	0	1	0	0	0
Superglue	0	0	0	0	0	0
Wet Powder	1	0	1	0	0	0
PEDOT	0	1	0	0	0	0
PAni	1	0	0	0	0	0

Table 6.1. The number of samples enhanced to a useable grade (3-4) for samples subjected to a range of environments for varying intervals of time.

6.4. Optimum Enhancement of Samples According to a Incompletely Known History

In the previous section the data were analysed in the context of a research study. The time intervals and environmental exposures were known. However, the outcomes, the abilities of five different techniques to enhance the prints, were unknown. In this

section the reverse is addressed; the outcomes are known but the specific scenario is not. Therefore according to the outcomes obtained in Section 6.3, a suitable technique (s) can be identified for the enhancement of a sample of incompletely known history.

The interpretation of the data for enhancement of fingerprints to useable levels (Figures 6.2b, 6.4b, 6.6b, 6.8b and 6.10b) has been divided into two different scenarios. Firstly, the situation that a print was of known age but had been subjected to uncertain conditions is considered. This corresponds to summation of the corresponding columns for each technique in Figures 6.2b, 6.4b, 6.6b, 6.8b and 6.10b; the outcomes are shown in Figure 6.12a-d, corresponding to fingerprints sampled after 1, 7, 14 and 28 days. In the data sets shown, summing the results across donors and environments means that each column represents a sample of 25 prints. Thus, anomalous behaviour of a single print (i.e. “bit error” associated with an outlier in terms of underlying print quality, enhancement protocol or assessment) is 4%. In practical terms, this scenario is realistic in (on the basis of other evidence) that one may frequently know when a crime was committed but have little or no knowledge of the history of the object in question.

Secondly, the scenario that a print had been subjected to a known environmental exposure but for an unknown time interval is considered. Inspection of the data in Figure 6.12 reveals four interesting features. First, superglue fuming was not effective on these samples subject to these environments. Therefore, in view of this outcome, data obtained using this method in the subsequent discussion is not included. Second, for relatively fresh (1 day old) prints, there was no significant difference in the effectiveness of the remaining four treatments. Third, for 7 day old prints, the PEDOT

variant of the electrochromic film treatment was unequivocally the best method. Interestingly, this method gave a better outcome for 7 day old prints than 1 day old prints. It is speculated that this may be associated with some form of compaction of the fingerprint deposit during ageing, which made the masking action of the deposit more effective. Third, for 14 day old prints, dusting was the most effective treatment. Fourth, for 28 day old prints, dusting was again the most effective treatment, but now even this optimum recovery level was low.

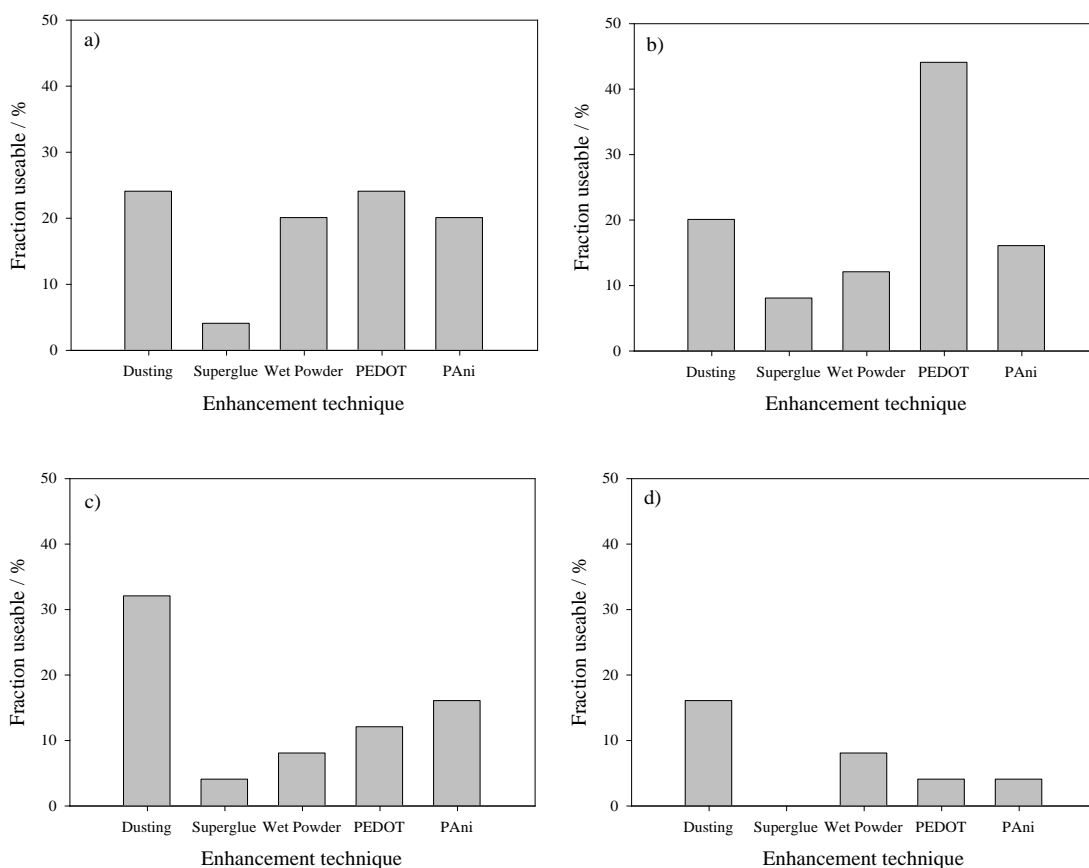


Figure 6.12. The enhancement to a useable grade of samples of an “unknown” environmental exposure for prints aged for; a) 1 day; b) 7 days; c) 14 days; d) 28 days.

A complementary situation is then considered, of fingerprints of known environment, but unknown age. This corresponds to summation of the columns *within* the individual panels of Figures 6.2b, 6.4b, 6.6b, 6.8b and 6.10b. Five distinct observations can be made on the outcomes, shown in Figure 6.13. First, superglue fuming was the least effective for three cases and not effective in the other two. Second, for the relatively unchallenging situation of prints on substrates kept under ambient conditions, that there was relatively little variation amongst the effectiveness of the remaining four treatments: dusting provided 50% recovery and the deposition of PANi provided 40% recovery. Third, for samples kept in water, dusting and the deposition of PANi were the most effective methods, with recovery rates of 30% and 24%, respectively. Fourthly, for acetone washed samples, only dusting provided significant enhancement. It is deduced that acetone was effective at removing the insulating non-polar organic components upon which the masking effect underlying the electrochromic film deposition approach relied. Finally, it is noted that the rather more challenging environments of extended heat treatment and soap washing prevented significant recovery by all but the deposition of PEDOT.

Finally, the integration of data both *within* the age rows in Figures 6.2b, 6.4b, 6.6b, 6.8b and 6.10b and, for each treatment, *between* the panels in these figures is considered. This corresponds to prints of unknown age *and* environment. In these aggregated data sets (Figure 6.14) the outcome for each enhancement method was assessed over 100 prints (exposed to 5 environments, of 4 ages and originating from 5 donors), strengthening the confidence about the observed variations in performance.

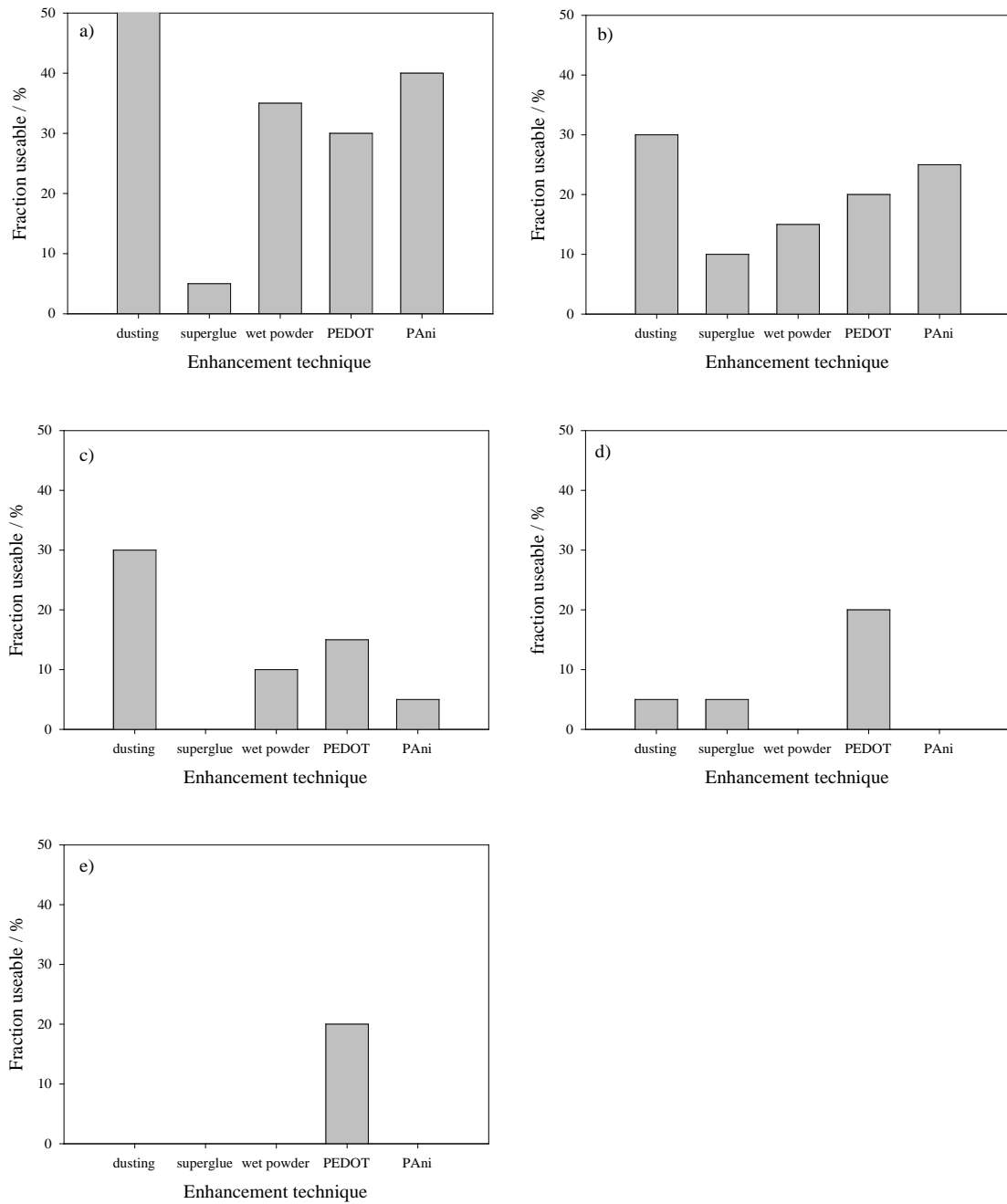


Figure 6.13. The enhancement to a useable grade, of samples of an “unknown” age for prints subject to storage under; a) ambient conditions; b) immersion in water; c) acetone wash; d) heat treatment; e) soap wash.

The overall outcome was that the two variants of the polymer enhancement were of comparable general performance to dusting and outperformed superglue and wet

powder for the types of sample studied. Of the two electrochromic films, PEDOT slightly outperformed all other methods and PANi was slightly less effective than dusting. In the absence of “history” information for an object, the statistically best option would be to use PEDOT. However, as the individual data sets for different film histories (Figures 6.2b, 6.4b, 6.6b, 6.8b and 6.10b) show, some knowledge about an object’s age or the environment to which it has been subjected may modify this conclusion. An alternative way of representing this latter issue is summarized in Table 6.2, which shows the enhancement technique that gave the highest number of improved samples (to a useable grade) for each environment and print age at enhancement. There are a few situations where no samples were improved to a useable extent. In these cases the technique that gave the best improvement was used; these cases are indicated by italic text. For samples washed with acetone and aged for 28 days there was no distinction between two techniques, dusting and PEDOT.

Time Interval	Ambient	High Temperature	Water Treated	Acetone Wash	Soap Wash
1 day	PEDOT	<i>PAni</i>	PEDOT	Wet Powder	PEDOT
7 days	Dusting	PEDOT	PAni	PEDOT	PEDOT
14 days	PEDOT	<i>PEDOT</i>	Dusting	Dusting	<i>PEDOT</i>
28 days	Dusting	PEDOT	Wet Powder	<i>Dusting/PEDOT</i>	<i>PEDOT</i>

Table 6.2. Enhancement technique giving the highest frequency of improvement (increase in fingerprint grade) for fingerprints of each age and environment studied.

Focusing on the polymer treatments, three significant observations can be made. The performance of the electrochromic polymers was better in more scenarios than the other three techniques combined. PEDOT was very effective at enhancing soap-washed samples and those kept at elevated temperature. Despite not producing the highest

number of useable prints, PANi was the most effective at *improving* water treated samples of varying ages; further refinement of the technique (for example making full use of *in-situ* potential control) may be valuable here.

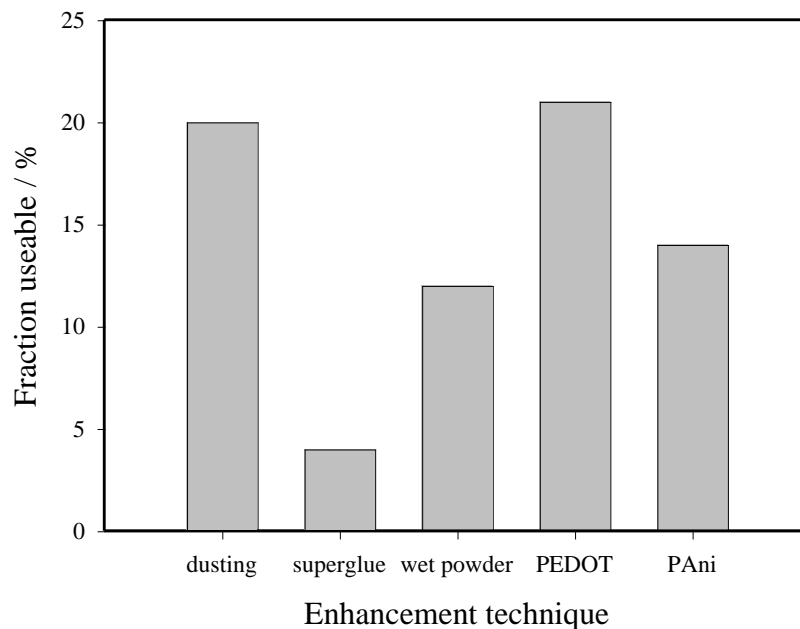


Figure 6.14. Enhancement via five individual techniques to a useable grade of prints of “unknown” age and environment.

Despite efforts to produce prints of consistent quality and composition for a given donor, variations are unavoidable even between fingers on the same hand or from the same finger. The survey of 500 prints was designed to allow exploration of key variables. However, for any given combination of circumstances (donor, print age, environment and enhancement method) this does not allow for replicates.

6.5. Conclusions

A survey was carried out on the effectiveness of a new electrochromic method for the enhancement of latent fingerprints on metal substrates. Fingerprints were deposited on stainless steel substrates, exposed to a range of environments representative of plausible crime scene situations and left for varying intervals prior to enhancement. Two variants of the electrochromic enhancement methodology, involving PANi and PEDOT films, were compared with three traditional methods, dusting with dry powder, wet powder and superglue fuming. The outcomes were assessed using the five point scale devised by Bandey, taking the view that prints of grade 0-2 are not useable and prints of grade 3 or 4 are useable.

Superglue fuming was generally the least effective method. This methodology, which is widely used to good effect on insulating materials (plastics), is complementary to the electrochromic methodology, which requires a conducting substrate. In broad terms, the best method for any selected example of the scenarios explored was either dusting or electrochromic enhancement; wet powder offered some enhancement but to a lesser extent.

Performance of the different techniques was assessed from the fine detail of fully known sample history, through partially known history to totally unknown history. For the relatively unchallenging case of samples stored under ambient conditions, with the exception of superglue treatment, there was little difference in performance of the different techniques for a given age of print. As the prints aged, the recovery rate declined, particularly in the step from 14 to 28 days. Samples washed with acetone

prior to storage were best treated by dusting. The poorer performance of the new electrochromic technique here was attributed to dissolution by acetone and removal from the surface of the non-polar organic components that form the insulating “mask” upon which the technique relies. Continuous and prolonged immersion in water generated a complex pattern of enhancement performance. Wet powder did not perform particularly well, but its performance did not decline greatly with immersion time. Dusting and electrochromic enhancement methods worked relatively well for samples up to age 14 days, but recovery rates declined sharply thereafter. For the most challenging environments of extended heat treatment and washing with soap solution, only the electrochromic enhancement procedure (with PEDOT as reagent) was effective.

Aggregation of the data by summation over all print ages (retaining environments separate), or over all environments (retaining print ages separate), or over both print ages and environments were considered. This allowed assessment of optimum approaches for evidence of unknown age, environmental exposure or both. Overall, in the absence of any sample history information, electrochromic enhancement by PEDOT provided the best chance of recovering a useable print; dusting and PANi electrochromic enhancement, in that order, were the next best methods. As one acquires more information on sample history, particularly environmental exposure, discrimination between dusting and electrochromic enhancement as the method of choice becomes possible.

It is concluded that electrochromic fingerprint enhancement will be competitive with presently used methods across a broad range of scenarios and may be pre-eminent in particular scenarios. There are two respects not explored in the simplistic assessment used here in which the electrochromic film methodology may further excel. The first is diversification to polymer films of different colours; a number of suitable materials are available. Second, the traditional approach involves use of monochrome black-and-white images but, by definition; electrochromic materials allow manipulation of optical properties (colour) by application of an external stimulus (voltage). Acceptance of this concept, for example using spectral imaging, would yield the benefits of an additional dimension of information.

6.6. References

1. A. L. Beresford, R. M. Brown, A. R. Hillman, J. W. Bond, *J. Forensic Sci.*, 2012, **57**, 93.
2. A. R. W. Jackson, J. M. Jackson, *Forensic Science*, 2004, Pearson Prentice House, Harlow, UK.
3. A. Girod, R. Ramotowski, C. Weyermann, *Forensic Sci. Int.*, 2012, **223**, 10.
4. H. C. Lee, R. E. Gaensslen, *Advances in Fingerprint Technology*, 2001, 2nd edn., CRC Press, London, UK.
5. G. S. Sodhi, J. Kaur, *Forensic Sci. Int.*, 2001, **120**, 172.
6. M. J. Choi, T. Smoother, A. A. Martin, A. M. McDonagh, P. J. Maynard, C. Lennard, C. Roux, *Forensic Sci. Int.*, 2007, **173**, 154.
7. L. Liu, S. K. Gill, Y. Gao, L. J. Hope-Weeks, K. H. Cheng, *Forensic Sci. Int.*, 2008, **176**, 163.
8. L. K. Seah, U. S. Dinish, W. F. Phang, Z. X. Chao, V. M. Murukeshan, *Forensic Sci. Int.*, 2005, **152**, 249.
9. F. Haque, A. D. Westland, J. Milligan, F. M. Kerr, *Forensic Sci. Int.*, 1989, **41**, 73.
10. G. Polimeni, B. F. Foti, L. Saravo, G. De Fulvio, *Forensic Sci. Int.*, 2004, **146**, 45.
11. P. Czekanski, M. Fasola, J. Allison, *J. Forensic Sci.*, 2006, **51**, 1323.
12. S. P. Wargacki, L. A. Lewis, M. D. Dadmun, *J. Forensic Sci.*, 2007, **52**, 1057.
13. A. L. Beresford, A.R. Hillman, *Anal. Chem.*, 2010, **82**, 483.
14. R. M. Brown, A. R. Hillman, *Phys. Chem. Chem. Phys.*, 2012, **14**, 8653.

15. H. L. Bandey, Fingerprint development and imaging newsletter: the powders process, study 1. Sandridge: Police Scientific Development Branch, Home Office, 2004; Report No.:54/04.
16. G. L. Thomas, T. E. Reynoldson, *J. Phys. D: Appl. Phys.*, 1975, **8**, 724.
17. C. E. Housecraft, E. C. Constable, *Chemistry: An Introduction to Organic, Inorganic and Physical Chemistry*, 2002, Pearson, Harlow, England.
18. G. Williams, N. McMurray, Latent, *Forensic Sci. Int.*, 2007, **167**, 102.
19. Y. Migron, D. Mandler, *J. Forensic Sci.*, 1997, **42**, 986.
20. E. Paterson, J. W. Bond, A. R. Hillman, *J. Forensic Sci.*, 2010, **55**, 221.
21. G. Williams, H. N. McMurray, D. A. Worsley, *J. Forensic Sci.*, 2001, **46**, 1085.
22. J. W. Bond, *J. Forensic Sci.*, 2008, **53**, 812.
23. M. Bailey, K. Hurst, *Advanced Modular Sciences*, 2000, Harper Collins, London, England.
24. J. Israelachvili, *Intermolecular and Surface Forces*, 1991, Academic Press, London, England.

Chapter Seven

7. Conclusions

The purpose of this work was to recover latent fingerprints from a selection of metallic surfaces, which have prospective forensic value, by the electropolymerisation of a polymer. The work aimed to utilise fingerprint residues to 'protect' the metal surface from polymer deposits, resulting in a negative image of the print. It was intended, where applicable, to exploit the electrochromic properties of the deposited polymer to adjust and optimise the contrast between print and substrate. The goal was to assess the technical performance of polymer enhancement in diverse environments, in a comparison with existing enhancement techniques to identify individual strengths and weaknesses. As well as environment, the study covered a range of fingerprint donors and ages of fingerprint deposits to consider the effects these might have on their subsequent enhancement. The facility to visualise fingerprints from a range of metal surfaces is desirable. Therefore the ultimate objective was to apply the technology to more challenging surfaces via the progression from model surfaces to elemental metals to alloys to evidentially viable items.

The electropolymerisation of PANi and PEDOT has been used to enhance fingerprints, on a range of diverse metals, including stainless steel, brass, copper and nickel plated brass. This was shown by the visualisation of ridge detail of both latent and visible prints previously lacking ridge definition. Latent fingerprints on both model and evidentially viable substrates were enhanced using the polymer treatment. The outcomes were assessed using the five point scale devised by Bandey, taking the view that prints of grade 0-2 are not useable and prints of grade 3 or 4 are useable. *Primary*,

secondary and *tertiary* detail was obtained through the use of digital imaging, optical microscopy and SEM. The ability to access all three levels of detail would allow a fingerprint expert to correctly identify a positive fingerprint match. These results indicate the polymer deposition technique to be a viable method for enhancing fingerprints.

Utilising PANi's electrochromic properties to optimise visual contrast between fingerprint and polymer proved extremely successful on stainless steel; accessing ridge detail that was both less well defined and obscured by an excess of polymer. This procedure resulted in 16% of the samples, previously unusable, to be enhanced to a level (assessed using the Bandey scale) that would be usable in court for a conviction.

The results discussed in Chapter 5 have also shown the polymer technique to work in a way that was not expected; obtaining both positive and negative enhancements on brass and copper. Instead of the fingerprint residue acting as a resist to polymer deposition, resulting in a negative enhancement, a positive enhancement was obtained due to the formation of a Schottky barrier between the corrosion products, as a result of fingerprint sweat, and the metal substrate. Limitations of the technique were found with unsuccessful enhancements on evidentially viable lead and nickel plated brass cartridges.

A survey was carried out on the effectiveness of the polymer deposition method for the enhancement of latent fingerprints on metal substrates. Fingerprints were deposited on

stainless steel substrates, exposed to a range of environments representative of plausible crime scene situations and left for varying intervals prior to enhancement. PANi and PEDOT deposition were compared with three traditional methods, dusting with dry powder, wet powder and superglue fuming. The outcomes were also assessed using the Bandey scale. Superglue fuming was generally the least effective method. This methodology, which has widespread use to good effect on insulating materials (plastics), is complementary to the electrochromic methodology, which requires a conducting substrate. In broad terms, the best method for any selected example of the scenarios explored was either dusting or electrochromic enhancement; wet powder offered some enhancement but to a lesser extent. The performance of the techniques was assessed from the fine detail of fully known sample history, through partially known history to totally unknown history.

It is concluded that the polymer deposition technique shows competitive enhancement with presently used methods across a broad range of scenarios. Enhancement on both copper and brass has proven to be the most useful, especially from previously fired brass cartridges, where substantial ridge detail has been developed. Despite the possibility of an enhancement producing either a positive or negative image, the technique has achieved something that happens rarely, successfully visualising latent ridge detail deposited onto a cartridge prior to its ejection from a firearm.

Future work in this area would be to explore a wider range of substrates, encompassing different metals to those already tested and other items that have forensic value. The range of polymer colours could also be extended which would widen the contrasting

possibilities. As well as expanding the colour palette, the use of fluorescence as an alternative method for visualising enhancements could be carried out. The next step in utilising the technique, as an approved method for fingerprint enhancement in criminal cases, would be to undertake pseudo-operational trials. The principle here is to establish whether the results obtained in a laboratory trial are replicable on items and surfaces that may be submitted to a fingerprint laboratory.

8. Appendices

The following published articles have been removed from of the electronic version of this thesis due to copyright restrictions:

Beresford, Ann L. and Hillman, A. Robert, Electrochromic Enhancement of Latent Fingerprints on Stainless Steel Surfaces, *Analytical Chemistry*, 2010, 82 (2), pp. 483–486. <http://dx.doi.org/10.1021/ac9025434>

Beresford, Ann L.; Brown, Rachel M.; Hillman, A. Robert; Bond, John W., Comparative Study of Electrochromic Enhancement of Latent Fingerprints with Existing Development Techniques, *Journal of Forensic Sciences*, 2012, 57 (1), pp. 93-102. <http://dx.doi.org/10.1111/j.1556-4029.2011.01908.x>